Universitat Autònoma de Barcelona

ELECTROCHEMICAL STRIPPING ANALYSIS AND NANOPARTICLES FOR AFFINITY BIOSENSORS

By

MARÍA TERESA CASTAÑEDA BRIONES

Thesis to opt for the Degree of Doctor in Chemistry

Program of Biotechnology

Group of Sensors & Biosensors
Department of Chemistry, Autonomous University of Barcelona.
Bellaterra, Barcelona, Spain
March 2008

The present thesis titled "Electrochemical Stripping Analysis and Nanoparticles for Affinity Biosensors" has been performed at the laboratories of the *Grup de Sensors i Biosensors* del *Departament de Química de la Universitat Autónoma de Barcelona* in collaboration with *Institut Català de Nanotecnologia* under the direction of Dr. Arben Merkoçi Hyka.

Bellaterra, March 2008

Dr. Arben Merkoçi Hyka
Research Professor
Grup de Sensors i Biosensors
Departament de Química
Universitat Autònoma de Barcelona
&
Group Leader
Nanobioelectronics & Biosensors Group
Institut Català de Nanotecnologia

Campus UAB, Bellaterra
Barcelona, Catalonia, Spain.

Grup de Sensors i Biosensors
Departament de Química, Universitat Autònoma de Barcelona
Edifici C s/n. Bellaterra. España
Tel. +34 93 581 2118 Fax: +34 93 581 2379

ABSTRACT

Although the main goal of my thesis was the design and construction of affinity biosensors I have started my work with the development of an electrochemical sensor for heavy metal detection. This sensor will be of great importance in the research group for future applications in DNA analysis by using heavy metal based quantum dots (QDs) as labels.

A special emphasis was given later to the development of different novel, rapid and sensitive biosensors for the electrochemical detection of DNA hybridization and proteins that take the advantage of a magnetic separation/mixing process and the use of gold nanoparticles as label, as well as the direct determination of gold nanoparticles by differential pulse voltammetry stripping technique.

This thesis is structured in seven chapters: Chapter 1 contains a general introduction about the biosensors field; explains the synthesis, properties and application of gold nanoparticles as well as its modification by using biological molecules and their use as label in electrochemical biosensors. At the same chapter are described the basis of DNA and protein analysis with interest for biosensor research. This chapter also describes previous methods used for hybridization detection and contains information that supports the theory of electrochemical detection as a fast, simple, and highly sensitive method of DNA hybridization as well as protein detection mostly using stripping voltammetry.

Chapter 2 establishes the objectives of the thesis.

Chapter 3 describes experimental section which is divided in three parts:

The first part focuses on the design and construction of a graphite–epoxy composite electrode (GECE) containing $Bi(NO_3)_3$ to different concentrations as a built-in bismuth precursor for anodic stripping individual or simultaneous detection of heavy metals such as lead, cadmium, copper and zinc, with interest for further applications in DNA or protein detection based on the use of metal nanoparticles. This part of the thesis was of a great interest for several reasons. A) The designed sensor was later on applied for cadmium sulphide quantum dots detection with interest for biosensor applications; B) The developed sensor opened the way for further development of free mercury screen-printed electrodes for environmental applications; C) The development of this work has been for me of great utility because it allowed me as a biologist, to get deeper in the electrochemistry field related to nanoscience and nanomaterials.

The second part describes the design and construction of a magnetic-graphite epoxy composite electrode (M-GECE). Its uses as transducers for electrochemical detection of DNA hybridization in model and sandwich systems in addition to gold nanoparticles of different sizes as labels are described at this same chapter.

The third part of the experimental section describes the use of gold nanoparticles as labels for protein analysis. Electrochemical in comparison to optical detection based on either the use of enzyme or gold nanoparticles as labels is described.

Chapter 3 also covers the study and optimization of the most important experimental parameters that affect the DNA and protein electrochemical detection

strategies described as well as some optical techniques applied to study working electrode surface and characterisation of paramagnetic beads and gold nanoparticles.

At Chapter 4 the global discussion of results is presented. In this chapter, some results of the assays reported are also discussed.

Chapter 5 summarises the general conclusions of the thesis.

Chapter 6 focuses on the proposals for future studies.

Finally, Chapters 7 and 8 show the publications that resulted from this thesis.

RESUMEN

Aun cuando el objetivo principal de mi tesis fue el diseño y la construcción de biosensores de afinidad, he comenzado mi trabajo desarrollando un sensor electroquímico para la detección de metales pesados. Este sensor será de gran importancia en nuestro grupo de investigación para futuras aplicaciones en el análisis de DNA usando puntos cuánticos (QDs) basados en metales pesados, como marca.

Un énfasis especial fue dado después al desarrollo de diferentes nuevos biosensores, rápidos y sensibles para la detección electroquímica de la hibridación de DNA y de proteínas, con las ventajas de ser procesos de mezclado y separación magnética y el uso de nanopartículas de oro como marca, así como la detección directa de las nanopartículas de oro mediante la técnica de voltametría de redisolución de pulso diferencial.

Esta tesis está estructurada en siete capítulos: El Capítulo 1 contiene una introducción general sobre el campo de biosensores; explica brevemente la síntesis, propiedades y aplicaciones de las nanopartículas de oro así como su modificación con moléculas biológicas y su uso como marca en biosensores electroquímicos. En el mismo capítulo son descritas las bases de análisis de proteínas y DNA de interés para la investigación de biosensores. Este capítulo describe también métodos usados anteriormente para la detección de hibridación y contiene la información que apoya la teoría de la detección electroquímica como un método rápido, simple y muy

sensible de hibridación del DNA así como la detección de proteínas sobre todo usando voltametría de redisolución.

El Capítulo 2 establece los objetivos de la tesis.

El Capítulo 3 describe la sección experimental que comprende tres partes:

La primera parte se enfoca en el diseño y construcción de un electrodo de composite grafito-epoxi (GECE) que contiene $Bi(NO_3)_3$ a concentraciones diferentes como un precursor de bismuto incorporado, para la detección individual o simultánea por redisolución anódica de metales pesados como plomo, cadmio, cobre y zinc, con interés para posteriores aplicaciones en la detección de DNA o proteínas basada en el uso de nanopartículas metálicas. Esta parte de la tesis fue de un gran interés por diversas razones. A) El sensor diseñado fue aplicado después para la detección de puntos cuánticos (QDs) con interés para aplicaciones en biosensores; B) El sensor desarrollado abrió el camino para el desarrollo posterior de electrodos serigrafiados libres de mercurio para aplicaciones ambientales; C) El desarrollo de este trabajo ha sido para mí de gran utilidad porque como biólogo esto me permitió profundizar en el campo de la electroquímica relacionada con nanociencia y nanomateriales.

La segunda parte describe el diseño y construcción de un electrodo de grafito-epoxi composite que contiene un imán integrado (M-GECE). Sus usos como transductores para la detección electroquímica de la hibridación de DNA, en los sistemas modelo y emparedado (*sandwich*), además para nanopartículas de oro de diferentes tamaños como marca, son descritos en este mismo capítulo.

La tercera parte de la sección experimental describe el uso de nanopartículas de oro como marca para el análisis de proteína. Se describe la detección electroquímica en comparación con la detección óptica basada en el uso de enzima o de nanopartículas de oro como marca.

El capítulo 3 cubre también el estudio y la optimización de los parámetros experimentales más importantes que afectan la detección electroquímica de DNA y proteínas en las estrategias propuestas, así como algunas técnicas ópticas utilizadas en el estudio de la superficie de los electrodos de trabajo y la caracterización de partículas paramagnéticas y nanopartículas de oro usadas.

En el capítulo 4 se presenta la discusión global de los resultados. En este capítulo algunos resultados de los ensayos reportados son discutidos también.

El capítulo 5 resume las conclusiones generales de la tesis.

El capítulo 6 se centra en las propuestas para estudios futuros.

Finalmente, los capítulos 7 y 8 muestran las publicaciones que resultaron del trabajo realizado en esta tesis.

AGRADECIMIENTOS

En primer lugar me gustaría expresar mi agradecimiento al catedrático Dr. Salvador Alegret quien me dio la oportunidad de integrarme a su grupo de trabajo así como la posibilidad para trabajar en su laboratorio. Del mismo modo también quiero expresar mi especial gratitud al Dr. Arben Merkoçi quien ha sido mi Director, por su confianza, su paciencia durante mi introducción al campo de la electroquímica y por todo su apoyo a lo largo de todo mi trabajo. Él siempre ha mostrado ser un investigador entusiasta y optimista, dispuesto a compartir sus conocimientos y a ofrecer el consejo cuando es necesario, por lo cual le estoy muy agradecida.

Estoy muy agradecida también hacia el Dr. Martin Pumera por su gran apoyo durante mi primer año de trabajo en el laboratorio.

Me gustaría también expresar mi agradecimiento a los Doctores Ramón Eritja, Fernando Domínguez y Lourdes Loidi, por su cálido recibimiento cuando visité sus respectivos laboratorios y por su buena disposición para colaborar.

Me gustaría agradecer también muy especialmente a todos mis compañeros de grupo, a los de siempre y a los que lo han sido en forma temporal: Briza, Anna, Sergi, Alfredo, Adriano, Gemma, Humberto, Raquel, Marisa, Gina, Paty y Humberto Luiz, por su honesta amistad y apoyo durante nuestro tiempo como compañeros de laboratorio. Los quiero mucho y los recordaré siempre.

Aprecio muchísimo los trabajos de colaboración realizados con Briza, Anna, Sergi, Adriano, Alfredo, Marisa y Paty, así como con Blanca y Francisco en el campo de la Genética.

Gracias al resto de los compañeros de laboratorio, tanto los anteriores como los actuales, quienes crearon siempre un agradable ambiente de trabajo: Sam, Xavi, Anabel, Anna González, Marinela, Oscar y Sandra.

Agradezco mucho al Departamento de Química, por el apoyo brindado durante mi trabajo, sobre todo gracias a Faly, Melina, Nacho y José Manuel. De la misma manera agradezco también al ICN por todas las facilidades brindadas en el último año para trabajar tanto en el laboratorio, como en los despachos que nos proporcionaron.

Agradezco también a mis amigos de aquí: Pilar y Simón, Carmen, Gladys, María Teresa y Alfonso, Lilia y Alberto, Julia y Antonio, Guillermo, Alicia, Jael y Oscar, Carmen Vivian y Antonio, y a los de lejos: Blanquis y Fausto, Beatriz y Alberto, Jorge y Maggie, Julieta, Mela, Agustín y Adelita, Rosalía, Alejandrina, Rosy, así como a todos mis compañeros de trabajo de la UAM-A, por su amistad y apoyo moral.

Estoy muy agradecida también con toda mi familia, sobre todo con mis hermanos Victoria, Catalina, Manuel, María Guadalupe, Porfirio, Juan Pablo, Alvaro y Sergio; con mis cuñados Juan, Arnulfo, Gloria, Francisca, Angel, María Sirenia, Francisco, Pedro y Maricela y resto de mi familia por su gran apoyo moral.

Finalmente agradezco infinitamente a mi esposo Margarito y a mis hijos Marisol e Ismael, mis tres amores, sin quienes no hubiera sido capaz de alcanzar esta meta.

Su amor, estímulo, enorme paciencia y el gran apoyo que siempre me han brindado, han sido invaluables. Su confianza en mí ha sido constante y ellos han sido para mí una fuente inagotable de fortaleza. ¡¡Los amo muchísimo!!!

A la memoria de mis padres

A mi familia

A mis amigos

INDEX

I. Sensitive stripping voltammetry of heavy metals by using a composite sensor based on a built-in-bismuth precursor. *Analyst*, 2005, 130, 971–976.

Castañeda M. T., Pérez B., Pumera M., Del Valle M., Merkoçi A., Alegret S.

II. Stripping analysis of heavy metals by using mercury-free composite based sensors. Chapter 1, pages 1–22, 'Applications of Analytical Chemistry in Environmental Research, 2005', Edited by Research SignPost, ISBN: 81-308-0057-8 Editor: Manuel Palomar, 2005.

Merkoçi Arben, Castañeda María Teresa, Alegret Salvador.

III. Gold nanoparticles in DNA and protein analysis. Chapter 38, pages 941–956. 'Electrochemical sensor analysis'. Amsterdam Elsevier, ISBN-13:978-0-444-53053-0. Editors: S. Alegret and A. Merkoçi, 2007.

Castañeda M. T., Alegret S., Merkoçi A.

IV. DNA analysis by using gold nanoparticle labels. Procedure 53, e381–388. 'Electrochemical sensor analysis'. Amsterdam Elsevier, ISBN-13:978-0-444-53053-9. Editors: S. Alegret and A. Merkoçi, 2007.

Castañeda M. T., Pumera M., Alegret S., Merkoçi A.

V. Electrochemical sensing of DNA using gold nanoparticles. *Electroanalysis*, 2007, 19, 743–753.

Castañeda M. T., Merkoçi A., Alegret S.

VI. Magnetically trigged direct electrochemical detection of DNA hybridization based Au_{67} Quantum Dot – DNA – paramagnetic bead conjugate. *Langmuir*. 2005, 21, 9625–9629.

Pumera M., Castañeda M. T., Pividori M. I., Eritja R., Merkoçi A., Alegret S.

VII. Electrochemical genosensors for biomedical applications based on gold nanoparticles. *Biosens, Bioelectron*. 2007, 22, 1961–1967.

Castañeda M. T., Merkoçi A., Pumera M., Alegret S.

VIII. Double-codified gold nanolabels for enhanced immunoanalysis. *Analytical Chemistry*, 2007, 79, 5232–5240.

Ambrosi A., Castañeda M. T., Killard A. J., Smyth M. R., Alegret S., Merkoçi A.

Chapter 8. ANNEX

I. Electrochemical detection of DNA Hybridization Using Micro and Nanoparticles. Humana Press methods book on biosensors, 2007. Accepted.

Castañeda M. T., Alegret S., Merkoçi A

ABBREVIATIONS

A	Adenine
AA	Ascorbic Acid
AAS	Atomic Absorption Spectrometry
Ab	Antibody
AbAg	Antibody/Antigen complex
AdSV	Adsorptive Stripping Voltammetry
AFM	Atomic Force Microscopy
Ag	Antigen
ASV	Anodic Stripping Voltammetry
ATR-FTIR	Attenuated Total Reflection-Fourier Transform Infrared Spectroscopy
AuNPs	Gold Nanoparticles
BSA	Bovine Serum Albumin
bp	Base pairs
C	Cytosine
CDRs	Complementarity Determining Regions
CE	Counter (auxiliary) electrode
CV	Cyclic voltammetry
CSV	Cathodic Stripping Voltammetry
ddH_2O	Double Distilled Water
DL	Limit of detection
DMF	N,N`-dimethylformamide
DNA	Deoxyribonucleic Acid
dsDNA	Double Stranded DNA
ssDNA	Single Stranded DNA
DPV	Differential Pulse Voltammetry

DTT	Dithiothreitol
EDS	Energy Dispersive X-ray Spectrometry
EIS	Electrochemical Impedance Spectroscopy
ELISA	Enzyme-Linked Immunosorbent Assay
***E*p**	Peak potential
FT-IR	Fourier Transform Infrared Spectroscopy
FRET	Fluorescence Resonance Energy Transfer
G	Guanine
GECE-M	Graphite-Epoxy Composite Electrode-Magnetic
GAD	Glutamic Acid Decarboxylase
HRP	Horse Radish Peroxidase
ICP-MS	Inductively coupled plasma mass spectrometry
Ig	Immunoglobulin (s)
IgG	Immunoglobulin G
IR	Infrared
ITO	Indium Tin Oxide
IUPAC	International Union of Pure and Applied Chemistry
***i*p**	Peak current
Kd	Dissociation constant
LSV	Linear Scan Voltammetry
M-GECE	Magnetic-Graphite-Epoxy Composite Electrode
NPs	Nanoparticles
OEG	Oligo(ethylene glycol)
PBS	Phosphate Buffered Saline
PCR	Polymerase Chain Reaction
PEG	Poly(Ethylene Glycol)
ppb	Parts per billion
PSA	Potentiometric Stripping Analysis
PV	Pulsed Voltammetry
QCM	Quartz Crystal Microbalance
QDs	Quantum Dots

RAIRS	Reflection Absorption Infrared Spectroscopy
RDE	Rotating Disk Electrode
RE	Reference Electrode
RNA	Ribonucleic Acid
SAM	Self-Assembled Monolayer
SAW	Surface Acoustic Wave
SCP	Stripping Chronopotentiometry
SDS	Sodium Dodecyl Sulphate
SEM	Scanning Electron Microscopy
SERS	Surface Enhanced Raman Scattering
S/N	signal-to-noise
SP	Stripping Potentiometry
SPR	Surface Plasmon Resonance
STM	Scanning Tunnelling Microscopy
SV	Stripping Voltammetry
SWAV	Square Wave Anodic Voltammetry
t	Time
T	Thymine
TEM	Transmission Electron Microscopy
T_m	Melting temperature
Tris	Tris(hydroxymethyl)-amino methane
XPS	X-ray Photoelectron Spectroscopy
V_H	Variable domains from on heavy chain
V_L	Variable domains from on light chain
WE	Working Electrode

Chapter 1. GENERAL INTRODUCTION

1. GENERAL INTRODUCTION

1.1 Sensors and Biosensors

A chemical sensor is defined as a device which responds to a particular analyte in a selective way through a chemical reaction and can be used for the qualitative or quantitative determination of this analyte.[1]

According to International Union of Pure and Applied Chemistry (IUPAC), recommendations, a biosensor is a self-contained integrated receptor-transducer device, which is capable of providing selective quantitative or semi-quantitative analytical information using a biological recognition element[2.]

Their two elements are essentials: first, the powerful molecular recognition capability of bioreceptors (biorecognition element) such as antibodies, DNA, enzymes and cellular components of living systems, and secondly, the transducer element to translate the interactions of the biorecognition element into a detectable signal.

The amount of signal generated is proportional to the concentration of the analyte, allowing for both quantitative and qualitative measurements in time[3]. Biorecognition element imparts the selectivity that enables the sensor to respond selectively to a particular analyte or group of analytes, thus avoiding interferences from other substances.[4]

Hence, a highly selective and sensitive biorecognition element is essential for the design of an efficient sensor.

1.1.1 Transducers

The transducer must be selected according to the product obtained in the biochemical reaction, and it can be electrochemical, optical, or piezoelectric[5].

1.1.1.1. Electrochemical transducers

The electrochemical transducers are classified into amperometric, potentiometric, and conductimetric.

Amperometric transducers are the most used for the design of biosensors, owing to their high sensitivity. Up till now, the amperometric transducers that gave the best sensitivities were glassy carbon[6-10] carbon paste[11-14] and diamond paste electrodes[15,16].

Diamond paste is a newly developed amperometric transducer obtained by mixing monocrystalline diamond powder with paraffin oil. Their advantages of utilizing it as a transducer in the biosensors technology are low background current, wide potential range, lack of adsorption, high signal-to-noise and signal-to-background ratios. Although diamond itself is a known insulator, boron-doped diamond films possess electronic properties ranging from semiconducting to semimetallic and are highly useful for electrochemical measurements[17].

Conducting composites are interesting alternatives for the construction of electrochemical transducers in general and for amperometric ones particularly. The capability of integrating various materials (i.e. graphite, polymers, catalysts etc.) is one of their main advantages. This incorporation is possible to be performed either through a previous modification of one of the component of the composite

before its preparation or through physical incorporation into the composite matrix. This kind of transducers offer many potential advantages compared to more traditional electrodes consisting of a surface-modified single conducting phase. Composite electrodes can often be fabricated with great flexibility in size and shape of the material, permitting easy adaptation to a variety of electrode configurations. Moreover these electrodes have higher signal-to-noise (S/N) ratio, compared to the corresponding pure conductors, that accompanies an improved (lower) detection limit.[18]

1.1.1.2. Optical transducers

These include vibrational (IR, Raman) and luminescence (Fluorescence, chemiluminescence). Surface Plasmon Resonance (SPR), has also been shown to be an effective optical transducer mechanism for biosensor use.

Fluorescence and chemiluminescence transducers are the most developed within the optical transducer class. Their limits of detection are the lowest that one can obtain using biosensors. Fiber-optic biosensors employ the absorbance or fluorescence of light by a product or reactant. Chemiluminescence occurs when the electron excitation energy necessary for photon emission is supplied by a chemical reaction.

Bioluminescence is a subdivision of chemiluminescence and occurs in living organisms such as fireflies, glow-worms and bacteria among others.[19] The main types of optical transducers used in biosensors technology are optical fibres[20,21], chemiluminescence[22] and SPR[23].

1.1.1.3. Piezoelectric or mass change transducers

The most commonly used are surface acoustic wave (SAW) and quartz crystal microbalance (QCM). The piezoelectric transducers allow a binding event to be converted into a measurable signal, for example resonance frequency changes. Changes in mass are sensed by variations in the frequency of oscillation in a piezoelectric crystal or surface acoustic wave. The principle is based on the piezoelectric properties of some material such as quartz crystals.

The development of a simple and multifunctional piezoelectric transducer, which can detect two or more species at one time, was reported by Li and Jiang.[24]

1.1.2. Operation principle and classification of biosensors

The operating principle of a biosensor involves detection of the biorecognition element and transforming it into another type of signal using a transducer that may produce either an optical, electrochemical or mass change (piezoelectric) signal.

The molecular recognition then corresponds to the association of the biological element and its target molecule (analyte) through an association such as: enzyme-substrate, antibody-antigen, receptor-hormone, complementary DNA sequencing, etc. These associations maximise the capacity of the biomolecules to recognise a unique substance among various substances.

A schematic representation of a biosensor is shown in Figure 1.1

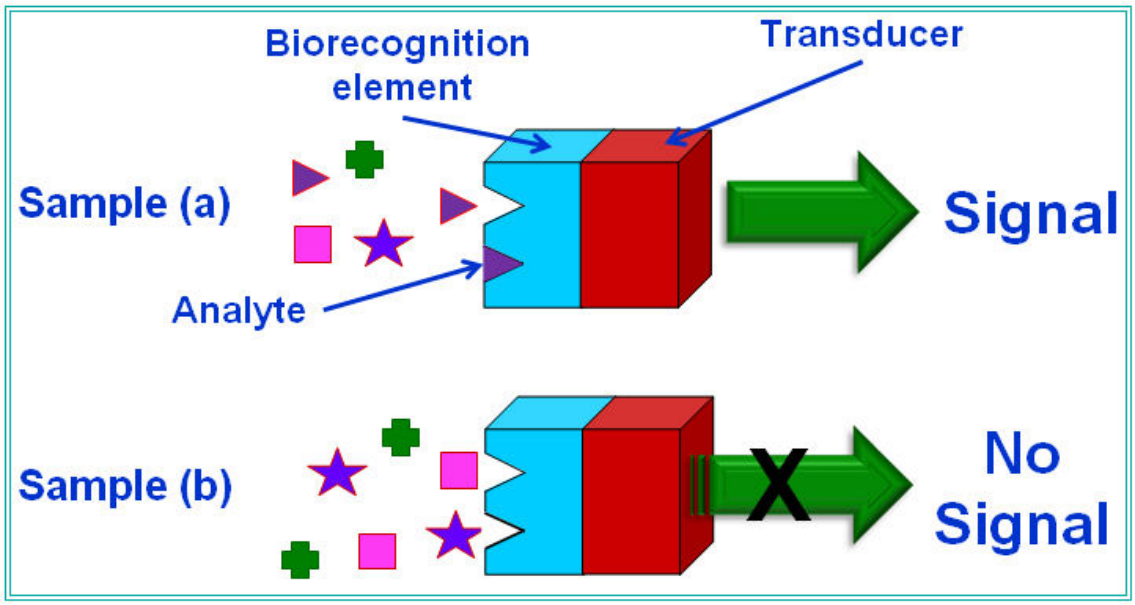

Figure 1.1. *Schematic representation of a biosensor. The analyte at sample (a) binds selectively with biorecognition element which is associated with the transducer and a measurable signal is obtained. At sample (b) the analyte is not present therefore no signal is obtained.*

In general, biosensors are classified either by their biological element or the transducer used. In some cases, the immobilization method used to attach the biological element to the transducer is used for classification.

Based on the type of used transducer, the biosensors are divided into optical[20,25-28], piezoelectric[29-33] thermometric[34-36] and electrochemical sensors[9,37-41].

The advantages of biosensors over traditional analytical devices include their potential for miniaturisation, short response times, high selectivity, ease of use and low cost.[42]

The biosensors have an important application in medical diagnostics[43-45] environmental monitoring[46-49] pathogenic microorganisms detection[50-53] food quality control[54], and other fields.

1.2. Electrochemical biosensors

1.2.1. General introduction and classification

Electrochemical biosensors combine the analytical power of electrochemical techniques with the specificity of biological recognition processes. Usually the bioreaction produces an electrical signal that relates to the concentration of an analyte. For this purpose, a biospecific reagent is either immobilized or retained at a suitable electrode, which converts the biological recognition event into a quantitative amperometric or potentiometric response. The combination of the electrode with a biomolecule offers new and powerful analytical tools that are applicable to many challenging problems.[17]

Electrochemical biosensors have been the most widely used classes of biosensors due to their faster response, greater simplicity, high sensitivity, and lower cost compared to optical, colorimetric, and piezoelectric biosensors.[55,56]

There are three types of electrochemical biosensors: Potentiometric, conductimetric and (volt)amperometric.

1.2.1.1. Classification based on the transduction mode

Depending on the transduction mode, the electrochemical biosensors can be classified in:

– ***Potentiometric biosensors***

Monitoring potentials at the working electrode with respect to the reference electrode, while changing the concentration of the analyte (logarithmic relationship) is the principle of a potentiometric biosensor.

These biosensors detect the accumulation of charge created by selective binding at the electrode surface.[57]

– ***Conductimetric biosensors***

Conductimetric sensors measure the effect of the biological and chemical changes upon the conductance between a pair of metal electrodes in a bulk solution, as a consequence of the immobilization and interaction of biomolecules.[58]

– ***(Volt)amperometric biosensors***

(Volt)amperometric biosensors possess linear concentration dependence, (compared to a logarithmic relationship in potentiometric biosensors) and measure changes in the current on the working electrode due to the direct oxidation/reduction of the products of a biochemical reaction in direct or indirect measuring systems.

(Volt)amperometric biosensors also have the advantages of high sensitivity, faster response, low cost, and disposable in comparison to other analytical devices.[59-61]

1.2.1.2. Classification based on the biological recognition element

In terms of nature of their biorecognition element, there are two categories of electrochemical biosensors:

– ***Biocatalytic biosensors***

Biocatalysts, such as enzymes, microbiological cells or tissues, are used to moderate a biochemical reaction, recognize, bind, and chemically convert a molecule.[17,59,62]

– ***Affinity biosensors***

Rely on the use of receptor molecules, such as antibodies, nucleic acids and membrane receptors to recognize and to bind irreversibly a particular target.[17-65] The high specificity and affinity of biochemical binding reactions (such as DNA hybridization and antibody–antigen complexation) lead to highly selective and sensitive sensing devices.

Alternative biorecognition elements include RNA and DNA aptamers[66,67] molecularly imprinted polymers[60,68] and templated surfaces[69].

The aptamers are functional nucleic acids selected from combinatorial oligonucleotide libraries by in vitro selection against a variety of targets, such as small organic molecules, peptides, proteins and even whole cells.[70]

1.2.2. Electrochemical techniques for the signal recording

There are three basic electrochemical processes that are useful in transducers for sensor applications: conductimetry, potentiometry and (volt)amperometry.

1.2.2.1. Conductimetry

The two main types of non-faradaic electrochemical analysis can be categorized as potentiometric, and conductimetric. Most reactions involve a change in the

composition of the solution. This will normally result in a change in the electrical conductivity of the solution, which can be measured electrically by an alternating current bridge method.[4]

There are two general types of devices for measuring conductance. The first, and most widely used, employs a pair of contacting electrodes, frequently platinum, immersed in the test liquid. The second type of instrumentation is noncontacting or "electrodeless" and depends on inductive or capacitive effects to measure conductance.

1.2.2.2. Potentiometry

Is a technique that involves the measurement of the potential of a cell at zero current. The potential is proportional to the logarithm of the concentration of the substance being determined.[4]

Potentiometric measurements require a reference electrode, a working electrode, and a reliable potential-measuring instrument, such as a voltmeter. The test solution must be in direct contact with the working electrode. The reference electrode may be placed in the test solution, or it can be brought into contact with the test solution through a salt bridge.

Owing to its simplicity and versatility, potentiometry is perhaps the most widely used analytical technique.[5]

1.2.2.3. Voltammetry

Voltammetry is an electroanalytical technique that measures current as a function of potential. When the current is recorded in a fixed potential as a function

of time, the technique is called chronoamperometry and when the potential may vary with time in a predetermined manner and the current is measured as a function of potential is called voltammetry or voltamperometry.

At voltammetry, an increasing (decreasing) potential is applied to the cell until oxidation (reduction) of the substance to be analysed occurs and there is a sharp rise (fall) in the current to give a peak current. The height of the peak current is directly proportional to the concentration of the electroactive material.

If the appropriate oxidation (reduction) potential is known, one may step the potential directly to that value and observe the current.[4]

The electrochemical cell, where the voltammetric experiment is carried out, consists of a working electrode (WE), a reference electrode (RE), and usually a counter (auxiliary) electrode (CE). The WE is where the reaction or transfer of interest is taking place.[71] The RE provides a known and stable potential, against which the potential of the WE is compared. The most common RE systems used in aqueous medium are the silver-silver chloride (Ag/AgCl) and the saturated calomel (Hg/Hg_2Cl_2) which have electrode potentials independent of the composition of electrolyte[72]. The CE is a current-carrying electrode, via which the current is measured. Inert conducting materials, such as a platinum wire or a graphite rod are often used as CE.[73] An electrochemical cell is shown in Figure 1.2

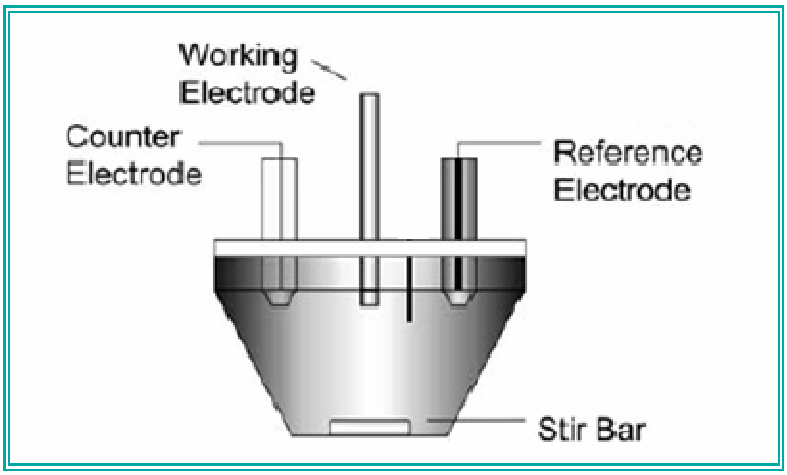

Figure 1.2. *An electrochemical cell used in voltammetry consists of a working electrode, a counter electrode, and a reference electrode. Adapted of Ref. 5*

The term voltammetry encompasses a broad area of electroanalytical chemistry that includes polarography, linear scan voltammetry (LSV), cyclic voltammetry (CV), pulsed voltammetry (PV), and stripping voltammetry (SV).

In general voltammetry is an analytical tool that can be used for the quantitative analysis of various redox-active compounds and is very useful in the analysis of the analytes that lack a chromophore or fluorophore. Overall, voltammetry is very versatile, and can be used for the analysis of many redox-active species.[5]

1.2.2.4. Stripping methods

Stripping analysis is commonly described as a two-step process:

Preconcentration: Deposition or adsorption of the analyte or analytes onto the surface or into the working electrode during time (t). This step often occurs under potential control or, possibly, at open circuit.

Stripping: The accumulated species is oxidized or reduced back into the solution. This can be achieved by varying the applied potential over time, applying a fixed current, or by inducing oxidation/reduction by another chemical species in

solution. In all cases, the resulting response is proportional to the concentration of that analyte in or on the electrode, and thus, the sample solution.

Of particular note, stripping voltammograms or chronopotentiograms can yield qualitative as well as quantitative information.

Owing to the possibility of preconcentrating the analyte onto the working electrode (by factors of 100 to more than 1000), stripping analysis has the lowest limits of detection among all electroanalytical methods (i.e., 10^{-11} M). With this technique is possible to analyze more than one (four to six) analyte at a time, with a relatively low cost.[5,17] Stripping analysis is an extremely sensitive, electrochemical technique for trace metals[74].

Numerous variants of stripping analysis exist currently, differing in their method of accumulation and measurement. In general stripping analysis include: cathodic stripping voltammetry (CSV), anodic stripping voltammetry (ASV), adsorptive stripping voltammetry (AdSV) and potentiometric stripping analysis (PSA).[17]

– ***Anodic stripping voltammetry***

ASV involves the electrochemical oxidation of a preconcentrated analyte. The term ASV should only be used when the analyte(s) is accumulated either by reduction (e.g., a metal ion) or by direct adsorption (e.g., organic compounds) and determined by its subsequent oxidation[74,75]

The first step involves the reduction of a metal ion to the metal, which usually forms an amalgam with the mercury electrode:

$$M^{n+} + ne^- + Hg \rightarrow M(Hg)$$

The applied potential on the working electrode should be maintained at least 0.4 V more negative than the standard. Under these conditions the deposition step is controlled by mass-transport. Thus, hydrodynamic control via rotation, stirring, or flow is typically used to facilitate the deposition step.

Increased mass transfer due to linear diffusion often avoids the need for hydrodynamic control for microelectrodes. The concentration of the reduced metal in the mercury, C_{Hg}, is given by Faraday's law:

$$C_{Hg} = \frac{i_L t_d}{nFV_{Hg}}$$

where i_L s the limiting current for the deposition of the metal, t_d is the length of the deposition period, n is the number of electrons transferred, F is the Faraday constant, and V_{Hg} the volume of the mercury electrode.

The stripping step is typically performed under quiescent conditions, and any stirring or flow is stopped, followed by a rest period (ca. 10–15 s) to allow the system to equilibrate.

At the end of the rest period, which is incorporated into the preconcentration step, the stripping step begins by the application of a potential–time waveform going in the positive direction.

When the potential reaches the standard potential of the metal–metal ion redox couple, that particular amalgamated metal is oxidized, or stripped (dissolved), from the mercury electrode:

$$M(Hg) \rightarrow M^{n+} + ne^- + Hg$$

Repetitive ASV runs can be performed with good reproducibility in connection to a short (30–60 s) "electrochemical cleaning" period at the final potential (e.g.,

+0.1 V using mercury electrodes). The potential–time sequence used in ASV, along with the resulting stripping voltammograms, is shown in Figure 1.3

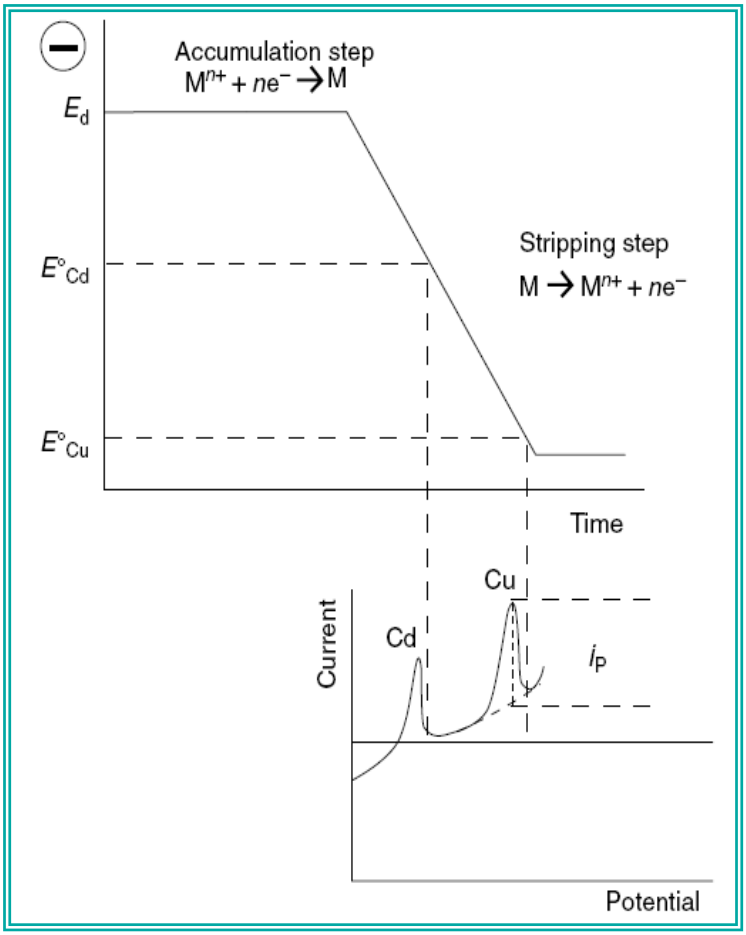

Figure 1.3. *Anodic stripping voltammetry: the potential-time waveform (top), along with the resulting voltammogram (bottom).*[17]

– *Potentiometric stripping analysis*

PSA and stripping potentiometry (SP) are general terms synonymous with stripping chronopotentiometry (SCP) which involves the determination of an accumulated analyte by observing the change of electrode potential with time during the stripping (at a constant rate) of the accumulated analyte either chemically or electrochemically.

PSA resembles ASV as the preconcentration step is similar in that the analyte is reduced and concertedly deposited onto a mercury electrode surface.

Rather than scanning a positive-going potential–time waveform and monitoring the current, the metal amalgam (M(Hg)) is oxidized ("stripped") chemically (using an oxidant) from the mercury electrode surface:

$$\text{M(Hg)} \xrightarrow{\text{oxidant}} \text{M}^{n+} + \text{Hg}$$

Typical oxidants used for the oxidation are O_2, Hg(II) and Cr(VI). In another approach, the amalgam can be stripped off by applying a constant anodic current to the electrode. By either means, the potential of the working electrode is recorded as a function of time, and a stripping curve, is obtained. A sudden change in potential occurs when all the metal deposited in the electrode has been oxidized from the surface. The transition time needed for the oxidation of a given metal, t_M, is a quantitative measure of the metal concentration $[M^{n+}]$ in the sample:

$$t_M \approx [M^{n+}] t_{dep}$$

where t_{dep} is the length of the deposition period.

For constant current PSA, the stripping time is inversely proportional to the applied stripping current. As predicted by the Nernst equation, the potential at which the reoxidation takes place serves as a quantitative identification of the different metals. The sigmoidal-shaped curves are easily converted to peaks by taking the first derivative of the analytical signal (i.e., dE/dt vs. E), which is easily accomplished with modern computer-controlled systems.[5]

1.3. Nanoparticles in biosensors design. Properties and applications

Although biosensors can be classified based on different criteria an interesting classification can be established based on the necessity of using additional reagents to obtain the analytical signal. In this way, biosensors can be divided in: *nonlabelled* or label-free types, which are based on the direct measurement of a phenomena occurring during the biochemical reactions on a transducer surface; and *labelled*, which relies on the detection of a specific label. Research into 'label-free' biosensors continues to grow[76], however 'labelled' ones are more common and are extremely successful in a multitude of platforms.

The labels used in electrochemical biosensors can be *enzymes* –the most used- or *electroactive compounds*. The last one presents the advantage of their lower cost and their operational simplicity.

Recently, the use of nanoparticles, mainly gold nanoparticles, as electroactive labels has received wide attention, due to their unique properties.

1.3.1. Properties of Nanoparticles

At the nanoscale, materials exhibit unique optical, electronic, and magnetic properties not seen at the bulk scale, which makes nanostructures attractive for a wide range of applications. The combination of these unique properties with the appropriate size scale has motivated the introduction of nanostructures into biology[77-84] The integration of nanotechnology with biology and bioengineering is producing many advances. The essence of nanotechnology is to produce and manipulate well defined structures on the nanometer scale with high accuracy.

Developments in nanotechnology have driven to research of nanoparticles (NPs) in the 1 to 100 nm range which can come in a variety of shapes of which the most commonly prepared are: spheres[85,86] rods[87], cubes[88], triangles[86] and ellipsoids[89]. Several reviews have addressed the synthesis and properties of different NPs.[3, 90-93]

An important application of NPs is at the field of electrochemical sensors and biosensors. Many kinds of NPs, such as metal, oxide and semiconductor nanoparticles also know as Quantum dots (QDs) have been used for constructing electrochemical sensors and biosensors, which play different roles: immobilization of biomolecules, the catalysis of electrochemical reactions, the enhancement of electron transfer between electrode surfaces and proteins, labelling of biomolecules and even acting as reactant in different sensing systems.[94]

The NPs offer a great potential in a variety of applications such as detection of infectious diseases[95], environmental monitoring[37] detection of pathogens[96], proteomics[97], genomics[98], drug delivery[99], catalytic[100] and others bioanalysis. Biological, medical and environmental applications of NPs are summarized by different authors. [78-101]

1.3.2. Use of nanoparticles as labels in affinity biosensors

Several compounds are being used as labels for affinity biosensors. Enzymes are the most reported and have shown to be very sensitive. Additionally, these labels have already well established methodologies. The only drawback is the lack of stability as well as the difficulty to be used for simultaneous detection. Fluorescent dyes, have been also reported for optical based sensors.

In the following part we will focus only to NPs as a novel alternative for labelling strategies.

The unique properties of nanoscale materials offer excellent prospects for interfacing biological recognition events with electronic signal transduction and for designing a new generation of bioelectronic devices exhibiting novel functions.[102]

Noble metal nanoparticles, such as gold[26,97,103-106], silver[107,108] and platinum[109], among others, as well as QDs such as CdS[110,111,], PbS[110], ZnS[110] CdTe[112] and others[113], have received considerable attention in recent years due to their use as labels.

The uses of these different metal nanoparticles and QDs have opened the door to the simultaneous detection of multiple targets. When several transducers or transducer-bioreceptor combinations are arrayed onto individual integrated circuit microchips, these biosensors are often referred to as biochips. In general, biochips consist of an array of individual biosensors that can be individually monitored and used to detect multiple analytes simultaneously[114].

Cai et al.[37] reported an electrochemical methodology that enables the rapid identification of different DNA sequences on the microfabricated electrodes.

Recently the field of biosensors for diagnostic purposes has acquired a great interest regarding the use of NPs as DNA and protein markers. Some biosensing assays based on bioanalytical application of NPs have offered significant advantages over conventional diagnostic systems with regard to assay sensitivity, selectivity, and practicality.[77,115,116]

1.3.3. Gold Nanoparticles

1.3.3.1 Synthesis and properties

In 1857 Faraday published a comprehensive study on the preparation and properties of colloidal gold.[117] A variety of methods have been developed for synthesis of gold nanoparticles (AuNPs), and among them, sodium citrate reduction of cloroauric acid at 100 ºC was developed by Turkevich[118] and remains the most commonly used method.

Recently, Lung et al. reported the preparation of AuNPs by arc discharge in water as an alternative, cheap, effective and environmentally friendly method.[119] Currently synthesis of novel AuNPs with unique properties and with applications in a wide variety of areas is subject of substantial research.[120-122]

The catalytic, optical, electrical, magnetic, and electrochemical properties that exhibit AuNPs have made them an integral part of research in nanoscience.[123]

In addition to their striking optical properties, AuNPs are important because they can be stabilized with a wide variety of molecules by taking advantage of well-known chemistry involving alkanethiol adsorption on gold.[124]

The attractive physicochemical properties of AuNPs are highly affected by its shape and size.[123,125] Ouacha et al.[126] reported the laser-assisted growth of AuNPs and concluded that this is a powerful method for controlling the shape of the Au-NPs irrespective of size. On the other hand, size and properties of AuNPs are highly dependent on their preparation conditions[12,100]. Synthesis of AuNPs of different shapes and sizes has been reported by Dos Santos et al.[127]

1.3.3.2. Modifications with biomolecules

In 1996, Mirkin's group and Alivisatos'group independently reported that AuNPs-DNA conjugates could serve as scaffolds for nanostructures.[128,129] The attachment of oligonucleotides onto the surface of a gold nanoparticle can be performed by simple adsorption[130] or via biotin-avidin linkage where the avidin is previously adsorbed onto the particle surface.[131,132]

The binding of streptavidin to biotin (*see* Figure 1.4A-C) as well as avidin has also been the subject of considerable fundamental and applied interest. This protein–ligand pair represents one of the strongest noncovalent affinities known. From the structure of the bound complex, it is known that the binding energy derives from multiple types of interactions between the protein and biotin.[133,134] Both streptavidin and avidin are the two homotetrameric proteins binding up to four molecules of biotin with an extraordinarily high affinity (Kd = 4 x 10^{-14} M for streptavidin and 6 x 10^{-16} M for avidin).[135] Streptavidin is isolated from *Streptomyces avidinii*, and avidin is a hen egg-white derived glycoprotein. Biotin is a small water-soluble vitamin, D-biotin (vitamin H).

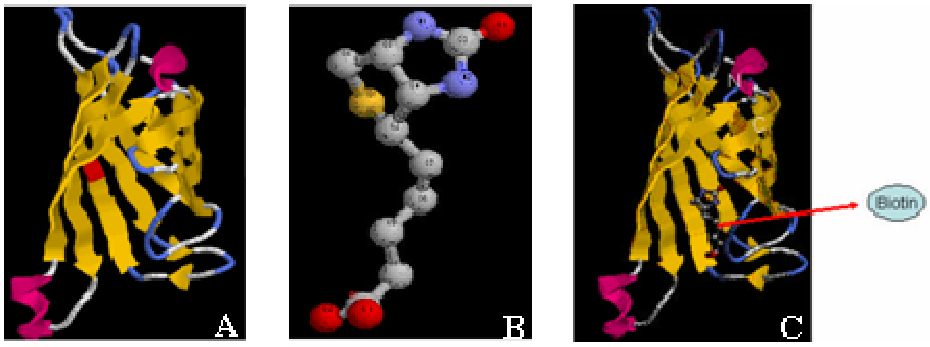

Figure 1.4. *Images of Streptavidin (A), structure of Biotin molecule ($C_{10}H_{16}N_2O_3S$) (B), and Streptavidin complex with Biotin ligand (C).*

However, the most commonly used method to attach oligonucleotides onto AuNPs is via thiol–gold bonds. Thiol-functionalized oligonucleotides stick strongly to gold surfaces.

The attachment via thiol linkage to nanocrystals is much stronger and more efficient than non-specific adsorption. Unfortunately, the number of oligonucleotides attached per nanoparticle cannot be directly controlled. However, gold nanocrystals with a controlled number of attached oligonucleotides can be isolated using gel electrophoresis.

Parak et al.,[136] Zanchet et al.,[137] as well as Park et al.,[138] employed gel electrophoresis to separated AuNPs modified with various densities of DNA, wherein the effective diameters of DNA-Au conjugates were derived from their relative gel mobilities as compared to the mobilities of bare AuNPs of different sizes. So far, the most widely used attachment scheme utilizes the covalent bond between thiol group on the 5′ or 3′ end of the oligo and gold nanoparticle, leaving the bases unobstructed for hybridization to its complement.[136-139]

DNA-functionalized AuNPs (DNA-AuNPs) have been widely used as important building blocks in nanotechnology and biosensing applications.[3,140] These DNA functionalized AuNPs can self-assemble into two- or three-dimensional superstructures,[141,142] and their aggregation causes shifts in plasmon bands that create high sensitivity for DNA sensing.[143] Because of the availability of many sites for DNA hybridization, a precise control over the number of hybridization events may sometimes be unfeasible, although AuNPs tethered with smaller numbers of DNA probes provide one mechanism by which to limit the number of hybridization events per particle.[137, 144-146]

These nanobioconjugates have been used in many areas such as diagnostics, therapeutics, sensors, and bioengineering.

Detection methods based on these nanobioconjugates show increased selectivity and sensitivity as compared with many conventional assays that rely on molecular probes.

1.3.3.3. Characterization techniques

− ***Optical characterization techniques of gold nanoparticles***

The development of scanning tunnelling microscopy (STM) and subsequently other scanning probe microscopy (SPM) such as atomic force microscopy (AFM) have opened up new possibilities for the characterization, measurement and manipulation of nanoparticles[147]. Combining with other techniques such as transmission electron microscopy (TEM)[97,148,149], high resolution transmission electron microscopy (HRTEM)[127], scanning electron microscopy (SEM), energy dispersive X-ray spectrometry (EDS), extended X-ray absorption fine-structure

(EXAFS)[149], Fourier transform infrared spectroscopy (FT-IR), reflection absorption infrared spectroscopy (RAIRS), fluorescent microscopy, X-ray difraction[150] and X-ray photoelectron spectroscopy (XPS) it is possible to study the nanoparticles to a great detail.

Inductively coupled plasma mass spectrometry (ICPMS) have been also used to detect gold nanoparticles.[151] UV-Vis spectra can also be used to determine the size and concentration of gold nanoparticles.[152]

- ***Electrochemical characterization techniques of gold nanoparticles***

Electrochemical techniques such as CV, differential pulse voltammetry (DPV), and chronoamperometry have shown to be appropriate for characterization of AuNPs.[148,150-155]

Stripping analysis is a powerful electroanalytical technique for trace metal measurements. Its remarkable sensitivity is attributed to the preconcentration step, during which the target metals are accumulated onto the WE.[17]

1.3.3.4. Applications in biosensors

The synthesis of AuNPs has received considerable interest due to their applications in a variety of fields: as catalysts[100,156,157,] electron microscopy markers[158,159], in nonlinear optical devices[160,161] or as biochemical labels or probes for detection and/or recognition of biomolecules[26,97,103-106] Recently the application areas of AuNPs are continuously growing up which have been reviewed by several authors.[3,78,162-164]

Some of these applications are described below.

– ***Labelling of biomolecules***

AuNPs have been successfully used as electroactive label in the detection of DNA sequences, based on the highly specific hybridization of complementary strands of DNA.[26,103-106,165,166]

Limoges et al.[103] developed a sensitive DNA sensor based on the labelling of oligonucleotide with 20 nm gold nanoparticles, and the sensor could detect the 406-base human cytomegalovirus DNA sequence at a concentration of 5 pM.

Dequaire et al.[105] reported an electrochemical metalloimmunoassay based on stripping voltammetric detection of a colloidal gold label. At this sandwich immunoassay the capture of the gold-labelled secondary antibody was carried out, followed by acid dissolution and anodic-stripping electrochemical measurement of the solubilized metal tracer. This protocol thus facilitated the detection of the target IgG protein down to the 3 picomolar level using a 35 mL sample volume.

– ***Enhancement of Electron Transfer***

The use of AuNPs in the construction of enzyme electrodes in order to enhance the electron transfer between the active centres of enzymes and electrodes acting as electron transfer mediators or electrical wires has been reported. Willner′s group[167] AuNPs were functionalized with N6-(2-aminoethyl)-flavin adenine dinucleotide, and then reconstituted with apo-glucose oxidase and assembled on a thiolated monolayer associated with a gold electrode. Alternatively, the functionalized AuNPs could be first assembled on the electrode, and apoglucose oxidase was reconstituted subsequently. The resulting enzyme electrode exhibited very fast electron transfer between the enzyme redox centre and the electrode with the help

of the AuNPs, and the electron transfer rate constant was found to be about 5000 s^{-1}, which is about seven times faster than that between glucose oxidase and its natural substrate, oxygen.

Wang et al.[168] self assembled AuNPs onto a three-dimensional silica gel network modified gold electrode, and obtained the direct electrochemistry of cytochrome c. These AuNPs acted as a bridge to electron transfer between protein and electrode.

– ***Catalysis of Electrochemical Reactions***

Many nanoparticles, especially metal nanoparticles such as AuNPs have excellent catalytic properties. The introduction of NPs with catalytic properties into electrochemical sensors and biosensors can decrease overpotentials of many analytically important electrochemical reactions, and even make possible the reversibility of some redox reactions, which are irreversible at common unmodified electrodes.

Ohsaka et al.[169] developed an electrochemical sensor for selective detection of dopamine in presence of ascorbic acid, which was based on the catalytic effect of AuNPs on the ascorbic acid (AA) oxidation. The oxidation potential of AA is shifted to less positive potential due to the high catalytic activity of Au nanoparticle.

1.3.4. Other nanoparticles: Quantum dots

QDs are made from inorganic colloidal semiconductors. They are single crystals, a few nanometers in diameter whose size and form can be precisely controlled by the duration temperature and ligand molecules used in the synthesis. Grieve et al.[90]

summarized recent work on the synthesis, characterisation and potential applications of QDs. Nanocrystal QDs are semiconductor materials where electrons are confined, yielding narrow, tunable, and highly stable photoluminescence compared to organic dyes.[170] QDs have shown great promise as biolabelling of DNA[111], protein[112], and cells.[171]

There are interesting studies on QDs conjugated with biomolecules as novel probes.[112,116,172] These nanometer-sized conjugates are water soluble and biocompatible, and provide important advantages over organic dyes and lanthanide probes.

Sapsford et al.[173] reported a review, at which they examine the progress in adapting QDs for various biosensing applications including use in immunoassays, as generalized probes, in nucleic acid detection and fluorescence resonance energy transfer (FRET) - based sensing. They also describe several important considerations when working with QDs mainly centred on the choice of material(s) and appropriate strategies for attaching biomolecules to the QDs.

Wang's group demonstrated the use of different inorganic-nanocrystal tracers for a multi-target electronic detection of DNA[174] or proteins.[175] (*See* Figure 1.5)

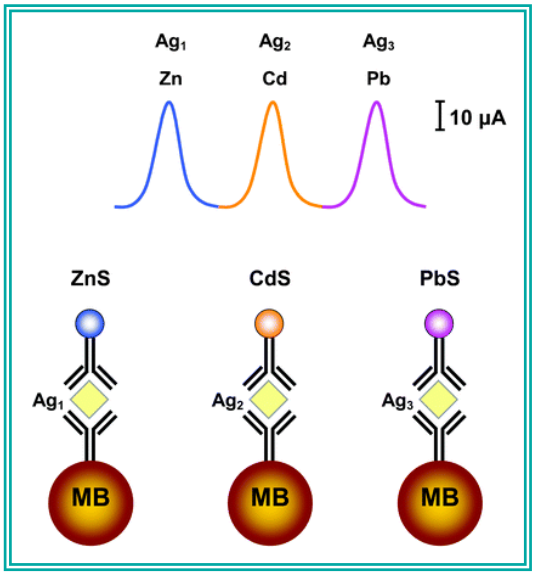

Figure 1.5. *Multi-antigen sandwich immunoassay protocol based on different inorganic-colloid (QDs) nanocrystal tracers.*[175]

Recently Wang et al.[176] reported a review which gives an overview of the emerging use of QDs in analysis.

1.4. DNA Analysis

1.4.1. DNA fundamentals

The nucleic acids, deoxyribonucleic acid (DNA) and ribonucleic acid (RNA) are polymers of nucleotides. They store and transmit genetic information. Both DNA and RNA contain two major purine bases, **adenine** (A), and **guanine** (G), and two major pyrimidines. In both DNA and RNA one of the pyrimidines is **cytosine** (C), but the second major pyrimidine is thymine (T) in DNA and uracil (U) in RNA. Only rarely does thymine occur in RNA or uracil in DNA.[177] The structures of the five major bases are shown in Figure 1.6.

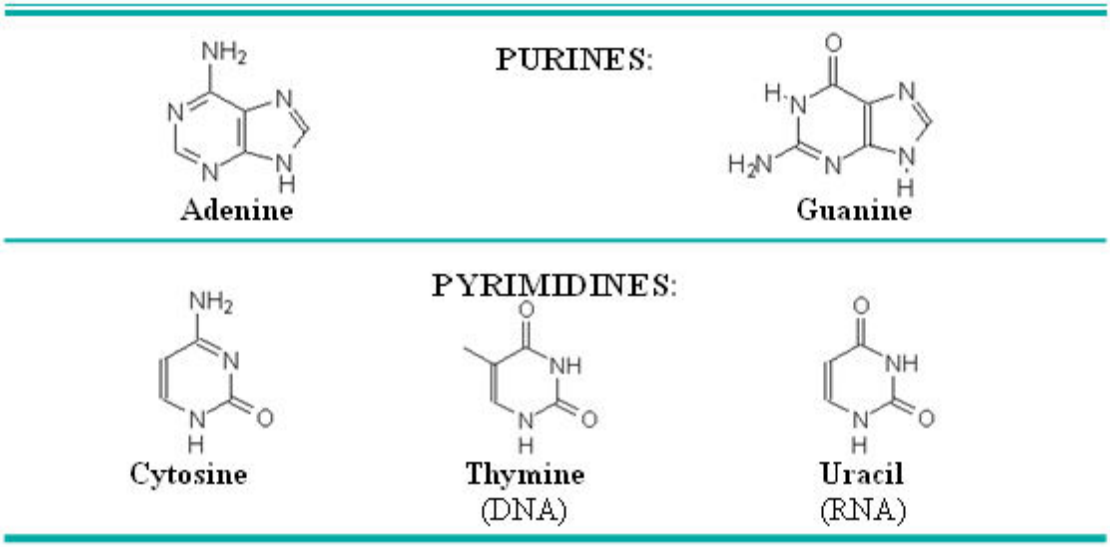

Figure 1.6. *Major purines and pyrimidines from which nucleic acids are built.*

Nucleic acids have two kinds of pentoses. The recurring deoxyribonucleotide units of DNA contain 2′deoxy-D-ribose, and the robonucleotide units of RNA contain D-ribose. In nucleotides, both types of pentoses are in their β-furanose (closed five-membered ring form). Figure 1.7 shows the corresponding structures.

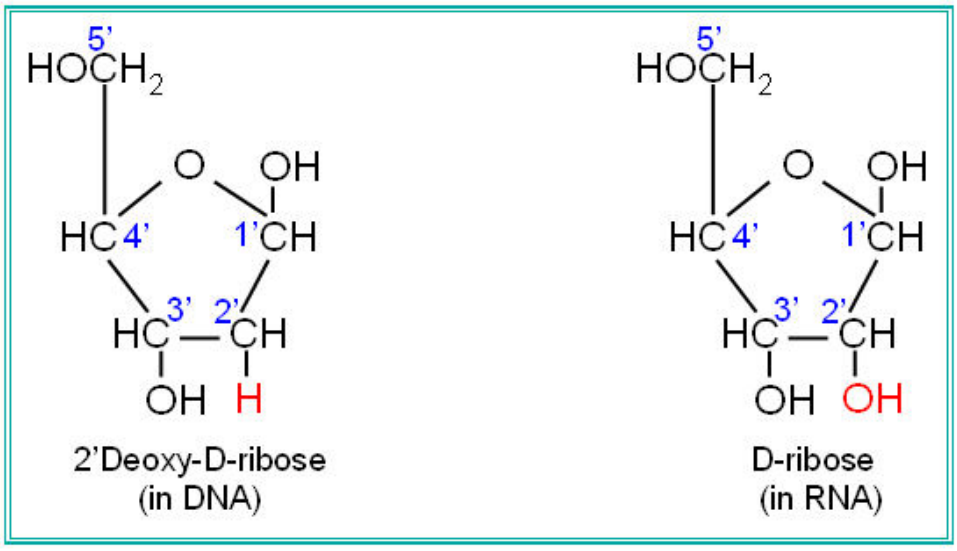

Figure 1.7. *Chemical structure of pentose which contains five carbon atoms, labelled as C1′ to C5′. The pentose is called* ***ribose*** *in RNA and* ***deoxiribose*** *in DNA because the DNA's pentose lacks an oxygen atom at C2′.*

A nucleotide is composed of three parts: pentose, base and phosphate group (*see* Figure 1.8).

In DNA or RNA, a pentose is associated with only one phosphate group, but a cellular free nucleotide (such as ATP) may contain more than one phosphate group. If all phosphate groups are removed, a nucleotide becomes a nucleoside.

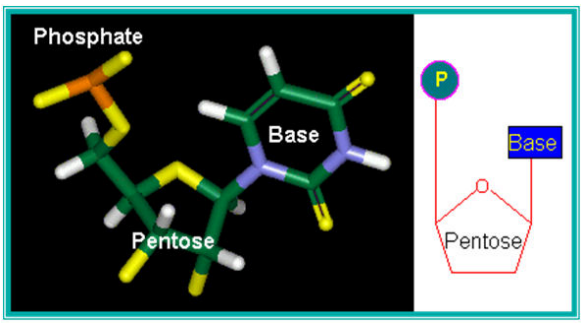

Figure 1.8. *The general structure of nucleotides. Left: computer model. Right: a simplified representation.*

The successive nucleotides of both DNA and RNA are covalently linked through phosphate-group "bridges," in which the 5′-hydroxyl group of one nucleotide unit is joined to the 3′-hydroxyl group of the next nucleotide by a phosphodiester linkage (*see* Figure 1.9). Thus the covalent backbones of nucleic acids consist of alternating phosphate and pentose residues, and the nitrogenous bases may be regarded as side groups joined to the backbone at regular intervals.[177]

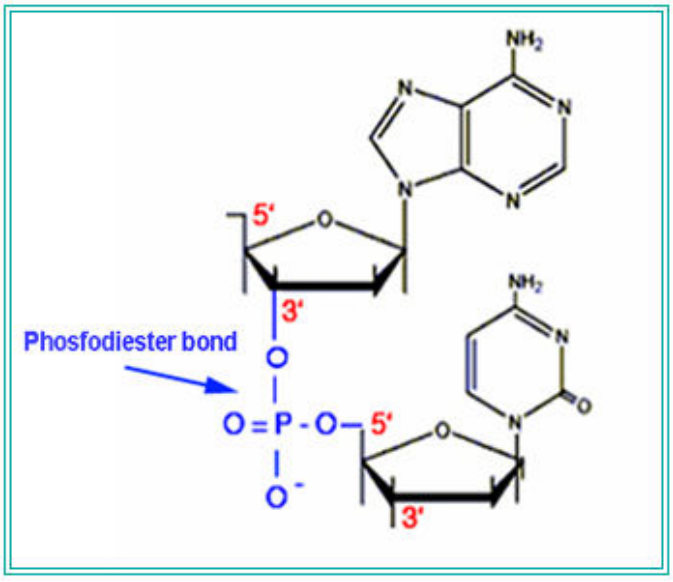

Figure 1.9. *Phosphodiester bond in the covalent backbone of DNA and RNA. The phosphodiester bonds link successive nucleotide units. A nucleotide is about 0.34 nm long.*

1.4.1.1. DNA structure

Watson and Crick's description, in 1953, of the double helical structure of the DNA molecule opened the door to a new era in biological understanding and research. Scientists, now knowing the molecular structure of the hereditary molecule, could begin both to elucidate and to manipulate its function.

DNA is the basic building block of life. Hereditary information is encoded in the chemical language of DNA and reproduced in all cells of living organisms. DNA consists of two long, twisted chains made up of nucleotides.[178] Each nucleotide contains one base (A, T, C or G), one phosphate molecule, and the sugar molecule deoxyribose[177] (*see* Figure 1.10). The double stranded helical structure of DNA is key for its use in self-assembly applications.

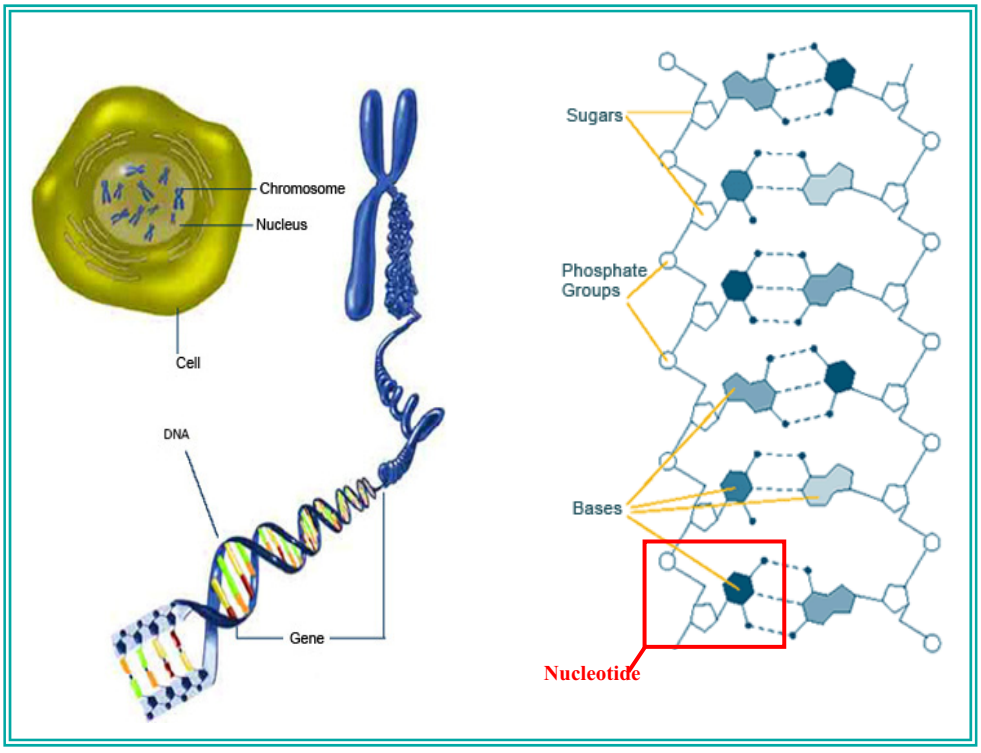

Figure 1.10. *Left: the long, stringy DNA that makes up genes is spooled within chromosomes inside the nucleus of a cell. Right: DNA is a double-stranded molecule twisted into a helix. Each strand, comprised of a sugar-phosphate backbone and attached bases, is connected to a complementary strand by hydrogen bonding between paired bases. The bases are adenine (A), thymine (T), cytosine (C) and guanine (G). At red square a nucleotide.*

The specific binding through hydrogen bonds between A and T, and C and G can result in the joining of two complementary single-stranded DNA to form a double-stranded DNA (*See* Figure 1.11).

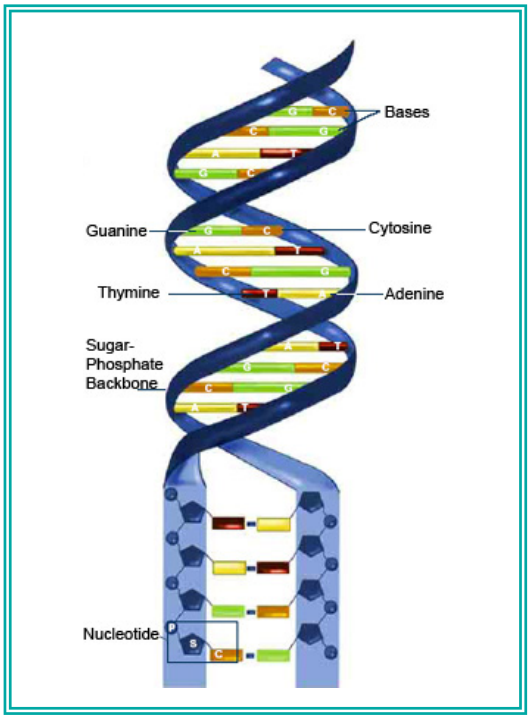

Figure 1.11. *Illustration of the double helical structure of the DNA molecule.*

There are two hydrogen bonds between A-T pairs and three hydrogen bonds between G-C pairs. (*See* Figure 1.12)

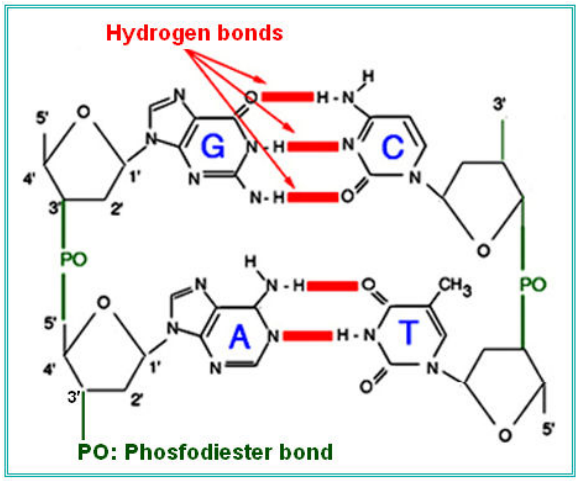

Figure 1.12. *A crucial property of the purines and pyrimidines is their ability to form hydrogen-bonded pairs (red colour) composed of one purine and one pyrimidine, such as guanine-cytosine (G-C), above and adenine-thymine (A-T), below.*

The phosphate ion carries a negative charge in the DNA molecule, which results in electrostatic repulsion of the two strands. In order to keep the two strands together, positive ions must be present in the solution to keep the negative charges neutralized.

1.4.1.2. DNA hybridization

The joining of two complementary single strands of DNA through hydrogen bonding to form a double-stranded DNA is called hybridization.[178] If a double-stranded DNA is heated above a certain temperature, the two strands will start to dehybridze and eventually separate into single strands. The center temperature of this transition is called the melting temperature, T_m, which is a sensitive function of environmental conditions such as ionic strength, pH, and solvent conditions. As the temperature is reduced, the two strands will eventually come together by diffusion and rehybridize to form the double stranded structure.[178] Similar hybridization reactions can occur between any single stranded nucleic acid chains: DNA/DNA, RNA/RNA, and DNA/RNA. These hybridization reactions can be used to detect and characterize nucleotide sequences using a particular nucleotide sequence as a probe. (*See* Figure 1.13)

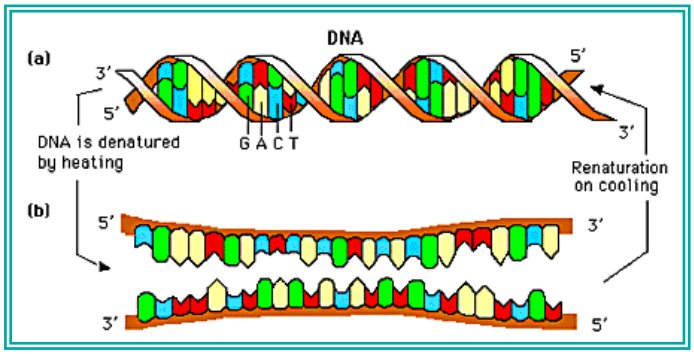

Figure 1.13. *The two strands of a DNA molecule are denatured by heating to about 100 °C = 212 °F (a to b). At this temperature, the complementary base pairs that hold the double helix strands together are disrupted and the helix rapidly dissociates into two single strands. The DNA denaturation is reversible by keeping the two single stands of DNA for a prolonged period at 65 °C = 149 °F (b to a). This process is called DNA renaturation or hybridization.*

1.4.2. DNA sensors

DNA biosensors represent a very important class of affinity biosensor in which the biorecognition molecules are oligonucleotides of known sequence and the recognition event is the hybridization with the complementary sequences.

Among the various types of DNA sensors, the electrochemical sensor has some advantage such as the use of very simple equipment to perform measurements, low cost and possibility of miniaturization in order to obtain high density arrays.

DNA biosensors based on DNA hybridization plays a more and more important role in DNA analysis.

1.4.3. Probe immobilization and characterization

One of the most important steps in the development of a DNA biosensor is the method used to immobilize the DNA (bioreceptor) on the transducer surface. A typical DNA biosensor (genosensor) is designed by the immobilization of a single stranded (ss) oligonucleotide (probe) on a transducer surface to recognize its complementary (target) DNA sequence via hybridization.[179] DNA has to be immobilized in a way that the bases remain available for further biorecognition of the complementary strand. In this sense, the nature of the electrode plays a very important role. In effect, depending on the compromise of the bases in the interaction with the electrode surface they could be or not be accessible for the double helix formation.[180]

The most relevant DNA immobilization approaches are:

1.4.3.1. Entrapment in a polymeric matrix

At this method the oligonucleotide can be retained in a matrix such as agar gel, polyacrilamide, or polypyrolle (PPy), which has been previously immobilized on a solid support. The matrix has a mesh size effective characterized by their large area of adsorption, which increases the amount of oligonucleotide strand attached, improving the sensitivity of the resulting system. The main disadvantage is the lack of oligonucleotide orientation, which decreases the accessibility to the captured molecule.

Pividori et al.[181] immobilized DNA target by its adsorption onto a nylon membrane.

Li et al. used a polylactic acid nanofiber membrane as a substrate for oligonucleotide assemblies.[182]

Recently, Vivek et al.[183] reported the possibility of immobilizing biomolecules on sol-gel matrices. Presently, sol-gel chemistry offers new and interesting possibilities for the promising encapsulation of heat-sensitive and fragile biomolecules (enzyme, protein, antibody and whole cells of plant, animal and microbes).

1.4.3.2. Covalent binding

The oligonucleotide is immobilized via covalent chemical bonds between the transducer and a functional group of the DNA, onto derivatized surfaces (glassy carbon or carbon paste modified electrodes and PPy, platinum or gold surfaces) or crosslinking where a bifunctional agent is used to bond chemically the transducer to

the oligonucleotide or by means of spacers such as glutaraldehyde, carbodiimide or a self-assembled monolayer of bifunctional silanes.

DNA molecule can be directly immobilized via the amino groups of its guanine nucleobases, its 50-phosphate groups, modified amino groups, or modified carboxylate groups binding with functionalized surface by cross-linking reaction.[184]

1.4.3.3. Adsorption

This method is based on the direct adsorption of DNA on the substrate such as nitrocellulose, nylon membranes, polystyrene, metal surfaces and carbon.

Adsorption mechanisms are generally categorized as either physical adsorption[9,185] which is carried out by soaking the surface with the solution that needs to be immobilised and leaving the surface to dry or electrochemical adsorption which uses the fact that the DNA backbone is negatively charged[186], so that a positive potential applied to an electrode attracts these biomolecules.

Adsorption has the advantages of its ease of operation and it does not require other reagents or any special nucleic acid modification but its principal disadvantage is the variability of the nucleic acid layer due to distortion of the molecule by adsorption and consequently the poor hybridization efficiency.

Arora et al.[9] reported the application of physically adsorbed double stranded calf thymus DNA (CT-dsDNA) onto polypyrrole-polyvinyl sulfonate (PPy–PVS) film coated onto ITO glass plate for sensing o-chlorophenol (OCP) and 2-aminoanthracene (2-AA) present in water and waste water samples.

1.4.3.4. Self-assembling monolayer

Self-assembling monolayer (SAM) of thiolated oligonucleotides or regular oligonucleotides.[179,187,188] is formed by spontaneous adsorption or chemical binding of molecules from a homogeneous solution onto a substrate. Most reports have immobilized DNA in the form of a SAM onto a gold surface using thiol chemistry.[179] SAM of terminally-thio-labeled oligonucleotides onto gold surfaces offers a direct method of chemisorption of DNA probes onto transducer surfaces based on the formation of gold-thiol bonds.[189]

The most widely used SAM in DNA immobilization is made by the adsorption of sulphur-based compounds such as thiols, disulphides or sulphide on glass or a metal surface such as gold, silver, palladium, copper and platinum. A mixed SAM consisting of single-stranded oligonucleotide (ssDNA)- and oligo(ethylene glycol) (OEG)-terminated thiol, was reported by Boozer et al.[190,191]

A sensor for detecting hepatitis B virus (HBV) DNA was prepared by immobilization of HBV-DNA fragments amplified by polymerase chain reaction (PCR) on a gold surface modified with a monolayer of thioglycolic acid (TGA) via carboxylate ester formation between the 30-hydroxy end of the DNA and the carboxyl residues of the TGA.[192] Once the thiolated monolayer was formed, the electrode was immersed in a solution containing the probe and (1-ethyl-3-(3-dimethylaminopropyl)carbodiimide for 1 h.

1.4.3.5. Affinity interactions

Streptavidin and avidin are of the most stable proteins known. Its properties along with the ability of biotin to be incorporated easily into various biological

materials, allow streptavidin to serve as a versatile, powerful affinity tag in a variety of biological applications.[193]

Due to the strong binding between streptavidin/avidin and biotin, the both have been the most widely used affinity interaction in ssDNA immobilization.[135,194]

Tetramer binding is formed between streptavidin and biotin, resulting in a very high affinity bond, with stability as high as a covalent bond. Because of this strong interaction, the complex formation is nearly unaffected by extreme conditions of pH or temperature, organic solvents, and denaturing agent. However, the presence of the large protein layer may results to non-specific binding sites and compromise the sensitivity and selectivity of certain types of sensors.[195] The effect of biotin binding on streptavidin structure and stability was studied by González et al.[196]

Mir and Katakis proposed the use of competitive displacement of labelled probes and they immobilized the biotin-capture probe through a biotin–streptavidin linkage.[197]

The avidin–biotin system also has become a “universal” tool in most of the fields of the biological sciences. The avidin–biotin system can contribute to the interaction between any two biomolecules in an indirect manner. Biotin can be chemically coupled to a binder molecule (e.g., a protein, DNA, hormone, etc.) without disturbing the interaction with its target molecule.[198]

1.4.3.6. Entrapment into a composite

In this method, the oligonucleotide is immobilized by mixing mineral oil and graphite powder and with this conductimetric paste the biosensor is constructed. This method does not require the modification of the oligonucleotide, however there

is a limited accessibility to the capture probe for the hybridization of the oligonucleotide target.[199]

DNA immobilization can be characterized by several means such as CV, TEM, AFM[200], QCM[201], SERS[202], fluorescence spectroscopy[201], SPR[201,203], EIS[204], etc.

Cho et al.[201] characterized the immobilization of thiol-modified oligomers on Au surfaces and subsequent hybridization with a perfectly matched or single-base mismatched target using a QCM and fluorescence spectroscopy.

SERS studies of self-assembled DNA monolayer – characterization of adsorption orientation of oligonucleotide probes and their hybridized helices on gold substrate were reported by Dong et al.[202]

1.4.4. Hybridization detection and amplification in DNA sensors

1.4.4.1. Hybridization detection techniques

The conventional methods for detection of specific gene sequences are based on hybridization, polymerase chain reaction (PCR), Southern blotting and various chemical methods. These expensive, time-consuming techniques require expertise and lengthy sample preparations.

To overcome these difficulties several researchers have reported DNA biosensors based on DNA probe immobilized onto a suitable matrix coupled to a physical transducer (optical, piezoelectric or electrochemical) that in turn generates a signal upon hybridization event occurring.

Development of nucleic acid-based detection systems is the main focus of many research groups and high technology companies. The enormous work done in this

field is particularly due to the broad versatility and variety of these sensing devices. From optical to electrical systems, from label-dependent to label-free approaches, from single to multi-analyte and array formats, this wide range of possibilities makes the research field very diversified and competitive.

The detection of DNA hybridization is of significant scientific and technological importance; consequently, a great variety of methods have been developed, including optical, piezoelectric, and electrochemical.

– ***Optical***

The most frequently used is the fluorescence transduction in which the oligonucleotides are labelled with fluorophores but also others kinds of optical methods can be used as transducers in DNA sensors such as colorimetry, chemiluminescence and SPR.

Mirkin[205] and Letsinger[206] one of the pioneers in the research into nanoparticle based biosensors, developed a methodology relied on the very simple principle that the optical properties of AuNPs is highly dependent on the size and structure of the particles. When 3 nm AuNPs are free floating in a solution the colour of this solution will be red, but if the nanoparticles are clustered the Plasmon resonance frequency will change, and thus changing the colour of the solution from red to blue. Mirkin and Letsinger used this principle to design a relatively simple DNA detection approach.

Nakamura et al.[207] developed the hybridization sandwich type of a target DNA using the DNA-AuNPs on a DNA self-assembled monolayer (DNA-SAM), was monitored *in situ* by SPR imaging in order to enhance the hybridization signal. SPR

imaging results strongly indicate that the hybridization signal is enhanced several times compared to the case of target DNA hybridization.

A wide range of different optical transducers for DNA sensors has been reported.[208-210]

– ***Piezoelectric***

The piezoelectric transducer has the advantage of high sensitivity without requiring any labelling of the interacting components. The most widely used piezoelectric readout is the QCM, which measures mass by detecting the change in frequency of a piezoelectric quartz crystal when it is disturbed by the addition of a small mass such as oligonucleotide strand.

Liu et al.[211] carried out the detection of DNA hybridization by QCM on a platinum quartz crystal modified with ssDNA probe immobilized on AuNPs. The acoustic is other alternative piezoelectric transducer which is also used for the detection of DNA hybridization.[212,213]

– ***Electrochemical***

Whereas optical detection methods with fluorescent dyes have dominated the DNA sensor industry and piezoelectric techniques can achieve low detection limits, the application of electrochemical methods can provide the significant advantages previously mentioned (*see* section 1.2.1.), including compatibility with microfabrication technology.[37,188,214-217] Electrochemical techniques broadly used for sensor transduction are voltammetry, amperometry and impedance spectroscopy. To know more details about the basic different pathways for

electrochemical detection of DNA hybridization *see* publication III (at chapter 7). Fewer of examples using potentiometry and conductimetry have been reported.

Nowadays, the most widely used techniques in the detection of DNA hybridization are based on metal nanoparticles labelling, particularly AuNPs as well as QDs (CdS, PbS, ZnS, CdSe, ZnSe, CdTe etc.)[93,173]

Wang et al.[104], one of the pioneers in the research of nanoparticle based biosensors, developed an approach using AuNPs combined with magnetic beads in a DNA hybridization electrochemical detection in which a biotinylated DNA probe was immobilized on a streptavidin coated magnetic bead and then a biotinylated target was captured by the probe, and labelled via a subsequent binding of streptavidin coated AuNPs. The AuNPs were detected down to a level of 4 nM using stripping voltammetry.

Further, similar approaches have been reported by different research groups.[103, 165,166]

Figure 1.14 shows a schematic of the most important strategies used to integrate AuNPs in DNA detection systems. *See* publication V (at chapter 7) in order to know more details.

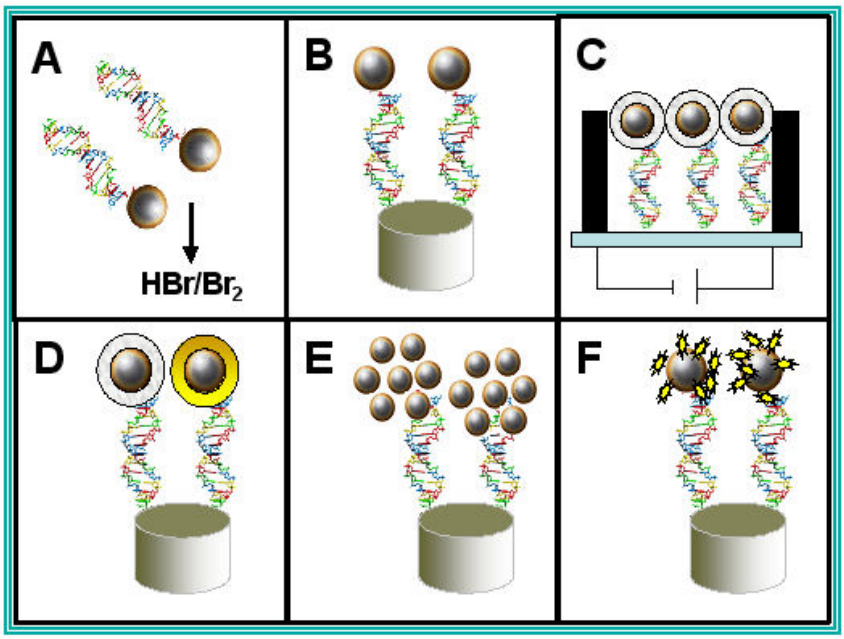

Figure 1.14. *Schematic (not in scale) of the different strategies used for the integration of gold nanoparticles (AuNPs) into DNA sensing systems: (A) Previous dissolving of AuNP by using HBr/Br₂ mixture followed by Au(III) ions detection; (B) Direct detection of AuNPs anchored onto the surface of the genosensor; (C) Silver enhancement using conductometric detection (D) Enhancement with silver or gold followed by detection; E) AuNPs as carriers of other AuNPs; F) AuNPs as carriers of other electroactive labels.*

Wang et al.[174] also developed a method for simultaneous analysis of different DNA targets at which three different DNA probe-modified magnetic beads hybridized with different DNA targets, and then a second hybridization with the labeled probe with different QDs, (ZnS, CdS and PbS). Stripping voltammetry of the metal ions resulting from the dissolution of the semiconductor nanoparticles yielded well defined and resolved stripping peaks at -1.12 V (Zn), -0.68 V (Cd) and -0.53 V (Pb) (vs. Ag/AgCl).

1.4.4.2. Amplification systems

The technologies used in recently reported DNA hybridization devices include AuNPs, enzyme-amplification, electrocatalysis, conducting polymers, surfactant

bilayers, surface-attached molecular beacons and ferrocene-labeled signaling probes.

A hybridization signal-amplified method, based on gold-nanoparticle-supported DNA sequences for electrochemical DNA sensors was reported by Zhang et al.[218] Thiol-tethered target oligonucleotides were assembled on the surface of AuNPs by means of sulphur–gold bonds, and then hybridized by complementary sequences immobilized on the electrode surface. $[Co(phen)_3]^{3+/2+}$ bonded to DNA molecules by both electrostatic and intercalative interactions were used as an indicator for hybridization detection.[218]

New electrochemical materials and modified substrates used as electrochemical transducers have also been explored to improve the sensitivity of DNA sensing.[219,220]

1.5. Protein Analysis

1.5.1. Antibodies fundamentals

Immunology involves a complex network of interacting molecules and cells that function to recognize and respond to foreign agents. It also has wide-ranging implications for the pharmaceutical, health-care and biotechnology industries.

All vertebrates have an immune system capable of distinguishing molecular “self” from “nonself” and then destroying those entities identified as nonself. In this way, the immune system eliminates viruses, bacteria, and other pathogens and molecules that may pose a threat to the organism. On a physiological level, the

response of the immune system to an invader is an intricate and coordinated set of interactions among many classes of proteins, molecules and cell types.

The immune response consists of two complementary systems, the humoral which is directed at bacterial infections and extracellular viruses (those found in the body fluids), but can also respond to individual proteins introduced into the organism, and cellular immune systems which destroys host cell infected by viruses and also destroys some parasites and foreign tissues. The proteins at the heart of the humoral immune response are soluble proteins called antibodies or immunoglobulins, (abbreviated as Ig).[177]

There are five antibody classes, with a distinctive structure and function. The five antibody classes are IgG, IgE, IgD IgM and IgA. The type of heavy chain of the molecule determines the immunoglobulin isotype (γ, ε, δ, μ, α, respectively).[177,221] IgE and IgD have similar structure of IgG. IgM occurs in either a monomeric, membrane-bound form or a sectreted form that is a cross-linked pentamer (or occasionally hexamers) of this basic structure. IgA, can be a monomer, dimmer, or trimer. (*See* Figure 1.15)

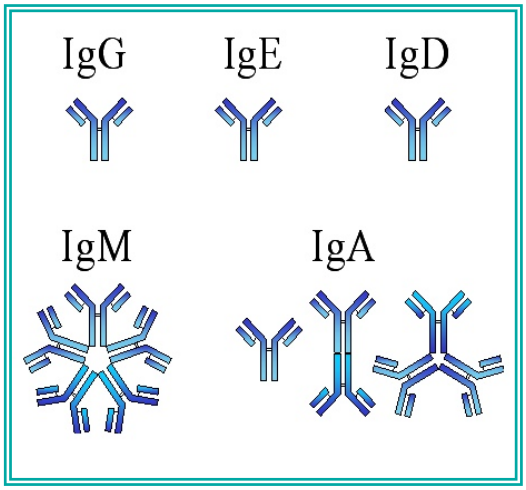

Figure 1.15. *Structures of different Immunoglobulin classes*

1.5.1.1. Antibody structure

Antibodies or Igs are composed of four polypeptide chains: two "light" (L) chains (lambda or kappa), and two "heavy" (H) chains (alpha, delta, gamma, epsilon or mu) joined to form a "Y" shaped molecule. L chains are composed of 220 amino acid residues while H chains are composed of 440-550 amino acids. Each chain has "constant" and "variable" regions (domains) as shown in the Figure 1.16. Variable domains are contained within the amino (NH_2) terminal end of the polypeptide chain (amino acids 1-110). When comparing one antibody to another, these amino acid sequences are quite distinct.

Constant regions or domains comprising amino acids 111-220 (or 440-550) are rather uniform in comparison from one antibody to another within the same isotype. "Hypervariable" regions or "Complementarity Determining Regions" (CDRs) are found within the variable regions of both the heavy and light chains. These regions or domains serve to recognize and bind specifically to antigen. The four polypeptide chains are held together by covalent disulfide (-S-S) bonds.[177,222] (*See* Figure 1.16)

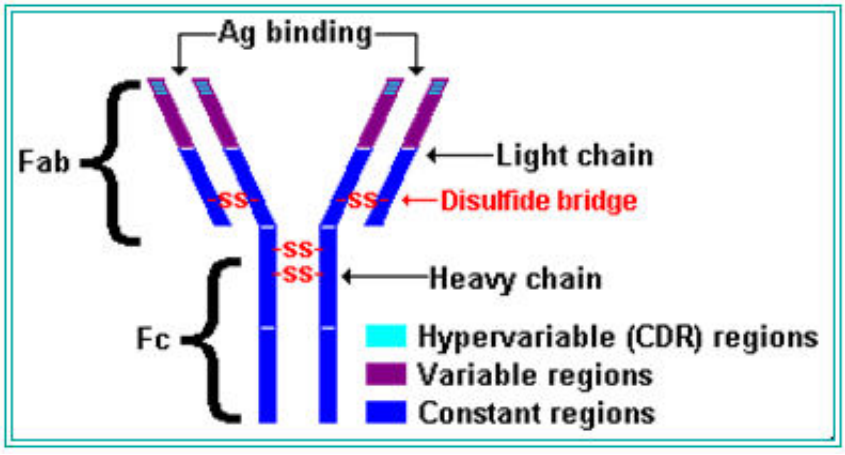

Figure 1.16. *Illustration of antibody general structure.*

IgG is the major class of antibody molecule and one of the most abundant proteins in the blood serum as well as also the most commonly used antibody in sensor applications. (*See* Figure 1.17.)

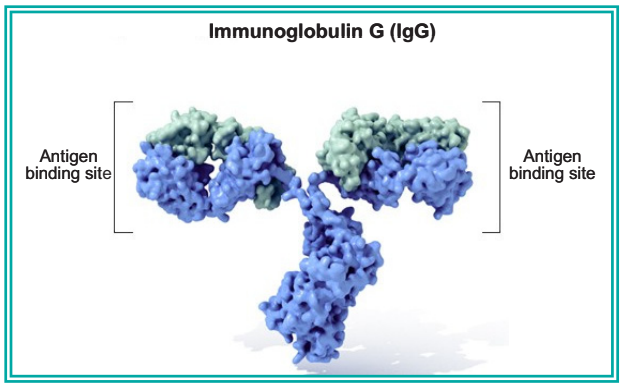

Figure 1.17. *Illustration IgG structure*

At its structure two antigen-binding sites are formed by the combination of variable domains from one light (V_L) and one heavy (V_H) chain. (*see* Figures 1.17 and 1.18.) Cleavage with papain separates the Fab and Fc portions of the protein in the hinge region. The Fc portion of the molecule also contains bound carbohydrate. Most antibody molecules contain a flexible hinge region where the two Fab regions join the Fc region. (*See* Figure 1.18)

The most important biological activities of antibodies are related to their effector functions, aimed at inactivation or removal of infectious agents and their products (e.g. bacteria, viruses, and toxins).

Antibodies of the IgG class exert two major effector functions: activation of complement and opsonisation (i.e. the induction of phagocytosis). These effectors functions, mediated via the (constant) Fc fragment are induced as a result of interaction of the antibody with its antigen via the (variable) Fab moiety.

Several studies that demonstrate effector functions of the antibodies have been reported.[223,224]

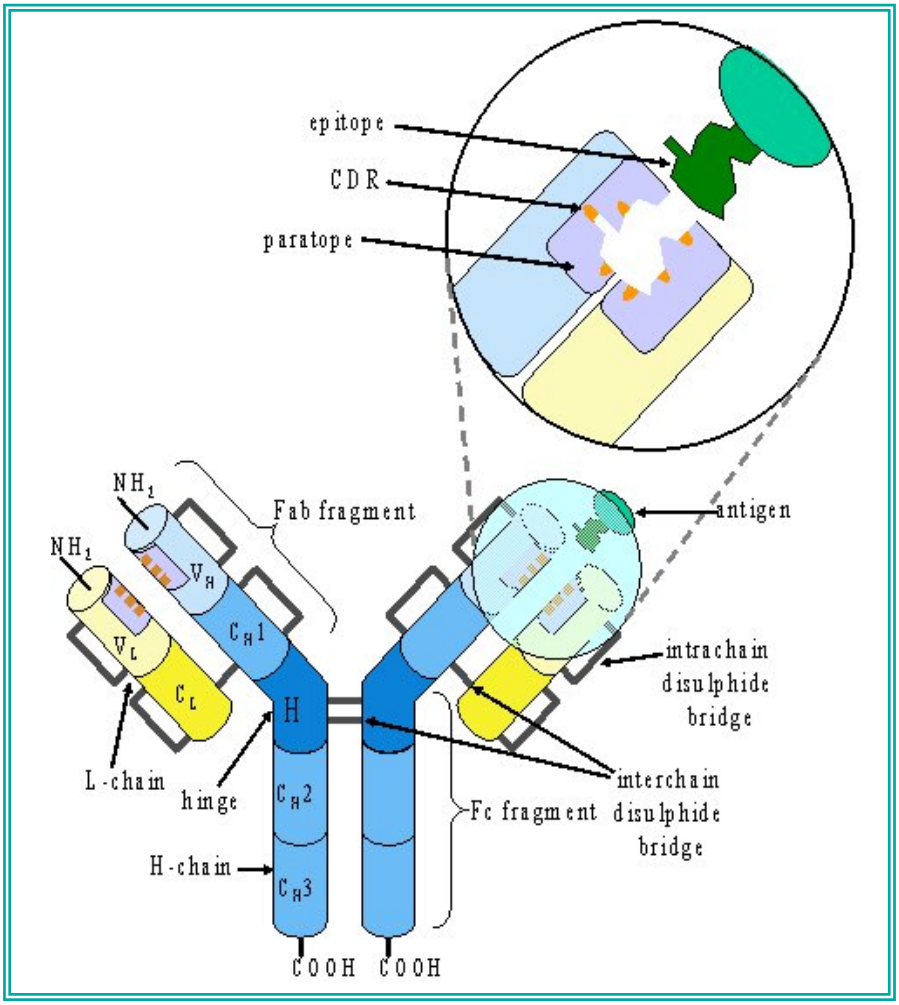

Figure 1.18. *Detailed structure of IgG.*

Immunoglobulin fragments produced by proteolytic digestion have proven to be very useful in elucidating structure/function relationships Igs:

– **Fab**. Digestion with papain breaks the immunoglobulin molecule in the hinge region before the H-H inter-chain disulfide bond. (*see* Figure 1.18.) This results in the formation of two identical fragments that contain the light chain and the V_H and C_H1 domains of the heavy chain. These fragments were called the Fab fragments because they contained the antigen binding sites of the antibody. Each

Fab fragment is monovalent whereas the original molecule was divalent. The combining site of the antibody is created by both V_H and V_L. An antibody is able to bind a particular antigenic determinant because it has a particular combination of V_H and V_L. Different combinations of a V_H and V_L result in antibodies that can bind a different antigenic determinant.

- **Fc** Digestion with papain also produces a fragment that contains the remainder of the two heavy chains each containing a C_H2 and C_H3 domain. This fragment was called Fc because it was easily crystallized. (*see* Figure 1.18) The effector functions of Igs are mediated by this part of the molecule. Different functions are mediated by the different domains in this fragment. Normally the ability of an antibody to carry out an effector function requires the prior binding of an antigen; however, there are exceptions to this rule.
- **$F(ab')_2$.** Treatment of immunoglobulins with pepsin results in cleavage of the heavy chain after the H-H inter-chain disulfide bonds resulting in a fragment that contains both antigen binding sites. This fragment was called $F(ab')_2$ because it was divalent.

  The Fc region of the molecule is digested into small peptides by pepsin. The $F(ab')_2$ binds antigen but it does not mediate the effector functions of antibodies.

1.5.1.2. Antibody-Antigen interaction

Antibodies or Ig are specialized immune proteins (glycoproteins), produced because of the introduction of an antigen into the body, and which possesses the remarkable ability to combine with the very antigen that triggered its production. So, antigen is any foreign substance that stimulates the body's immune system to

produce antibodies. Most antigens are macromolecules: proteins, polysaccharides, even DNA and RNA.

The main advantage of antibodies is their specificity directed against an antigen. (*see* Figure 1.19) The immune system of the humans generates over 10^8 different antibodies with distinct binding specifities.[222]

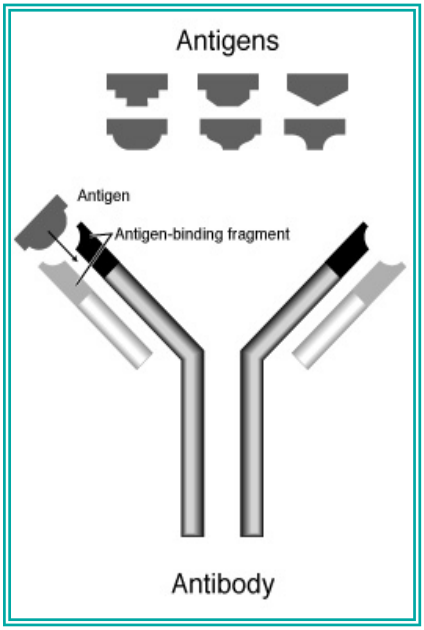

Figure 1.19. *Specificity Ab-Ag interaction*

The binding specificity of an antibody is determined by the amino acid residues in the variable domains of its H and L chains. (*See* Figure 1.20)

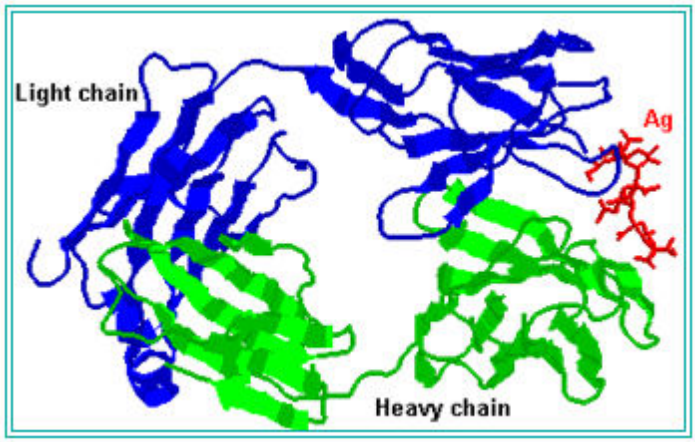

Figure 1.20. *Antigen binding within Fab fragment.*

Several different types of chemical bonds may be involved in Ab-Ag binding.- The interaction occurs by noncovalent forces (like that between enzyme and their substrate) between the antigen-combining site on the antibody called **paratope** and a portion of the antigen called the **antigenic determinant** or **epitope**. (*See* Figure 1.18)

A typical antibody-antigen interaction is quite strong, characterized by K_d values as low as 10^{-10}_M. The bonds that hold the antigen to the antibody combining site are all non-covalent in nature. These include hydrogen bonds (*see* Figure 1.21), electrostatic bonds, Van der Waals forces and hydrophobic bonds.

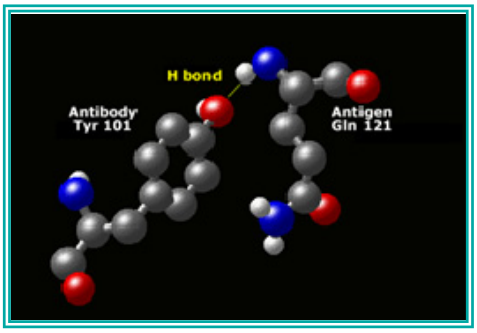

Figure 1.21. *Close-up of a hydrogen bond − The Tyr 101 of the antibody forms a hydrogen bond with the Gln 121 of the antigen.*

Multiple bonding between the antigen and the antibody ensures that the antigen will be bound tightly to the antibody. The K_d reflects the energy derived from the various bonding that stabilize the binding. Since antigen-antibody reactions occur via non-covalent bonds, they are by their nature reversible.

The extraordinary binding affinity and specificity of antibodies makes them valuable analytical reagents. Two types of antibody preparations are in use:

– **Polyclonal antibodies**

Policlonal antibodies are those produced by many different B-lymphocytes responding to one antigen, such as a protein injected into an animal. Cells in the population of B lymphocytes produce antibodies that bind specific, different epitopes within the antigen. Thus, polyclonal preparations contain a mixture of antibodies that recognize different parts of the protein.

– **Monoclonal antibodies**

In contrast, monoclonal antibodies are synthesized by a population of identical B cells (a clone) grown in cell culture. These antibodies are homogeneous, all recognizing the same epitope. The techniques for producing monoclonal antibodies were developed by Georges Köhlerl and Cesar Milstein in 1975.[177]

The specificity of antibodies has practical uses. An antibody is attached to a label or some other reagent that makes it easy to detect.

When the antibody binds the target protein, the label reveals the presence of the protein in a solution or its location in a gel or even a living cell.

1.5.2. Immunosensors

Immunosensors are affinity ligand-based biosensors in which the immunochemical reaction is coupled to a transducer[225]. These biosensors use antibodies as the biospecific sensing element, and are based on the ability of an antibody to form complexes with the corresponding antigen.[226]

Immunoassays are among the most specific of the analytical techniques. They provide extremely low detection limits, and can be used for a wide range of

substances. As research moves into the era of proteomic, such assays become extremely useful for identifying and quantifying proteins.

Immunosensors are based on immunological reactions involving the shape recognition of the Ag by the Ab binding site to form the Ab/Ag stable complex:

$$Ab + Ag \leftrightarrow AbAg$$

IgG, which is mainly produced during the secondary immune response or fragments of IgG are predominantly used in immunosensor applications. However, other Igs are also available.

Immunoassays, based on the specific reaction of Abs with the target substances (Ags) to be detected, have been widely used for the measurement of targets of low concentration in clinical biofluid specimen such as urine and blood and the detection of the trace amounts of drugs and chemicals such as pesticides in biological and environmental samples.

According to the nature of a label, immunoassay can be classified as label-free immunoassay, radio-immunoassay, enzyme immunoassay, fluorescent immunoassay, chemiluminescent immunoassay, bioluminescent immunoassay etc.

Metalloimmunoassay (immunoassay involving metals) have been developed and extended later on to the use of a variety of other metal-based labels such as colloidal metal particles.[105,106,]

1.5.2.1. Protein immobilization and characterization

During the last years, significant progress has been made and well-defined methodologies for the immobilization of proteins (e.g. antibodies) and nucleic acids have been established.

The protein immobilization methods are the commonly used as in DNA, which were explained at 1.4.3 See section. Such methods are: entrapment in a polymeric matrix, adsorption[227,228], self-assembled monolayer[229-233], covalent binding[231], affinity interactions and entrapment into a composite, as well as the combination of them[234]. Some examples are described below:

A piezoelectric immunosensor was developed for rapid detection of *Escherichia coli* O157:H7. It was based on the immobilization of affinity-purified antibodies onto a monolayer of 16-mercaptohexadecanoic acid (MHDA), a long-chain carboxylic acid-terminating alkanethiol, self-assembled on an AT-cut quartz crystal's Au electrode surface with N-hydroxysuccinimide (NHS) ester as a reactive intermediate. The stepwise assembly of the immunosensor was characterized by means of both QCM and CV techniques.[230]

Hepatitis B surface antibody (HBsAb) was immobilized to the surface of platinum electrode modified with colloidal gold and polyvinyl butyral (PVB) as matrices to detect hepatitis B surface antigen (HBsAg) via EIS[235]. Preparation of the PVB-HBsAb-modified is displayed at Figure 1.22

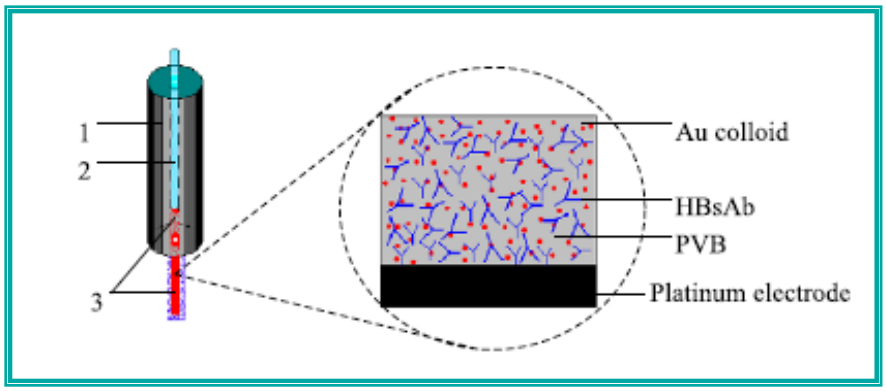

Figure 1.22. *Schematic diagram of the immunosensor showing: (1) PVC tube, (2) cuprum write, (3) platinum electrode modified with HBSaB-Au-PVB.* [235]

1.5.2.2. Protein detection and amplification

– ***Detection***

In the area of protein diagnostics the extremely high selectivity and affinity of antibody molecules to their corresponding antigens have widely been exploited by the enzyme-linked immunosorbent assay (ELISA) which relies on fluorophore labelling and is extraordinarily general.[236,237]

In immunosensors, which represent the logical further development of immunoassays, the required transduction of the biological recognition into a physical signal is in most cases achieved either optical[23,233,238,239] or electrochemically[97,227,228,232,234-237,240-244]

Electrochemical detection at immunosensors is generally achieved by using electroactive compounds as labels including metallic ions[245-247] nanoparticles. Several electrochemical immunosensors by using AuNPs as label are described at publication III (at chapter 7).

Immunosensors are of great interest because of their utility as specific, simple, and direct detection devices with reduced size, cost and time of analysis compared to conventional immunoassay techniques.

While the biological systems based on Ag-Ab pairs provide high selectivity, the immunosensors, with the integrated immunological reagents onto the transducer surfaces, ensure an increased sensitivity and simplicity of the analytical process.[234-236,243]

– ***Amplification***

Different signal amplification systems at immunosensors have been recently reported: AuNPs, enzyme-amplification, electrocatalysis among others.

An electrochemical stripping metalloimmunoassay based on silver-enhanced gold nanoparticle label,[106] a novel, sensitive electrochemical immunoassay has been developed based on the precipitation (reduction) of silver on colloidal gold labels which, after silver metal dissolution in an acidic solution, was indirectly determined by ASV at a glassy-carbon electrode. The reached sensibility was picomolar level.

The sensitivity of immunosensors also is strongly dependent on the amount of immobilised antibodies and their remaining antigen binding properties. The use of smaller and well-oriented antibody fragments as bioreceptor molecules influences the final immunosensor signal.[231]

AuNPs and precipitation of an insoluble product formed by HRP-biocatalyzed oxidation of 3,3′-diaminobenzidine (DAB) in the presence of H_2O_2 were used to enhance the signal obtained from a SPR biosensor. AuNPs functionalized with HS-OEG_3-COOH by SAM technique were covalently conjugated with HRP and anti

IgG antibody to form the Au–anti IgG–HRP complex which was applied in enhancement of SPR immunoassay using a sensor chip for detection of anti-glutamic acid decarboxylase antibody (anti-GAD antibody). The DL found was as low as 0.03 ng/mL of anti-GAD antibody (or 200 fM) which is much higher than that of previous reports.[23]

Das et al.[242] reported a nanocatalyst-based electrochemical assay for proteins. Ultrasensitive detection has been achieved by signal amplification combined with noise reduction: the signal is amplified both by the catalytic reduction of p-nitrophenol to p-aminophenol by gold-nanocatalyst labels and by the chemical reduction of p-quinone imine to p-aminophenol by $NaBH_4$; the noise is reduced by employing an indium tin oxide electrode modified with a ferrocenyl-tethered dendrimer and a hydrophilic immunosensing layer.

An ultrasensitive label-free bioelectrochemical method for rapid determination of thrombin has been developed by directly detecting the redox activity of adenine (A) nucleobases of anti-thrombin aptamer using a pyrolytic graphite electrode. The bioelectrochemical protocol involves a sandwich format. Thrombin, captured by immobilzed anti-thrombin antibody on microtiter plates, is detected by anti-thrombin aptamer-Au nanoparticle bio bar codes. DPV was employed to investigate the electrochemical behaviours of the purine nucleobases. Because the nanoparticle carries a large number of aptamers per thrombin binding event, there is substantial amplification and thrombin can be detected at a very low level of detection (0.1 ng/mL).[244]

1.6. References

[1] Catterall, R.W. Chemical Sensors. 1997, Oxford, UK: Oxford University Press.

[2] Thevenot D. R., Toth K., Durst R. A., Wilson G. S. Electrochemical Biosensors: Recommended Definitions and Classification (Technical Report) *Pure Appl. Chem*. **1999**, 71, 2333–2348.

[3] Niemeyer C. M. Nanoparticles, Proteins, and Nucleic Acids: Biotechnology Meets Materials Science. *Angew. Chem. Int. Ed.* **2001**, 40, 4128–4158.

[4] Eggins, B. R., Chemical Sensors and Biosensors. Analytical Techniques in the Sciences, ed. D. J. Ando. 2002, Northern Ireland, UK: John Wiley & Sons, LTD. 273.

[5] Ewing's analytical instrumentation handbook. Edited by Jack Cazes. Marcel Der, New York, 3rd edition, 2005.

[6] Wang J., Li M., Shi Z., Li N., Gu Z. Direct electrochemistry of cytochrome C at a glassy carbon electrode modified with single-wall carbon nanotubes. *Anal. Chem*. **2002**, 74, 1993–1997.

[7] Evtugyn G. A., Goldfarb O. E., Budnikov H.C., Ivanov A.N., Vinter V.G. Amperometric DNA-Peroxidase Sensor for the Detection of Pharmaceutical Preparations. *Sensors* **2005**, 5, 364−376.

[8] Ugo P., Zangrando V., Moretto L. M., Brunetti B. Ionexchange voltammetry and electrocatalytic sensing capabilities of cytochrome c at polyestersulfonated ionomer coated glassy carbon electrodes. *Biosens. Bioelectron*. **2002,** 17, 479–487.

[9] Arora K., Chaubey A., Singhal R., Singh R. P., Pandey M. K., Samanta S. B., Malhotra B. D., Chand S. Application of electrochemically prepared polypyrrole-polyvinyl sulphonate films to DNA biosensor. *Biosens. Bioelectron.* **2006**, 21, 1777–1783.

[10] Arvinte A., Valentini F., Radoi A., Arduini F., Tamburri E., Rotariu L., Palleschi G., Bala C. The NADH Electrochemical Detection Performed at Carbon Nanofibers Modified Glassy Carbon Electrode. *Electroanalysis* **2007**, 19, 1455−1459.

[11] Ming L., Xi X., Liu J. Electrochemically platinized carbon paste enzyme electrodes: A new design of amperometric glucose biosensors. *Biotech. Letters* **2006**, 28, 1341−1345.

[12] Miscoria S. A., Barrera G. D., Rivas G. A. Enzymatic biosensor based on carbon paste electrodes modified with gold nanoparticles and polyphenol oxidase. *Electroanalysis* **2005**, 17, 1578–1582.

[13] Cui X., Liu G., Lin Y. Amperometric Biosensors Based on Carbon Paste Electrodes Modified with Nanostructured Mixed-valence Manganese Oxides and Glucose Oxidase. *Nanomedicine*, **2005**, 1, 130−135.

[14] Erdem A., Ariksoysal D. O., Karadeniz H., Kara P., Sengonul A., Sayiner A. A., Ozsoz M. Electrochemical genomagnetic assay for the detection of hepatitis B virus DNA in polymerase chain reaction amplicons by using disposable sensor technology. *Electrochem. Comm.* **2005,** 7, 815–820.

[15] Stefan R. I., Nejem R. M., van Staden J. F., Aboul-Enein H. Y. New Amperometric Biosensors Based on Diamond Paste for the Assay of L- and D- Pipecolic Acids in Serum Samples. *Preparative Biochemistry & Biotechnology* **2004**, 34, 135–144.

[16] Stefan R. I., Bokretsion R. G., van Staden J. F., Aboul-Enein H. Y. Simultaneous determination of creatine and creatinine using amperometric biosensors. *Talanta* **2003**, 60, 844–847.

[17] Wang J., Analytical Electrochemistry 3rd Ed. 2006, A. John Wiley & Sons. New York.

[18] Alegret S., Merkoci A., Pividori M. I., Del Valle M., Chapter: "Electrochemical (bio)sensors based on rigid conducting carbon-polymer composites", Enciclopedia of Sensors, Edited by: Craig A. Grimes, Elizabeth C. Dickey, and Michael V. Pishko. Volume 3, 23–44, 2006.

[19] Horswell J., Weitz H. J., Percival H. J., Speir T. Impact of heavy metal amended sewage sludge on forest soils as assessed by bacterial and fungal biosensors. *Biol. fertil. soils* **2006**, 42, 569–576.

[20] Campbell D. W., Müller C., Reardon K. F. Development of a Fiber Optic Enzymatic Biosensor for 1,2-dichloroethane. *Biotech. Letters* **2006**, 28, 883–887.

[21] Kwakye S., Baeumner A. A microfluidic biosensor based on nucleic acid sequence recognition. *Anal. Bioanal. Chem.* **2003,** 376, 1062–1068.

[22] Li B. X., Zhang Z. J., Jin Y. Plant tissue-based chemiluminescence flow biosensor for determination of unbound dopamine in rabbit blood with on-line microdialysis sampling. *Biosens. Bioelectron*. **2002**, 17, 585–589.

[23] Cao C., Sim S. J., Signal enhancement of surface plasmon resonance immunoassay using enzyme precipitation-functionalized gold nanoparticles: A femto molar level measurement of anti-glutamic acid decarboxylase antibody. *Biosens. Bioelectron*. **2007**, 22, 1874−1880.

[24] Li F., Jiang Z. Design and Analysis of a Biosensor Transducer with Multifunctions. *J. Intelligent Mat. Syst. Struct.* **2006**, 17, 823−830.

[25] Okamoto A., Kanatani K., Saito I. Pyrene-Labeled Base-Discriminating Fluorescent DNA Probes for Homogeneous SNP Typing. *J. Am. Chem. Soc.* **2004**, 126, 4820–4827.

[26] Storhoff J. J., Lucas A. D., Garimella V., Bao Y. P., Müller U. R. Homogeneous detection of unamplified genomic DNA sequences based on colorimetric scatter of gold nanoparticle probes. *Nature Biotechnol***. 2004**, 22, 883–887.

[27] Kumar J., Kumar Jha S., D'Souza S. F. Optical microbial biosensor for detection of methyl parathion pesticide using Flavobacterium sp. whole cells adsorbed on glass fiber filters as disposable biocomponent. *Biosens. Bioelectron*. **2006**, 21, 2100–2105.

[28] Satu J. V., Kurittu J. S., Karp M. T. A Luminescent Escherichia coli Biosensor for the High Throughput Detection of ß-Lactams. *J Biomol Screen.* **2002**, 7, 127–134.

[29] Tombelli S., Minunni M., Santucci A., Spiriti M. M., Mascini M. A DNA-based piezoelectric biosensor: Strategies for coupling nucleic acids to piezoelectric devices. *Talanta* **2006**, 68, 806–812.

[30] Dell'Atti D., Tombelli S., Minunni M., Mascini M. Detection of clinically relevant point mutations by a novel piezoelectric biosensor. *Biosens. Bioelectron*. **2006**, 21, 1876–1879.

[31] Pohanka M., Pavliš O., Skládal P. Diagnosis of tularemia using piezoelectric biosensor technology. *Talanta* **2007**, 71, 981–985.

[32] Hwang Il-H., Lee J.-H. Self-actuating biosensor using a piezoelectric cantilever and its optimization. *J. Physics: Conference Series* **2006**, 34, 362–367.

[33] Cooper M. A., Singleton V. T. A survey of the 2001 to 2005 quartz crystal microbalance biosensor literature: applications of acoustic physics to the analysis of biomolecular interactions *J. Molecular Recognition* **2007**, 20, 154–184.

[34] Yi-hua Z., Tse-chao, Fei X. novel thermal biosensor based on enzyme reaction for pesticides measurement. *J. Environ. Sci.* **2005**, 17, 615–619.

[35] Wang L., Lin Q. Theory and Experiments of MEMS Thermal Biosensors. *Conf. Proc. IEEE Eng. Med. Biol. Soc.* **2005**, 2, 1301–1304.

[36] Ramanathan K., Danielsson B. Principles and applications of Thermal biosensors. *Biosens. Bioelectron*. **2001**, 16, 417–423.

[37] Cai H., Shang C., Hsing I. M. Sequence-specific electrochemical recognition of multiple species using nanoparticle labels. *Anal. Chim. Acta* **2004**, 523, 61–68.

[38] Kerman K., Matsubara Y., Morita Y., Takamura Y. Peptide nucleic acid modified magnetic beads for intercalator based electrochemical detection of DNA hybridization. *Science and technology of Advanced Materials* **2004**, 5, 351–357.

[39] Erdem A., Pividori M. I., Lermo A., Bonanni A., Del Valle M., Alegret S. Genomagnetic assay based on label-free electrochemical detection using magneto-composite electrodes. *Sensors and Actuators B* **2006**, 114, 591–598.

[40] Helali S., Martelet C., Abdelghani A., Maaref M. A., Jaffrezic-Renault N. A. Disposable immunomagnetic electrochemical sensor based on functionalised magnetic

beads on gold surface for the detection of atrazine. *Electrochimica Acta* **2006,** 51, 5182–5186.

[41] Boon E. M., Salas J. E., Barton J. K. An Electrical probe of protein-DNA interactions on DNA-modified surfaces. *Nature Biotechnology* **2002**, 20, 282–286.

[42] Castillo J., Gáspár S., Leth S., M. Niculescu M., Mortari A., Bontidean I., Soukharev V., Dorneanu S. A., Ryabov A. D., Csöregi E. Biosensors for life quality Design, development and applications. *Sensors and Actuators B* **2004**, 102, 179–194.

[43] Tansil N. C., Xie F., Xie H., Gao Z. An ultrasensitive nucleic acid biosensor based on the catalytic oxidation of guanine by a novel redox threading intercalator. *Chem. Commun.* **2005**, 1064–1066.

[44] Nebling E., Grunwald T., Albers J., Scha¨fer, P., Hintsche R. Electrical detection of viral DNA using ultramicroelectrode arrays. *Anal. Chem.* **2004**, 76, 689–696.

[45] Viswanathan S., Wu L. C., Huang M. R., Ho J. A. A. Electrochemical immunosensor for cholera toxin using liposomes and poly(3,4-ethylenedioxythiophene)-coated carbon nanotubes. *Anal. Chem.* **2006**, 78, 1115–1121.

[46] Kramer K., Hock B. Recombinant antibodies for environmental analysis. *Anal. Bioanal. Chem.* **2003**, 377, 417–426.

[47] Mascini M. Affinity electrochemical biosensors for pollution control. *Pure Appl. Chem.* **2001**, 73, 23–30.

[48] Rodriguez-Mozaz S., Marco M-P., Lopez de Alda M. J., Barceló D. Biosensors for environmental monitoring of endocrine disruptors: a review article. *Anal. Bioanal. Chem,* **2004**, 378, 588–598.

[49] Vaiopoulou E., Melidis P., Kampragon E., Aivasidis A. On-line load monitoring of wastewaters with a respirographic microbial sensor. *Biosens. Bioelectron.* **2005**, 21, 365–371.

[50] Díaz-González M., González-García M. B., Costa-García A. Immunosensor for mycobacterium tuberculosis on screen-printed carbon electrodes. *Biosens. Bioelectron.*, **2005**, 20, 2035–2043.

[51] Wang S. H., Zhang J. B., Zhang Z. P., Zhou Y. F., Yang R. F., Chen J., Guo Y. C., You F., Zhang X. E. Construction of single chain variable fragment (scFv) and Bi-scFv-alkaline phosphatase fusion protein for detection of Bacillus anthracis. *Anal. Chem.* **2006,** 78, 997–1004.

[52] Miranda-Castro R., De-los-Santos-Álvarez P., Lobo-Castañón M. J., Miranda-Ordieres A. J., Tuñón-Blanco P. Hairpin-DNA Probe for Enzyme-Amplified Electrochemical Detection of *Legionella pneumophila. Anal. Chem.* **2007**, 79, 4050–4055.

[53] Maalouf R., Fournier-Wirth C., Coste J., Chebib H., Saïkali Y., Vittori O., Errachid A., Cloarec J.-P., Martelet C., Jaffrezic-Renault N. Label-free detection of bacteria by electrochemical impedance spectroscopy: comparison to surface plasmon resonance. *Anal. Chem.* **2007**, 79, 4879–4886.

[54] Susmel S., Guilbault G. G., O'Sullivan C. K. Demonstration of label-less detection of food pathogens using electrochemical redox probe and screen printed gold electrodes. *Biosens. Bioelectron*. **2003**, 18, 881–889.

[55] Wang J. Electrochemical biosensors: Towards point-of-care cancer diagnostics. *Biosens. Bioelenctron.* **2006**, 21, 1887–1892.

[56] Mehrvar M., Abdi, M. Recent Developments, Characteristics, and Potential Applications of Electrochemical Biosensors. *Anal. Sciences* **2004**, 20, 1113–1126.

[57] Lakard B., Herlem G., Lakard S., Antoniou A., Fahys B. Urea potentiometric biosensor based on modified electrodes with urease immobilized on polyethylenimine films. *Biosens. Bioelectron*. **2004**, 19, 1641–1647.

[58] Chouteau C., Dzyadevych S., Chovelon J.-M., Durrieu C. Development of novel conductometric biosensors based on immobilised whole cell *Chlorella vulgaris* microalgae. *Biosens. Bioelectron*. **2004**, 19, 1089–1096.

[59] Kulys J., Baronas R. Modelling of Amperometric Biosensors in the Case of Substrate Inhibition. *Sensors* **2006**, 6, 1513–1522.

[60] Kirsch N., Honeychurch K. C., Hart J. P., Whitcombe M. J. Voltammetric Determination of Urinary 1-Hydroxypyrene Using Molecularly Imprinted Polymer-Modified Screen-Printed Carbon Electrodes. *Electroanalysis* **2005**, 17, 571–578.

[61] Zhuo Y., Yuan R., Chai Y., Zhang Y., Li X., Zhu Q., Wang N. An amperometric immunosensor based on immobilization of hepatitis B surface antibody on gold electrode modified gold nanoparticles and horseradish peroxidase, *Anal. Chim. Acta* **2005**, 548, 205–210.

[62] Ramanavičius A., Kaušaitė A., Ramanavičienė A., Polypyrrole-coated glucose oxidase nanoparticles for biosensor design. Sensors *and Actuators B* **2005**, 111-112, 532–539.

[63] Textor M., Kuennemann E., Knoll W. Combined Affinity and Catalytic Biosensor: In Situ Enzymatic Activity Monitoring of Surface-Bound Enzymes. *J. Am. Chem. Soc*. **2005**, 127, 13084–13085.

[64] Chen Q., Huang J., Yin Huijun, Chen K., Osa T. The applications of affinity biosensors: IAsys biosensor and quartz crystal microbalance to the study on interaction between *Paeoniae radix* 801 and endothelin-1. *Sensors and Actuators B* **2006,** 115, 116–122.

[65] Cosnier S. Affinity Biosensors Based on Electropolymerized Films. *Electroanalysis* **2005,** 17, 1701–1715.

[66] Xu D. K., Xu D. W., Yu X. B., Liu Z. H., He W., Ma Z. Q. Label-free electrochemical detection for aptamer-based array electrodes. *Anal. Chem*. **2005**, 77, 5107–5113.

[67] Savran, C. A., Knudsen, S. M., Ellington, A. D., Manalis, S. R. Micromechanical detection of proteins using aptamer-based receptor molecules. *Anal. Chem*. **2004**, 76, 3194–3198.

[68] Hayden O., Bindeus R., Haderspock C., Mann K. J., Wirl B., Dickert F. L. Study on the Molecular Imprinted Polymers with Recognition Properties Towards to Dibenzoyl-L-tartaric Acid Prepared by Photo-Polymerization Method. Photo-polymerization Conditions. *Sensors and Actuators B-Chemical* **2003**, 91, 316–319.

[69] Rick J., Chou T-C. Using protein templates to direct the formation of thin-film polymer surfaces. *Biosens. Bioelectron*. **2006**, 22, 544–549.

[70] Cho E. J., Collett J. R., Szafranska A. E., Ellington A. D. Optimization of aptamer microarray technology for multiple protein targets. *Anal. Chim. Acta* **2006**, 564, 82–90.

[71] Settle, F. A., ed., *Handbook of Instrumental Techniques for Analytical Chemistry*, Prentice Hall, Upper Saddle River, New Jersey, 1997.

[72] Kellner R., Mermet J.-M., Otto M., Widmer H. M. Analytical Chemistry, Wiley-VCH, Weinheim, 1998.

[73] Wang J., Armalis S. Stripping voltammetry at microdisk composite electrode assembly. *Electroanalysis* **1995**, 7, 958–961.

[74] Wang, J., Stripping Analysis: Principles, Instrumentation and Applications, VCH Publishers, Deerfield Beach, FL, 1985.

[75] Fogg A. G., Wang J. Terminology and Convention for Electrochemical Stripping Analysis (Technical Report). *Pure Appl. Chem*. **1999,** 71, 891–897.

[76] Cooper M. A. Label-free screening of bio-molecular interactions. *Analytical & Bioanalytical Chemistry* **2003**, 377, 834–842.

[77] Alivisatos A. P. The use of nanocrystals in biological detection. *Nat. Biotechnol*., **2004**, 22, 47–52.

[78] Katz E., Willner I. Integrated nanoparticle-biomolecule hybrid systems: Synthesis, properties and applications. *Angew. Chem. Int. Ed*. **2004**, 43, 6042–6108.

[79] Rosi N. L., Mirkin C. A. Nanostructures in biodiagnostics. *Chem. Rev*. **2005**, 105, 1547–1562.

[80] McNeil S. E. Nanotechnology for the biologist. *J. Leukocyte Biol.* **2005,** 78, 585–594.

[81] Hernández-Santos D., González-García M. B., Costa-García A. Metal-nanoparticles based electroanalysis. *Electroanalysis* **2002,** 14, 1225–1235.

[82] Salata O. V., Applications of nanoparticles in biology and medicine. *J. Nanobiotech.* **2004**, 2, 3–9.

[83] Azzazy H. M. E., Mansour M. M. H., Kazmierczak S. C. Nanodiagnostics: A New Frontier for Clinical Laboratory Medicine. *Clinical Chemistry* **2006**, 52, 1238–1246.

[84] Whitesides G. M. The 'right' size in nanobiotechnology. *Nat. Biotechnol*. **2003**, 21, 1161–1165.

[85] DeBenedetti B., Vallauri, D. Deorsola F. A., Martínez García M. Synthesis of TiO2 nanospheres through microemulsion reactive precipitation. *J. Electroceramics* **2006**, 17, 37–40

[86] Shiv S., Suresh B., Murali S. Synthesis of Gold Nanospheres and Nanotriangles by the Turkevich Approach. *J. Nanosci. Nanotechnol*. **2005,** 5, 1721–1727.

[87] Tai H. H., Koo H.-J., Chung B. H. Shape-Controlled Syntheses of Gold Nanoprisms and Nanorods Influenced by Specific Adsorption of Halide Ions. *J. Phys. Chem. C* **2007**, 111, 1123–1130.

[88] Hyuk Im S., Tack Lee Y., Wiley B., Xia, Y. Large-Scale Synthesis of Silver Nanocubes: The Role of HCl in Promoting Cube Perfection and Monodispersity. *Angew. Chem. Int. Ed*. **2005**, 44, 2154–2157.

[89] Mendoza-Reséndez R., Bomati-Miguel O., Morales M. P., Bonville P., Serna C. J. Microstructural characterization of ellipsoidal iron metal nanoparticles. *Nanotechnology* **2004,** 15, S254–S258.

[90] Grieve K., Mulvaney P., Grieser F. Synthesis and electronic properties of semiconductor nanoparticles/quantum dots. *Curr. Opin. in Colloid & Interface Science* **2000**, 5, 168–172.

[91] Bönnemann H., Richards R. M. Nanoscopic Metal Particles – Synthetic Methods and Potential Applications, *Eur. J. Inorg. Chem*. **2001**, 10, 2455–2480.

[92] Penn S. G., He L., Natan M. J. Nanoparticles for bioanalysis. *Curr. Opin. in Chem. Biology* **2003**, 7, 609–615.

[93] Gupta A. K., Gupta M. Synthesis and surface engineering of iron oxide nanoparticles for biomedical applications. *Biomaterials* **2005**, 26, 3995–4021.

[94] Luo X., Morrin A., Killard A. J., Smyth M. R., Application of Nanoparticles in Electrochemical Sensors and Biosensors. *Electroanalysis* **2006**, 18, 319–326.

[95] Pejcic B., De Marco R., Parkinson G. The role of biosensors in the detection of emerging infectious diseases. *Analyst* **2006**, 131, 1079–1090.

[96] Lin F. Y. H., Sabri M., Alirezaie J., Li D., Sherman P. M. Development of a Nanoparticle-Labeled Microfluidic Immunoassay for Detection of Pathogenic Microorganisms. *Clin. Diagn. Lab. Immunol*. **2005**, 12, 418–425.

[97] Ambrosi A., Castañeda M. T., Killard A. J., Smyth M. R., Alegret S., Merkoçi, A., Double-codified gold nanolabels for enhanced immunoanalysis. *Anal. Chem.* **2007**, 79, 5232–5240.

[98] Zhang J., Song S., Zhang L., Wang L., Wu H., Pan D., Fan Ch. Sequence-Specific Detection of Femtomolar DNA via a Chronocoulometric DNA Sensor (CDS): Effects of Nanoparticle-Mediated Amplification and Nanoscale Control of DNA Assembly at Electrodes. *J. Am. Chem. Soc*. **2006**, 128, 8575–8580.

[99] Sinha R., Kim G. J., Nie, S., Dong M. Shin. Nanotechnology in cancer therapeutics: bioconjugated nanoparticles for drug delivery. *Mol. Cancer Ther.* **2006**, 5, 1909–1917.

[100] Cuenya B. R., Hyeon Baeck S., Jaramillo T. F., McFarland E. W. Size-and Support-Dependent Electronic and Catalytic Properties of Au^0/Au^{3+} Nanoparticles Synthesized from Block Copolymer Micelles. *J. Am. Chem. Soc*. **2003**, 125, 12928–12934.

[101] Andreescu S., Sadik O. A., Trends and challenges in biochemical sensors for clinical and environmental monitoring. *Pure Appl. Chem*. **2004**, 76, 861–878.

[102] Wang J. Nanomaterial-based electrochemical Biosensors. *Analyst*, **2005**, 130, 421−426.

[103] Authier L., Grossiord C., Brossier P., Limoges B. Gold nanoparticle-based quantitative electrochemical detection of amplified human cytomegalovirus DNA using disposable microband electrodes. *Anal. Chem.* **2001**, 73, 4450–4456.

[104] Wang J., Xu D.K., Kawde A.N., Polsky R., Metal nanoparticle based electrochemical stripping potentiometric detection of DNA hybridization. *Anal. Chem.* **2001,** 73, 5576–5581.

[105] Dequaire M., Degrand C., Limoges B. An electrochemical metalloimmunoassay based on a colloidal gold label. *Anal. Chem*. **2000**, 72, 5521–5528.

[106] Chu X., Fu X., Chen K., Shen G.-L., Yu R.-Q. An electrochemical stripping metalloimmunoassay based on silver-enhanced gold nanoparticle label. *Biosens, Bioelectron.* **2005,** 20, 1805–1812.

[107] Liu C.-H., Li Z.-P., Du B.-A., Duan X.-R., Wang Y.-C. Silver Nanoparticle-Based Ultrasensitive Chemiluminescent Detection of DNA Hybridization and Single-Nucleotide Polymorphisms. *Anal. Chem*. **2006**, 78, 3738–3744.

[108] Cai H., Xu Y., Zhu N., He P., Fang Y. An electrochemical DNA hybridization detection assay based on a silver nanoparticle label. *Analyst* **2002**, 127, 803–808

[109] Polsky R, Gill R, Kaganovsky L, Willner I. Nucleic Acid-functionalized Pt nanoparticles: catalytic labels for the amplified electrochemical detection of biomolecules. *Anal. Chem*. **2006**, 78, 2268–2271.

[110] Wang J., Liu G., Jan M. R., Zhu Q. Electrochemical detection of DNA hybridization based on carbon-nanotubes loaded with CdS tags. *Electrochem. Commun.* **2003**, 5, 1000–1004

[111] Hansen J. A., Mukhopadhyay R., Hansen J. Ø, Gothelf K. V. Femtomolar Electrochemical Detection of DNA Targets Using Metal Sulfide Nanoparticles. *J. Am. Chem. Soc*. **2006**, 128, 3860–3861.

[112] Wolcott A., Gerion D.e, Visconte M., Sun J., Schwartzberg A., Chen S., Zhang J. Z. Silica-Coated CdTe Quantum Dots Functionalized with Thiols for Bioconjugation to IgG Proteins. *J. Phys. Chem*. B **2006**, 110, 5779–5789.

[113] Zhang C.-Y., Johnson L. W. Homogenous rapid detection of nucleic acids using two-color quantum dots. *Analyst* **2006**, 131, 484–488

[114] Knopf G. K, A. S. Bassi, Smart Biosensor Technology. C. R. C. Press. 2007.

[115] Alivisatos A. P., Biological applications of colloidal nanocrystals. *Nanotechnology* **2003**, 14, R15–R27.

[116] Chan W. C. W., Maxwell D. J., Gao X. H., Bailey R. E., Han M. Y., Nie S. A., Luminescent quantum for multiplexed biological detection and imaging. *Curr. Opin. Biotech*. **2002,** 13, 40–46.

[117] Faraday M., Experimental relations to gold (and other metals) to light. *Phil. Trans. Roy. Soc. London*. **1857**, 147, 145–181.

[118] Turkevich J., Stevenson P. C., Hiller J. A study of the nucleation and growth processes in the synthesis of colloidal gold. *Discuss. Faraday Soc.* **1951**, 11, 55–75.

[119] Lung, J. K., Huang J-C., Tien D-C, Liao C-Y, Tseng K-H, Tsung T-T, Kao, W-S, Tsai T-H, Jwo C-S, Lin H-M, Stobinski L., Preparation of gold nanoparticles by arc discharge in water. *J. Alloys and Compounds* **2007**, 434-435, 655–658.

[120] Panda B. R., Chattopadhyay, A. Synthesis of Au Nanoparticles at "all" pH by H_2O_2 Reduction of $HAuCl_4$. *J. Nanosci. Nanotechnol*. **2007**, 7, 1911–1915.

[121] Luo Y., Sun X. Sunlight-Driving Formation and Characterization of Size-Controlled Gold Nanoparticles. *J. Nanosci. Nanotechnol*. **2007**, 7, 708–711.

[122] Liang Z., Zhang J., Wang L., Song S., Fan C., Li G. A Centrifugation-based Method for Preparation of Gold Nanoparticles and its Application in Biodetection. *Int. J. Mol. Sci.* **2007**, 8, 526–532.

[123] Burda C., Chen X., Narayanan R., El-Sayed M. A. Chemistry and Properties of Nanocrystals of Different Shapes. *Chem. Rev*. **2005**, 105, 1025–1102.

[124] Love J. C., Estroff L. A., Kriebel J. K., Nuzzo R. G., Whitesides G. M. Self-Assembled Monolayers of Thiolates on Metals as a Form of Nanotechnology. *Chem. Rev.* **2005**, 105, 1103–1169.

[125] Liz-Marzan L. M. Nanometals: Formation and color. *Materials Today*. **2004**, 7, 26–31.

[126] Ouacha H., Hendrich C., Hubenthal F., Träger. Laser-assisted growth of gold nanoparticles: Shaping and optical characterization. *Appl. Phys. B* **2005**, 81, 663–668.

[127] Dos Santos Jr. D. S., Alvarez-Puebla R. A., Oliveira Jr., O. N., Aroca R. F. Controlling the size and shape of gold nanoparticles in fulvic acid colloidal solutions and their optical characterization using SERS. *J. Mater. Chem*. **2005**, 15, 3045–3049.

[128] Mirkin C. A., Letsinger R. L., Mucic R. C., Storhoff J. J. A DNA-based method for rationally assembling nanoparticles into macroscopic materials. *Nature* **1996**, 382, 607–609.

[129] Alivisatos A. P., Johnsson K. P., Peng X. G., Wilson T. E., Loweth C. J., Bruchez M. P., Schultz P. G. Organization of 'nanocrystal molecules' using DNA. *Nature* **1996**, 382, 609–611.

[130] Gearheart L. A., Ploehn H. J., Murphy C. J. Oligonucleotide Adsorption to Gold Nanoparticles: A Surface-Enhanced Raman Spectroscopy Study of Intrinsically Bent DNA. *J. Phys. Chem. B* **2001**, 105, 12609–12615.

[131] Shaiu W. L., Larson D. D., Vesenka J., Henderson E. Atomic force microscopy of oriented linear DNA molecules labeled with 5 nm gold spheres. *Nucl. Acids. Res.* **1993**, 21, 99–103.

[132] Sastry M., Lala N., Patil V., Chavan S. P., Chittiboyina A. G. Optical absorption study of the biotinavidin interaction on colloidal silver and gold particles. *Langmuir* **1998**, 14, 4138–4142.

[133] Hendrickson W. A., Pahler A., Smith J. L., Satow Y., Merritt E. A., Phizackerley R. P. Crystal structure of core streptavidin determined from multiwavelength anomalous diffraction of synchrotron radiation. *Proc. Natl. Acad. Sci.* **1989**, 86, 2190–2194.

[134] Weber, P. C., Ohlendorf, D. H., Wendoloski, J. J., Salemme, F. R. Structural origins of high-affinity biotin binding to streptavidin. *Science* **1989**, 243, 85–88.

[135] Green N. M. Avidin and streptavidin. *Methods Enzymol*. **1990**, 184, 51–67.

[136] Parak W. J., Pellegrino T., Micheel C. M., Gerion D., Williams S. C., Alivisatos A. P. Defined DNA/nanoparticle conjugates. *Nano Lett.* **2003**, 3, 33–36.

[137] Zanchet D., Micheel C. M., Parak W J., Gerion D., Alivisatos A. P. Electrophoretic Isolation of Discrete Au Nanocrystal/DNA Conjugates. *Nano Lett*. **2001**, 1, 32–35.

[138] Park, S., Brown K. A., Hamad-Schifferli K. Changes in Oligonucleotide Conformation on Nanoparticle Surfaces by Modification with Mercaptohexanol. *Nano Lett.* **2004**, 4, 1925–1929.

[139] Cao Y.J., Jin R., Mirkin C. A. DNA-modified core-shell Ag/Au nanoparticles. *Am. Chem. Soc*. **2001**, 123, 7961–7962.

[140] Shipway A. N., Willner I. Nanoparticles as structural and functional units in surface-confined architectures. *Chem. Commun*. **2001**, 2035–2045.

[141] Taton T. A., Mucic R. C., Mirkin C. A., Letsinger R. L. *J.* The DNA-mediated formation of supramolecular moo-and multilayered nanoparticle structures. *Am. Chem. Soc*. **2000**, 122, 6305–6306.

[142] Patolsky F., Ranjit K. T., Lichtenstein A., Willner I. Dendritic amplification of DNA analysis by oligonucleotide-functionalized Au-nanoparticles. *Chem. Commun.* **2000**, 1025–1026.

[143] Storhoff J. J., Lazaride, A. A., Mucic R. C., Mirkin C. A., Letsinger R. L., Schatz G. C. What controls the optical properties of DNA-linked gold nanoparticles assemblies. *J. Am. Chem. Soc.* **2000**, 122, 4640–4650.

[144] Sung K. M., Mosley D. W., Peelle B. R., Zhang S., Jacobson J. M. Synthesis of Monofunctionalized Gold Nanoparticles by Fmoc Solid-Phase Reactions. *J. Am. Chem. Soc.* **2004**, 126, 5064–5065.

[145] Claridge S. A., Goh S. L., Frechet J. M. J., Williams S. C., Micheel C. M., Alivisatos, A. P. Directed assembly of discrete gold nanoparticle groupings using branched DNA scaffolds. *Chem. Mater*. **2005**, 17, 1628–1635.

[146] Xu X., Rosi N. L., Wang Y., Huo F., Mirkin C. A. Asymetric functionalization of gold nanoparticles with oligonucleotides. *J. Am. Chem. Soc*. **2006**, 128, 9286–9287.

[147] Chirea M., García-Morales V., Manzanares J.A., Pereira C., Gulaboski R., Silva F. Electrochemical characterization of polyelectrolyte/gold nanoparticle multilayers self-assembled on gold electrodes. *J. Phys. Chem. B*. **2005**, 109, 21808–21817.

[148] Ito M., Tsukatani T., Fujihara H. Preparation and characterization of gold nanoparticles with a ruthenium-terpyridyl complex, and electropolymerization of their pyrrole modified metal nanocomposites. *J. Mater. Chem.* **2005**, 15,960−964.

[149] Frenkel A. I., Nemzer S., Pister I., Soussan L., Harris T., Sun Y., Rafailovich M. H. Size-controlled synthesis and characterization of thiol-stabilized gold nanoparticles. *J. Chem. Phys.* **2005**, 123, 184701.

[150] El-Deab M. S., Sotomura T., Ohsaka T. Morphological Selection of Gold Nanoparticles Electrodeposited on Various Substrates. *J. Electrochem. Soc*. **2005**, 152, C730−C737.

[151] Merkoci A., Aldavert M., Tarrasón G., Eritja R., Alegret S., Toward an ICPMS-linked DNA assay based on gold nanoparticles immunoconnected through peptide sequences. *Anal. Chem*. **2005**, 77, 6500−6503.

[152] Haiss W., Thanh N. T. K., Aveyard J., Fernig D. G. Determination of Size and Concentration of Gold Nanoparticles from UV-Vis Spectra. *Anal. Chem*. **2007**, 79, 4215−4221.

[153] Quinn B. M., Liljeroth P., Ruiz V., Laaksonen T., Kontturi K. Electrochemical resolution of 15 oxidation states for monolayer protected gold nanoparticles. *J. Am. Chem. Soc.* **2003**, 125, 6644−6645.

[154] Balasubramanian R., Guo R., Mills A. J., Murray R. W. Reaction of $Au_{55}(PPh3)_{12}Cl_6$ with Thiols Yields Thiolate Monolayer Protected Au_{75} Clusters *J. Am. Chem. Soc.* **2005**, 127, 8126−8132.

[155] Hernández J., Solla-Gullón J., Herrero E. Gold nanoparticles synthesized in a water-in-oil microemulsion: electrochemical characterization and effect of the surface structure on the oxygen reduction reaction. *J. Electroanal. Chem.* **2004**, 574, 185−196.

[156] Remediakis I. N., N. Lopez, Nørskov J. K. CO oxidation on gold nanoparticles: Theoretical studies. *Applied Catalysis A.* **2005**, 291, 13–20.

[157] Grzybowska-Świerkosz B. Nano-Au/oxide support catalysts in oxidation reactions: Provenance of active oxygen species. *Catalysis Today* **2006**, 112, 3–7.

[158] Horisberger M. Colloidal gold: a cytochemical marker for light and fluorescent microscopy and for transmission and scanning electron microscopy. *Scanning Electron Microsc*. **1981**, 11, 9–31.

[159] Thiberge S., Nechushtan A., Sprinzak D., Gileadi O., Behar V., Zik O., Chowers Y., Michaeli S., Schlessinger J., Moses E. Scanning electron microscopy of cells and tissues under fully hydrated conditions. *Proc. Natl. Acad. Sci.* **2004**, 101, 3346–3351.

[160] Hohenau A., Krenn J. R., Garcia-Vidal F. J., Rodrigo S. G., Martin-Moreno L., Beermann J., Bozhevolnyi S. I. Spectroscopy and nonlinear microscopy of gold nanoparticle arrays on gold films. *Phys. Rev. B* **2007**, 75, 085104.

[161] Wang W., Wang Y., Z. Dai Z., Sun Y., Sun Y. Nonlinear optical properties of periodic gold nanoparticle arrays. *Applied Surface Science* **2007**, 253, 4673–4676.

[162] Merkoçi A., Aldavert M., Marin S., Alegret S. New materials for electrochemical sensing V. Nanoparticles for DNA labeling. *Trends Anal. Chem*. **2005**, 24, 341−349.

[163] Guoa S., Wang E. Synthesis and electrochemical applications of gold nanoparticles.

Anal. Chim. Acta **2007**, 598, 181–192.

[164] Castañeda M. T., Merkoçi A., Alegret S. Electrochemical sensing of DNA using gold nanoparticles. *Electroanalysis* **2007**, 19, 743–753.

[165] Pumera M., Castañeda M. T., Pividori M. I., Eritja R., Merkoçi A., Alegret S. Magnetically trigged direct electrochemical detection of DNA hybridization based Au67 Quantum Dot – DNA – paramagnetic bead conjugate. *Langmuir.* **2005**, 21, 9625–9629.

[166] Castañeda M. T., Merkoçi A., Pumera M., Alegret S. Electrochemical genosensors for biomedical applications based on gold nanoparticles. *Biosens, Bioelectron*. **2007**, 22, 1961–1967.

[167] Xiao Y., Patolsky F., Katz E., Hainfeld J. F., Willner I., "Plugging into Enzymes": Nanowiring of Redox Enzymes by a Gold Nanoparticle. *Science* **2003**, 299, 1877−1881.

[168] Wang L., Wang E. K. Direct electron transfer between Cytochrome c and a gold nanoparticles modified electrode. *Electrochem. Commun*. **2004**, 6, 49–54.

[169] Raj C. R., Okajima T., Ohsaka T. Gold nanoparticle arrays for the voltammetric sensing of dopamine. *J. Electroanal. Chem.* **2003**, 543, 127–133.

[170] Medintz I. L., Uyeda H. T., Goldman E. R., Mattoussi H. Quantum dot bioconjugates for imaging, labelling and sensing. *Nat. Mater*. **2005**, 4, 435–446.

[171] Parak W. J., Gerion D., Pellegrino T., Zanchet D., Micheel C., Williams S. C., Boudreau R., Le Gros M. A., Larabell C. A., Alivisatos A. P. Biological applications of colloidal Nanocrystals. *Nanotechnology* **2003**, 14, R15–R27.

[172] Hansen J. A., Wang J., Kawde A. N., Xiang Y., Gothelf K. V., Collins, G. Quantum-dot/aptamer-based ultrasensitive multi-analyte electrochemical biosensor. *J. Am. Chem. Soc*. **2006**, 128, 2228–2229.

[173] Sapsford K. E., Pons T., Medintz I.L., Mattoussi H. Biosensing with Luminescent Semiconductor Quantum Dots. *Sensors* **2006**, 6, 925–953.

[174] Wang J., Liu G., Merkoçi A. Electrochemical Coding Technology for Simultaneous Detection of Multiple DNA Targets. *J. Am. Chem. Soc*. **2003**, 125, 3214–3215.

[175] Liu G., Wang J., Kim J., Jan M. R., Electrochemical Coding for Multiplexed Immunoassays of Proteins. *Anal. Chem*. **2004**, 76, 7126–7130.

[176] Wang X., Ruedas-Rama M. J., Hall E. A. H. The Emerging Use of Quantum Dots in Analysis. *Analytical Letters* **2007**, 40, 1497–1520.

[177] Nelson D. L., Cox M. M., Lehninger Principles of Biochemistry. Third Edition. Worth Publishers. New York, N.Y. 2000.

[178] Sun Y., Kiang C-H. DNA-based Artificial Nanostructures: Fabrication, Properties, and Applications. Chapter V in "Handbook of Nanostructured Biomaterials and Their Applications in Nanobiotechnology," Ed. by Nalwa, American Scientific Publishers (2005).

[179] Gooding J. J. Electrochemical DNA Hybridization Biosensors. *Electroanalysis* **2002**, 14, 1149–1156.

[180] Rivas G. A., Pedano M. L., Ferreyra N. F. Electrochemical Biosensors for Sequence-Specific DNA Detection. *Analytical Letters* **2005**, 38, 2653–2703.

[181] Pividori M. I., Merkoçi A., Alegret S. Classical dot–blot format implemented as an amperometric hybridisation genosensor. *Biosens. Bioelectron*. **2001**, 16, 1133–1142.

[182] Li D., Frey M. W., Baeumner A. J. Electrospun Polylactic Acid Nanofiber Membranes as Substrates for. Biosensor Assemblies. *J. Membrane Science* **2006**, 279, 254–263.

[183] Vivek K., Vijay T., Huangxian J. Immobilization of Biomolecules in Sol-Gels: Biological and Analytical Applications. *Crit. Rev. Anal. Chem*. **2006**, 36, 73–106.

[184] De-los-Santos-Álvarez P., Lobo-Castañón, M. J., Miranda-Ordieres A. J. Tuñón Blanco P. Electrochemistry of Nucleic Acids at Solid Electrodes and Its Applications. *Electroanalysis.* **2004**, 16, 1193–1204.

[185] De la Escosura-Muñiz A., González-García M. B., Costa-García A. DNA hybridization sensor based on aurothiomalate electroactive label on glassy carbon electrodes. *Biosens. Bioelectron*. **2007,** 22, 1048–1054.

[186] Díaz-González M., De la Escosura-Muñiz A., González-García M.B., Costa García A. DNA hybridization biosensors using polylysine modified SPCEs. *Biosens. Bioelectron.* **2008,** d.o.i: 101016/j.bios.2007.12.001.

[187] Foultier B., Moreno-Hagelsieb L., Flandre, D., Remacle J. Comparison of DNA Detection Methods Using Nanoparticles and Silver Enhancement. *IEE Proc. Nanobiotechnology* **2005**, 152, 3.

[188] Pividori M. I., Merkoci A., Alegret S., Electrochemical genosensor design: immobilisation of oligonucleotides onto transducer surfaces and detection methods. *Biosens. Bioelectron.* **2000**, 15, 291–303.

[189] Steel A. B., Levicky R. L., Herne T. M., Tarlov M. J. Immobilization of Nucleic Acids at Solid Surfaces: Effect of Oligonucleotide Length on Layer Assembly. *Biophysic. J.* **2000**, 79, 975–981.

[190] Boozer C., Chen S., Jiang S., Controlling DNA Orientation on Mixed ssDNA/OEG SAMs. *Langmuir* **2006**, 22, 4694–4698.

[191] Abad-Valle P., Fernández-Abedul M. T., Costa-García A. Genosensor on gold films with enzymatic electrochemical detection of a SARS virus sequence. *Biosens. Bioelectron.* **2005,** 20, 2251–2260.

[192] Ju H. X., Ye Y. K., Zhao J. H., Zhu Y. L., Hybridization Biosensor Using di(2,2′-bipyridine)osmium (III) as Electrochemical Indicator for Detection of Polymerase Chain Reaction Product of Hepatitis B Virus DNA. *Anal. Biochem*. **2003**, 313, 255–261.

[193] Wilchek M., Bayer E. A., Applications of avidin-biotin technology: literature survey. *Methods Enzymol*. **1990**, 184, 14–45.

[194] Hernández-Santos D., González-García M.B., Costa-García A. Genosensor based on platinum (II) complex as electrocatalytic label**.** *Anal. Chem.* **2005***,* 77, 2868–2874.

[195] Jones, M. L., Kurzban G. P., Non cooperatives of biotin binding to tetrameric streptavidin. *Biochemistry* **1995**, 34, 11750−11756.

[196] González M., Bagatolli L. A., Echabe I., Arrondo J. L. R., Argaraña C. E., Cantor C. R., Fidelio G. D. Interaction of Biotin with Streptavidin. Thermostability and conformational changes upon binding. *J. Biol. Chem.* **1997,** 272, 11288–11294.

[197] Mir M., Katakis I. Towards a fast-responding, label-free electrochemical DNA biosensor. *Anal. Bioanal*. *Chem*. **2005**, 381, 1033–1035.

[198] Wilchek M. My life with affinity. *Protein Sci.* **2004,** 13, 3066−3070

[199] Millan K. M., Mikkelsen, S. R. Sequence-selective biosensor for DNA based on electroactive hybridisation indicators. *Anal.Chem*. **1993**, 65, 2317–2323.

[200] Lallemand D., Rouillati M. H., Dugas V., Chevolot Y., Souteyrand E., Phaner-Goutorbe M. AFM characterization of ss-DNA probes immobilization: a sequence effect on surface organization. *Journal of Physics: Conference Series* **2007**, 61, 658–662.

[201] Cho Y.-K., Kim S., Kim Y. A., Lim H. K., Lee K., Yoon D. S., Lim G., Pak Y. E., Ha T. H., Kim K. Characterization of DNA immobilization and subsequent hybridization using in situ quartz crystal microbalance, fluorescence spectroscopy, and surface plasmon resonance. *J. Colloid and Interface Science*. **2004**, 278, 44−52.

[202] Dong L. Q., Zhou J. Z., Wu L. L., Dong P., Lin Z. H. SERS studies of self-assembled DNA monolayer – characterization of adsorption orientation of oligonucleotide probes and their hybridized helices on gold substrate. *Chem. Physics Letters* **2002**, 354, 458−465.

[203] Peterson A. W., Heaton R. J., Georgladis R. M. The effect of surface probe density on DNA hybridization. *Nucleic Acids Research* **2001**, 29, 5163−5168.

[204] Cloarec J. P., Deligianis N., Martin J. R., Lawrence I., Souteyrand E., Polychronakos C., Lawrence M. F. Immobilization of homooligonucleotide probe layers onto Si/SiO_2

substrates: characterization by electrochemical impedance measurements and radiolabelling. *Biosens. Bioelecron*. **2002**, 17, 405−412.

[205] Elghanian R., Storhoff J. J., Mucic R. C., Letsinger R. L., Mirkin C. A., Selective Colorimetric Detection of Polynucleotides Based on the Distance-Dependent Optical Properties of Gold Nanoparticles. *Science* **1997**, 277, 1078−1081.

[206] Storhoff J. J., Elghanian R., Mucic R. C., Mirkin C. A., Letsinger R. L. J. One-Pot Colorimetric Differentiation of Polynucleotides with Single Base Imperfections Using Gold Nanoparticles Probes. *J. Am. Chem. Soc.* **1998,** 120, 1959−1964.

[207] Nakamura F., Ito M., Manna A., Tamada K., Hara M., Knoll W. Observation of Hybridization on a DNA Array by Surface Plasmon Resonance Imaging using Au Nanoparticles. *Japanese J. Appl. Phys.* **2006**, 45, 1026−1029.

[208] Gaylord B. S., Heeger A. J., Bazan G. C. DNA detection using water-soluble conjugated polymers and peptide nucleic acid probes. *Proc. Natl. Acad. Sci. USA* **2002,** 99, 10954–10957

[209] Peterson A. W., Wolf L. K., Georgiadis R. M. J. Hybridization of mismatched or partially matched DNA at surfaces. *J. Am. Chem. Soc*. **2002,** 124, 14601–14607.

[210] Taton T. A. Two-color Labeling of Oligonucleotide Arrays via Size-Selective Scattering of Nanoparticle Probes. *J. Am. Chem. Soc.* **2001**, 123, 5164–5165.

[211] Liu S. F., Li J. R., Jiang L. Surface modification of platinum quartz crystal microbalance by controlled electroless deposition of gold nanoparticles and its enhancing effect on the HS-DNA immobilization. *Colloids and Surfaces A: Physicochemical and Engineering Aspects* **2005**, 257-258, 57–62

[212] Cooper M. A., Dultsev F. N., Minson T., Ostanin V. P., Abell, C., Klenerman D. Direct and sensitive detection of a human virus by rupture event scanning. *Nat. Biotechnol*. **2001,** 19, 833–837.

[213] Hook F., Ray, A., Norden B., Kasemo B. Characterization of PNA and DNA Immobilization and Subsequent Hybridization with DNA Using Acoustic-Shear-Wave Attenuation Measurements. *Langmuir* **2001,** 17, 8305–8312.

[214] Palecek, E. Past, present and future of nucleic acids electrochemistry. *Talanta* **2002**, 6, 809–819.

[215] Wang J., Xu D., Erdem A., Polsky R., Salazar M. A. Genomagnetic electrochemical assays of DNA hybridization. *Talanta* **2002**, 56, 931–938.

[216] Cao Y. W. C., Jin R. C., Mirkin C. A. Nanoparticles with Raman Spectroscopic. Fingerprints for DNA and RNA Detection. *Science* **2002**, 297, 1536–1540.

[217] Park S. J., Taton T. A., Mirkin C. A. Array-based electrical detection of DNA with nanoparticle probes. *Science* **2002,** 295, 1503–1506.

[218] Zhang Z.-L., Pang, D.-W., Yuan H., Cai R.-X., Abruña H. D. Electrochemical DNA sensing based on gold nanoparticle amplification. *Anal Bioanal Chem*. **2005,** 381, 833–838.

[219] Pividori M. I., Merkoci A., Alegret S. Graphite-epoxy composites as a new transducing material for electrochemical genosensing. *Biosens. Bioelectron*. **2003**, 19, 473−484.

[220] Pividori M. I., Alegret S. Graphite-Epoxy Platforms for Electrochemical Genosensing. *Anal. Letters* **2003**, 36, 1669−1695.

[221] Male D. Immunology: An Illustrated Outline. 4th Edition. Elsevier, London, U.K., 2003.

[222] Killard A. J., Deasy B., O'Kennedy R., Smyth M. R. Antibodies: production, functions and. applications in biosensors. TrAC - *Trends in Anal. Chem.* **1995**, 14, 257–266.

[223] Taylor L., Bachler M., Duncan I., Keen S., Fallon R., Mair C., McDonald T. T., Schwarz H.. In vitro and in vivo activities of OX40 (CD134)-IgG fusion protein isoforms with different levels of immune-effector functions. *J. Leukocyte Biology* **2002,** 72, 522−529.

[224] Lazar G. A., Dang W., Karki S., Vafa O., Peng J. S., Hyun L., Chan C., Chung H. S., Eivazi A., Yoder S. C., Vielmetter J., Carmichael D. F., Hayes R. J., Dahiyat B. I.. Engineered antibody Fc variants with enhanced effector function. *Proc. Natl. Acad. Sci.* **2006**, 103, 4005–4010.

[225] Luppa P. B., Sokoll L. J., Chan D. W. Immunosensors—principles and applications to clinical chemistry. *Clin. Chim. Acta* **2001**, 314, 1–26.

[226] Chan W. C. W., Maxwell D. J., Gao X. H., Bailey R. E., Han M. Y., Nie S. A. Luminescent quantum dots for multiplexed biological detection and imaging. *Curr. Opin. Biotechnol*., **2002**, 13, 40–46.

[227] Fernández-Sánchez C., Costa-García A. Adsorption of immunoglobulin G on carbon paste electrodes as a basis for the development of immunoelectrochemical devices. *Biosens. Bioelectron*. **1997**, 12, 403−413.

[228] Fernández-Sánchez C., González-García M. B., Costa-García A., AC voltammetric carbon paste-based enzyme immunosensors. *Biosens. Bioelectron*. **2000**, 14, 917−924.

[229] Wu Z., Wang B., Cheng Z., Yang X., Dong S., Wang E. A facile approach to immobilize protein for biosensor: self-assembled supported bilayer lipid membranes on glassy carbon electrode. *Biosens. Bioelectron*. **2001**, 16, 47–52.

[230] Su X-Li, Li Y. A self-assembled monolayer-based piezoelectric immunosensor for rapid detection of Escherichia coli O157:H7. *Biosen. Bioelectron*. **2004**, 19, 563−574.

[231] Bonroy K., Frederix F., Reekmans G., De Wolf E., De Palma R., Borghs G., Declerck P., Goddeeris B. Comparison of random and oriented immobilisation of antibody fragments on mixed self-assembled monolayers. *J. Immunological Methods* **2006**, 312, 167−181.

[232] Chen H., Jiang J.-H., Huang Y., Deng T., Li J.-S., Shen G.-L., Yu R-Q. An electrochemical impedance immunosensor with signal amplification based on Au-colloid labeled antibody complex. *Sensors and Actuators B: Chemical* **2006**, 117, 211−218.

[233] Lee W., Oh B.-K., Lee W. H., Choi J.-W. Immobilization of antibody fragment for immunosensor application based on surface plasmon resonance. *Colloids and Surfaces B: Biointerfaces* **2005**, 40, 143−148.

[234] Tang D., Yuan R., Chai Y., Zhang L., Zhong X., Liu Y., Dai J. Preparation and application on a kind of immobilization method of anti-diphtheria for potentiometric immunosensor modified colloidal Au and polyvinyl butyral as matrixes. *Sensors and Actuators B: Chemical* **2005**, 104, 199−206.

[235] Tang D., Yuan R., Chai Y., Dai J., Zhong X., Liu Y., A novel immunosensor based on immobilization of hepatitis B surface antibody on platinum electrode modified colloidal gold and polyvinyl butyral as matrices via electrochemical impedance spectroscopy. *Bioelectrochemistry* **2004**, 65, 15–22.

[236] Santandreu M., Céspedes F., Alegret S., Martínez-Fàbregas E., Amperometric Immunosensors Based on Rigid Conducting Immunocomposites, *Anal. Chem,* **1997**, 69, 2080–2085.

[237] Sole S., Alegret S., Cespedes F., Martinez-Fabregas E., Diez- Caballero T., Flow injection immunoanalysis based on a magnetoimmunosensor system, *Anal. Chem.* **1998**, 70, 1462–1467.

[238] Barzen C., Brecht A., Gauglitz G., Optical multiple-analyte immunosensor for water pollution control. *Biosens. Bioelectron*. **2002**, 17, 289–295.

[239] Rodriguez-Mozaz, S., Reder S., Lopez de Alda M., Gauglitz G., Barceló D., Simultaneous multi-analyte determination of estrone, isoproturon and atrazine in natural waters by the RIver ANAlyser (RIANA), an optical immunosensor. *Biosens. Bioelectron*. **2004**, 10, 633–640.

[240] Navratilova I., Skladal P., The immunosensors for measurement of 2,4-dichlorophenoxyacetic acid based on electrochemical impedance spectroscopy. *Bioelectrochem*. **2004**, 62, 11–18.

[241] Aguilar Z. P. Sirisena M. Development of automated amperometric detection of antibodies against Bacillus anthracis protective antigen. *Anal. Biol. Chem*. **2007**, 389, 507−515

[242] Das J., Aziz Md. A., Yang H. A Nanocatalyst-Based Assay for Proteins: DNA-Free Ultrasensitive Electrochemical Detection Using Catalytic Reduction of p-Nitrophenol by Gold-Nanoparticle Labels. *J. Am. Chem. Soc*. **2006**, 128, 16022−16023.

[243] Santandreu M., Sole S., Fabregas E., Alegret S., Development of electrochemical immunosensing systems with renewable surfaces. *Biosens. Bioelectron*. **1998**, 13, 7–17.

[244] He P., Shen L., Cao Y., Li D. Ultrasensitive Electrochemical Detection of Proteins by Amplification of Aptamer-Nanoparticle Bio Bar Codes. *Anal. Chem*. **2007**, 79, 8024−8029.

[245] De la Escosura-Muñiz A., González-García A., Costa-García A. Determination of human serum albumin using aurothiomalate as electroactive label, *Anal. Bioanal. Chem.* **2006**, 384, 742–750.

[246] De la Escosura-Muñiz A., González-García A., Costa-García A. Aurothiomalate as an electroactive label for the determination of Immunoglobulin M, using glassy carbon electrodes as immunoassay transductors. *Sens. Actuators B* **2006,** 114, 473–481.

[247] De la Escosura-Muñiz A., González-García A., Costa-García A Electrocatalytic detection of aurothiomalate on carbon electrodes. Application as a non-enzymatic label to the quantification of proteins. *Anal. Chim. Acta* **2004,** 524, 355–363.

Chapter 2. OBJECTIVES

2. OBJECTIVES

The general objective of this thesis is to design, construct and study affinity biosensors for the electrochemical detection of DNA hybridization and proteins by using nanoparticles as labels and electrochemical stripping analysis as measurement technique.

In order to carry out this general objective, the following particular objectives were established:

1. To design and construct built-in bismuth sensor based on graphite-epoxy composite ($Bi(NO_3)_3$-GECE) for quantitative electrochemical stripping detection and determination of heavy metals – the main constituent of most of the quantum dots.
2. To determine heavy metals by using the built-in bismuth precursor based sensor and electrochemical stripping analysis, as an important step to be studied prior nanoparticle detection.
3. To design and develop a genosensor based on graphite-epoxy composite and an integrated magnet (M-GECE) able to collect paramagnetic microparticles modified with biological molecules labelled with nanoparticles.
4. To modify gold nanoparticles with DNA strands and antibodies and characterise accordingly prior applications in affinity biosensors.
5. To develop different strategies for DNA hybridization detection by using M-GECE and gold nanoparticles as labels easy to be directly detected by electrochemical stripping analysis without previous dissolving.

6. To demonstrate the possibility of using gold nanoparticles as labels for a immunosensor based on graphite-epoxy composite and an integrated magnet (GECE-M) that can detect antigen human IgG as a model protein.

Chapter 3. EXPERIMENTAL

3. EXPERIMENTAL

3.1. Metal analysis using voltammetric stripping sensors

3.1.1. Introduction

Among various environmental pollutants, heavy metals such as cadmium (Cd) and lead (Pb) are considered hazardous, with toxic effects for the living organisms.

To support the development and implementation of environmental monitoring programs, quantitative technologies are necessary for measuring heavy metals exposure.

Environmental monitoring of heavy metals has always relied on highly sensitive different detection methods such as atomic absorption spectrometry (AAS)[1,2], inductively coupled plasma atomic emission spectrometry[3,4], and anodic stripping voltammetry (ASV)[4-6] Often these methods require complex sample preparation and expensive instrumentations. In contrast ASV have some advantages such as little or no sample pre-treatment, is simple, fast, and low cost instrumentation, for which is widely used. Detection limits as low as 10^{-10} have been achieved for many trace metals using ASV.[7]

Mercury film and hanging mercury drop electrodes are routinely used as working electrodes in ASV[8]. This is because mercury has a high overvoltage for hydrogen and also forms metal amalgams that help preconcentrate the analyte metal at the electrode and give well-defined stripping peaks, hence lowering the detection limits. However, the toxicity of mercury limits its use, and this has prompted the

exploration of alternative electrode materials. Use of thin films of bismuth deposited onto different substrates has recently been proposed as a possible alternative to mercury[9-12].

In this thesis a Hg-free sensor for the simultaneous and individual anodic stripping analysis of heavy trace metals such as Pb and Cd among others was constructed. The new sensor was prepared with graphite-epoxy composite electrode (GECE) containing bismuth nitrate $Bi(NO_3)_3$ as built-in bismuth precursor ($Bi(NO_3)_3$-GECE). Different concentrations of $Bi(NO_3)_3$ (0.1, 0.5 and 2 % W/W) in its construction were studied.

Bismuth is an electrode material characterized by its low toxicity and its ability to form alloys with some metals of interest like Cd, Pb or Zn, allowing their preconcentration at the electrode surface.

On the other hand conducting composites represent an effort in designing mercury free sensors for stripping analysis. The capability of integrating various materials is one of their main advantages.

Composite sensors offer many potential advantages including higher signal-to-noise (S/N) ratio[13-18] compared to more traditional electrodes consisting of single conducting phase.

The suitability of $Bi(NO_3)_3$-GECE for analysis of heavy metals was also evaluated by ASV of Pb and Cd in this work, demonstrating the successful response of this new sensor. Its use in the detection of heavy metals applying ASV appears very promising, advantageous and alternative to conventional methods due to their inherent specificity, simplicity and fast response.

This improved analytical sensor will facilitate the establishment of environmental monitoring programs in order to detect Pb and Cd either in soil, water, foods and other real samples with high reproducibility and sensitivity.

Beside environmental applications, the developed sensors should be of great interest for further applications in Quantum Dot (QD) detection and currently in use in the research group for DNA analysis based on QDs (i.e. CdS).

3.1.2. Experimental

3.1.2.1. Apparatus

- SWASV voltammograms were obtained using an electrochemical analyzer Autolab PGSTAT 20 (Eco Chemie, The Netherlands) connected to a personal computer.
- Platinum electrode (model 52-67 1, Crison, Spain); that served as an auxiliary electrode or CE.
- Double junction Ag/AgCl (Orion 900200, Spain) as reference electrode.
- $Bi(NO_3)_3$-GECE as WE (home made as described at section 3.1.3).
- A Hitachi S-570 scanning electron microscope (SEM) was used to observe the surface of the working electrodes.

3.1.2.2. Reagents and Materials

- Epoxy resin (Epotek H77A) and hardener (Epotek H77B), (Epoxy Technology, Inc., USA).
- Graphite powder of particle size 50 μm, (BDH, U.K.).

- Bismuth nitrate, $Bi(NO_3)_3$; Potassium acetate, CH_3-COOK; nitric acid, 65 %; Lead nitrate (II), $Pb(NO_3)_2$ and cadmium nitrate, $Cd(NO_3)_2$, (Sigma-Aldrich).
- Hydrochloric acid to 37 % (PanReac, Barcelona, Spain).

3.1.2.3. Buffers and solutions preparation

All solutions including trace metals (Pb and Cd) were prepared from analytical reagent grade chemicals in deionized water. The Pb and Cd stock solutions were prepared by dissolving the corresponding nitrates in Milli-Q ultrapure water. Acetate buffer (0.1 M, pH 4.5) or HCl 0.5 M were used as supporting electrolyte. The experiments were conducted at 25 ± 1 ºC.

3.1.2.4. Electrode construction

The $Bi(NO_3)_3$-GECE was constructed in two steps, as follows:

— ***Transducer body***

A connection female of 2 mm of diameter is used and a metallic thread placed on it. This connection is welded in its extreme to the centre of the copper disk (6 mm o.d. and 0.5 mm thickness), with the concavity up. (*See* Figure 1A) Previously the copper disk is cleaned by dipping it in HNO_3 solution (1:1) in order to remove copper oxide and rinsed well with bi-distilled water in order to avoid the decrease of the electrical conductivity of the transducer. This connection is introduced into a cylindrical PVC sleeve (6 mm i.d., 8 mm o.d. and 20 mm longitude). (*See* Figure 1B-C). The metallic thread allows that the connection remains fixed well in the end of the cylindrical PVC sleeve, whereas

in another end there stays a cavity of approximately 3 mm deep in which will be placed the conducting paste.

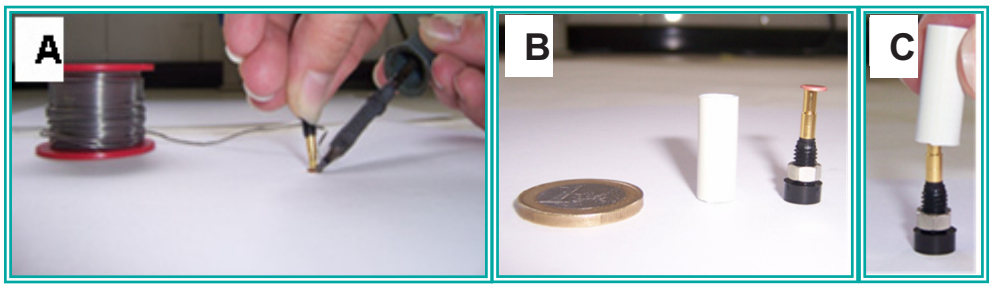

Figure. 3.1. *Pictures of transducer body construction.*

– $Bi(NO_3)_3$-GECE preparation

The graphite powder plus the corresponding percentage of $Bi(NO_3)_3$ (0.1, 0.5, or 2.0 %) are mixed well using a small spatula. The percentage of $Bi(NO_3)_3$ was calculated from of the part of graphite. The epoxy resin and hardener in a ratio 20:3 (w/w) are also mixed well using a small spatula. When the resin and hardener are well-mixed, the graphite powder in the ratio 1:4 (w/w) is added and mixed thoroughly for 30 min to obtain an homogeneous paste of $Bi(NO_3)_3$-graphite-epoxy composite. Table 1 shows the paste composition for $Bi(NO_3)_3$-GECEs.

The resulting conducting paste is introduced into the cylindrical transducer body previously prepared. The electrical contact is completed using the copper disk connected to a copper wire into a cylindrical PVC sleeve (6 mm i.d., 8 mm o.d. and 160 mm longitude) leading to the electrochemical workstation. Afterwards the conducting composite is cured in a dry heat oven at 40 °C for one week or at higher temperature and a minor time.

Once the resin is hardened, prior to use, the surface of the electrode is polished with abrasive papers of higher at lower rugosity grade and then with alumina paper (polishing strips 301044-001, Orion, Spain) and rinsed carefully with bidistilled water.

The prepared working electrode was ready for later measurements connected with the measuring system as will be described in the next sections.

After each measurement the electrode surface could be newly smoothed or polished to provide fresh active material ready to be used in a new assay.

Table 1. *Paste composition of $Bi(NO_3)_3$-GECE.*

$Bi(NO_3)_3$ %−mg	Graphite mg	Resin mg	Hardener mg
0.1−0.7	139.3	243.478	36.5217
0.5−3.5	136.5	243.478	36.5217
2.0−14	126.0	243.478	36.5217

3.1.2.5. Electrode surface characterization

The surface morphologies of $Bi(NO_3)_3$-GECEs (containing 0.1, 0.5 and 2 % of $Bi(NO_3)_3$ salt) before and after the preconcentration step (electrolysis at 21.3 V during 120 s) were observed by SEM. To know more details see publication I (at Chapter 7)

3.1.2.6. Electrochemical procedure

Experiments were carried out using an electrochemical analyzer Autolab PGSTAT 20 (Eco Chemie, The Netherlands) connected to a personal computer. SWASV measurements were performed in the presence of dissolved oxygen. The square wave parameters have been previously optimised in order to maximise the stripping signal.[12]

$Bi(NO_3)_3$-GECE as WE, Ag/AgCl as RE and platinum as auxiliary electrode were immersed into the electrochemical cell containing 25 mL 0.1 M acetate buffer (pH 4.5) as electrolyte. The deposition potential of 21.3 V was applied to $Bi(NO_3)_3$-GECE while the solution was stirred. Following a 120 s deposition step, the stirring was stopped and after 15 s of equilibrium, the voltammogram was recorded by applying a square-wave potential scan between 21.3 and 20.3 V with a frequency of 50 Hz, amplitude of 20 mV and potential step of 20 mV. Aliquots of the target metal standard solution were introduced after recording the background voltammograms. A 60 s conditioning step at +0.6 V (with solution stirring) was used to remove the remaining reduced target metals and bismuth, prior to the next cycle. The electrodes were washed thoroughly with deionized water between each test. The indicated procedure was employed unless stated otherwise.

The influence of the $Bi(NO_3)_3$ has been studied for the different percentages of this salt used in the sensor construction following the same protocol.

A scheme of the sensing design based on $Bi(NO_3)_3$-GECE is shown at Figure 3.2.

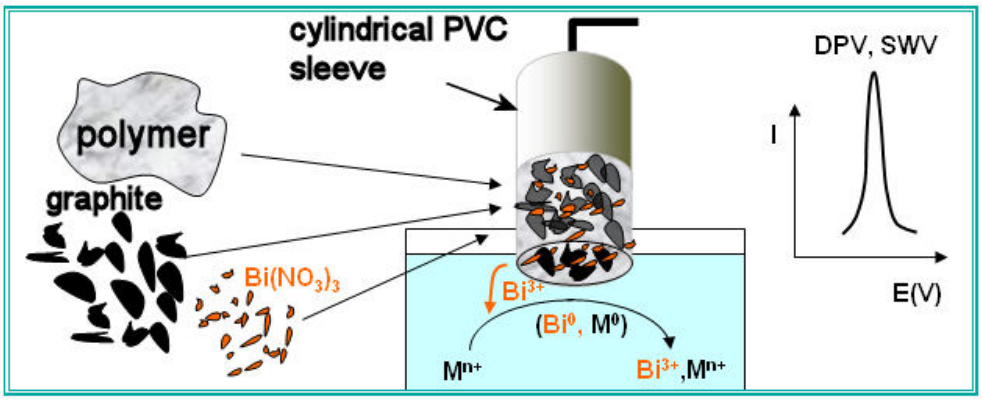

Figure 3.2. *Schematic of the sensing design based on $Bi(NO_3)_3$-GECE. It represents GECE modified internally with bismuth nitrate salt which serves as built-in bismuth precursor for bismuth film formation. The $Bi(NO_3)_3$ modifier particles exposed on the polished surface of the electrode, can be electrochemically reduced in the contact with the measuring solution during the SWASV process, together with the target analytes.*

3.1.3. Results and discussion

The characteristics of the electrodes must be very dependent on the amounts of $Bi(NO_3)_3$ used for the $Bi(NO_3)_3$-GECEs preparation. The Figure 3.3 shows the effect of $Bi(NO_3)_3$ loadings (0.1, 0.5 and 2.0 %, w/w) in the SWASV for Pb^{2+} at the range of 10-70 ppb. The best results were obtained for $Bi(NO_3)_3$-GECE with 0.1 % of $Bi(NO_3)_3$.

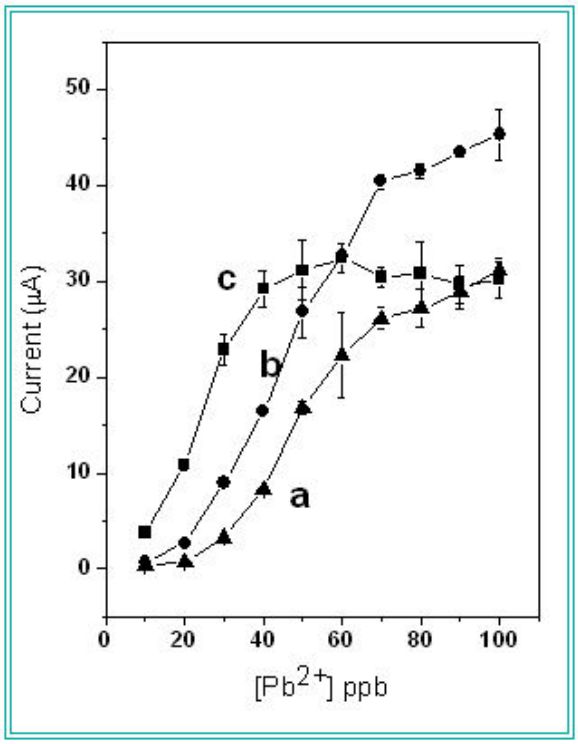

Figure 3.3 *Effect of the bismuth concentration: (a) 0.5 %, (b) 0.1 % y (c) 2 %. SWASV for different concentrations of Pb^{2+} (range 10-70 ppb of Pb^{2+}. Conditions: 0.1 M acetate buffer pH=4.5 as electrolytic cell. Square-wave voltammetric scan with a frequency of 50 Hz, potential step of 20 mV and amplitude of 20 mV*

Individual and simultaneous SWASV measurements of Pb and Cd with the $Bi(NO_3)_3$-GECE were carried out.

The $Bi(NO_3)_3$-GECE exhibited well-defined and separated stripping signals for both metal ions, Cd^{2+} and Pb^{2+}, surrounded with low background contribution and a relatively large negative potential range. The $Bi(NO_3)_3$-GECE revealed good linear behavior in the examined concentration range from 10 to 90 μgL^{-1} for Cd and 10-70 μgL^{-1} for Pb metal ions, with a DL of 7.23 μgL^{-1} for Cd and 11.81 μgL^{-1} for Pb obtained after a 120 s deposition step. The dependences of current responses on heavy metals concentration, as well as calibration curves inside are shown in Figure 3.4.

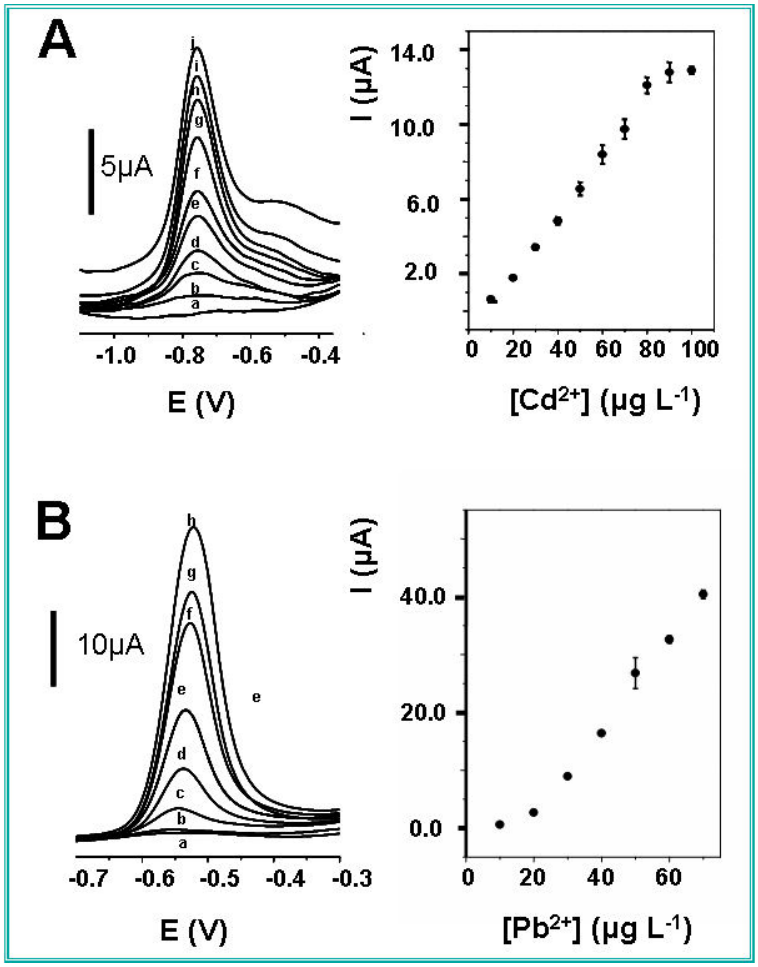

Figure 3.4 *Square-wave stripping voltammograms for increasing concentration of cadmium (A) in 10 μgL^{-1} steps (b–j) and lead (B) in10 μgL^{-1} steps (b–h). Also are shown the corresponding blank voltammograms (a) and the calibration plots (right) over the ranges 10–90 μgL^{-1} cadmium and 10–70 μgL^{-1} lead; solutions 0.1M acetate buffer (pH 4.5); square-wave voltammetric scan with a frequency of 50 Hz, potential step of 20 mV and amplitude of 20 mV; deposition potential of 21.3 V for 120 s.*

3.1.4. Conclusions

A novel and simple GECE that incorporates $Bi(NO_3)_3$ salt in the sensing matrix was developed. SWASV of Pb and Cd was performed demonstrating the successful response of this new $Bi(NO_3)_3$-GECE.

The combination of $Bi(NO_3)_3$-GECE developed with SWASV has been shown to be particularly advantageous for trace heavy metal ions. The main advantages of

this new procedure are the sensitive response, simplicity, low-cost of equipments. Moreover, the surface of the $Bi(NO_3)_3$-GECE could be renewed easily by simple polishing so that the utility of the sensor is improved.

An additional advantage of this approach is the small volume of sample necessary. The small volume of analyte sample helps to reduce contamination effects.

The developed sensors have been with interest for the detection of heavy metal based quantum dots[19] for applications in DNA sensors and immunosensors. This work is still in process at our research group.

3.1.5. References

1 Doner G., Ege A.Determination of copper, cadmium and lead in seawater and mineral water by flame atomic absorption spectrometry after coprecipitation with aluminum hydroxide. *Anal. Chim. Acta* **2005**, 547, 14−17.

2 Kara D., Fisher A., Hill S. J. Preconcentration and determination of trace elements with 2,6-diacetylpyridine functionalized Amberlite XAD-4 by flow injection and atomic spectroscopy. *Analyst* **2005**, 130, 1518−1523.

3 Knauthe B., Otto M., Martin F. A systematic approach to optimum working conditions with inductively coupled plasma atomic emission spectrometry. *Fresenius' J. Anal. Chem*. **2000**, 367, 679−685.

4 Ochsenkühn-Petropoulou M., Ochsenkühn K.-M. Comparison of inductively coupled plasma-atomic emission spectrometry, anodic stripping voltammetry and instrumental neutron-activation analysis for the determination of heavy metals in airborne particulate matter. *Fresenius' J. Anal. Chem*. **2001**, 369, 629−632.

5 Desmond D., Lane B., Alderman J., Hill M., Arrigan D. W. M., Glennon J. D. An environmental monitoring system for trace metals using stripping voltammetry. *Sensors and Actuators B: Chemical* **1998**, 48, 409−414.

6 Baldo M. A., Daniele S. Anodic Stripping voltammetry at bismuth-coated and uncoated carbon microdisk electrodes. *Anal. Lett*. **2004**, 37, 995−1011.

[7] Wang, J. Stripping Analysis: Principles, Instrumentation and Applications, VCH Publishers, Deerfield Beach, FL, 1985.

[8] Economou A., Voulgaropoulos A., LabVIEW-based sequential-injection analysis system for the determination of trace metals by square-wave anodic and adsorptive stripping voltammetry on mercury-film electrodes. *J. Autom. Meth. Manag. Chem*. **2003**, 25, 133−140.

[9] Adraoui I., Rhazi M. E., Amine A. Fibrinogen-Coated Bismuth Film Electrodes for Voltammetric Analysis of Lead and Cadmium using the Batch Injection Analysis. *Anal. Lett.* **2007**, 40, 349−368.

[10] Wang J., Lu J. Bismuth film electrodes for adsorptive stripping voltammetry of trace nickel. *Electrochem. Communications* **2000**, 2, 390−393.

[11] Wang J. Stripping Analysis at Bismuth Electrodes: A Review. *Electroanalysis* **2005**, 17, 1341−1346.

[12] Kirgöz U. A., Marín S., Pumera M., Merkoçi A., Alegret S. Stripping voltammetry with bismuth modified graphite-epoxi composite electrodes. *Electroanalysis* **2005**, 17, 881−886.

[13] Alegret S. Integrated analytical systems, ed. A. Merkoçi and S. Alegret, Elsevier, Amsterdam, **2003**, pp. 377–412.

[14] Moreno-Baron L., Merkoçi A., Alegret S. Graphite-epoxy composite as an alternative material to design mercury free working electrodes for stripping voltammetry. *Electrochim. Acta* **2003**, 48, 2599–2605.

[15] Carrégalo S., Merkoçi A., Alegret S. Applicattion of Graphite-Epoxy Composite Electrodes in Differential Pulse Anodic Stripping Voltammetry of Heavy Metals. *Microchim. Acta* **2004**, 147, 245–251.

[16] Céspedes F., Alegret S. New materials for electrochemical sensing II. Rigid carbon–polymer biocomposites. *Trends Anal. Chem*. **2000**, 19, 276−285.

[17] Alegret S., Fàbregas E., Céspedes F., Merkoçi A., Solé E., Alvareda M., Pividori M. I., The strategy of biosensor surface renewal: past, present and future. A review. *Quim. Anal.* **1999**, 18, 23−29.

[18] Alegret S., Merkoci A., Pividori M. I., Del Valle M., Chapter: "Electrochemical (bio)sensors based on rigid conducting carbon-polymer composites", Encyclopedia of Sensors, Edited by: Craig A. Grimes, Elizabeth C. Dickey, and Michael V. Pishko. **2006**, Volume 3, 23−44.

[19] Merkoçi A., Marin S., Castañeda M. T. , Pumera M., Ros J., Alegret S., Crystal and electrochemical properties of water dispersed CdS nanocrystals obtained via reverse micelles and arrested precipitation, *Nanotechnology* **2006**, 17, 2553−2559.

3.2. DNA analysis based on electrochemical stripping of gold nanoparticles

3.2.1. Introduction

The attractive physicochemical properties of AuNPs are highly affected by its shape and size[1,2]. The size and properties of AuNPs are highly dependent on their preparation conditions[3,4]. Dos Santos et al. have reported the synthesis of AuNPs of different shapes and sizes[5].

Currently synthesis of novel AuNPs with unique properties and with applications in a wide variety of areas is subject of substantial research[6,7].

Among noble-metal nanoparticles, AuNPs have been the most extensively used in electrochemical biosensor applications. This is also due to the fact that the biochemical activity of the labelled receptor biomolecules (i.e. proteins and DNA among others) is retained when AuNPs are coupled to them[8-10].

Nucleic acid biosensors are based on affinity reactions involving DNA molecules and particularly AuNPs have been successfully used as electroactive label in the detection of DNA sequences, based on the highly specific hybridization of complementary strands of DNA[11-16].

On the other hand microscopic magnetic beads on the micron size scale have become useful platforms in order to immobilize biomolecules at different biological assays such those related to antibodies[17], oligonucleotides[13,15,16,18] and another applications[18-20] (*see* Figure 3.5.). Using a magnetic separator the beads allow

isolation and subsequent handling of target molecules in a highly specific manner. Capture, washing steps and detection are easily performed and optimised.

Four different AuNPs-based electrochemical DNA hybridization detection protocols involving the use of either 10 nm diameter AuNP -streptavidin or 1.4 nm diameter monomaleimide-Nanogold – as labels and microparticles –magnetic beads (MB) 2.8 μm diameter– as platforms for DNA probe immobilization were developed at this thesis.

The first two designs are model system assays that consist of the hybridization between a capture DNA strand which is linked with paramagnetic beads and another complementary DNA strand used as target which is labelled with AuNPs. At one of these model system assays a DNA sequence related with breast cancer was used as target.

The other two DNA biosensors designs are sandwich system assays. At these assays the DNA strand related with cystic fibrosis which was used as a target is sandwiched between two complementary DNA probes: the first one linked with paramagnetic beads and a second one labelled with AuNPs either via biotin-streptavidin or thiol-monomaleimide reactions.

Several parameters affecting the hybridization and analytical performance of the developed genosensors were optimized.

AuNPs bound to a DNA can be detected directly or an alternative is the indirect detection by oxidatively dissolving the AuNPs into aqueous metal ions and then electrochemically sensing the ions. The great majority of the AuNPs-based assays have been based on chemical dissolution of the AuNPs tag (in an hydrobromic

acid/bromine mixture) followed by accumulation and stripping analysis of the resulting Au^{3+} solution.[16,21,22]

The HBr/Br_2 solution is highly toxic and therefore methods based on direct electrochemical detection of AuNPs tags, which would replace the chemical oxidation agent, are urgently need[13].

Direct detection of AuNPs but not in connection with the detection of DNA hybridization was reported earlier by our group and Costa-García's group.[23,24]

All the assays developed by our group were based on a magnetically induced direct electrochemical DPV detection of gold tags on magnetic graphite-epoxy composite electrode without need of acidic dissolution.

The developed genomagnetic sensors provide a reliable discrimination against noncomplementary DNA as well against one and three-base mismatches.

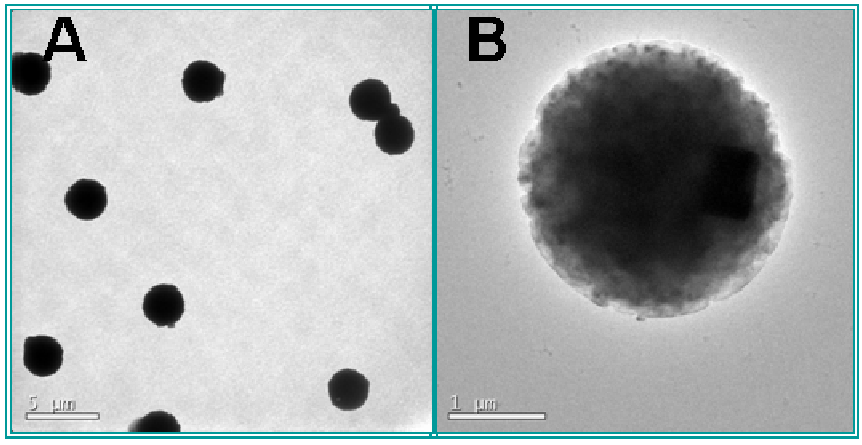

Figure 3.5. *TEM images of paramagnetic beads 2.8 µm diameter (MB) at: (A) 600X and (B) 4000X magnifications.*

3.2.2. Experimental

Apparatus, some reagents and procedures described at this section are common to the different strategies developed at this thesis, but the protocols of the assays will be described separately.

3.2.2.1. Apparatus

- Electrochemical analyzer Autolab PGSTAT 20 (Eco Chemie, The Netherlands) connected to a personal computer for DPV analysis.
- Platinum electrode (model 52-67 1, Crison, Spain); that served as an auxiliary electrode.
- Double junction Ag/AgCl (Orion 900200, Spain) as reference electrode.
- Magnetic graphite epoxy composite electrode (M-GECE) as working electrode (home made as is described at section 3.2.2.5.).
- TS-100 Thermo Shaker (Spain) for the binding of streptavidin-coated paramagnetic beads (MB) with biotinylated probe (Immobilization DNA) and hybridization events.
- MCB 1200 biomagnetic processing platform (Sigris, CA, USA), in order to carry out the magnetic separation.
- Power supply, 3000V/300mA/300W (Code PS3003, Ecogen, S.R.L., Spain).

- A BlueMarine 100 (Inverness Medical Ibérica, S.A.U., Barcelona, Spain) horizontal electrophoresis unit tray is used in order to carry out the gel electrophoresis.
- TEM images were taken using a Jeol JEM-2011 electronic microscope (Jeol Ltd., Tokyo, Japan).
- Melting curves were generated in a spectrophotometer (Jasco V550) equipped with a temperature controller.

3.2.2.2. Reagents and materials

All reagents and materials used in DNA analysis are listed below:

- Tris (hydroxymethyl) methylamine (Tris), sodium chloride, sodium citrate, ethylenediamine tertraacetic acid disodium salt (EDTA), lithium chloride, tween 20, boric acid, nitric acid 65 %, bovine serum albumin (BSA), (Molecular Biology reagent, Ref. B428, glycerol (G8773-500 mL), 2-Propanol and bromophenol blue sodium salt (B8026) from Sigma-Aldrich.
- Hydrochloric acid to 37 % (PanReac, Barcelona, Spain).
- Xylenecyanol FF, (95600-10G, Fluka).
- Agarose (Molecular Biology grade, Roche).
- Streptavidin-coated paramagnetic beads of diameter 2.8 µm (concentration: 10 mg/mL) –Dynabeads M-280 Streptavidin– (Dynal Biotech, Norway).
- Monomaleimide-Nanogold, 1.4 nm diameter (also named here maleimide-Au_{67} quantum dots or AuNPs) (Nanoprobes Inc., NY.).
- Gold Streptavidin (AuNPs 10 nm diameter), Sigma-Aldrich.

- Epoxy resin (Epotek H77A) and hardener (Epotek H77B), (Epoxy Technology, Inc., USA).
- Graphite powder of particle size 50 μm, (BDH, U.K.).
- Neodymium magnet (diameter 3 mm, height 1.5 mm), Halde Gac Sdad, Spain. (catalog number N35D315)

3.2.2.3. Oligonucleotides

Biotinylated probe oligonucleotide and no modified oligonucleotides were received from Alpha DNA, Canada. Oligonucleotides modified with thiol (–SH) group were synthesized in our laboratory on an automatic Applied Biosystems DNA synthesizer, model 392, and according described procedure[25].

Oligonucleotides purchased from Alpha DNA, Canada arrived in pellet form. These were rehydrated in autoclaved Milli-Q water and split in 100 μL aliquots which were stored in a −20 ºC freezer and when required an aliquot was thawed just prior to use and were touched only with gloved hands in order to avoid any contamination. Oligonucleotide sequences and modifications used in the different assays are listed in Tables 2, 3, 4 and 5.

3.2.2.4. Buffers and solutions preparation

All buffers and stock solutions used in this thesis were prepared using deionized and autoclaved water and stored in refrigerator (4 ºC) until its use. These are outlined below:

- 2xB&W: 10 mM Tris HCl (pH 7.5), 1 mM EDTA and 2.0 M NaCl.

- B&W: was prepared from 2xB&W diluting with the deionized autoclaved water.
- TTL buffer: 100 mM Tris.HCl, pH 8.0; 0.1 % Tween 20; and 1M LiCl.
- TT buffer: 250 mM Tris–HCl, pH 8.0; and 0.1 % Tween 20.
- TTE buffer: 250 mM Tris–HCl, pH 8.0; 0.1 % Tween 20; and 20 mM Na_2 EDTA, pH 8.0.
- Hybridization solution: 750 mmol/L NaCl, 75 mmol/L sodium citrate.
- Supporting electrolyte: HCl 0.1 M solution.
- 5X Tris-Borate-EDTA Buffer (TBE) as running buffer, Composition of 10X TBE Buffer, for 1 Liter: 108 g Tris, 55 g Boric acid, 40 mL 0.5 M EDTA (pH 8.0) and Milli-Q water to 1 L. The pH is 8.3 and requires no adjustment. Dilute 1 in 20 to obtain 5X TBE buffer.
- Dyes: Bromophenol blue and xylenecyanol FF. For a 10X concentrated solution, the composition is the following: 0.2 % xylenecyanol FF, 0.2 % bromophenol blue, 50 % glycerol and 10X TBE buffer Milli-Q Water. For preparing 100 mL add: 0. 2 g of xylenecyanol, 0.2 g of bromophenol blue, 50 g of glycerol, 10 mL TBE 10X and 40 mL of Milli-Q water. Add 1 µL by each 9 mL of solution.
- BSA at 10 %: Weigh 10 g of BSA powder and place it in a 125 mL flask, then add 100 mL of hybridization solution (prepared previously as in 4) to the flask. Swirl to mix the solution.

3.2.2.5. Electrode construction

The construction of the working electrode (M-GECE) involved the following two steps:

– Transducer body construction

This is similar as previously has been described (*See* Section 3.1.2.4.) but in this case the cylindrical PVC sleeve used is of a longitude of 22 mm owing to that a cavity of a higher depth is required.

– M-GECE preparation

The epoxy resin and hardener are mixed manually in a ratio 20:3 (w/w) using a small spatula. When the resin and hardener are well-mixed, the graphite powder in the ratio 20:80 (w/w) is added and mixed thoroughly for 30 min to obtain a homogeneous paste of graphite-epoxy composite. The resulting conducting paste of graphite epoxy composite is introduced into the cylindrical transducer body where a neodymium magnet is previously introduced, 2 mm under the surface of the electrode in such a way that the small neodymium magnet stays between 2 layers of graphite epoxy composite. (*See* Figure. 3.6A)

The electrical contact is completed using the copper disk connected to a copper wire into a cylindrical PVC sleeve (6 mm i.d., 8 mm o.d. and 160 mm longitude) leading to the electrochemical workstation. (*See* Figure 3.6B) The conducting composite is cured, polished and smoothed in the same way as for $Bi(NO_3)_3$GECE preparation (see Section 3.1.2.4.). The prepared M-GECE was ready for later

measurements in a three electrode set-up (*see* Figure 3.6C) connected with the measuring system (*see* Figure 3.6D) as will be described in section 3.2.2.6.

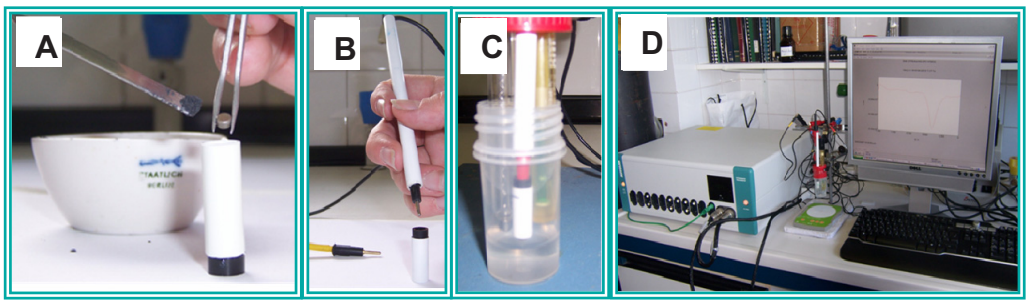

Figure. 3.6. *Pictures of M-GECE-M preparation (A-B); system of three electrodes, from left to right: auxiliary, working and reference immersed into electrochemical cell (C); electrochemical analyzer Autolab PGSTAT 20 connected to a personal computer, at which DPV electrochemical detection of AuNPs was carried out (D).*

3.2.2.6. Electrochemical detection

The electrochemical detection is an extensively used method to analyze specific DNA sequences by means of the hybridization event due to its simplicity, selectivity, instrumentation of low cost and high sensitivity.

At all the assays developed in this part of the thesis, the amount of AuNPs tag was determined by DPV according to the following procedure. The following parameters have been used: deposition potential, +1.25 V; duration, 120 s; conditioning potential, 1.25 V; step potential, 10 V; modulation amplitude, 50 mV. A blank was run by triplicate immersing the three electrodes: M-GECE as working electrode, the Ag/AgCl as reference electrode and the platinum electrode as auxiliary in an electrochemical cell containing 10 mL of HCl 0.1 M as supporting electrolyte. The responses were saved. (*See* Figure 3.6C). The electrodes were rinsed well with Milli-Q water. Afterwards the sample was

placed onto the surface of M-GECE during 60 s time during which is accumulated on it due to the inherent magnetic field of the electrode. The sample measurement was carried out by immersing also the three electrodes in the electrochemical cell containing 10 mL of HCl 0.1 M solution as supporting electrolyte. The response was saved. (*See* Figure 3.6C)

The electrochemical oxidation of AuNPs to $AuCl_4^-$ was performed at +1.25 V (vs. Ag/AgCl) for 120 s in the nonstirred solution. Immediately after the electrochemical oxidation step, was performed DPV. During this step scan the potential from +1.25 V to 0 V with step potential 10 mV, modulation amplitude 50 mV, scan rate 33.5 mVs^{-1}, no stirred solution. The influence of time and potential of electrochemical oxidation of AuNPs to $AuCl_4^-$ upon the DPV signal also are studied in order to establish the optimal values.

The response saved for the blank was subtracted from the sample response using the Autolab software. The result which is an analytical signal due to the reduction of $AuCl_4^-$ at potential +0.4 V was saved.[23] The DPV peak height at the potential of +0.4 V as the analytical signal was used in all of the measurements. Figure 3.7a shows the typical differential pulse voltammogram for the oxidation signal of Au during a sandwich assay.

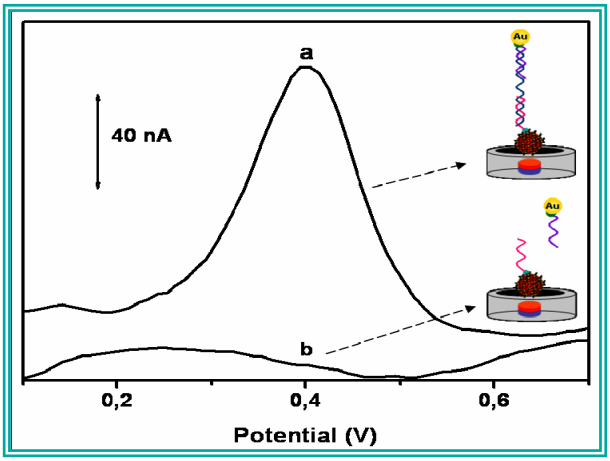

Figure 3.7. *Typical DPV voltammograms for the oxidation signals of Au during a sandwich assay to 38 pmol of target (a) and sandwich assay without target used as control (b). Conditions: hybridization time, 15 min; hybridization temperature, 42 ^{o}C; amount of paramagnetic beads, 50 µg; electrooxidation potential, +1.25 V; electrooxidation time, 120 s; DPV scan from +1.25 V to 0 V, step potential 10 mV, modulation amplitude 50 mV, scan rate 33.5 mVs^{-1}, nonstirred solution.*

The Au reduction signal current is proportional to the amount of AuNPs, which corresponds to the concentration of hybridized DNA target. The quantitative result is obtained from the corresponding calibrate plot. Figure 3.7b shows the DPV response (almost negligible) to control assay owing to the fact that the sandwich is not formed.

3.2.2.7 Model system assay for DNA hybridization electrochemical detection by using 1.4 nm Au_{67} quantum dot tag linked to the target DNA

The first assay developed was a model system as an initial strategy proposed. At this assay the binding of the capture probe DNA to the MB is achieved via streptavidin-biotin interaction and then hybridized with the target DNA labelled previously with Au_{67} (monomaleimide-Nanogold of 1.4 nm diameter) in the ratio 1:1.

— ***Oligonucleotide sequences***

The oligonucleotide sequences used at this assay are shown in Table 2.

Table 2. *Oligonucleotide sequences used at model system assay using Au_{67} as tag*

NAME	USE	SEQUENCE[1]
DNA1	**Target**	**5′TCT CAA CTC GTA-phosphate-O$(CH_2)_3$-CONH-CH(CH_2SH)-CONH-$(CH_2)_6$-0H**
DNA2	**Capture**	**5′TAC GAG TTG AGA-biotin3′**
DNA-NC	**Noncomplementary**	**thiohexyl-5′CGA GTC ATT GAG TCA TCG AG3′**

— ***Preparation of the Au Quantum dot modified DNA (1:1 Au_{67}-DNA1)***

The binding of maleimide-Au_{67} quantum dot to the thiol DNA1 in the ratio 1:1 was preformed as described previously[25] (for reaction scheme, *see* Figure 3 of publication VI, Chapter 7 of this thesis). Briefly: Mix aliquots of lyophilized maleimide- Au_{67} nanoparticles (6 nmols) with thiol-oligonucloetides (6 nmols) dissolved in 10 % 2-propanol. Keep the resulting mixtures overnight at room temperature and store the resulting solutions in refrigerator until further use.

Gel electrophoresis was used to determine the purity of discrete Au_{67} nanocrystal-DNA1 conjugates in 2 % agarose gel at 80 V, with electrophoresis time 20 min, using 0.5x TBE as a running buffer.[26,27] This procedure is described in more detail at section 3.2.2.10. of this thesis.

— ***Immobilization of the DNA probe (DNA2) onto paramagnetic beads***

The binding of the biotinylated probe with MB was carried out using a slightly modified procedure recommended by Dynal Biotech.[28] Briefly:

100 μg of MB were transferred into 1.5 mL Eppendorf tube. The MB were washed with 100 μL B&W buffer three times, resuspended in 50 μL of B&W buffer, and then 5 μg of probe DNA2 were added. The volume was adjusted to 100 μL as well as the concentration of NaCl to 1.0 M by 2xB&W buffer and autoclaved water. The resulting solution was incubated for 15 min at temperature of 25 °C with gentle mixing in a TS-100 ThermoShaker. The MB with immobilized probe from the incubation solution were magnetically separated by placing the tube on magnetic processing platform and washed 3 times with 100 μL of B&W buffer. (*See* Figure 3.8) Completed the preparation process by resuspending the DNA2 modified beads in 50 μL of B&W buffer were ready for the corresponding hybridization. (*See* Figure 3.9A).

Figure 3.8. *MCB 1200 biomagnetic processing platform in which magnetic separations are carried out.*

— ***Hybridization procedure***

The desired amount of Au_{67} marked DNA1 was added in the solution (50 µL) of DNA2 modified beads in B&W buffer prepared previously, and the volume adjusted to 100 µL keeping the NaCl concentration at 1.0 M by adding 2xB&W buffer and autoclaved water. (*See* Figure 3.9B) The hybridization reaction was carried out during 15 min at 42 °C in TS-100 Thermo Shaker (if not stated otherwise). (*See* Figure 3.9C) The final Au_{67}-DNA1/DNA2-paramagnetic bead conjugates (*see* Figure 3.9C) was washed 3 times with 100 µL of B&W buffer and resuspended in 50 µL of B&W buffer. The surface of magnetic graphite-epoxy composite electrode was then brought into contact for 60 s with the solution containing Au_{67} -DNA1/DNA2-paramagnetic beads conjugates which accumulated on it due to the inherent magnetic field of the electrode. (*See* Figure 3.9D).

— ***Electrochemical detection***

The electrochemical method used was DPV which has been explained at section 3.2.2.6. (*See* Figure 3.9E).

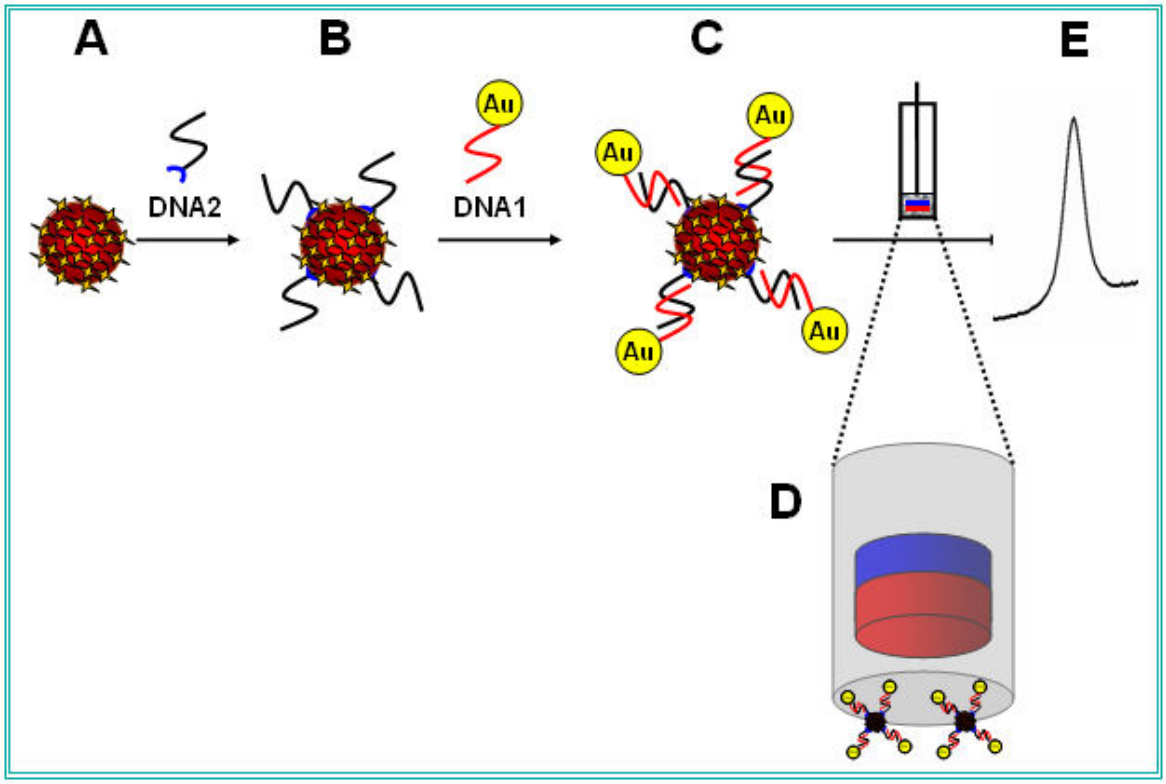

Figure 3.9. *Schematic representation of the analytical protocol (not in scale): (A) introduction of streptavidin coated paramagnetic beads; (B) immobilization of the biotinylated probe (DNA2) onto the paramagnetic beads; (C) addition of the 1:1 Au_{67}-DNA1 target; (D) accumulation of Au_{67}-DNA1/DNA2- paramagnetic bead conjugate on the surface of magnetic electrode; (E) magnetically trigged direct DPV electrochemical detection of gold quantum dot tag in Au_{67}-DNA1/DNA2- paramagnetic bead conjugate. Adapted of publication VI (at chapter 7)*

— ***Discrimination study***

To study the discrimination between DNA-NC (noncomplementary) and three base mismatches DNA and the DNA1 (target DNA) (*see* sequences in Table 2) in order to demonstrate the selectivity of the genomagnetic model system assay protocol the same protocol above described, was performed but supplying non complementary DNA or three base mismatches DNA by DNA1. On the other hand an assay by using graphite-epoxy composite electrode without magnet (GECE) was carried out in order to demonstrate the effective magnetic triggering of M-GECE. For more details see publication VI (at chapter 7).

3.2.2.8. Model system assay for DNA hybridization electrochemical detection. Use of a *BRCA1* breast cancer gene related DNA strand as target and 10 nm diameter AuNPs as label

This assay is based on the hybridization between a capture DNA strand modified with biotin which is linked with paramagnetic beads via streptavidin- biotin and another DNA strand related to *BRCA1* breast cancer gene used as a target also modified with biotin and which is marked with 10 nm diameter streptavidin modified Au-NPs also via streptavidin-biotin linkage.

— *Oligonucleotide sequences*

The oligonucleotide sequences used in this assay are listed at Table 3.

Table 3. *Oligonucleotide sequences for model system assay by using 10 nm diameter AuNPs as label*

NAME	USE	SEQUENCE[1]
BC-A	**Capture**	**biotin-5′GAT TTT CTT CCT TTT GTT C3′**
BC-T[2]	**Target**	**biotin-5′GAA CAA AAG GAA GAA AAT C3′**
BC-MX3	**Three base mismatch**	**biotin-5′GAA CAA ATC TAA GAA AAT C3′**
BC-NC	**Noncomplementary**	**biotin-5′GGT CAG GTG GGG GGT ACG CCAGG3′**

[1] Red colour nucleotides correspond to mismatches
[2] Target related to *BRCA1* breast cancer gene

– Immobilization of the capture DNA probe (BC-A) onto paramagnetic beads

100 μg of MB (*see* Figure 3.10A) were transferred into 0.5 μL Eppendorf tube. The MB were magnetically separated (*see* Figure 3.8), decanted and washed once with 100 μL of TTL buffer and then separated, decanted and resuspended in 20 μL of TTL buffer.

The desired amount of BC-A (capture DNA) was added. (*See* Figure 3.10B) The resulting solution was incubated for 15 min at temperature of 25 ºC with gentle mixing in a TS-100 ThermoShaker, so as to ensure immobilization. Then the MB with the immobilized BC-A were separated from the incubation solution, decanted and washed sequentially with 100 μL of TT, TTE and TT buffers with the appropriate magnetic separation steps and then decanted and resuspended in 50 μL of hybridization solution. The suspension of MB-modified with BC-A was ready for the hybridization.

– Hybridization procedure

The desired amount of BC-T (target DNA) was added to the previous suspension (50 μL of MB/BC-A conjugate) (See Figure 3.10C), then was incubated at 42 ºC for 15 min and with gentle mixing in TS-100 Thermo Shaker in order to carry out the hybridization reaction. The formed MB/BC-A/BC-T conjugate was washed twice with 100 μL of TT buffer and resuspended in 20 μL of TTL buffer. It was ready for adding streptavidin–gold nanoparticles (AuNPs) label.

— ***Binding of the streptavidin-coated AuNPs***

The desired amount of AuNPs was added to the resulting MB/BC-A/BC-T conjugate (*see* Figure 3.10D) and then incubated for 15 min at 25 ºC and with gentle mixing in TS-100 Thermo Shaker. The resulting MB/BC-A/BC-T/AuNPs conjugate was washed twice with 100 µL of TT buffer and then separated, decanted and resuspended in 50 µL of hybridization solution. The surface of M-GECE was brought into contact for 60 s with the solution containing the MB/BC-A/BC-T/Au-NPs conjugate that is accumulated on it due to the inherent magnetic field of the electrode. (*See* Figure 3.10E) The M-GECE was ready for the immediate DPV detection of AuNPs labels anchored onto the surface through the conjugate.

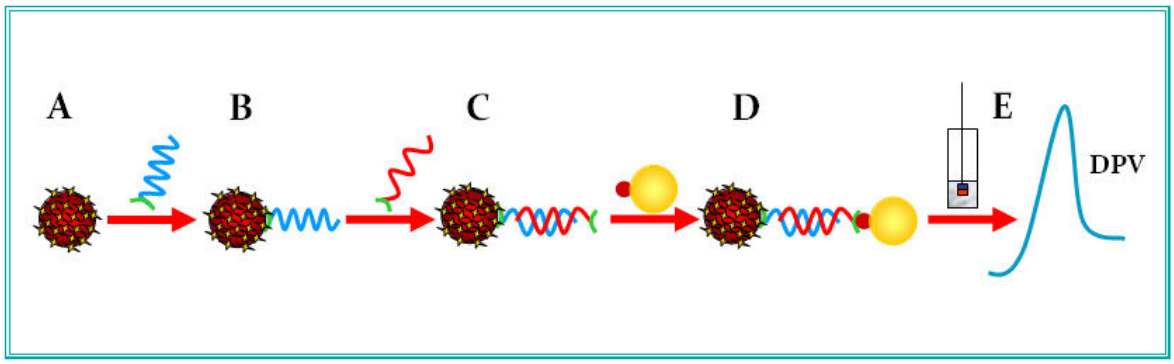

Figure 3.10. *Schematic representation of the analytical protocol (not in scale): (A) introduction of the streptavidin-coated magnetic beads; (B) immobilization of the biotinylated BC-A probe onto the magnetic beads; (C) addition of the biotinylated BC-T probe, hybridization event; (D) addition and capture of the streptavidin-gold nanoparticles; (E) accumulation of final AuNPs-BCT/BC-A-magnetic beads conjugate on the surface of the M-GECE and magnetically trigged direct DPV electrochemical detection of AuNPs tag in the conjugate.*

— ***Discrimination study***

A study of discrimination between BC-MX3 (three base mismatch) and BC-NC (noncomplementary) and the BC-T (target DNA) (*see* sequences in Table 3) in

order to demonstrate the selectivity of the genomagnetic model system assay protocol was performed following the same protocol above described. Of the same way here a study of the DPV response of BC-T on GECE was carried out.

See more details about the procedure of this assay in publication IV (at chapter 7).

– ***Electrochemical detection***

The electrochemical detection was carried out at the same way as has been described at section 3.2.2.6.

3.2.2.9. Sandwich system assay for DNA hybridization electrochemical detection. Use of a cystic fibrosis related DNA strand as target and 10 nm diameter AuNPs as label

In this sandwich assay the target is sandwiched between two complementary DNA probes in which the first one (capture DNA probe) modified with biotin is linked with paramagnetic beads via streptavidin-biotin and a second one which is modified with biotin and labelled with AuNPs of 10 nm diameter modified with streptavidin, also is linked via streptavidin biotin.

– **Oligonucleotide sequences**

The sequences of the oligonucleotides used at this assay are shown at Table 4

Table 4. *Oligonucleotide sequences used at sandwich system assay using 10 nm diameter AuNPs as label*

NAME	USE	SEQUENCE[1]
CF-A	**Capture**	**5′-TGC TGC TAT ATA TAT-biotin-3′**
CF-T[2]	**Target**	**5′-ATA TAT ATA GCA GCA GCA GCA GCA GCA GAC GAC GAC GAC TCT C-3′**
CF-B	**Signaling**	**biotin-5′GAG AGT CGT CGT CGT-3′**
CF-MX1	**One base mismatch**	**5′-ATA TAT AAA GCA GCA GCA GCA GCA GCA GAC GAC GAC GAC TCT C-3′**
CF-MX3	**Three base mismatches**	**5′-ATA TAT CCC GCA GCA GCA GCA GCA GCA GAC GAC GAC GAC TCT C-3′**
CF-NC	**Noncomplementary**	**biotin-5′GGT CAG GTG GGG GGT ACG CCA GG-3′**

[1] Red colour nucleotides correspond to mismatches
[2] Target related to Cystic fibrosis gene

— Immobilization of the capture DNA probe (CF-A) onto paramagnetic beads

100 μg of MB (*see* Figure 3.11A) were transferred into 0.5 μL Eppendorf tube The MB were magnetically separated (*see* Figure 3.8), decanted and washed once with 100 μL of TTL buffer and then separated, decanted and resuspended in 20 μL of TTL buffer. The desired amount of CF-A (capture DNA) was added. (*See* Figure 3.11B) Then the resulting solution was incubated for 15 min at temperature of 25 ºC with gentle mixing in a TS-100 ThermoShaker, so as to ensure immobilization.

The MB with the immobilized CF-A were separated from the incubation solution, decanted and washed sequentially with 100 μL of TT, TTE and TT buffers with the appropriate magnetic separation steps and then decanted and resuspended in 50 μL of hybridization solution, which is ready for the first hybridization.

— First hybridization procedure

The desired amount of CF-T (target DNA) was added to the 50 μL of MB/CF-A conjugate obtained in the previous step. (*See* Figure 3.11C) and was incubated at 25 ºC for 15 min and with gentle mixing in TS-100 Thermo Shaker in order to carry out the first hybridization reaction. (*See* Figure 3.11C) The formed MB/CF-A/CF-T conjugate was washed twice with 100 μL of TT buffer and resuspended in 20 μL of TTL buffer. It was ready for the second hybridization reaction.

— Second hybridization procedure

The desired amount of CF-B (signaling DNA) was added to the 50 μL of MB/CF-A/CF-T conjugate obtained in the previous step (*See* Figure 3.11D) Then incubated at 25 ºC for 15 min and with gentle mixing in TS-100 Thermo Shaker in order to carry out the second hybridization reaction. (*See* Figure 3.11D) The formed MB/CF-A/CF-T/CF-B conjugate was washed twice with 100 μL of TT buffer and resuspended in 20 μL of TTL buffer. It was ready for adding streptavidin–gold nanoparticles (Au-NPs) label.

— Binding of the streptavidin-coated AuNPs

The desired amount of Au-NPs was added to the resulting MB/CF-A/CF-T/CF-B conjugate (*see* Figure 3.11E) and then incubated for 15 min at 25 ºC and with gentle mixing in TS-100 Thermo Shaker.

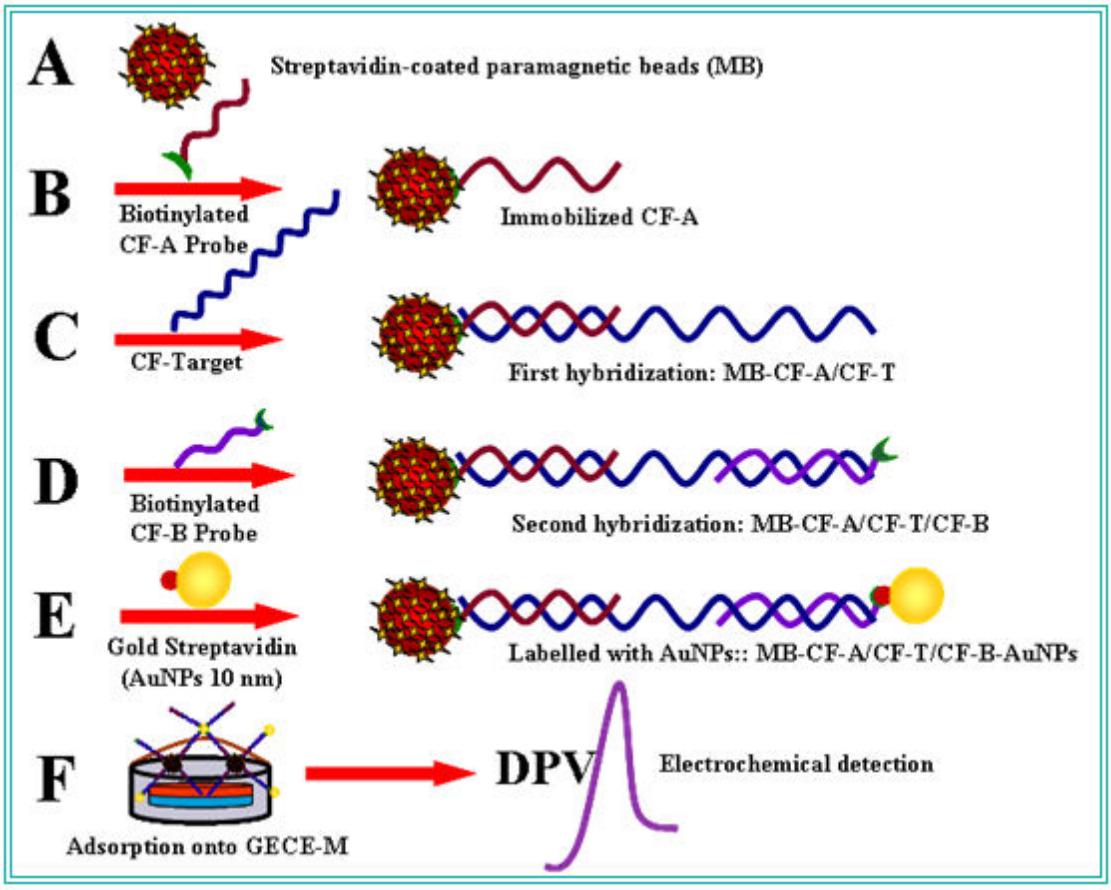

Figure 3.11 *Schematic representation of the sandwich system analytical protocol (not in scale): (A) Streptavidin-coated magnetic beads; (B) immobilization of the biotinylated CF-A probe onto the magnetic beads; (C) addition of CF-T (first hybridization event); (D) addition of biotinylated CF-B probe (second hybridization event); (E) labelling by using the streptavidin-gold nanoparticles; (F) accumulation of Au-NPs-DNA-magnetic bead conjugate on the surface of M-GECE and magnetically trigged direct DPV electrochemical detection of Au-NPs tag in the conjugate.*

The resulting MB/CF-A/CF-T/CF-B/Au-NPs conjugate was washed twice with 100 μL of TT buffer and then separated, decanted and resuspended in 50 μL of hybridization solution. (*See* Figure 3.11E) The surface of M-GECE into was brought in contact for 60 s with the solution containing the MB/CF-A/CF-T/CF-B/Au-NPs conjugate that is accumulated on it due to the inherent magnetic field of the electrode. (*See* Figure 3.11F) The M-GECE is ready for the immediate

DPV detection of Au-NPs labels anchored onto the surface through the conjugate.

― ***Discrimination study***

A study of discrimination between CF-MX, CF-MX3, CF-NC and the CF-T (*see* sequences in Table 4) in order to demonstrate the selectivity of the genomagnetic sandwich assay protocol was performed following the same protocol above described as well as with GECE in order to know the DPV response of CF-T.

― ***Electrochemical detection***

The electrochemical detection was carried out at the same way as has been described at section 3.2.2.6.

3.2.2.10. Sandwich system assay for DNA hybridization electrochemical detection. Use of a cystic fibrosis related DNA strand as target and 1.4 nm diameter AuNPs as label

In this approach the DNA sensor design is based on a sandwich detection strategy in which a cystic fibrosis related DNA strand is used as target sandwiched between two complementary DNA probes: the DNA capture probe immobilized on MB via streptavidin-biotin and the DNA signaling probe modified with thiol and labelled with AuNPs via reaction of thiol group with monomaleimide so as to ensure a 1:1 AuNP-DNA probe connection. DPV is used for a direct voltammetric detection of AuNPs onto M-GECE.

— ***Functionalization of monomaleimide-Nanogold 1.4 nm***

Monomaleimide-Nanogold 1.4 nm *(*AuNPs) was functionalized with signaling DNA (CF-B). This oligonucleotide modified with thiol (–SH) group is directly bound to the surface of AuNPs tags.

The binding is carried out via reaction of maleimide-thiol group as has been described previously. Figure 3.12A shows a schematic illustration of the method to functionalization of AuNPs with thiol DNA CF-B. Briefly:

Aliquots of lyophilized AuNPs (6 nmol) with CF-B (6 nmol) were mixed and dissolved in 10 % 2-propanol.

The mixture was kept overnight at room temperature and the resulting solution stored in refrigerator until further use. The maleimide group reacts specifically with sulfhydryl groups when the pH of the reaction mixture is between pH 6.5 and 7.5 and forms a stable thioether linkage that is not reversible. (*See* Figure 3.12B)

The obtained DNA-functionalized AuNPs carry a negative surface charge provided by the anionic thiolated oligonucleotide.

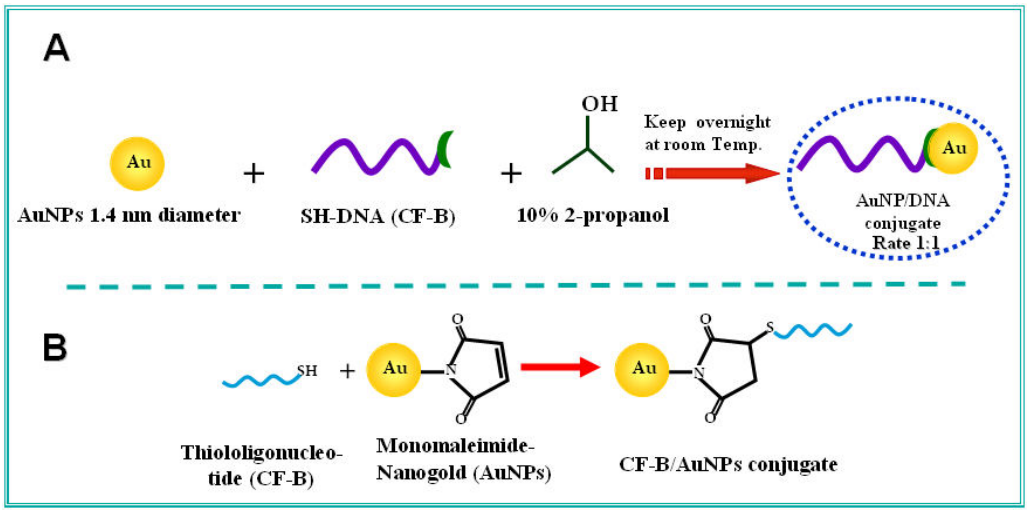

Figure 3.12. *Schematic illustrations (not in scale) of functionalization of monomaleimide-Nanogold with thiol-DNA (CF-B) (**A**) and monomaleimide-Nanogold with thiol-oligonucleotide reaction (**B**).*

— *Oligonucleotide sequences*

The sequences of the oligonucleotides used at this assay are shown at Table 5.

Table 5. *Oligonucleotide sequences used at sandwich system assay using 1.4 nm diameter AuNPs as label*

NAME	USE	SEQUENCE[1]
CF-A	Capture	5′-TGC TGC TAT ATA TAT-biotin-3′
CF-T[2]	Target	5′-ATA TAT ATA GCA GCA GCA GCA GCA GCA GAC GAC GAC GAC TCT C-3′
CF-B	Signaling	thiol-5′GAG AGT CGT CGT CGT-3′
CF-MX1	One base mismatch	5′-ATA TAT AAA GCA GCA GCA GCA GCA GCA GAC GAC GAC GAC TCT C-3′
CF-MX3	Three base mismatch	5′-ATA TAT CCC GCA GCA GCA GCA GCA GCA GAC GAC GAC GAC TCT C-3′
CF-NC	Noncomplementary	biotin-5′GGT CAG GTG GGG GGT ACG CCA GG-3′

[1] Red colour nucleotides correspond to mismatches
[2] Target related to Cystic fibrosis gene

— ***Agarose gel electrophoresis of the DNA-functionalized AuNPs***

To verify the purity of the functionalization of AuNPs with CF-B a gel electrophoresis was carried out. The CF-B/AuNPs conjugate sample and control dyes (bromophenol blue and xylenecyanol FF) were loaded in the wells of a 2 % agarose gel and a 80 V voltage was applied along the gel, with electrophoresis time of 20 min, using 0.5X tris-borate-EDTA (TBE) buffer as a running buffer. A detailed description of the procedure is given in the following two sections.

— ***Agarose gel to the 2 %***

To prepare gel agarose 1 g of agarose powder was weighted and dissolved in 50 mL of 1X TBE buffer (50 mL are needed for a single gel). The solution was mixed and heated in the microwave until the solution is completely clear and no small floating particles were visible (about 2 minutes). (*See* Figure 3.13A) The solution was cooled to 55 ºC before pouring the gel into the plastic casting tray and the plastic comb was placed in the slots on the side of the gel tray. The agarose mixture was poured into the gel tray until the comb teeth are immersed about 6 mm or 1/4 " into the agarose. *See* Figure 3.13B) The agarose gel was allowed to be cooled until solidified. The gel appears as cloudy white colour after cooling during about 20 minutes. See more details in Annex of this thesis.

— ***Gel electrophoresis***

To carrier out the electrophoresis, the comb from the wells by pulling straight up on the comb was removed. The tape from both ends of the gel tray was removed

carefully. The gel tray in the gel box with the wells closest to the negative (black) electrode was placed. Enough 1X TBE buffer was added to fill the electrophoresis chamber and submerge the gel about 1/4 of inch. 20 µL of control dyes into the first well and 20 µL of MB-CFA conjugate in the next well were loaded. Then the top of the electrophoresis chamber was closed and the leads pluged into the electrophoresis chamber. (*See* Figure 3.13C) The gel was run at 80 V until the loading dye had migrated 1/2 of the way down the gel approximately (about 20 minutes). (*See* Figure 3.13D) The power supply was turned off. The migration of the CF-B/AuNPs conjugate towards the '+' electrode and the discrete band of the conjugate, which indicate its successful preparation was observed.

The gel was then observed and scanned using an overhead projector. (*See* Figure 3.13E) The obtained conjugate as resulted from functionalization could then assemble with target DNA. See more details at Annex of this thesis.

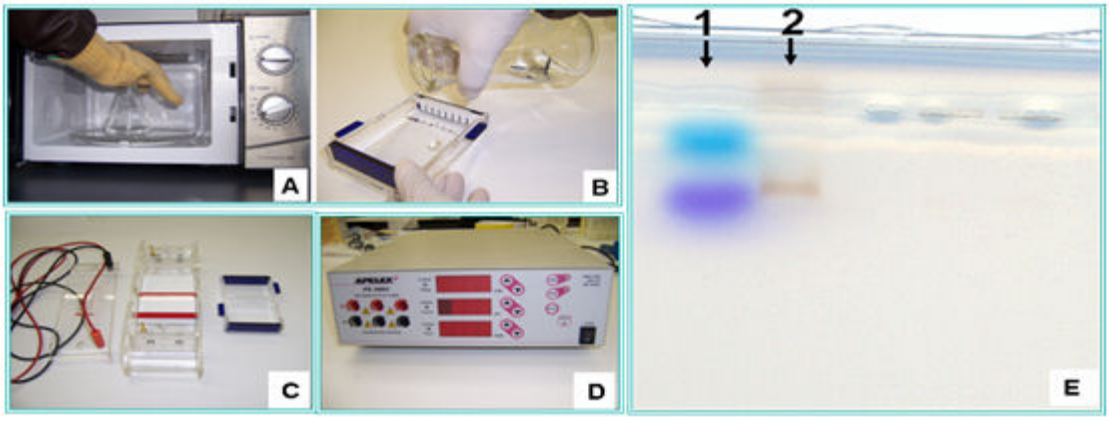

Figure 3.13. *Agarose gel to 2% dissolution at microwave (A), Pour the agarose mixture into the gel tray until the comb teeth are immersed about 6 mm or 1/4" into the agarose. Gel electrophoresis chamber (C), Power supply (D). Agarose gel in which the corresponding bands of control of bromophenol blue and xylenecyanol dyes (**1**) and DNA/monomaleimide-Nanogold 1.4 nm conjugate (**2**) are observed (E). Conditions: 80 V, electrophoresis time 20 min using 0.5X Tris-borate-EDTA buffer as running buffer.*

– Immobilization of capture DNA probe onto paramagnetic beads

The binding of the biotinylated capture DNA probe (CF-A) with MB was carried out using a modified procedure recommended by Bangs Laboratories[28], as follows: 50 μg (5 μL) of MB were transfered into 0.5 mL Eppendorf tube. The amount of MB used in this protocol was the result of an optimization between 25 and 150 μg for the same concentration of CF-T (38 pmol). The MBs were washed once with 100 μL of TTL buffer. The washing steps were carried out using gentle rotation or occasional mixing by gently tapping the tubes, approximately during 1 min. The magnetic separation was performed by placing the tube on MCB 1200 biomagnetic processing platform (magnet) for 1 min (*see* Figure 3.8). Then the supernatant is removed with a micropipette (while the tube remains on the magnet) and resuspended gently in 20 μL TTL buffer, removing the tube from the magnet previously. Then 200 pmol of biotin modified capture DNA probe (CF-A), were added (*see* Figure 3.14-I) and the volume was adjusted to 100 μL by adding deionised and autoclaved water. The resulting MB/CF-A conjugate was incubated during 15 min at temperature of 25 °C with gentle mixing in a TS-100 Thermo Shaker in order to immobilize CF-A. The influence of the time and the temperature of hybridization on DPV response were also optimized. When the immobilization was completed, the resulting MB/CFA conjugate (MB with the immobilized CF-A), was magnetically separated from the incubation solution by placing the tube on the magnet for 1 minute. The supernatant is removed with a micropipette while the tube remains on the magnet. The remaining part was washed sequentially with 100 μL

of TT buffer, 100 μL of TTE buffer and 100 μL of TT buffer using gentle rotation or occasional mixing by gently tapping the tubes. It was separated magnetically by placing the tube on the magnet for 1 min. The supernatant was removed and resuspended gently in 50 μL of hybridization solution and it was ready for the first hybridization.

— First hybridization

38 pmol (if no stated otherwise) of target DNA (CF-T) were added in the solution (50 μL) of the MB/CF-A conjugate obtained in the previous step (*see* Figure 3.14-II). The volume was adjusted to 100 μL by adding deionised and autoclaved water and incubated at 42 °C with gentle mixing during 15 min. When the hybridization was complete the obtained MB/CF-A/CF-T conjugate was magnetically separated and washed twice with 100 μL of TT buffer using gentle rotation or occasional mixing by gently tapping the tubes. It is then resuspended gently in 50 μL of hybridization solution and was ready for the second hybridization.

— Second hybridization

38 pmol (should be added as minimum the same concentration as CF-T DNA) were added AuNPs functionalized with CF-B in the ratio 1:1 in the solution (50 μL) of the MB/CF-A/CF-T conjugate obtained in the previous step. (*See* Figure 3.14-III) The necessary volume of BSA at 10 % and autoclaved water was added in order to obtain a final volume of 100 μL and a final concentration of the BSA of 5% approximately. With the BSA used as blocking agent and the effective washing

steps non-specific adsorption was eliminated. At 42 °C with gentle mixing during 15 min the incubation was carried out. When the hybridization was complete the resulting MB/CF-A/CF-T/CF-B-AuNPs conjugate was washed three times with 100 µL of TT buffer, using gentle rotation or occasional mixing by gently tapping the tubes. Separate magnetically by placing the tube on the magnet for 1 min. The supernatant is resuspended in 50 µL of hybridization solution and it is ready for to do the corresponding measurement. The solution containing the final conjugate was placed on the surface of GECE-M during 60 s which was accumulated on it due to the inherent magnetic field of the electrode. (*see* Figure 3.14-IV) This protocol can be adapted for other fields such as biotechnological and environmental. Finally the direct DPV electrochemical detection of AuNPs tags in the conjugate after the DNA hybridization event was carried out without the need of acidic (i.e. HBr/Br_2) dissolution[13,15], according to the established conditions. (*See* Figure 3.14-V)

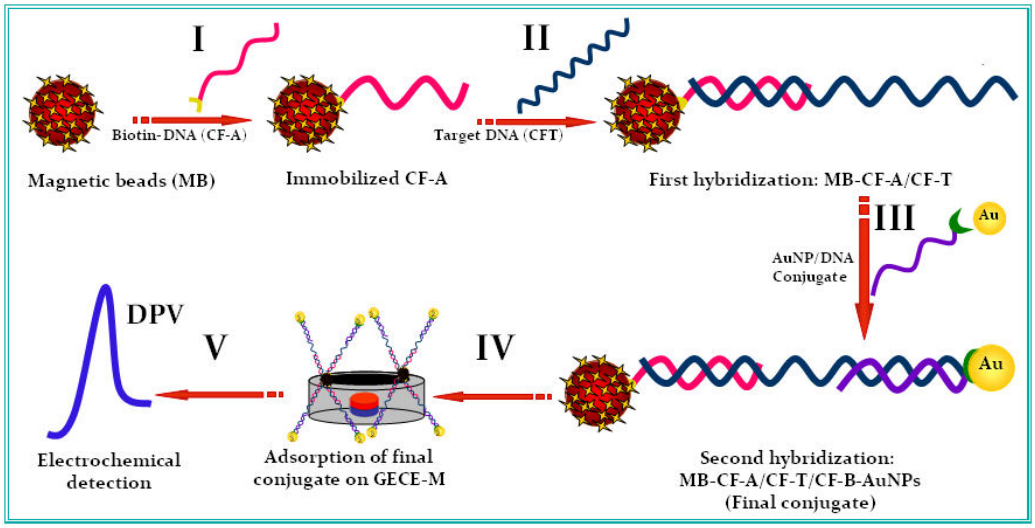

Figure 3.14. *Schematic representation (not in scale) of the analytical protocol of sandwich assay by using AuNPs 1.4 nm of diameter (I): Immobilization of the biotinylated CF-A probe onto streptavidin-coated paramagnetic beads (MB), (II): addition of Target CF to the first hybridization event, (III): addition of monomaleimide-nanogold (AuNPs) functionalized with signaling thiolated CF-B probe to the second hybridization event, (IV): adsorption of final conjugate on the surface of the M-GECE, and (V): magnetically trigged direct DPV electrochemical detection of AuNPs labels in the conjugate.*

— ***Electrochemical detection***

The electrochemical detection was carried out using the same way as the one described at section 3.2.2.6.

— ***Discrimination study***

The discrimination between CF-MX1, CF-MX, CF-NC and the CF-T (*see* sequences in Table 5) in order to demonstrate the selectivity of the genomagnetic sandwich assay protocol (performed following the same protocol as described above) has been studied.

— ***Melting experiments***

Melting experiments were performed as follows. Solutions of equimolar amounts of oligonucleotides (1000 pmol of CF-A, CF-B and CF-T) were mixed in buffer appropriate. The solutions were heated to 90 ºC, allowed to cool slowly to room temperature, and stored at 4 ºC until the UV was measured. The DNA concentration was determined by UV absorbance measurements (260 nm) at 90 ºC. UV absorption spectra and melting experiments (absorbance vs., temperature) were recorded in 1 cm path length cells using a spectrophotometer, with a temperature controller and a programmed temperature increase rate of 1 ºC min^{-1}.

The studies of melting temperature (T_m) experiments were carried out in duplicates.

– TEM characterization of 1.4 nm diameter AuNPs

The 1.4 nm diameter AuNPs were diluted previously in Milli-Q water, in a ratio 1:1 (25 µl of sample 25 µl of H_2O). Then the dissolution was placed in ultrasound bath during 5 min in order to avoid aggregates from AuNPs and TEM characterization was carried out.

3.2.3. Results and discussion

3.2.3.1. Model system assay for DNA hybridization electrochemical detection by using 1.4 nm Au_{67} quantum dot tag linked to target DNA

– Preparation of the Au Quantum dot modified DNA (1:1 Au_{67}-DNA1)

The figure 3.15 shows the results of agarose gel electrophoresis for purity control of Au_{67} nanoparticles (A), as well as target DNA (B), and noncomplementary DNA (C) labelled with Au_{67} nanoparticle, and finally dyes used as control (D).

As can be seen, in (A) Au_{67} nanoparticles do not migrates owing to the fact that they do not have charge. However target (B) and noncomplementary DNA-Au_{67} (C) conjugates have negative charge because the DNA strands are negatively charged. If Au_{67} is completely linked to the target and noncomplementary DNA the gold is charged negatively and therefore the conjugates migrate towards the positive pole.

On the other hand can be observed the good separation of the dyes used as control (D), which is used as a control for the good development of gel electrophoresis.

The result of this gel electrophoresis leads to the conclusion that target and noncomplementary DNA have been efficiently labelled with Au_{67}.

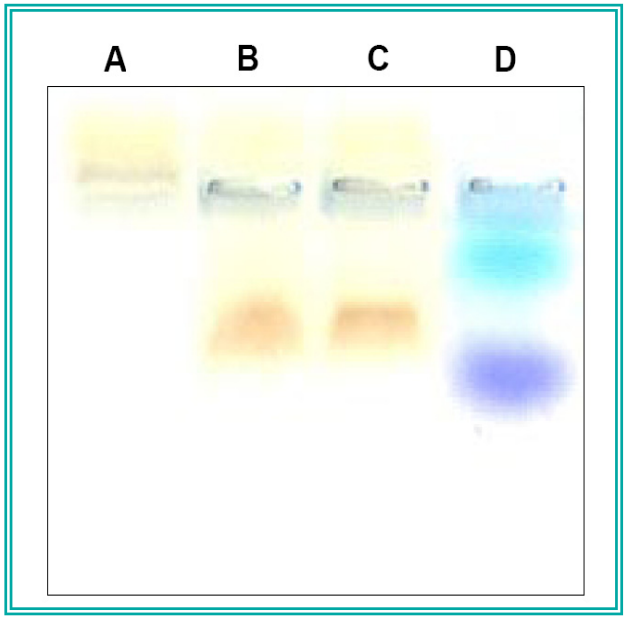

Figure 3.15. *Purity control of discrete Au_{67} nanocrystal-DNA conjugates. (A) maleimide Au_{67} nanocrystals; (B) target DNA marked with Au_{67} nanoparticle; (C) non-complementary DNA marked with Au_{67} nanoparticle; (D) bromophenol blue and xylenecyanol dyes. Conditions: gel electrophoresis in 2% agarose gel at 80 V, with electrophoresis time 20 min, using 0.5× TRIS-borate-EDTA (TBE) buffer as a running buffer.*

— *Discrimination study*

The results of discrimination study are shown in Figure 3.16A-D The discrimination or selectivity study among target (Figure 3.16A) and three base mismatches (Figure 3.16B), as well as noncomplementary DNA (Figure 3.16C) provides a high level of selectivity as can be seen in the DPV hybridization responses on M-GECE. Effective magnetic triggering of the transducing event is

also demonstrated in Figure 3.16A and Figure 3.16D, showing the well-defined signal hybridization response on the magnetic and no electrochemical response on nonmagnetic electrode, respectively. For more details see publication VI (at chapter 7)

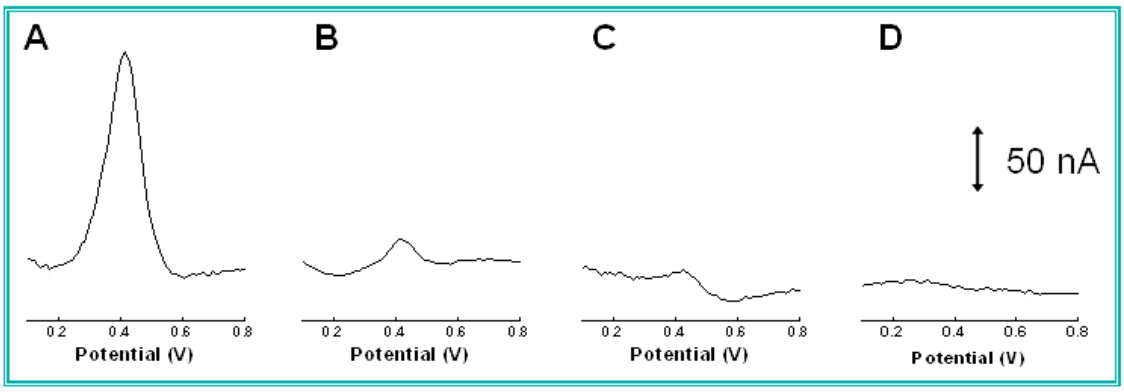

Figure 3.16. *DPV hybridization response of 500 nM target (A), 500 nM three-base mismatch (B), 1000 nM noncomplementary DNA (C) on magnetic graphite-epoxy composite electrode. DPV hybridization response of 500 nM target on non magnetic graphite-epoxy composite electrode (D). Conditions: hybridization time, 15 min; hybridization temperature, 42 °C; amount of MB, 100 μg; electrooxidation potential, +1.25 V; electrooxidation time, 120 s, DPV scan from +1.25 V to 0 V, step potential 10 mV, modulation amplitude 50 mV, scan rate 33.5 mV* s^{-1}*, nonstirred solution. Publication VI (at chapter 7).*

— *Parameters optimization*

The influence of different parameters involved in the genomagnetic protocol such as the amount of MB, hybridization time, hybridization temperature, and electrooxidation potential and electrochemical oxidation time of the Au_{67} were examined and optimized.

An amount of 100 μg of MB, 15 min as hybridization time, 42 ºC as hybridization temperature, +1.25 V as electrooxidation potential and electrooxidation time of 120 s were chosen as optimal for the proposed DNA hybridization detection.

The voltammetric responses are shown in publication VI (at chapter 7), which are widely discussed.

— ***Concentration dependence***

The new Au_{67} quantum dot-based DNA hybridization direct detection protocol shows defined concentration dependence (*see* Figure 3.17). The calibration plot was linear over the range from 10 nM to 40 nM of target DNA with sensitivity of 0.97 nA nM^{-1} and intercept of –0.83 nA (correlation coefficient of 0.991).

The DL (based on upper limit approach[29]) reached was of 12 nM of target DNA. This DL is comparable to LOD of HBr/Br_2 dissolution based 5 nm-Au nanoparticle-DNA-paramagnetic bead (m:n) assay (15 nM)[16] but it is achieved with much smaller, 1.4 nm AuNPs (containing 45 times less gold atoms than 5 nm Au nanoparticle), reflecting high sensitivity of presented direct electrochemical detection of n:1 Au_{67}QD – DNA – paramagnetic bead protocol.

Very good precision is an attractive feature of the presented magnetically trigged Au_{67}QD marked direct electrochemical detection DNA hybridization. It reflects a well-defined and highly reproducible magnetic collection of Au_{67}- DNA1/DNA2-paramagnetic bead conjugates on the surface of the electrode with a built-in magnet and also a well defined structure of these conjugates, without any irreproducible three-dimensional Au-paramagnetic bead DNA linked network, typical for previously developed configurations.[16,30]

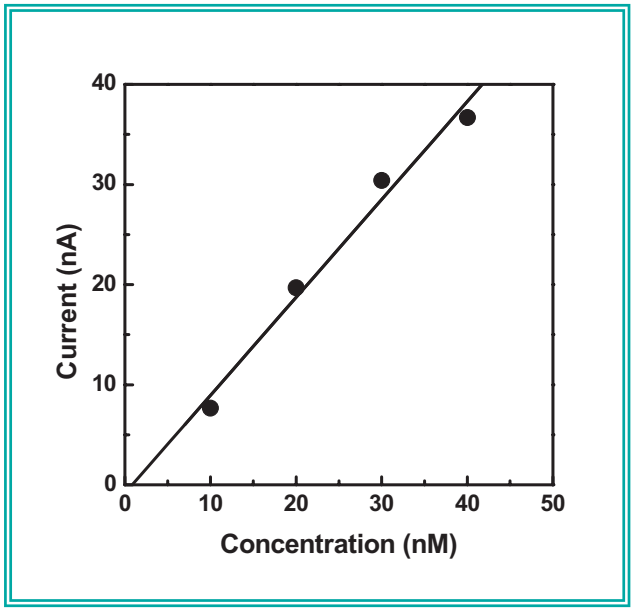

Figure 3.17. *Calibration plot for target DNA. Hybridization time, 20 min; amount of paramagnetic beads, 50 µg. Other conditions, as in Figure 3.16A. Publication VI (at chapter 7)*

3.2.3.2. Model system assay for DNA hybridization electrochemical detection. Use of a *BRCA1* breast cancer gene related DNA strand as target and 10 nm diameter AuNPs as label

– Discrimination study

At this genomagnetic assay using as target a DNA strand related to the *BRCA1* breast cancer gene a discrimination study also was carried out. The DPV hybridization response of 2.5 $\mu g.mL^{-1}$ of target (BC-T), three-base mismatches (BC-MX3) and non complementary (BC-NC) DNAs on M-GECE can be observed in Figure 3.18 A-D.

A well-defined signal for BC-T is observed. (*see* Figure 3.18A) The Figure 3.18B shows a significantly much lower signal for BC-MX3. A practically null gold

signal is observed for BC-NC (Figure 3.18C). The results obtained show that the magnetically trigged direct electrochemical detection of NPs tags corresponds to an effective hybridization along with an efficient magnetic attraction of the MB/BC-A/BC-T/Au-NPs conjugate onto the sensor surface with the tiny magnet inside (M-GECE).

Finally in Figure 3.18D no electrochemical response is observed for BC-T conjugate on conventional GECE (without a built-in magnet), because of the absence of magnetic or adsorptive accumulation of MB.

The discrimination of BC-MX3 and BC-NC is significantly better than that observed in previous assay. See publication VI (at chapter 7).

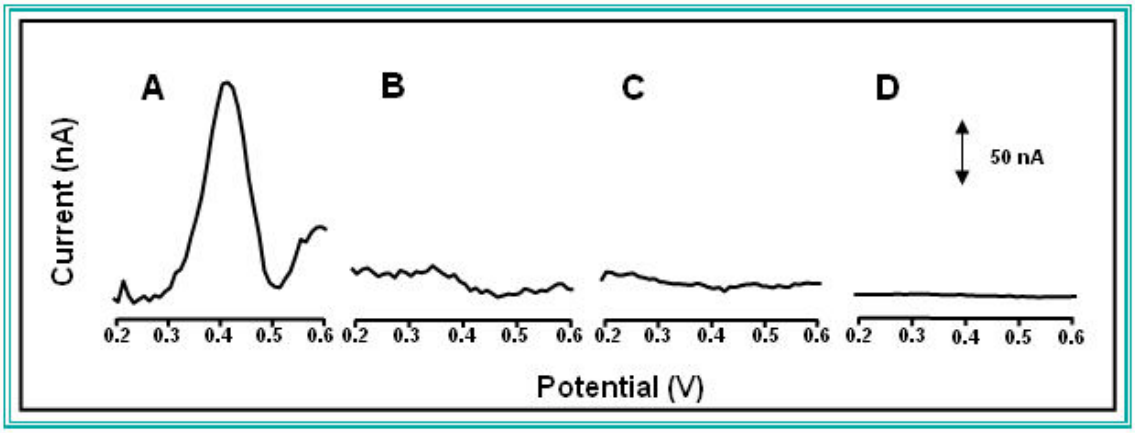

Figure 3.18. *DPV hybridization response of 2.5 µg.mL^{-1} of: BC-T (A), BC-MX3 (B), BC-NC (C) on magnetic graphite-epoxy composite electrode and 2.5 µg.mL^{-1} of BC-T on non-magnetic graphite-epoxy composite electrode (D). Conditions: amount of paramagnetic beads, 50 µg; amount of Au nanoparticles, 9 x 10^{12}; hybridization time, 15 min; hybridization temperature, 42 ^{o}C; oxidation potential, +1.25 V; oxidation time, 120 s; DPV scan from +1.25 V to 0 V; step potential, 10 mV; modulation amplitude, 50 mV; scan rate, 33.5 mV.s^{-1}; non-stirred solution.*

— *Parameters optimization*

Figure S1 A-C (See Supplementary Information at publication VII at chapter 7) displays the effect of amount of the Au-NPs (S1A), MB (S1B) and hybridization

time (S1C) upon the hybridization response. The amounts of MB and Au-NPs affect the quantity of bound probes and captured tags, respectively, which have a great effect upon the sensitivity. An amount of 9 x 10^{12} AuNPs as label, 50 µg of MB and a hybridization time of 15 min were chosen as optimal for this assay.

— ***Concentration dependence***

Figure 3.19 shows the BC-T defined concentration dependence.

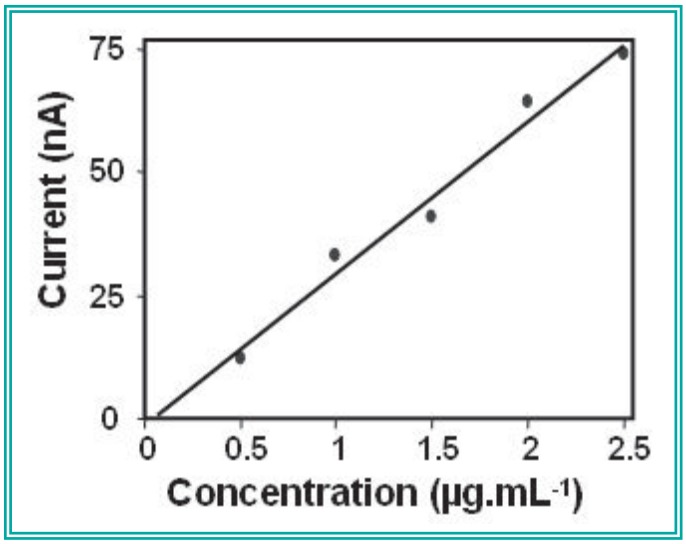

Figure 3.19 *Calibration plot for BC-T DNA over the 0.5-2.5 µg.mL^{-1} range with a correlation coefficient of 0.9784. Hybridization time, 15 min; amount of paramagnetic beads, 50 µg; oxidation potential, +1.25 V; oxidation time, 120 s. DL: 0.198 µg.mL^{-1} of BC-T (33 pmol in 50 µL sample volume).*

The calibration plot was linear over a concentration range from 0.5-2.5 $\mu g.mL^{-1}$ of BC-T, with a correlation coefficient of 0.9784 and a DL of 0.198 $\mu g.mL^{-1}$ of BC-T, based on upper limit approach.[29] This DL corresponds to 33 pmol in the 50 µL sample volume which was compared with that reported at others works. See publication VII (at chapter 7). The proposed method could be a useful approach for future applications in clinical diagnostic and others fields.

3.2.3.3. Sandwich system assay for DNA hybridization electrochemical detection. Use of a cystic fibrosis related DNA strand as target and 10 nm diameter AuNPs as label

— ***Discrimination study***

Figure 3.20 A-D shows the hybridization detection studies with CF-T.

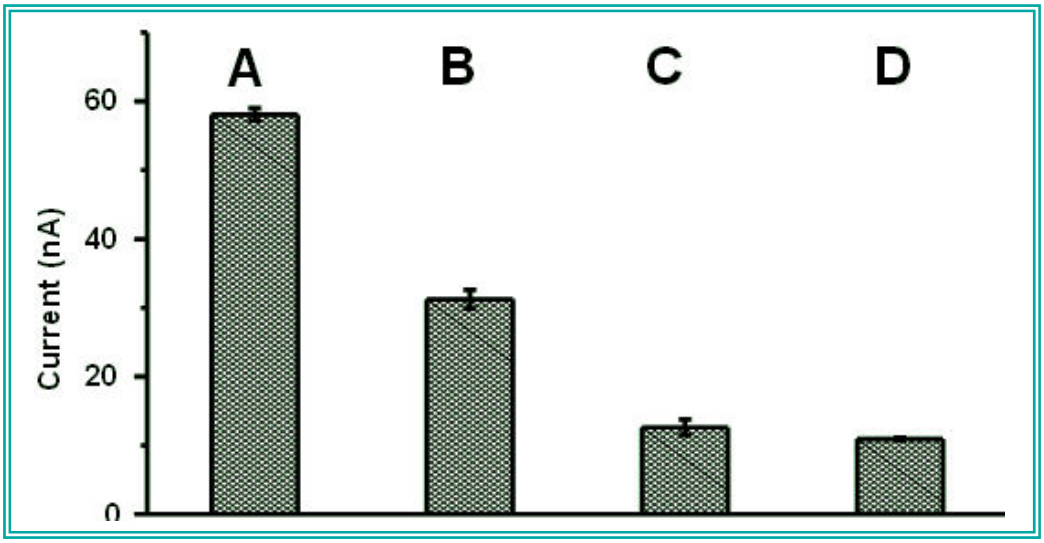

Figure 3.20. *Histogram that shows the current intensities of DPV peaks obtained for the hybridization responses of 8 µg.mL-1 of: target associated with cystic fibrosis (A), CF-MX1 (B), CF-MX-3, and CF-NC on M-GECE.. Error bars show the mean and the standard deviations of the measurements taken from three independent experiments. Conditions: Hybridization time, 15 min; hybridization temperature, 25 ºC; amount of MB, 100 µg; electrooxidation potential, +1.25 V; electrooxidation time, 120 s; DPV scan from +1.25 V to 0 V; step potential, 10 mV; modulation amplitude, 50 mV; scan rate, 33.5 mV s^{-1}; nonstirred solution.*

Data are given in vertical bars that show the current intensities of DPV signals obtained for the hybridization responses of 8 μg.mL-1 of: CF-T, CF-MX-1, CF-MX3 and CF-NC on M-GECE.

Error bars show the mean and the standard deviations of the measurements taken from three independent experiments. In Figure 3.20A is observed the higher current intensity which represents the efficient hybridization electrochemical response on the M-GECE because of magnetic attraction of the MB/CF-A/CF-T/CF-B/AuNPs conjugate to its surface.

Low responses for CF-MX1 (Figure 3.20B) and significantly lower for CF-MX3 (Figure 3.20C) and CF-NC (Figure 3.20D) are observed according to the difference in current intensities. The discriminations can be improved by avoiding the nonspecifically adsorbed oligonucleotides by a better control of the washing step or increasing the concentration of CF-A.

— Parameters optimization

The analyzed parameters at this assay were: hybridization time, hybridization temperature and amount of MB upon the hybridization response. *See* Figure S2 A-D (Supplementary Information of publication VII) (at chapter 7). Figure S2 A represents a typical differential pulse voltammogram for the signals of Au at M-GECE after hybridization with CF-T in this sandwich assay.

A hybridization time of 15 min; hybridization temperature of 25 °C and an amount of MB of 100 μg were chosen as the optimal. The amount of MB is of great

importance because of its influence in the immobilization of CF-A which will determine the sensitivity and reproducibility of the genosensor.

Electrooxidation potential and electrochemical oxidation were investigated and optimized previously. See publication VI (at chapter 7). Hence, a potential of +1.25 V and 120 s were selected as optimal for electrooxidation of Au-NPs upon the DPV signal.

3.2.3.4. Sandwich system assay for DNA hybridization electrochemical detection. Use of a cystic fibrosis related DNA strand as target and 1.4 nm diameter AuNPs as label

— Discrimination study

The specificity of the new magnetically trigged direct electrochemical detection of DNA hybridization was evaluated by detecting the DPV signals obtained for CF-T, CF-XI, CF-X3 and CF-NC DNA strand (*see* sequences at Table 5) at a concentration of 38 pmol. Figure 3.21 shows the voltammograms obtained during the assay.

As shown in Figure 3.21A, a well-defined DPV response arising from CF-T (complementary DNA) is observed. The Figures 3.21B and 3.21C show a significantly lower signal for CF-MX1 and much lower for CF-MX3, respectively. At Figure 3.21D practically null signals is observed for CF-NC and finally, also null response for 38 pmol of CF-T is observed when GECE nonmagnetic electrode is used as WE (Figure 3.21E).

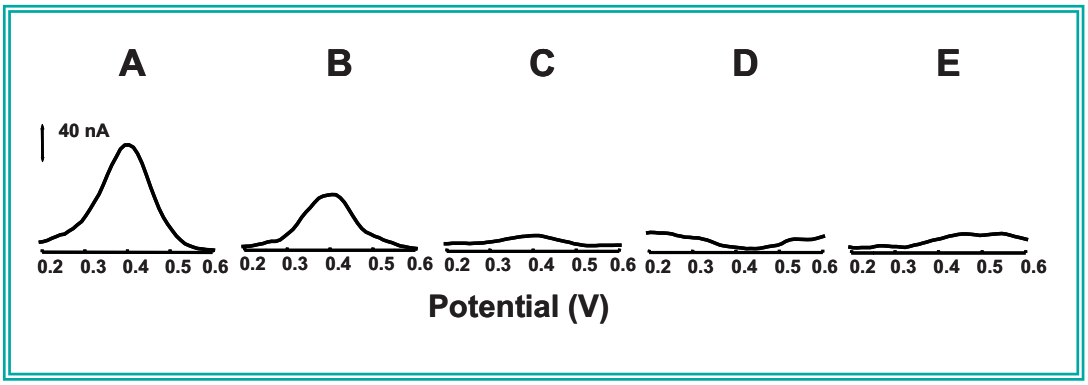

Figure 3.21 *DPV hybridization response of 38 pmol of: target (A), single base mismatch (B) three-base mismatch (C), non-complementary DNA (D) on M-GECE and of target on non-magnetic GECE (E).Conditions amount of paramagnetic beads, 50 µg; hybridization time, 15 min; hybridization temperature, 42 ºC; oxidation potential, +1.25 V; oxidation time, 120 s; DPV scan from +1.25 V to 0 V; step potential, 10 mV; modulation amplitude, 50 mV; scan rate, 33.5 mV.s^{-1}; non-stirred solution.*

Also as in all the previous assays, an effective magnetic accumulation is observed. Figures 3.21A and 3.21E, show an effective hybridization along with an efficient magnetic attraction of the AuNPs-CF-B/CF-T/CF-A-MB conjugate onto the surface of M-GECE (*see* Figure 3.21A), whereas no electrochemical response is obtained for the same conjugate onto GECE because of the absence of magnetic or adsorptive accumulation of MB (*see* Figure 3.21E). These results demonstrate that M-GECE has a high specificity for DNA hybridization electrochemical detection.

— ***Parameters optimization***

The effect of MB amount upon the analytical signal was studied for the range 25 to 150 µg, being the concentration of CF-T the same (38 pmol). The DPV response increased with increasing of MB concentration and then decreased as MB increases further, reaching a maximum at 50 µg, which was chosen as optimal in this bioassay.

The effect of the hybridization time (incubation time required until hybridization reaction occurs) on DPV response was also investigated. The studied hybridization times were between 5 and 30 min using the same CF-T concentration. The highest signal was obtained for 15 min, therefore this time was chosen as optimal for subsequent studies to evaluate the analytical performance of the genomagnetic sensor.

With respect to hybridization temperatures values of 25, 30, 37 and 42 ºC were investigated. DPV response increased with the increasing temperature up to 42 ºC which was chosen as optimal for this bioassay.

The influence of the electrochemical oxidation time of the AuNPs upon the DPV signal was also studied. The signal displays an increase in the interval from 30 to 120 s and levels off thereafter. This leads to the conclusion that the electrooxidation time of 120 s is sufficient for reaching the steady-state response.

Optimization of the electrooxidation potential of the AuNPs was performed in an interval of +1.15 to +1.35 V. A potential of +1.25 V was selected as optimal for electrooxidation of AuNPs.

— Concentration dependence

Figure 3.21 shows the CF-T defined concentration dependence at the assay by using 1.4 nm diameter AuNPs.

The calibration plot (*see* Figure 3.22) was linear over a concentration range from 10-60 pmol of CF-T, with a correlation coefficient of 0.9936 and a DL as low as 3 pmol of CF-T in the 50 μL sample volume (based on upper limit approach[29]). The

obtained DL is lower compared to that obtained for the model system assays developed at this thesis.

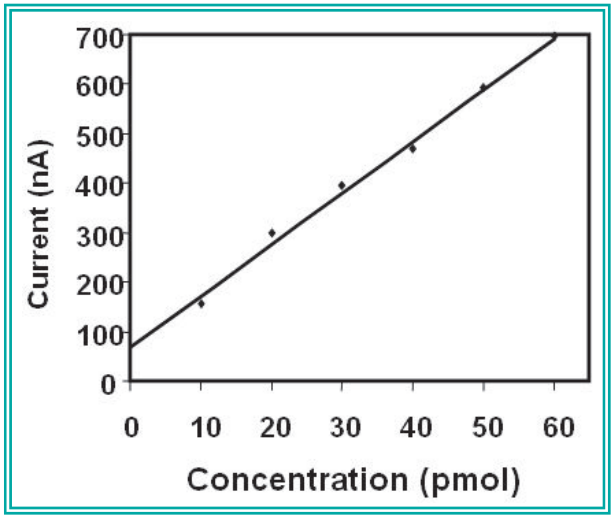

Figure 3.22 *Calibration plot for CF-T DNA over the range 10-60 pmol with a correlation coefficient of 0.9936. Hybridization time, 15 min; amount of magnetic beads, 50 µg; oxidation potential, +1.25 V; oxidation time, 120 s. DL: 3 pmol in 50 µL sample volume.*

The best analytical performances were obtained by using monomaleimide nanogold (1.4 nm) as tag. This is due to the fact that these NPs ensure a 1:1 AuNP / DNA connection avoiding the NP network formation that leads to an 'inhibited' detection.

The specific streptavidin-biotin interaction, may lead to the formation of interconnected three-dimensional network of the final conjugate (*see* Figure 3.23-left).

This phenomenon does not happen when the 1:1 Au-DNA connection is used (*see* Figure 3.23-right).

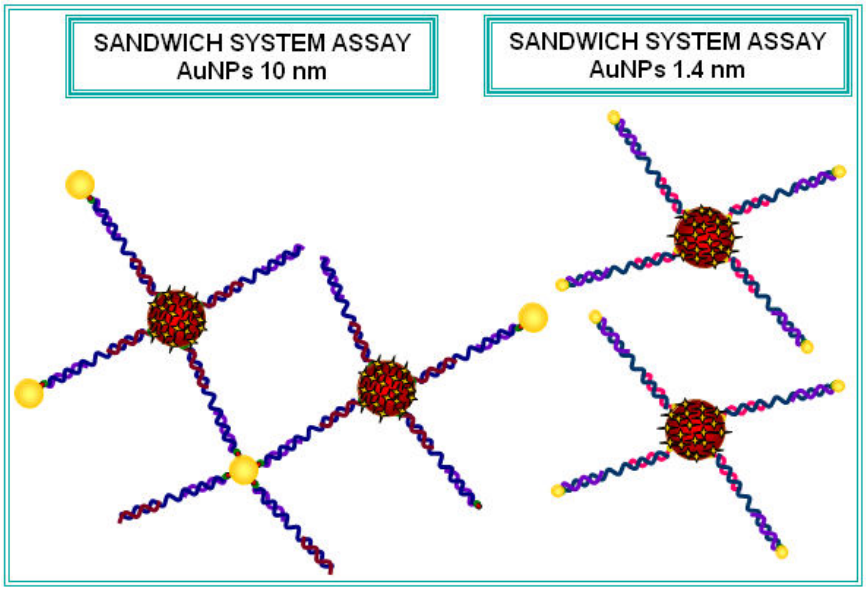

Figure 3.23. *Schematic that shows the formation of particle linked DNA network structure due to the interconnection between paramagnetic beads MB in the case where 10 nm diameter AuNPs modified with more than one DNA strands are used in sandwich system assay (A). Such network is not created in sandwich system assay by using 1.4 nm diameter AuNPs DNA connection in ratio 1:1 (B).*

— *Melting experiments*

Figure 3.24 shows the melting experiments results. All of the absorbance versus temperature plots showed sigmoidal curves. The T_m obtained during this study (two samples) were 65.9 ºC and 65.3 ºC.

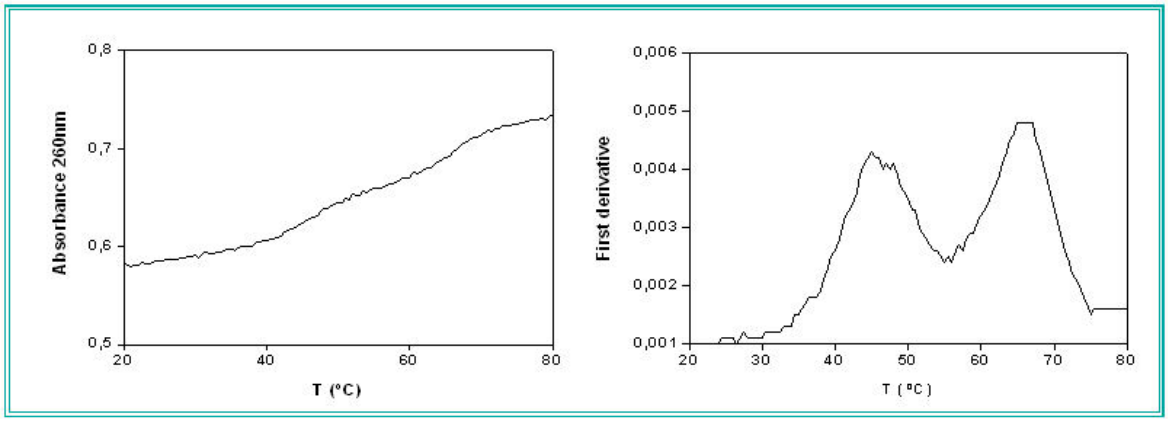

Figure 3.24. *UV melting profile (260 nm) for CF-T+CF-A+CF-B, pH 7.5, 0.15 M NaCl (A) and first derivative of the corresponding melting curve.*

– ***TEM characterization of 1.4nm diameter AuNPs***

TEM images were recorded on a Jeol JEM-2011 electronic microscope (Jeol Ltd., Tokyo, Japan) using an accelerating voltage of 200 kV, in order to characterize the size of the 1.4 nm diameter AuNPs. The samples used for TEM observation were prepared by placing a drop of sample onto a copper grid coated with a layer of amorphous carbon. The TEM image obtained indicated a size of 1.4 nm of these AuNPs. (*See* Figure 3.25)

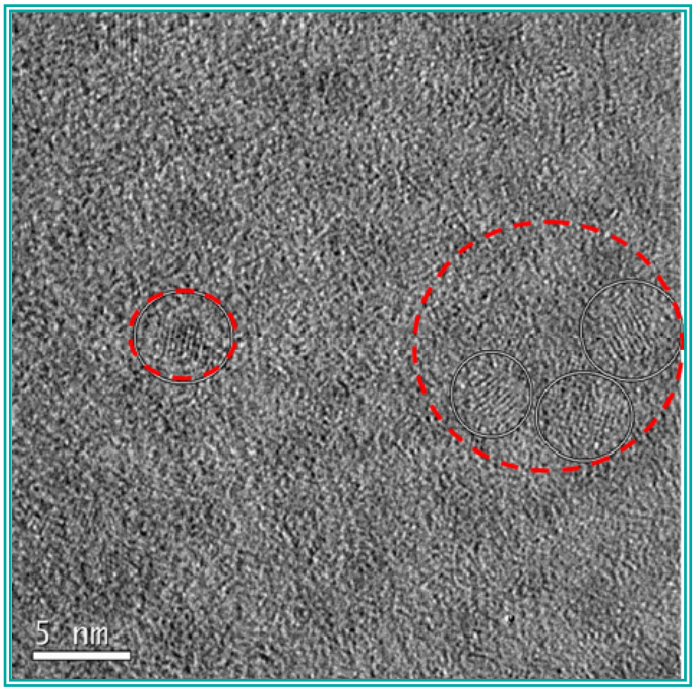

Figure 3.25. *TEM image of 1.4 nm diameter AuNPs at 500000X magnifications.*

3.2.4. Conclusions

The proof of the concept of magnetically trigged direct electrochemical detection for monitoring DNA hybridization has been demonstrated.

The different strategies developed for electrochemical DNA hybridization detection using AuNPs as labels in combination with MB as platform to immobilize capture DNA probe was successfully demonstrated on the M-GECE constructed. *See* publications VI and VII (at chapter 7).

Well defined signals for target DNA with an effective discrimination against three mismatches and non-complementary DNA strands were observed at first model system assay (*see* publication VI at chapter 7), against three base mismatches and non complementary DNA at second model system assay (*see* publication VII at chapter 7) as well as against one and three base mismatches and non complementary DNA at the two sandwich system assays (*see* publication VII at chapter 7. An important advantage of all the protocols developed at this thesis, is the elimination of the need of acid dissolution which greatly simplifies particle-based electrical bioassays and obviates the need for a toxic HBr/Br_2 solution. (*See* publications VI and VII at chapter 7).

The use of a 1:1 AuNPs-DNA conjugate avoids the creation of an interconnected network of Au-DNA/MB compared to previously developed DNA assays (which relied on multiple duplex links between MB and nanoparticles) pushing down the achievable DLs and facilitating potential manipulation of individual either Au_{67} quantum dot-DNA1/DNA2-paramagnetic beads (*see* publication VI at chapter 7) or

AuNPs-CF-B/CF-T/CF-A-MB conjugates in microfluidic channel arrays, offering the possibility parallel multiple DNA detection[31] in the future.

The high performance of the method is also attributed to the sensitive ASV determination of AuNPs on M-GECE.

The developed assays offer good selectivity, simplicity, low cost, a fast response time and are highly sensitive and potentially useful for medical and environmental applications among others fields.

The best analytical performances were obtained by using AuNPs of 1.4 nm.

The developed methods have a sufficient DL for real-world analysis in regard to diagnosis. The application of the developed designs can be extended to other fields such as environmental related analysis where fast DNA analysis is of special importance. (*See* publication VII at chapter 7)

Current effort in our laboratory is directed to the optimization of the experimental conditions in order to improve the sensitivity and reproducibility in order to adapt these assays to the pathogenic microorganism detection. (*See* publication VII at chapter 7)

The systems developed should be studied in order to be applied at real samples.

3.2.5. References

[1] Liz-Marzan L. M., Nanometals: Formation and color. *Materials Today* **2004**, 7, 26–31.

[2] Burda C., Chen X., Narayanan R., El-Sayed M. A. Chemistry and Properties of Nanocrystals of Different Shapes. *Chemical Reviews* **2005**, 105, 1025–1102.

[3] Cuenya B. R., Hyeon Baeck S., Jaramillo T. F., McFarland E. W. Size-and Support-Dependent Electronic and Catalytic Properties of Au^0/Au^{3+} Nanoparticles Synthesized from Block Copolymer Micelles. *J. Am. Chem. Soc.* **2003**, 125*,* 12928–12934

[4] Miscoria S. A., Barrera G. D., Rivas G. A. Enzymatic biosensor based on carbon paste electrodes modified with gold nanoparticles and polyphenol oxidase. *Electroanalysis* **2005**, 17, 1578–1582.

[5] Dos Santos Jr. D. S., Alvarez-Puebla R. A., Oliveira Jr. O. N., Aroca R. F. Controlling the size and shape of gold nanoparticles in fulvic acid colloidal solutions and their optical characterization using SERS. *J. Mater. Chem*. **2005**, 15, 3045–3049.

[6] Panda B. R., Chattopadhyay A. Synthesis of Au Nanoparticles at "all" pH by H_2O_2 Reduction of $HAuCl_4$. *J. Nanosci. Nanotechnol.* **2007***,* 7, 1911–1915.

[7] Luo Y., Sun X. Sunlight-Driving Formation Characterization of Size-Controlled Gold Nanoparticles. *J. Nanosci. Nanotechnol.* **2007***,* 7, 708–711.

[8] Castañeda M. T., Alegret S., Merkoçi A. Electrochemical sensing of DNA using gold nanoparticles, *Electroanalysis* **2007**, 19, 743–753.

[9] Merkoçi A. Electrochemical biosensing with nanoparticles. *FEBS Journal* **2007***,* 274, 310–316.

[10] Luo X., Morrin A., Killard A. J., Smyth M. R. Application of Nanoparticles in Electrochemical Sensors and Biosensors. *Electroanalysis* **2006**, 18, 319–326.

[11] Burda C., Chen X., Narayanan R., El-Sayed M. A. Chemistry and Properties of Nanocrystals of Different Shapes. *Chemical Reviews* **2005**, 105, 1025–1102.

[12] Dos Santos Jr. D. S., Alvarez-Puebla R. A., Oliveira Jr. O. N., Aroca R. F. Controlling the size and shape of gold nanoparticles in fulvic acid colloidal solutions and their optical characterization using SERS. *J. Mater. Chem*. **2005**, 15, 3045–3049.

[13] Pumera M., Castañeda M. T., Pividori M. I., Eritja R., Merkoçi A., Alegret S. Magnetically Trigged Direct Electrochemical Detection of DNA Hybridization Using Au_{67} Quantum Dot as Electrical Tracer. *Langmuir* **2005**, 21, 9625–9629.

[14] Ozsoz M., Erdem A., Kerman K., Ozkan D., Tugrul B., Topcuoglu N. Electrochemical Genosensor Based on Colloidal Gold Nanoparticles for the Detection of Factor V Leiden Mutation Using Disposable Pencil Graphite Electrodes. *Anal. Chem*. **2003**, 75, 2181–2187.

[15] Castañeda M. T., Merkoçi A., Pumera M., Alegret S., Electrochemical genosensors for biomedical applications based on gold nanoparticles. *Biosens. Bioelectron*. **2007**, 22, 1961–1967.

[16] Wang J., Xu D., Kawde A. N., Polsky R. Metal nanoparticle-based electrochemical stripping potentiometric detection of DNA hybridization. *Anal. Chem.* **2001***,* 73**,** 5576–5581.

[17] Ambrosi A., Castañeda M. T., Killard A. J., Smyth M. R., Alegret S., Merkoçi A., Double-codified gold nanolabels for enhanced immunoanalysis. *Anal. Chem.*, **2007**, 79, 5232–5240.

[18] Palecek E., Fojta M., Jelen F. New approaches in the development of DNA sensors: hybridization and electrochemical detection of DNA and RNA at two different surfaces. *Bioelectrochemistry* **2002**, 56, 85–90.

[19] Gijs M. A. M., Magnetic bead handling on-chip: new opportunities for analytical applications. *Microfluidics and Nanofluidics* **2004**, 1, 22–40.

[20] Lim C. T., Zhang Y. Bead-based Microfluidic Immunoassays: The Next Generation. *Biosens. Bioelectron*. **2007**, 22, 1197–1204.

[21] Authier L., Grossiord C., Brossier P., Limoges B. Gold nanoparticle-based quantitative electrochemical detection of amplified human cytomegalovirus DNA using disposable microband electrodes. *Anal. Chem.* **2001**, 73, 4450–4456.

[22] Kawde A-N., Wang J. Amplified Electrical Transduction of DNA Hybridization Based on Polymeric Beads Loaded with Multiple Gold Nanoparticle Tags. *Electroanalysis* **2004**, 16, 1–2.

[23] Pumera M., Aldavert M., Mills C., Merkoçi A., Alegret S. Direct Voltammetric Determination of Gold Nanoparticles Using Graphite-Epoxy Composite Electrodes*. Electrochim. Acta* **2005***,* 50, 3702–3707.

[24] González García M. B., Costa García A., Adsorptive stripping voltammetric behaviour of colloidal gold and immunogold on carbon paste electrode, *Bioelectrochem. Bioenerg*. **1995**, 38, 389–395.

[25] Torre B. G., Morales J. C., Avino A., Iacopino D., Ongaro A. Fitzmaurice D., Murphy D., Doyle H., Redmond G., Eritja R. Synthesis of Oligonucleotides

Carrying Anchoring Groups and Their Use in the Preparation of Oligonucleotide -Gold Conjugates. *Helv. Chim. Acta* **2002**, 85, 2594–2607.

[26] Loweth C. J., Caldwell W. B., Peng X., Alivisatos A. P., Schultz P. G. DNA-based assembly of gold nanocrystals. *Angew. Chem., Int. Ed. Engl.* **1999**, 38, 1808–1812.

[27] Zanchet D., Micheel C. M., Parak W. J., Gerion D., Alivisatos A. P. Electrophoretic Isolation of Au Nanocrystal/DNA conjugates. *Nano Lett.* **2001**, 1, 32–35.

[28] Bangs Laboratories Inc., *TechNote* 101 (1999).

[29] Mocak J., Bond A. M., Mitchell S. Scollary G. A statistical overview of standard (IUPAC and ACS) and new procedures for determining the limits of detection and quantification: Application to voltammetric and stripping techniques (Technical Report). *Pure & Appl. Chem.* **1997**, 69, 297–328.

[30] Wang J., Xu D., Polsky R. Magnetically-Induced Solid-State Electrochemical Detection of DNA Hybridization. *J. Am. Chem. Soc*. **2002**, 124, 4208–4209.

[31] Fan Z. H., Mangru S., Granzow R., Heaney P., Ho W., Dong Q., Kumar R. Dynamic DNA Hybridization on a Chip Using Paramagnetic Beads. *Anal. Chem.* **1999**, 71, 4851−4859.

3.3. Protein analysis based on electrochemical stripping of gold nanoparticles

3.3.1. Introduction

Several methods, such as ELISA[1], radioimmunoassay[2], fluorescence immunoassay[3], chemiluminescence assay[4,5], bioluminescence[5], immuno-PCR assay[6], among others, have been developed for protein detection. However, most methods, unfortunately, have some drawbacks. They either are hazardous to the health, have time-consuming procedures and complexity, or require highly qualified personnel and sophisticated instrumentation, which have motivated the findings of new technologies.

The electrochemical technique is attractive for the immunoassay of biomarkers, owing to its high sensitivity, inherent simplicity, miniaturization, and low cost.

On the basis of a specific reaction of the Ab and Ag, electrochemical immunosensors provide a sensitive and selective tool for the determination of proteins.

The emergence of nanotechnology is opening new horizons for highly sensitive electrochemical assays of biomarkers.[7-9] By incorporation with NPs, electrochemical biosensors have shown great promise for diagnosis of trace biomolecules because the nanoparticle-based amplification platforms and

amplification processes have been reported to dramatically enhance the intensity of the electrochemical signal and lead to ultrasensitive bioassays.[8-10]

Metal nanoparticles[11-13] and semiconductors[14] have been used as electroactive labels to amplify electrochemical detection of DNA and proteins.

AuNPs have attracted considerable scientific interest because of their unique properties[15]. AuNPs have been widely used for labelling proteins in connection to microscopy imaging.

The use of gold as electrochemical label for voltammetric monitoring of protein interactions was pioneered in 2000 by González-García et al.[16] and Dequaire et al.[11] Recently, several electrochemical immunosensors by using AuNPs as label have been reported[17-19]. Others works have been described at Publication III (at chapter 7).

In addition, the bio-bar-code method is a strategy that has made a marked impact on the field of gold nanoparticle-based biodiagnostics, by providing a protocol to detect proteins.[20] The bio–bar code assay appeared in the early 2000's as a promising analytical tool for high sensitivity detection of proteins.

The use of MB has also recently attracted much attention in controlling bio-related systems owing to its operational convenience and separation efficiency[21,22].

At this work the combination of optical and electrochemical properties of AuNPs with the catalytic activity of the HRP enzyme will be demonstrated now with a new double-codified (DC) label. It represents a gold nanoparticle modified with a model anti-human IgG peroxidase-conjugated antibody (anti-human IgG-HRP). The used label offers several analytical routes for immunodetection.

Spectrophotometric analysis based on either gold nanoparticle absorption or HRP enzymatic activity and the electrochemical detection based on gold nanoparticle will be presented and compared. Optical sensitivity enhancement attributable to the use of AuNPs as a multi-IgG-HRP carrier, which therefore amplifies the enzymatic signal, as well as the high sensitivity in the direct electrochemical detection, represents the most important achievements due to the use of this double-codified nanolabel, which can potentially be exploited in several other future applications

The magnetic particle allows the separation of reacted target molecules from unreacted ones. The nanoparticles aim at amplifying and detecting the target of interest.

3.3.2. Experimental

3.3.2.1. Apparatus

- All voltammetric experiments were carried out in a 5-mL voltammetric cell at room temperature (25 °C), using the same electrochemical analyzer and three-electrode configuration as for DNA analysis. *See* section 3.2.2.1 and Figure 3 at publication VIII (at chapter 7).
- The binding of streptavidin coated paramagnetic beads with biotinylated primary antibody and all the incubations were performed in a TS-100 ThermoShaker.
- Magnetic separation was carried out with a MCB1200 biomagnetic processing platform (Sigris).

- The spectrophotometric measurements were performed using a Tecan Sunrise absorbance microplate reader.
- Transmission electron micrographs were taken using a Jeol JEM-2011 (Jeol Ltd., Tokyo, Japan).
- Scanning electron microscopy characterizations were performed with a Jeol JSM- 6300 (Jeol Ltd.) linked to an energy-dispersive spectrometer LINK ISIS-200 (Oxford Instruments, Bucks, England) for the energydispersive X-ray analysis.

3.3.2.2. Reagents and materials

All buffer reagents and other inorganic chemicals were supplied by Sigma, Aldrich, or Fluka, unless otherwise stated. All chemicals were used as received, and all aqueous solutions were prepared in doubly distillated water.

- Streptavidin-coated magnetic beads (M-280), from Dynal Biotech.
- Biotin conjugate-goat anti-human IgG (sigma B1140, developed in goat and ç-chain specific), human IgG from serum, goat IgG from serum, anti-human IgG peroxidase conjugate (Sigma A8667, developed in goat and whole molecule), o-phenylenediamine dihydrochloride (OPD), hydrogen tetrachloroaurate(III) trihydrate ($HAuCl_4.3H_2O$, 99.9%), trisodium citrate, and hydrogen peroxide were purchased from Sigma-Aldrich.

3.3.2.3. Buffers and solutions preparation

These are listed below:

- Phosphate buffer solution (PBS): 0.01 M phosphate-buffered saline, 0.137 M NaCl, and 0.003 M KCl (pH 7.4).
- Blocking buffer: PBS solution with added 5 % (w/v) (BSA; pH 7.4).
- The binding and washing (B&W) buffer: PBS solution with added 0.05 % (v/v) Tween 20 (pH 7.4).
- Supporting electrolyte: 0.1 M HCl solution.
- OPD-H_2O_2 solution for spectrophotometric analysis: dissolving one Sigma OPD tablet in 25 mL of phosphate-citrate buffer (pH 5.0), and then immediately before the analysis, add 10 μL of a 30 % H_2O_2 solution.

3.3.2.4. Electrode construction

The electrode construction was carried out in the same way as previously has been described. See section 3.2.2.5.of this thesis, but here is named GECE-M instead of M-GECE.

3.3.2.5. Procedures

– ***Synthesis and characterization of gold nanoparticles***

AuNPs were synthesized by reducing tetrachloroauric acid with trisodium citrate, a method pioneered by Turkevich et al.[23] Briefly, 200 mL of 0.01 % $HAuCl_4$ solution were boiled with vigorous stirring. 5 mL of a 1 % trisodium citrate solution were added quickly to the boiling solution. When the solution turned deep red, indicating the formation of AuNPs, the solution was left stirring and cooling down. (*See* Figure 3.26)

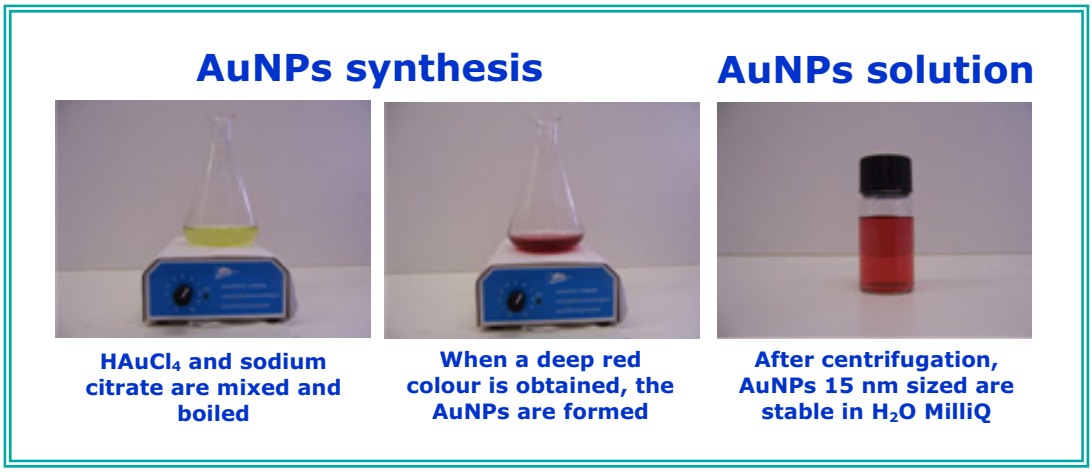

Figure 3.26. *Illustration of synthesis of AuNPs.*

The figure 3.27 shows a schematic representation of the synthesis AuNPs reaction.

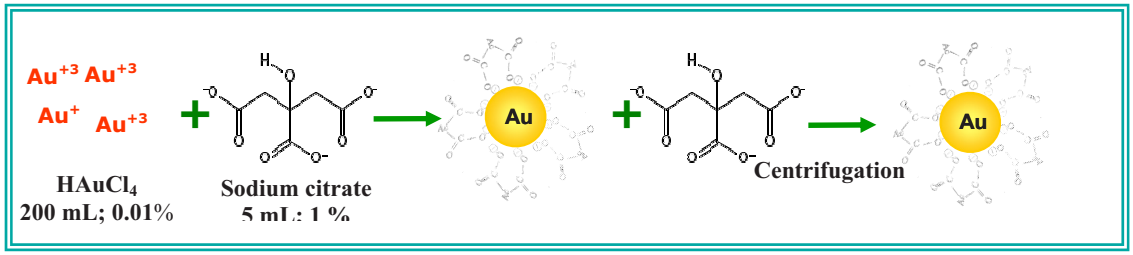

Figure 3.27. *Schematic representation of the AuNPs synthesis reaction.*

– **Preparation of the DC-AuNP**

The DC-AuNP, which represents a gold-labelled antihuman IgG-peroxidase conjugate antibody, was prepared by following the published procedure.[24] (*see* Figure 3.28 (upper part) The binding of the biotinylated anti-human IgG with streptavidin-coated paramagnetic beads was carried out using a slightly modified procedure recommended by Dynal Biotech.[25]

– **Preparation of Magnetic Beads Sandwich-Type Immunocomplexes**

150 μL (15 μL from the stock solution) of MB were transferred (I in Figure 3.28) into a 0.5-mL Eppendorf tube. The MB were washed twice with 150 μL of B&W buffer and then resuspended in 108 μL of B&W buffer and 42 μL (from stock solution 0.36 mg/mL) of biotinylated anti-human IgG were added. The resulting MB and anti-human IgG solution was incubated for 30 min at temperature of 25 °C with gentle mixing in a TS-100 ThermoShaker. The formed MB/anti-human IgG (II in Figure 3.28) was separated from the incubation solution and washed three times with 150 μL of B&W buffer. The MB/anti-human IgG was resuspended in 150 μL of blocking buffer (PBS-BSA 5 %) to block any remaining active surface of MB, and i the mixture was incubated at 25 °C for 20 min.

The excess of DC-AuNP conjugate was magnetically separated from MB/anti-human IgG/human IgG/DC-AuNP conjugate (Va in Figure 3.28) for spectrophotometric analysis either HRP or AuNPs residuals.

Finally, the two magnetic bead sandwich immunocomplexes prepared without AuNP (MB/anti-human IgG/human IgG/anti-human HRP; see IVb in Figure 3.28) and with AuNP (MB/anti-human IgG/human IgG/DC-AuNP; see Vb in Figure 3.28) in the secondary antibody conjugate were analyzed spectrophotometrically and/or electrochemically in order to evaluate the benefits in using AuNPs. See details of spectrophotometric analysis in publication VIII (chapter 7).

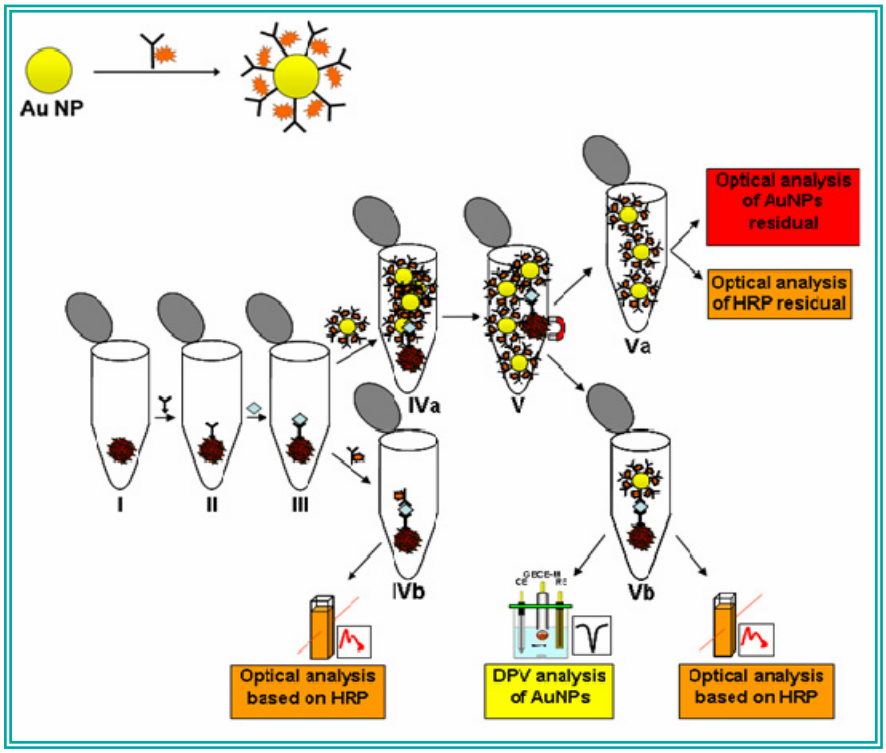

Figure 3.28. *Schematic (not in scale) of (upper part) preparation of double-codified label using AuNPs (13 nm) and anti-human IgG peroxidise conjugated antibody (anti-human-HRP) and (lower part) general assay procedure and characterizations, consisting of the following steps. (I) Introduction of streptavidin-coated paramagnetic beads (MBs). (II) Incubation with the primary biotinylated anti-human IgG antibody. (III) Incubation with different concentrations of the antigen human IgG. (IVa) Incubation with gold-labeled anti-human-HRP. (V) Separation of the magnetic bead immunocomplex from unbound gold-labeled anti-human-HRP. (Va) Gold-labeled anti-human-HRP residual for spectrophotometric analysis of gold and HRP. (IVb) Incubation with anti-human-HRP and spectrophotometric calibration based on HRP. (Vb) Magnetic bead immunocomplex with gold-labeled anti-human-HRP ready for double detection: spectrophotometric based on HRP and electrochemical based on direct DPV analysis of AuNPs.*

– **Electrochemical Analysis**

The MB/antihumanIgG/human IgG/DC-AuNP immunocomplex was resuspended in 150 μL of double-distilled water. A 50 μL aliquot of this suspension was brought into contact for 5 min with the surface of the magnetic graphite-epoxy composite electrode in order to allow AuNP to accumulate on it. After 5 min, the electrode was transferred without any washing steps to an electrochemical cell

containing 0.1 M HCl. A preconcentration process to oxidize AuNPs to $AuCl_4^-$ was performed at +1.25 V (vs Ag/AgCl) for 120 s in a stirred solution. Immediately after the electrochemical oxidation, DPV was performed as, scan rate 33.5 mVs^{-1}, nonstirred solution), resulting in an analytical signal due to the reduction of $AuCl_4^-$ at potential +0.45 V[26]. *See* Figure 3.29.)

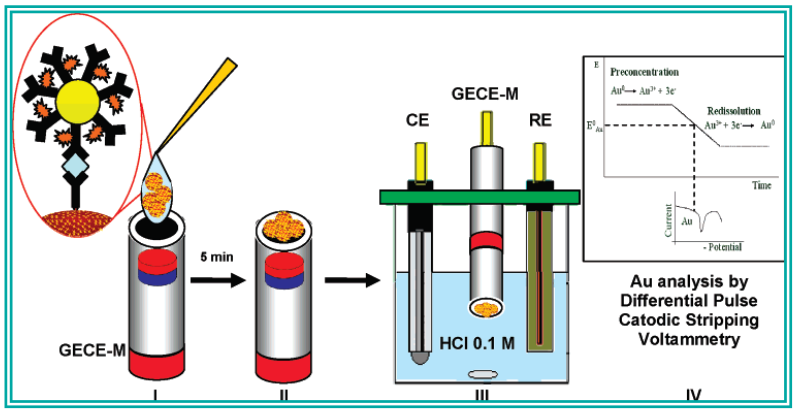

Figure 3.29. *Electrochemical analysis procedure consisting of the following. (I) Deposition of 50 µL of the MB-AuNP immunocomplex sample onto the electrode surface. (II) Adsorption of the added immunocomplex on the electrode surface for 5 min at open circuit. (III) Introduction of the electrode without a washing step in the measurement cell containing 0.1 M HCl as electrolyte buffer. (IV) Electrochemical analysis consisting of a preconcentration step at 1.25 V for 150 s, followed by a DP cathodic scan from 1.25 to 0 V, and measurement of the peak current at 0.45* V (step potential 10 mV, amplitude 50 mV, scan rate 33 mV/s (vs Ag/AgCl).

3.3.3. Results and discussion

– ***Preparation of the DC-AuNP***

The gold aggregation test was performed to detect salt-induced colloidal gold aggregation and find by this way the Ab concentration to be used for conjugation with AuNPs. The Ab concentration that prevents gold aggregation was determined by measuring the difference between the absorbance at 520 nm and at 580 nm and plotting it against the concentration used (*see* Figure S7 Supporting information of

publication VIII) (at chapter 7). The minimum antibody concentration giving the highest absorbance difference was 7 μg for 1 mL of AuNPs and that corresponded to the number of protein molecules of 10 for each gold nanoparticle. See more details at publication VIII (at chapter 7).

Transmission electron micrographs (*see* Figure 3.30) show AuNPs surrounded by anti-human-HRP antibodies. The multiple small dots present inside the biological mass could be associated with Fe atoms of the prosthetic heme group of HRP enzymes.

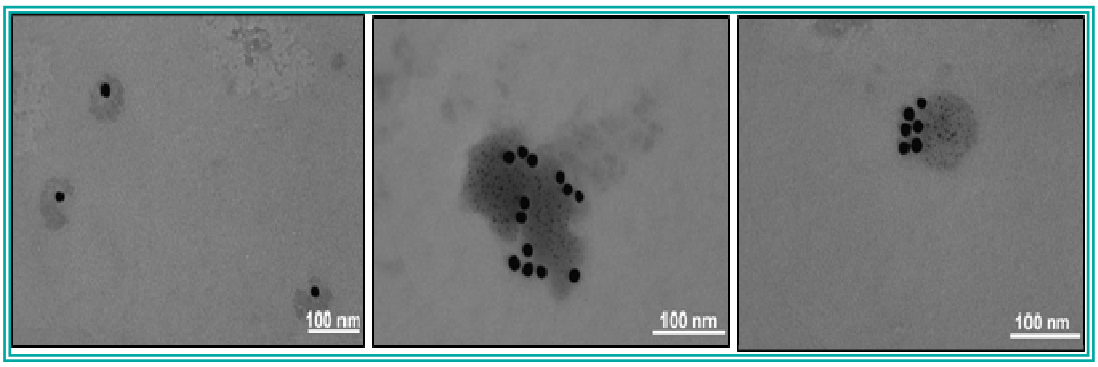

Figure 3.30. *Transmission electron micrographs showing anti-human-HRP antibodies conjugated to AuNPs. The small spots around the black AuNPs can be associated to iron metals present in the heme group of HRP. The experimental conditions of the conjugate preparation are explained in section 3 of the main text of publication VIII (at chapter 7)*

– ***Spectrophotometric Analysis***

In order to know these results, see publication VIII (chapter 7), where have been explained widely.

– ***Electrochemical Measurements***

The sandwich-type immunocomplex MB/anti-human IgG/ human IgG/ DC-AuNP (Vb in Figure 3.28) obtained after magnetic separation of the unbound DC-

AuNP was directly detected using the differential pulse cathodic scan, obviating the use of toxic HBr/Br_2 solutions. The results obtained (*See* Figure 6 of publication VIII) (at chapter 7) show an attractive performance of the magnetically trigged electrochemical detection of the immunoreaction based on DCAuNP labeling.

Figure 6A (*See* Figure 6 of publication VIII) (at chapter 7) shows typical DPV curves corresponding to the DC-AuNPs connected to the immunocomplex for human IgG concentrations ranging from 2.5×10^{-6} to 1 μg/mL.

Various parameters involved in the preparation of DC-AuNP based immunocomplexes as well as in the electrochemical detection including the deposition time of MB immunocomplexes on the electrode surface, before the electrochemical measurement were examined and optimized. See graphs and more details at publication VIII (at chapter 7)

Figure 6E (*See* publication VIII) (at chapter 7) shows the calibration curve for the DPV analysis of the MB immunocomplex. A sensitivity of 0.5066 μA/ln μg.mL^{-1} can be observed with a detection limit of 0.26 ng of human IgG for 1 mL of sample (that corresponds to 1.7 pM).

The method showed a very good precision, which represents an attractive and important feature for novel electrochemical immunoassays. The results obtained are related to the well-defined and highly reproducible magnetic collection of the MB/antihuman IgG/human IgG/DC-AuNP immunocomplexes on the electrode surface and overall to the direct detection of AuNPs without the need of any preliminary dissolving step that might affect the sensitivity as well as the

reproducibility of the method (a series of 3 repetitive immunoreactions for 1 μg of human IgG/ mL showed a RSD of ~3%).

The use of DC-AuNP label resulted in a significantly improved response for both the electrochemical and the spectrophotometric detection techniques, compared to the classical immunoassays exploiting HRP or other enzymes as labels. The lowest DL was for spectrophotometric detection (52 pg/mL or 0.33 pM); however, electrochemical analysis was the most sensitive and with a DL (260 pg/mL or 1.69 pM) still much lower or comparable with those reported by other authors based on either electrochemical or optical detections.[27]

The results obtained show that besides the optical-electrochemical application and opens new possibilities for in-field analysis in connection with low-cost and easy-to-use instrumentation.

The use of DC-AuNP label resulted in a significantly improved response for both the electrochemical and the spectrophotometric detection techniques, compared to the classical immunoassays exploiting HRP or other enzymes as labels. The lowest DL was obtained using spectrophotometric detection (52 pg/mL or 0.33 pM); however, electrochemical analysis was the most sensitive and with a DL (260 pg/mL or 1.69 pM) still much lower or comparable with those reported by other authors based on either electrochemical or optical detections.[27]

3.3.4. Conclusions

A versatile gold-labelled detection system based on either a spectrophotometric or an electrochemical method was developed.

The novel double-codified label consisting of AuNPs conjugated to an HRP-labelled anti-human IgG Ab, is used to detect human IgG as a model protein. MBs were used as supporting material for the preparation of the sandwich-type immunocomplexes.

A magnetic separation was then used to isolate the complexes from the unbound components, reducing considerably incubation and washing times. M-GECE allowed an efficient and very reproducible collection of the MB immunocomplexes on the electrode surface for enhanced adsorption and subsequently the direct electrochemical determination of AuNPs.

The DC-AuNP label allows us to perform immunoassays using both the electrochemical and the spectrophotometric techniques, obtaining for both detection methods better results in terms of DL (0.33 and 1.69 pM for the Ag by the optical-HRP-based and the electrochemical-AuNP-based analysis, respectively), and in terms of method sensitivity, if compared to the classical ELISA.

This proof of concept of a double-codified immunodetection method shows a very good performance, it is rapid, straightforward, and inexpensive (no special equipment is required).

In addition, this system establishes a general detection methodology that can be applied to a variety of immunodetection and DNA detection systems including lab-on-a-chip technology.

3.3.5. References

[1] Yates A. M., Elvin, S. J., Williamson D. E. The optimisation of a murine TNF-alpha ELISA and the application of the method to other murine cytokines. *J. Immunoassay* **1999**, 20, 31−44.

[2] Huang F., Cockrell D. C., Stephenson T. R., Noyes J. H., Sasser R. G. A Serum Pregnancy Test with a Specific Radioimmunoassay for Moose and Elk Pregnancy-Specific Protein B *J. Wildlife Management* **2000**, 64, 492−499.

[3] Choi J.-W., Jun H. P., Lee Woochang, Oh B.-K. Min J., Won Hong L. Fluorescence immunoassay of HDL and LDL using protein A LB film. *J. Microbiol. Biotechnol.* **2001**, 11, 979−985.

[4] Wang J. Huang W., Liu Y., Cheng J., Yang J. Capillary Electrophoresis Immunoassay Chemiluminescence Detection of Zeptomoles of Bone Morphogenic Protein-2 in Rat Vascular Smooth Muscle Cells. *Anal. Chem*. **2004**, 76, 5393−5398.

[5] Roda A., Pasini P., Mirasoli M., Michelini E., Guardigli M. Biotechnological applications of bioluminescence and chemiluminescence. *Trends in Biotechnology* **2004**, 22, 295−303.

[6] Adler M., Wacker R., Niemeyer C. M. A real-time immuno-PCR assay for routine ultrasensitive quantification of proteins. *Biochem. Biophys. Res. Comm.* **2003**, 308, 240−250.

[7] Wang, J. Nanomaterial-Based Amplified Transduction of Biomolecular Interactions. *Small* **2005**, 1, 1036−1043.

[8] Daniel M. C., Astruc D. Gold Nanoparticles: Assembly, Supramolecular Chemistry, Quantum-Size-Related Properties, and Applications toward Biology, Catalysis, and Nanotechnology. *Chem. Rev*. **2004**, 104, 293−346.

[9] Katz E., Willner I. Integrated nanoparticle-biomolecule hybrid systems: Synthesis, properties and applications. *Angew. Chem. Int. Ed*. **2004**, 43, 6042–6108.

[10] Wang J. Nanoparticle-Based Electrochemical Bioassays of Proteins. *Electroanalysis* **2007**, 19, 769–776.

[11] Dequaire M., Degrand C., Limoges B. An electrochemical metalloimmunoassay based on a colloidal gold label. *Anal. Chem*. **2000**, 72, 5521–5528.

[12] Wang J., Xu D.K., Kawde A.N., Polsky R., Metal nanoparticle based electrochemical stripping potentiometric detection of DNA hybridization. *Anal. Chem.* **2001,** 73, 5576–5581.

[13] Authier L., Grossiord C., Brossier P., Limoges B. Gold nanoparticle-based quantitative electrochemical detection of amplified human cytomegalovirus DNA using disposable microband electrodes. *Anal. Chem.* **2001**, 73, 4450–4456.

[14] Wang J., Liu G., Merkoçi A. Electrochemical Coding Technology for Simultaneous Detection of Multiple DNA Targets. *J. Am. Chem. Soc*. **2003**, 125, 3214–3215.

[15] Hernández-Santos D., González-García M. B., Costa-García A. Metal-nanoparticles based electroanalysis. *Electroanalysis* **2002,** 14, 1225–1235.

[16] M. B. González-García, C. Fernández-Sánchez, A. Costa-García. Colloidal gold as an electrochemical label of streptavidin–biotin interaction. *Biosens. Bioelectron*. **2000**, 15, 315−321.

[17] Das J., Aziz Md. A., Yang H. A Nanocatalyst-Based Assay for Proteins: DNA-Free Ultrasensitive Electrochemical Detection Using Catalytic Reduction of p-Nitrophenol by Gold-Nanoparticle Labels. *J. Am. Chem. Soc*. **2006**, 128, 16022−16023.

[18] Chen H., Jiang J.-H., Huang Y., Deng T., Li J.-S., Shen G.-L., Yu R-Q. An electrochemical impedance immunosensor with signal amplification based on Au-colloid labeled antibody complex. *Sensors and Actuators B: Chemical* **2006**, 117, 211−218.

[19] Chu X., Fu X., Chen K., Shen G.-L., Yu R-Q. An electrochemical stripping metalloimmunoassay based on silver-enhanced gold nanoparticle label. *Biosens. Bioelectron.* **2005**, 20, 1805−1812.

[20] Stoeva S. I., Lee J.-S.,Smith J. E., Rosen S. T., Mirkin C. A. Multiplexed Detection of Protein Cancer Markers with Biobarcoded Nanoparticle Probes. *J. Am. Chem. Soc.* **2006**, 126, 8378−8379.

[21] Willner I., Katz E. Magnetic control of electrocatalytic and bioelectrocatalytic processes. *Angew. Chem. Int. Ed. Engl.* **2003**, 42, 4576–4588.

[22] Nam J.-M., Thaxton C. S., Mirkin C. A. Nanoparticle-based bio-bar codes for the ultrasensitive detection of proteins. *Science* **2003**, 301, 1884–1886.

[23] Turkevich J., Stevenson P. C., Hiller J. A study of the nucleation and growth processes in the synthesis of colloidal gold. *Discuss. Faraday Soc*. **1951**, 11, 55–75.

[24] Beesley J. Colloidal Gold. A new perspective for cytochemical marking; Royal Microscopical Society Handbook 17; Oxford Science Publications. Oxford University Press: Oxford, England, 1989.

[25] Dynal Biotech, Technote 010 for product 112.05.

[26] Pumera M., Aldavert M., Mills C., Merkoçi A., Alegret S. Direct Voltammetric Determination of Gold Nanoparticles Using Graphite-Epoxy Composite Electrodes. *Electrochim. Acta* **2005**, 50, 3702–3707.

[27] Wang M., Wang L., Yuan H., Ji X., Sun C., Ma L., Li J.H., Bai Y., Li T. Immunosensors Based on Layer-by-Layer Self-Assembled Au Colloidal Electrode for the Electrochemical Detection of Antigen. *Electroanalysis* **2004**, 16, 757–764.

Chapter 4. GLOBAL DISCUSSION OF RESULTS

4. GLOBAL DISCUSSION OF RESULTS

Bismuth modified sensor. One of the principal advantages of the $Bi(NO_3)_3$GECE is the decreased toxicity and improved environmental safety using this bismuth-based electrode instead of mercury based electrodes for heavy metal analysis. The prepared sensors can be safely disposed without adverse environmental considerations. They give reproducible response, have low cost and are compatible with mass production technologies.

DNA sensing with M-GECE. The developed M-GECE showed great capacity and efficiency for DNA modified MB accumulation / immobilization. This sensor allow the direct detection of Au-NPs tags, anchored through the DNA hybridization event without the need of previous acidic dissolution.

The different genosensor strategies developed show an excellent discrimination against noncomplementary DNA as well as for one and/or three base mismatches. In these cases, when replaced the target, DPV signals with very low intensity or even null responses were observed. These indicate that we could selectively identify the target DNA sequence without interferences from excess non-complementary DNA.

Gel electrophoresis has been performed in order to verify the purity of the functionalization of 1.4 nm diameter AuNPs with thiol-oligonucleotides (target, noncomplementary and one and/or three mismatches and signaling DNAs.

In all the developed assays the capture DNAs modified with biotin were immobilized onto MBs used as platform by means of the streptavidin-biotin

linkage. At assay model system the capture DNA was hybridized with the Au_{67}-labelled complementary target and non complementary and three base mismatches sequences.

In order to improve the efficiency of the proposed protocol for sandwich system assay (using a cystic fibrosis related DNA strand as target and 10 nm diameter AuNPs as label) BSA as a blocking agent in the corresponding step at the second hybridization is used. In parallel, and also to avoid the non specific adsorption the washing steps were improved.

Furthermore, the preliminary linking step of AuNPs with signaling thiol-oligonucleotide ensuring the ratio 1:1 AuNPs/DNA, allows the elimination of one step of the assay and, consequently, the analysis time was reduced.

Model protein sensing with M-GECE. M-GECE was also studied for protein detection giving promising results. The effect of relevant experimental variables, including the reaction time of antigen with antibody, the dilution ratio of the colloidal gold-labeled antibody and the parameters of the anodic stripping operation, upon the peak current was examined and optimized.

AuNPs labels for both DNA and protein sensing were directly determined by ASV on M-GECE without necessity of acidic dissolution. The lowest DL obtained for genosensors was of 3 pmol for sandwich system assay by using 1.4 nm diameter AuNPs and for immunosensor, using spectrophotometric detection (52 pg/mL or 0.33 pM); however, electrochemical analysis (protein detection) was the most sensitive and with a DL (260 pg/mL or 1.69 pM). The high performance of the method is attributed to the sensitive ASV determination of AuNPs on M-GECE.

Chapter 5. GENERAL CONCLUSIONS

5. GENERAL CONCLUSIONS

In this thesis a new graphite-epoxy composite electrode (GECE) containing $Bi(NO_3)_3$ [$Bi(NO_3)_3$-GECE)] as built-in bismuth precursor, as a possible alternative for electrochemical stripping analysis of trace heavy metals has been developed. The results clearly show the advantages of the $Bi(NO_3)_3$-GECE in combination with SWASV technique for metal heavy metals detection.

Fast and effective analyses of trace metal ions such as Pb and Cd among others in environmental samples of soil, natural waters and effluents can be carried out by using the Bi electrode constructed. The inherent advantages of no necessity of mercury remove many of the objections for the use of electrochemical methods in the measurement of such species in these media. The electrode surface can be polished after each measurement and being used with the same efficient results in others measurements because the electrode is very robust.

When comparing the $Bi(NO_3)_3$-GECE with the commonly used mercury film electrode and previously developed bismuth film electrode, the newly proposed electrode offers a remarkable performance in analysis of trace heavy metals, which can be advantageous in electrochemical, hence contributing to the wider applicability of electrochemical stripping techniques in connection with "mercury-free" electrodes.

Beside environmental applications the developed bismuth based electrode would have special interest for application to heavy metal based quantum dots. Such applications are currently in the studying process at the research group for DNA detection.

Affinity electrochemical genosensors based on labelling with AuNPs and the use of MB as platform for the immobilization of capture DNA probe have been also developed in this thesis in order to demonstrate the effective magnetic triggering of M-GECE. As also has been demonstrated, with this magnetically assisted DNA sensor, target DNA leaded to very well defined signal whereas essentially no signal was observed for non-complementary DNA.

Beside the advantage of its use as capture platform, the MB can be separated from other species of the matrix simply by applying the magnetic force. This takes advantage of rapid magnetic separation (~30 s), which is in sharp contrast to conventional bioseparation processes (usually hours), such as chromatography and centrifugation.

During the development of this thesis has been demonstrated that the use of MB offers unprecedented advantages in this respect, because are sufficiently robust to allow repetitive washing under moderately stringent conditions, thus exhibiting the ability to efficiently remove non-specific species.

A novel, sensitive electrochemical immunoassay has been also developed based in AuNPs as label. The method was evaluated for a noncompetitive heterogeneous immunoassay of an IgG as a model.

The electrochemical detection of AuNPs labels in affinity biosensors using stripping methods allows the detailed study of DNA hybridization as well as immunoreactions with interest in genosensor or immunosensor applications.

Electrochemical methods used for AuNPs label detection may be very promising taking into account their high sensitivity, low detection limit, selectivity, simplicity, low cost, and availability of portable instruments.

As final conclusion, the DNA and protein electrochemical analysis strategies were successfully demonstrated and its use for real samples is viable. Such DNA biosensors and immunosensor hold an enormous application potential principally for clinic diagnostic and environmental monitoring among other fields.

Chapter 6. FUTURES PERSPECTIVES

6. FUTURES PERSPECTIVES

As reported in this thesis the lowest DL obtained for genosensors was of 3 pmol for sandwich system assay by using 1.4 nm diameter AuNPs. For protein sensing using spectrophotometric detection the DL was 52 pg/mL (0.33 pM) and for electrochemical analysis was the most sensitive but being the DL 260 pg/mL (1.69 pM).

However the obtained DL could be further lowered at these protocols by using diverse amplification techniques. Silver enhancement method, based on the catalytic effect of AuNPs on the chemical reduction (electro catalytic deposition) of silver ions can be used, Hydrogen catalysis too should be also promising alternative to improve detection limits.

Although two sizes (1.4 and 10 nm) AuNPs for DNA sensing and one size AuNP (~ 20 nm) for protein sensing have been already studied in this thesis further research should be necessary in the future for a better understanding of the effect the AuNP size toward the electrochemical signal might present.

Current works at our laboratory aims the triplex DNA electrochemical detection as a novel detection tool to be applied for *Listeria innocua* related DNA strand as target. M-GECE as working electrode and 1.4 nm diameter AuNPs functionalized with thiol-DNA as labels in a triplex assay and different parallel-stranded DNA clamps (capture DNA probes) to carry out the DNA triplex formation are being used.

The developed genosensing method should have special interest for single-nucleotide polymorphisms (SNPs) in real samples. The objective should be to establish an SNP electrochemical detection protocol using AuNPs and apply it to study the human genomic DNA samples for Factor II of coagulation gene (prothrombine, linked with thrombosis problems) with and without PCR. Table 6 shows oligonucleotide sequences to SNP electrochemical detection assay

As a further work we will employ human serum samples containing the genotypes of Factor II of coagulation can be employed. Real samples of the three possible genotypes of the Factor II of coagulation gene (prothrombine) linked with thrombosis problems: G/G, G/A and A/A are already supplied by the Unidad de Medicina Molecular-FPGMX, Clínica Universitaria Hospital de Santiago, Santiago de Compostela. This work is now in process by the research group.

Table 6. *Oligonucleotide sequences to SNP electrochemical detection assay*

NAME	USE	SEQUENCE
P1-FII	**Capture**	**5′-TCACTTTTATTGGGAACCA-3′**
P2-FII	**Signaling**	**SH-5′-GGAGCATTGAGGCTCGCTG-3′**
T1-FII	**Target**	**5′TGGTTCCCAATAAAAGTGACTCTCAGCGA GCCTCAATGCTCC-3′**
T2-FII	**Target**	**5′TGGTTCCCAATAAAAGTGACTCTCAGCA AGCCTCAATGCTCC-3′**

The fragment sequence that present the SNP of interest is shown below:

Fragment of the gene F2 GenBank agreement M17262.

SNP signaled at red G/A, rs1799963

26461 tatctagaaa cagttgcctg gcagaggaat actgatgtga ccttgaactt gactctattg

26521 gaaacctcat ctttcttctt cagagcccct ttaacaaccg ctggtatcaa atgggcatcg

26581 tctcatgggg tgaaggctgt gaccgggatg ggaaatatgg cttctacaca catgtgttcc

26641 gcctgaagaa gtggatacag aaggtcattg atcagtttgg agagtagggg gccactcata

26701 ttctgggctc ctggaaccaa tcccgtgaaa gaattatttt tgtgtttcta aaactatggt

26761 tcccaataaa agtgactctc agcgagcctc aatgctccca gtgctattca tgggcagctc

26821 tctgggctca ggaagagcca gtaatactac tggataaaga agacttaaga atccaccacc

26881 tggtgcacgc tggtagtccg agcactcggg aggctgaggt gggaggat

The future development of DNA and immunosensors based on the developed strategies aim at the mass production of these devices for several other applications.

Chapter 7. Publications

I

Sensitive stripping voltammetry of heavy metals by using a composite sensor based on a built-in-bismuth precursor.

Castañeda M. T., Pérez B., Pumera M., Del Valle M., Merkoçi A., Alegret S., *Analyst*, 2005, 130, 971-976.

Sensitive stripping voltammetry of heavy metals by using a composite sensor based on a built-in bismuth precursor

M. T. Castañeda,† B. Pérez, M. Pumera, M. del Valle, A. Merkoçi* and S. Alegret

Received 17th February 2005, Accepted 12th April 2005
First published as an Advance Article on the web 27th April 2005
DOI: 10.1039/b502486m

A new graphite–epoxy composite electrode (GECE) containing $Bi(NO_3)_3$ as a built-in bismuth precursor for simultaneous and individual anodic stripping analysis of heavy trace metals like lead and cadmium is reported. The developed $Bi(NO_3)_3$-GECE is compatible with bismuth film electrodes reported previously including the composite electrodes (Bi-GECE) recently reported by our group. $Bi(NO_3)_3$-GECE displays the ability for the detection of both individual and simultaneous determination of heavy trace metals and exhibits well defined, reproducible and sharp stripping signals. The sensitive response is combined with the minimal toxicity of $Bi(NO_3)_3$. This novel sensor would be an appropriate alternative tool to sensors using bismuth in solution during their utilization in environmental quality monitoring as well as other applications.

1. Introduction

Mercury-modified electrodes coupled with stripping techniques have been recognised as the most sensitive methods for determination of heavy metals.[1] However, the potential dangers associated with mercury have led to developing mercury-free sensors. Unmodified electrodes like bare carbon, gold or iridium[2–4] graphite–epoxy composites[5–7] recordable CDs[8] or silver-plated rotograved carbon electrodes[9] have been used as an alternative to mercury based electrodes. Efforts have been done also to use electrodes modified with various metal affinity compounds such as tetraphenylporphyrin,[10] Nafion[11,12] *N-p*-chlorophenylcinnamohydroxamic acid,[13] dithizone,[14] *etc*.

One of the excited alternatives to mercury based electrodes is that based on bismuth. Bismuth film electrodes (BiFE) display an attractive stripping voltammetric performance which compares favourably with that of common mercury-film electrodes (HgFE).[15] The low toxicity of bismuth makes it an alternative material to mercury in terms of trace metal determination.

The remarkable stripping performance of BiFE can be due to the binary and multicomponent 'fusing' alloys formation of bismuth with metals like lead and cadmium.[16] Bismuth film, with an attractive stripping voltammetric behaviour, prepared by electrodeposition onto the micro disc,[17] gold,[18] carbon paste,[19] glassy carbon,[20–23] rotating glassy carbon disc[24] electrodes have been reported. *In situ* or *ex-situ* preparation[25] of the BiFE including the effect of bismuth precursor salt used to prepare the film and a variety of substrate surfaces (platinum, gold, glassy carbon, carbon paste, carbon fibre)[26] for bismuth plating were carefully examined for their effects in the preconcentration and stripping steps, including the constant-current potentiometric stripping.[27]

Conducting composites represent another effort in designing mercury free sensors for stripping analysis. The capability of integrating various materials is one of their main advantages. Composite sensors offer many potential advantages including higher signal-to-noise (S/N) ratio[28–32] compared to more traditional electrodes consisting of single conducting phase. Composite electrodes can often be fabricated with great flexibility in size and shape of the material, permitting easy adaptation to a variety of electrode configurations. Their surfaces can be smoothed or polished to provide fresh active material ready to be used in a new assay. Each new surface yields reproducible results because all individual compounds are homogeneously dispersed or compressed in the bulk of the composite.

Fig. 1 represents the schematic of the rigid graphite–epoxy composite electrode (GECE) configurations (I, II) that have been used by our group as well as the new one (III configuration) that is presented in this work. The first configuration was based on GECE sensors without modifications. These sensors have been studied firstly for PSA determination of heavy metals by using stripping with constant current mode or chemical oxidation by dissolved oxygen.[5] Later on the same GECE without any modification have been characterised in their use in DPASV.[6,7]

The second configuration, Bi-GECE[33] was based on GECE without modification but bismuth film formation due to the presence of bismuth in the measuring solution. In the present work we present a novel configuration (Fig. 1, III) $Bi(NO_3)_3$-GECE, that represents GECE modified internally with bismuth nitrate salt which serves as a built-in bismuth precursor for bismuth film formation. This represents an integrated configuration of bismuth based GECEs for stripping analysis.

2. Experimental

Reagents and solutions

All solutions used in this study were prepared from analytical reagent grade chemicals. The lead and cadmium stock solutions were prepared by dissolving the corresponding

† On leave from: Departamento de Ciencias Básicas, Universidad Autónoma Metropolitana-Azcapotzalco, Av. San Pablo 180, Col. Reynosa Tamaulipas 022000, Mexico.
*arben.merkoci@uab.es

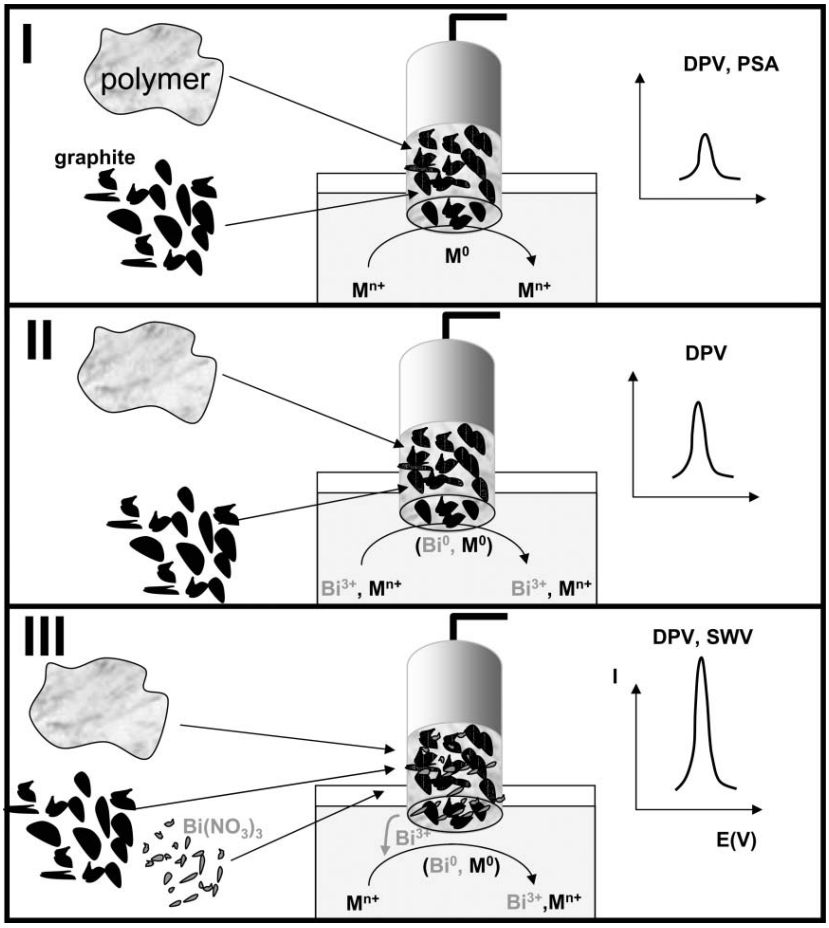

Fig. 1 Schematics of the sensing designs. The unmodified or modified GEC pastes have been introduced into a PVC cylindrical sleeve body (upper part) which has an inner electrical copper disc. Shown are: (I) sensing based on GECE sensors without modifications; (II) sensing based on Bi-GECE. It represents GECE without modification but in the presence of bismuth in the measuring solution. (III) Sensing based on $Bi(NO_3)_3$-GECE. It represents GECE modified internally with bismuth nitrate salt.

nitrates in water obtained from an ion-exchange system Milli-Q (Millipore). Acetate buffer (0.1 M, pH 4.5) or HCl 0.5 M were used as supporting electrolyte.

Electrode fabrication

The $Bi(NO_3)_3$-GECE were prepared using graphite powder with a particle size of 50 μm (BDH, UK), Epotek H77 (epoxy resin), hardener (both from Epoxy Technology, USA) and $Bi(NO_3)_3$ (Aldrich). Graphite powder and $Bi(NO_3)_3$ salt were first mixed together. The obtained dried mixture was mixed well with epoxy resin (mixed with hardener) in a ratio of 1 : 4 (w/w) as described in a previous work.[34,35] The percentage of $Bi(NO_3)_3$ in the prepared paste was varied, being 0.1, 0.5 and 2.0% (w/w).

The resulting $Bi(NO_3)_3$ containing graphite–epoxy paste was placed into a PVC cylindrical sleeve body (6 mm id), which has an inner electrical copper contact, to a depth of 3 mm. The conducting composite material glued to the copper contact was cured at 40 °C during one week. Before each use, the surface of the electrode was wet with doubly distilled water and then thoroughly smoothed, first with abrasive paper and then with alumina paper (polishing strips 301044-001, Orion).

Instrumentation

A platinum auxiliary electrode (model 52–67 1, Crison, Spain) and double junction Ag/AgCl reference electrode (Orion 900200) with 0.1 M KCl as external reference solution and $Bi(NO_3)_3$-GECE as working electrode were used. Square wave anodic stripping voltammetry (SWASV) experiments were performed using an Autolab PGSTAT 20 System (Eco-chemie, The Netherlands). A Hitachi S-570 scanning electron microscope (SEM) was used to observe the surface of the working electrodes.

Electrochemical procedures

SWASV measurements were carried out in the presence of dissolved oxygen. $Bi(NO_3)_3$-GECE as working, Ag/AgCl as reference and platinum as auxiliary electrodes were immersed into the electrochemical cell containing 25 mL 0.1 M acetate buffer (pH 4.5). The deposition potential of −1.3 V was applied to $Bi(NO_3)_3$-GECE while the solution was stirred. Following a 120 s deposition step, the stirring was stopped and after 15 s equilibration, the voltammogram was recorded by applying a square-wave potential scan between −1.3 and

−0.3 V with a frequency of 50 Hz, amplitude of 20 mV and potential step of 20 mV. Aliquots of the target metal standard solution were introduced after recording the background voltammograms. A 60 s conditioning step at +0.6 V (with solution stirring) was used to remove the remaining reduced target metals and bismuth, prior to the next cycle. The electrodes were washed thoroughly with deionized water between each test. The indicated procedure was employed unless stated otherwise.

Measurements in the phosphate buffer for the study of the pH effect as well as in HCl medium were also performed in the same experimental conditions as described above.

3. Results and discussion

The prepared $Bi(NO_3)_3$-GECE revealed physical and mechanical properties similar with the non-modified GECEs studied earlier.[28] The polished surface was smooth and shiny. Since fresh $Bi(NO_3)_3$ modifier particles are exposed on the surface upon polishing, they can be reduced electrochemically upon their contact with the measuring solution during the SWASV process along with the target analytes (see Fig. 1 III).

Surface characterisation

The surface morphologies of $Bi(NO_3)_3$-GECEs (containing different quantities of $Bi(NO_3)_3$ salt) before and after the preconcentration step (electrolysis at −1.3 V during 120 s) were observed by scanning electron microscopy (SEM).

As can be seen, the surface of $Bi(NO_3)_3$-GECE, with different concentration of $Bi(NO_3)_3$, before the preconcentration step (Fig. 2A) appears to have clusters of conducting material gathered in random areas. This is due to the graphite particles randomly distributed and randomly oriented in the epoxy resin.[36] Microcrystalline $Bi(NO_3)_3$ particles should also be distributed randomly, but due to the very low percentage (0.1–2.0%, w/w) were not visible. The darker coverage of the same $Bi(NO_3)_3$-GECEs after the preconcentration step (Fig. 2B) compared to $Bi(NO_3)_3$-GECE before preconcentration (Fig. 2A) is clearly visible. This is due to the bismuth film formation coming from the $Bi(NO_3)_3$ salt inside the sensor matrix. The quantity of $Bi(NO_3)_3$ did not have any visible effect on the sensor surface. The images 2B (a–c) have similar darkness. It seems that for different quantities of $Bi(NO_3)_3$ used, the bismuth film has the same configuration.

For all the $Bi(NO_3)_3$-GECEs after the preconcentration step there can also be seen dimensional fibril-like networks onto their surfaces, which is in correlation with an earlier report of a Bi-film on carbon surface.[15] The black and thick appearance of bismuth deposit can be attributed to carbon substrate that has positive effect on the nucleation and growth of the bismuth film. The same deposition of bismuth was clearly observed for GECE used in connection with bismuth in measuring solution.[33] In this way the bismuth film formation is clearly demonstrated in both configurations Bi-GECE and $Bi(NO_3)_3$-GECE (Fig. 1).

Measuring parameters

In order to obtain efficient SWASV response of $Bi(NO_3)_3$-GECE some important parameters such as step potential, amplitude and frequency were optimized as in a previous work.[33] For this purpose, the step potential from 5 to 50 mV with an increment of 5 mV, the amplitude from 5 to 50 mV increment of 5 mV and the frequency from 10 to 100 Hz increment of 10 Hz were scanned for 20 ppb Pb^{2+} in 0.1 M acetate buffer of pH 4.5 at deposition potential of −1.3 V for 120 s. According to the obtained voltammograms (results not shown) step potential of 20 mV, amplitude of 20 mV and frequency of 50 Hz were chosen as the optimum parameters.

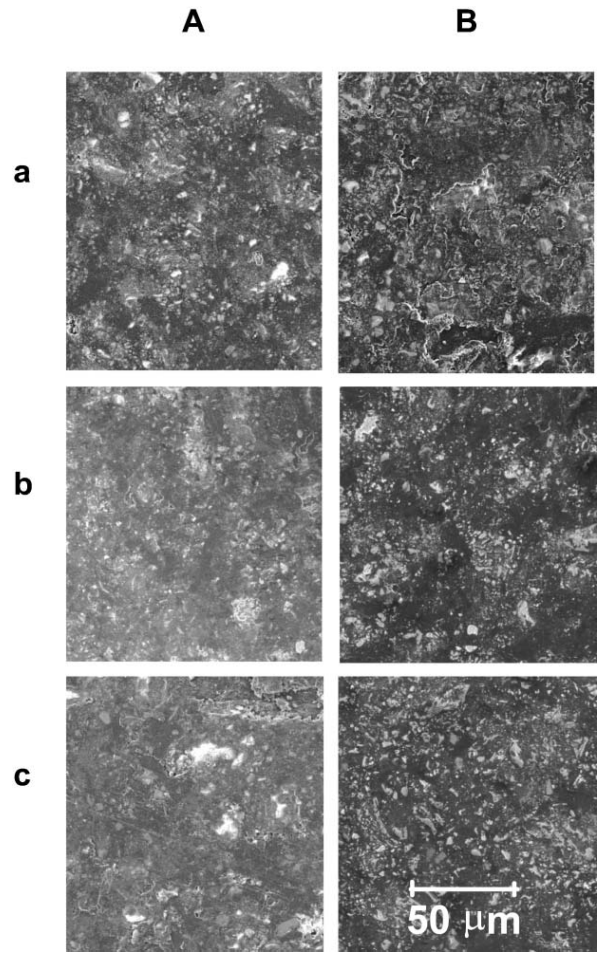

Fig. 2 Scanning electron microscopy images for $Bi(NO_3)_3$-GECE before (A) and after (B) the preconcentration step from solutions of 0.1 M acetate buffer (pH 4.5) at −1.3 V during 120 s. All electrode surfaces have been polished in the same way as explained in the text. The same accelerated voltage (10 kV) and resolution (10 μm) were used. The $Bi(NO_3)_3$ concentrations in the prepared sensors were 0.1 (a), 0.5 (b) and 2.0% (c) (w/w).

The characteristics of the electrodes must be very dependent on the amounts of $Bi(NO_3)_3$ used for the $Bi(NO_3)_3$-GECEs preparation. The effect of $Bi(NO_3)_3$ loadings (0.1–2.0%, w/w) in the SWASV of the resulting $Bi(NO_3)_3$-GECEs were studied for a 70 ppb solution of Pb^{2+} at 0.1 M acetate buffer of pH 4.5. The increase of $Bi(NO_3)_3$ content in the composite electrode increases the bismuth ion release during the contact with the measuring solution, and consequently the bismuth film formation capability. On the other hand, the higher $Bi(NO_3)_3$ content may reduce the conductivity of the $Bi(NO_3)_3$-GECE.

A maximum response was observed for $Bi(NO_3)_3$-GECE containing 0.1% $Bi(NO_3)_3$ chosen as a compromise between the two factors which affects oppositely the $Bi(NO_3)_3$-GECE response.

The effect of pH on the calibration curves of $Bi(NO_3)_3$-GECE (with 0.1% $Bi(NO_3)_3$) for lead in 0.1 M phosphate buffer were also tested. A decrease of the response by increasing the pH was observed indicating that the use of this built-in $Bi(NO_3)_3$-GECE at pH $>$ 6 is unfavourable most probably, as in the case of *in-situ* bismuth film formation, due to Bi(III) hydrolysis.[26] The maximal response was achieved at lower pH values.

It has been observed that GECE, when in long-term contact with aqueous solutions of extreme pH values ($>$10 or $<$2), begin to deteriorate. However as the working electrode surface can easily be renewed by a simple polishing, even very acidic medium can be used. In this work, HCl 0.5 M beside the 0.1 M acetate buffer (pH 4.5) has been used as a measuring medium.

Stripping voltammetry of trace metals

The stripping performance of $Bi(NO_3)_3$-GECE was tested for lead and cadmium and the resulting voltammograms were given in Fig. 3. The figure demonstrates the square wave stripping voltammograms for increasing concentration of cadmium (A) in 10 μg L^{-1} steps (b–j) and lead (B) in 10 μ L^{-1} steps (b–h). Also shown are the corresponding blank voltammograms (a) and the calibration plots (right) over the ranges 10–90 μg L^{-1} cadmium and 10–70 μg L^{-1} lead. The $Bi(NO_3)_3$-GECE displays well-defined and single peaks for cadmium (E_p = −0.76 V) and lead (E_p = −0.54 V). Detection limits of 7.23 and 11.81 μg L^{-1} can be estimated for cadmium and lead, respectively, based on the upper limit approach (ULA),[37] which utilizes the one-sided confidence band around the calibration line. Lower detection limits are expected in connection with longer deposition periods. Also in the concentration ranges mentioned above, the calibration plots (right) were linear exhibiting the R values of 0.9968 and 0.9953 for cadmium and lead, respectively.

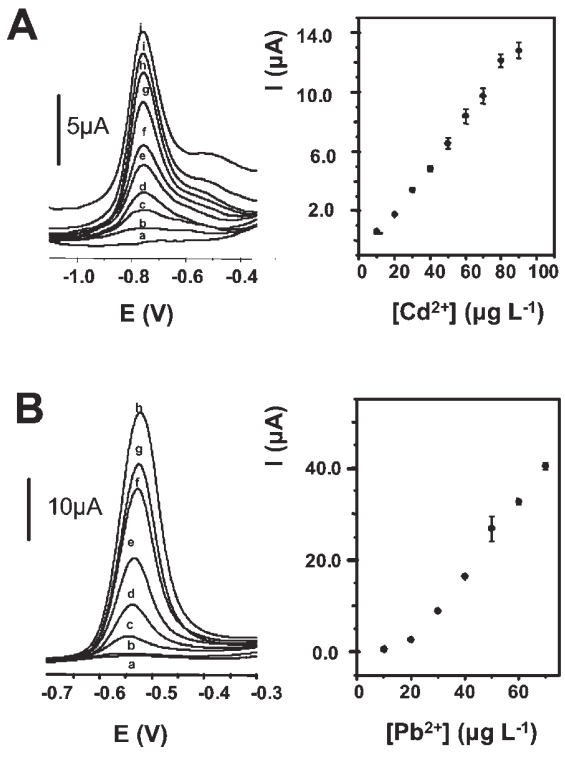

Fig. 3 Square-wave stripping voltammograms for increasing concentration of cadmium (A) in 10 μg L^{-1} steps (b–j) and lead (B) in 10 μg L^{-1} steps (b–h). Also are shown the corresponding blank voltammograms (a) and the calibration plots (right) over the ranges 10–90 μg L^{-1} cadmium and 10–70 μg L^{-1} lead; solutions 0.1 M acetate buffer (pH 4.5); square-wave voltammetric scan with a frequency of 50 Hz, potential step of 20 mV and amplitude of 20 mV; deposition potential of −1.3 V for 120 s.

The difference in peak shapes (sharper for lead and cadmium) and in detection limits of these heavy metals can be explained by the binary and multicomponent 'fusing' alloys formation of lead and cadmium with bismuth.[16]

As in the case of Bi-GECE the bismuth film formation onto $Bi(NO_3)_3$-GECE is shown to be a homogenous and uniform one due to the novel supporting material. The rich microstructure of $Bi(NO_3)_3$-GECE, composed of a mixture of carbon microparticles forming internal microarrays might have a profound effect upon the bismuth film structural features. The obtained peak widths of 20 mV for lead and cadmium were similar to other bismuth film electrodes reported previously.

The simultaneous measuring of lead and cadmium with $Bi(NO_3)_3$-GECE was also performed as shown at Fig. 4. This figure displays square wave stripping voltammograms for cadmium (E_p = −0.72 V) and lead (E_p = −0.54 V) for increasing concentrations in 10 μg L^{-1} steps (Pb) and 20 μg L^{-1} steps (Cd) (b–e). The well resolved peaks increase linearly with the metal concentration. The voltammogram clearly indicates that these metals can be measured simultaneously following a short deposition time of 2 min. In the concentration range from 10–40 μg Cd L^{-1} and 20–80 μg Cd L^{-1} the stripping signals remained undistorted and the resulting calibrating plots of this concentration range are linear, exhibiting the R values of 0.9562 and 0.9762, respectively,

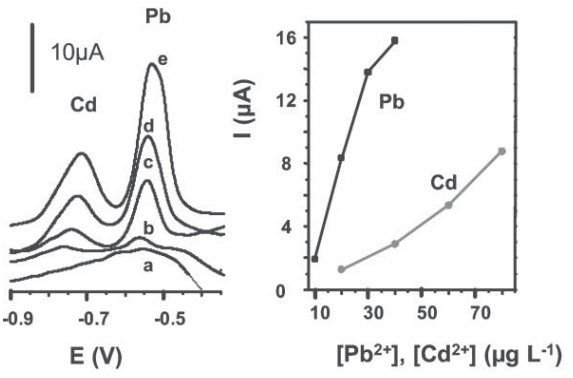

Fig. 4 Determination of cadmium and lead for increasing concentrations in 10 μg L^{-1} steps (Pb) and 20 μg L^{-1} steps (Cd); concentration ranges of 10–40 (Pb) and 20–80 (Cd) μg L^{-1}. Also shown is the blank (a) and the corresponding calibration plots. Experimental conditions as in Fig. 3.

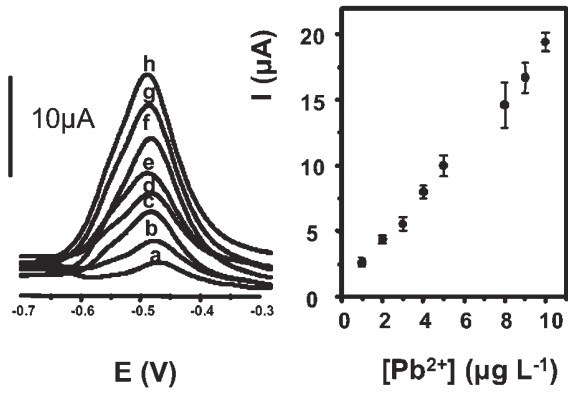

Fig. 5 Square-wave stripping voltammograms for increasing concentration of lead: (a) 1, (b) 2, (c) 3, (d) 4, (e) 5, (f) 8, (g) 9, (h) 10 μg L^{-1}. Also shown is the corresponding calibration plot (right) over the range 1–10 μg L^{-1} lead. The measuring solution was 0.5 M HCl. Other experimental conditions as in Fig. 3.

for lead and cadmium. Detection limits of around 19.1 and 35.8 μg L^{-1} can be estimated for lead and cadmium, respectively, based on the same method.[37]

A more sensitive measurement was observed for lead at 0.5 M HCl as measuring solution. Fig. 5 represents typical subtractive square-wave stripping voltammograms (removing blanks) for increasing concentration of lead ranging from 1 to 10 μg L^{-1} steps (a–h). Also, the calibration plot (right) over the studied range is shown. This highly sensitive response in HCl medium, as expected also from the study of the pH effect is probably related to an improved bismuth release and alloy formation in this medium.

The stability of the $Bi(NO_3)_3$-GECEs in 10 consecutive measurements for 50 ppb cadmium in 0.1 M acetate buffer of pH 4.5 and using the same surface was tested. It was observed that the reproducibility of the obtained current peak was comparable with that of the Bi-GECE[33] developed previously, that uses bismuth solution. It seems that the Bi precursor in the $Bi(NO_3)_3$-GECEs surface keeps ensuring the same heavy metal preconcentration. The relative standard deviation of this measurement was 9.33%.

Although the $Bi(NO_3)_3$ particles were not uniform in size they were expected to be exposed in a reproducible way onto the freshly obtained $Bi(NO_3)_3$-GECE surfaces after each mechanical polishing procedure. This was confirmed by checking the reproducibility of the measurements for a series of 10 different surfaces of the same $Bi(NO_3)_3$-GECE. The relative standard deviations of these measurements performed in the same experimental conditions as for the stability study was 10.69% for cadmium measurements.

4. Conclusions

A novel GECE that incorporates $Bi(NO_3)_3$ salt in the sensing matrix is developed. The resulted $Bi(NO_3)_3$-GECE is compatible with bismuth-film electrodes for use in stripping analysis of heavy metals. The built-in bismuth property is the distinctive feature of this $Bi(NO_3)_3$ modified GECE which can be utilized for the generation of bismuth adjacent to the electrode surface. The developed $Bi(NO_3)_3$-GECE is related with an *in-situ* bismuth ions generation and film formation without the necessity of external addition of the bismuth in the measuring solution. The good stability (9.33% for cadmium measurements) of the $Bi(NO_3)_3$-GECE is owing to the unique surface morphology resulting in enhanced contact between the GECE matrix and the electrochemically reduced bismuth. Moreover, the surface of the $Bi(NO_3)_3$-GECE could be renewed easily by simple polishing, so that the utility of the sensor is improved.

The convenience of this built-in bismuth sensor in voltammetric analysis will be greatly improved if this novel composite should be used by screen-printed technology. The utilization of the $Bi(NO_3)_3$-GECE for real heavy metal samples along with other applications are underway in our laboratory.

Acknowledgements

This work was financially supported by (1) Ministry of Education and Culture (MEC) of Spain (Projects BIO2004-02776, MAT2004-05164 and the grant MEC 2003-022 given to Dr M.Pumera); (2) Spanish Foundation Ramón Areces (project 'Bionanosensores'). A. Merkoci thanks the ''Ramón y Cajal'' program of MEC (Spain). The authors acknowledge Anna Puig's efficient technical assistance.

M. T. Castañeda,† B. Pérez, M. Pumera, M. del Valle, A. Merkoçi* and S. Alegret
Grup de Sensors i Biosensors, Departament de Química, Universitat Autònoma de Barcelona, 08193 Bellaterra, Catalonia, Spain.
E-mail: arben.merkoci@uab.es; Fax: 34-93581 2379; Tel: 34-935811976

References

1 J. Wang, *Stripping Analysis*, VCH Publishers, Deerfield Beach, 1985.
2 E. Achterberg and P. Braungardt, *Anal. Chim. Acta*, 1999, **400**, 381.
3 J. Wang and B. Tian, *Anal. Chem.*, 1993, **65**, 1529.
4 M. A. Nolan and S. P. Kounaves, *Anal. Chem.*, 1999, **71**, 3567.
5 M. Serradell, S. Izquierdo, L. Moreno, A. Merkoçi and S. Alegret, *Electroanalysis*, 2002, **14**, 1281.
6 L. Moreno, A. Merkoçi and S. Alegret, *Electrochim. Acta*, 2003, **48**, 2599.
7 S. Carrégalo, A. Merkoçi and S. Alegret, *Microchim. Acta*, 2004, **147**, 245.
8 L. Angnes, E. M. Richter, M. A. Augelli and G. H. Kume, *Anal. Chem.*, 2000, **72**, 5503.
9 P. R. M. Silva, E. Khakami, M. Chaker, A. Dufrense and F. Courchesne, *Sens. Actuators, B*, 2001, **76**, 250.
10 H. H. Frey, C. J. McNeil, R. W. Keay and J. V. Bannister, *Electroanalysis*, 1998, **10**, 480.
11 A. Merkoçi, M. Vasjari, E. Fabregas and S. Alegret, *Mikrochim. Acta*, 2000, **135**, 29.
12 Z. Hu, C. J. Seliskar and W. R. Heineman, *Anal. Chim. Acta*, 1998, **369**, 93.
13 T. H. Degefa, B. S. Chandravanshi and H. Alemu, *Electroanalysis*, 1999, **11**, 1305.
14 I. Palchetti, C. A. Upjohn, P. F. Turner and M. Mascini, *Anal. Lett.*, 2000, **33**, 1231.
15 J. Wang, J. Lu, S. B. Hocevar, P. A. Farias and B. Ogorevc, *Anal. Chem.*, 2000, **72**, 3218.
16 J. Wang, J. Lu, Ü. A. Kirgöz, S. B. Hocevar and B. Ogorevc, *Anal. Chim. Acta*, 2001, **434**, 29.
17 M. A. Baldo and S. Daniele, *Anal. Lett.*, 2004, **37**, 995.
18 H. P. Chang and D. C. Johnson, *Anal. Chim. Acta*, 1991, **248**, 85.
19 G. U. Flechsig, O. Korbout, S. B. Hocevar, S. Thongngamdee, B. Ogorevc, P. Grundler and J. Wang, *Electroanalysis*, 2002, **14**, 192.

20 E. A. Hutton, B. Ogorevc, S. B. Hocevar, F. Weldon, M. R. Smyth and J. Wang, *Electrochem. Commun.*, 2001, **3**, 707.
21 J. Wang and J. Lu, *Electrochem. Commun.*, 2000, **2**, 390.
22 G. Kefala, A. Economou, A. Voulgaropoulos and M. Sofoniou, *Talanta*, 2003, **61**, 603.
23 L. Lin, N. S. Lawrence, S. Thongngamdee, J. Wang and Y. H. Lin, *Talanta*, 2005, **65**, 144.
24 E. Chatzitheodorou, A. Economou and A. Voulgaropoulos, *Electroanalysis*, 2004, **16**, 21, 1745.
25 E. A. Hutton, J. T. van Elteren, B. I. Ogorevc and M. R. Smyth, *Talanta*, 2004, **63**, 849.
26 S. B. Hocevar, B. Ogorevc, J. Wang and B. Pihlar, *Electroanalysis*, 2002, **14**, 1707.
27 S. B. Hocevar, J. Wang, R. P. Deo and B. Ogorevc, *Electroanalysis*, 2002, **14**, 112.
28 S. Alegret, *Integrated analytical systems*, ed. A. Merkoçi and S. Alegret, Elsevier, Amsterdam, 2003, pp. 377–412.
29 S. Alegret, *Analyst*, 1996, **121**, 1751.
30 F. Céspedes, E. Fàbregas and S. Alegret, *Trends Anal. Chem.*, 1996, **15**, 296.
31 F. Céspedes and S. Alegret, *Trends Anal. Chem.*, 2000, **19**, 276.
32 S. Alegret, E. Fàbregas, F. Céspedes, A. Merkoçi, S. Solé, M. Albareda and M. I. Pividori, *Quím. Anal.*, 1999, **23**, 18.
33 Ü. A. Kırgöz, S. Marín, M. Pumera, A. Merkoçi and S. Alegret, *Electroanalysis*, 2005, published online 24 February.
34 M. Santandreu, F. Céspedes, S. Alegret and E. Martínez-Fàbregas, *Anal. Chem.*, 1997, **69**, 2080.
35 A. Merkoçi, S. Braga, E. Fàbregas and S. Alegret, *Anal. Chim. Acta*, 1999, **391**, 65.
36 S. Ramirez-Garcia, S. Alegret, F. Céspedes and R. J. Forster, *Analyst*, 2002, **127**, 1512.
37 J. Mocak, A. M. Bond, S. Mitchell and G. Scollary, *Pure Appl. Chem.*, 1997, **69**, 297.

II

Stripping analysis of heavy metals by using mercury-free composite based sensors. Chapter 1, pages 1-22, ‘Applications of Analytical Chemistry in Environmental Research, 2005’, Edited by Research SignPost, ISBN: 81-308-0057-8 Editor: Manuel Palomar, 2005.

Merkoçi Arben, Castañeda María Teresa, Alegret Salvador.

Research Signpost
37/661 (2), Fort P.O., Trivandrum-695 023, Kerala, India

Applications of Analytical Chemistry in Environmental Research, 2005:
ISBN: 81-308-0057-8 Editor: Manuel Palomar

1 Stripping analysis of heavy metals by using mercury-free composite based sensors

Arben Merkoçi, Maria Teresa Castañeda* and Salvador Alegret
Grup de Sensors & Biosensors, Departament de Química, Universitat Autònoma de, Barcelona, 08193 Bellaterra, Catalonia, Spain

Abstract

Stripping analysis (SA) has proved to be a powerful electroanalytical technique for trace-metal measurements. This technique offers excellent sensitivity and the possibility for multielement determination. The performance of SA is strongly affected by the working electrode material. To date a range of materials have been used as working electrodes for detection of heavy metals, the most popular being mercury based electrodes.

It is the potential dangers that are associated with mercury which has led to the development of various

*On live from: Departamento de Ciencias Básicas, Universidad Autónoma Metropolitana-Azcapotzalco, Av. San Pablo 180, Col. Reynosa Tamaulipas 022000, México, D. F., Mexico

Correspondence/Reprint request: Dr. Arben Merkoçi, Grup de Sensors & Biosensors, Departament de Química Universitat Autònoma de, Barcelona, 08193 Bellaterra, Catalonia, Spain. E-mail: arben.merkoci@uab.es

electrodes where the manipulation of large quantities of toxic mercury solutions may be avoided. In recent years, a growing interest in the use of mercury-free sensors has occurred. Graphite-epoxy composite (GEC) sensors for various SA techniques such as the differential pulse anodic stripping voltammetry (DPASV), square wave voltammetry (SWV) or potentiometric stripping (PS) of heavy metals have been used in our laboratories. The use of these types of sensors is a simpler alternative to the use of mercury for analysis of trace levels of heavy metals.

A general analytical study accompanied by scanning electron microscopy observations of GEC sensors, before and after the stripping step of heavy metals will be presented. Some comparative data obtained by classical electrodes along with a wide revision of the reported results obtained by other authors will also be presented.

GEC sensors show accumulation properties for heavy metals and consequently acceptable behaviour to be used as working electrode in various SA techniques. Heavy metal determination in real water samples in batch system or flow through systems will be presented. The obtained results show that these low cost and easy to prepare sensors can be with interest for future research in SA of heavy metals as well as for other analytes.

1. Introduction

1.1. Heavy metal analysis with electrochemical stripping techniques

There is an increasing demand for heavy metals monitoring as result of their high toxicity over human health. At present, the most common methods used for the analysis of heavy metals are flame atomic absorption spectrometry, graphite furnace-atomic absorption spectrometry, inductively coupled plasma-atomic emission spectroscopy and inductively coupled plasma-mass spectrometry. These techniques, commonly used for measuring trace metals in the central laboratory are not suitable for the task of on-site assays [1]. Electrochemical methods compared to the mentioned techniques, offers several advantages related with cost and simplicity. The most used methods for heavy metals analysis, between electrochemical methods, are stripping techniques. These techniques enhance selectivity and sensitivity by combining separation, pre-concentration and determination in one process [2,3].

1.2. State of the art of the mercury free electrodes

The performance stripping techniques is strongly affected by the working electrode material. An ideal working electrode should possess low ohmic resistance, chemical and electrochemical inertness over a broad range of

potentials, high hydrogen and oxygen overvoltage resulting in a wide potential window, low residual current, ease of reproduction of the electrode surface, maximum versatility, low cost and no toxicity.

To date a range of materials have been used as working electrodes for detection of heavy metals, the most popular being mercury based electrodes. The usefulness of mercury electrodes for the determination of metal ions is due to their ability to form amalgams, allowing for preconcentration of the metal ions prior to their determination by voltammetric stripping methods. Another advantage of using mercury in working electrodes is associated with the high overpotential of hydrogen evolution on such electrodes [4].

A common stripping procedure involves electrochemically generating the mercury film onto a graphite substrate. Mercury-modified electrodes coupled with stripping techniques have been recognised as the most sensitive methods for determination of heavy metals, especially the detection of lead. The use of hanging mercury drop electrode (the most common mercury electrode) and mercury film electrode has allowed a sub-ppb lead determination [5]. However, these techniques require tedious experimental precautions regarding the stability and recovery of mercury drop after each experiment or careful manipulation of mercury solutions for film deposition.

The potential dangers associated with mercury has led to the developing of various electrodes such that use of a mercury solution may be avoided. Among those electrodes which have been developed are the coating of glassy carbon electrodes (GCE) with a mercury - film modified with Nafion [6,7], cellulose acetate [8], naphtol derivative [9], cysteine [2] etc.. Even composite electrode containing HgO as a built-in mercury precursor, which supply mercury film formation, has been reported to avoid the use of mercury solution [10].

In recent years, as the result of the potential dangers that are associated with mercury, a growing interest in the use of mercury free electrodes has occurred. Modified as well as unmodified electrodes are reported for this purpose. A mercury-free voltammetric sensor for a hand-held instrument, for detection of copper, based on chemical accumulation of the trace metal onto the surface of glassy carbon electrode modified with tetraphenylporphyrin has been reported [11]. Similar efforts have resulted in the use of electrodes modified with PAN / Nafion [12] or N-p-chlorophenylcinnamohydroxamic acid [13]. Disposable screen-printed electrodes for lead determination based on carbon inks mixed with dithizone, Nafion or ionophore have been also developed [14]. Unmodified electrodes like bare carbon, gold or iridium as possible alternative to mercury have been used also. [15-18] Gold electrodes from recordable CDs [19] have been another material studied for its possible use in stripping voltammetry. Lastly, a silver-plated rotograved carbon electrodes was also reported [20].

Bismuth film electrodes (BiFEs), consisting of a thin bismuth-film deposited on a suitable substrate, have been shown to offer comparable performance to MFEs in ASV heavy metals determination. [21] The remarkable stripping performance of BiFE can be due to the binary and multi component 'fusing' alloys formation of bismuth with metals like lead and cadmium. [22] Besides the attractive characteristics of BiFE, the low toxicity of bismuth makes it an alternative material to mercury in terms of trace metal determination. Various substrates for bismuth film formation are reported. Bismuth film was prepared by electrodeposition onto the micro disc by applying an in-situ electroplating procedure.[23] Bismuth deposition onto gold [24], carbon paste [25] or glassy carbon [26-28] electrodes have been reported to display an attractive stripping voltammetric behaviour. In situ or ex-situ preparation [29] of the bismuth film electrodes including bismuth precursor salt and a variety of substrate surface (platinum, gold, glassy carbon, carbon paste, carbon fiber)[30] for bismuth plating were carefully examined for their effects in the preconcentration and stripping steps including the constant-current potentiometric stripping.[31]

1.2. Composite electrodes

Composite represents one of the most interesting materials for the preparation of working electrodes to be applied in electrochemical analysis. A composite results from the combination or integration of two or more dissimilar materials. Each individual component maintains its original characteristics while giving the composite distinctive chemical, mechanical and physical qualities. These qualities are different from those shown by the individual elements of the composite [32].

In general composites are classified by the nature of the conducting material (platinum, gold, carbon, etc.) and the arrangement of its particles (i.e. whether the conducting particles are dispersed in the polymer matrix or if they are grouped randomly in clearly defined conducting zones and insulating zones). Furthermore, using a given conducting material we may use different types of polymers thus establishing a new typification: epoxy composites, methacrylate composites, silicone composites, etc. Moreover, composites can be classified according their rigidity as rigid composites or soft composites, also, known as pastes or inks.

Conducting composites and biocomposites are interesting alternatives for the construction of electrochemical (bio)sensors. The capability of integrating various materials are one of their main advantages. Some materials which are incorporated within the composite result in enhanced sensitivity and selectivity. This incorporation is possible to be performed either through a previous modification of one of the component of the composite before its

preparation or through physical incorporation into the composite matrix. Composite and biocomposite electrodes offer many potential advantages [33-36] compared to more traditional electrodes consisting of a surface-modified single conducting phase. Composite electrodes can often be fabricated with great flexibility in size and shape of the material, permitting easy adaptation to a variety of electrode configurations.

Composite surfaces can be smoothed or polished to provide fresh active material ready to be used in a new assay. Each new surface yields reproducible results because all individual compounds are homogeneously dispersed or compressed in the bulk of the composite.

Composite electrodes have higher signal-to-noise (S/N) ratio, compared to the corresponding pure conductors, that accompanies an improved (lower) detection limit. Another advantage is the possibility to obtain composite electrodes from precious metals in a form with less weight and lower cost compared to their pure conductor counterparts.

Recent developments in the field of conducting composites applied to electrochemistry have opened a new range of possibilities for the construction of electrochemical sensors. The main features of these materials have been described elsewhere [33-36].

2. Designs and characterizations of metal sensors

2.1. Designs

Figure 1 represents the schematics of the metal sensing designs based on graphite epoxy composite electrodes (GECE) I) Sensing based on GECE sensors without modifications [37-39] II) Sensing based on Bi-GECE. [40] It represents GECE without modification but in the presence of bismuth in the measuring solution III) Sensing based on $Bi(NO_3)_3$-GECE. [41] It represents GEC modified internally with bismuth nitrate salt.

The GECE were prepared using graphite powder with a particle size of 50 μm (BDH, UK) and Epotek H77 (epoxy resin) and hardener (both from Epoxy Technology, USA). Graphite powder and epoxy resin (mixed with hardener) were hand-mixed in a ratio of 1:4 (w/w) as described in a previous work [42,43]. Bismuth nitrate salt was added in the GECE paste before curing so as to prepare the $Bi(NO_3)_3$-GECE.

The resulting pastes, for all cases, were placed into a PVC cylindrical sleeve body (6 mm i.d.), which has an inner electrical copper contact, to a depth of 3 mm. The conducting composite material glued to the copper contact was cured at 40ºC during a week. Before each use, the surface of the electrode was wet with doubly distilled water and then thoroughly smoothed, first with abrasive paper and then with alumina paper (polishing strips 301044-001, Orion).

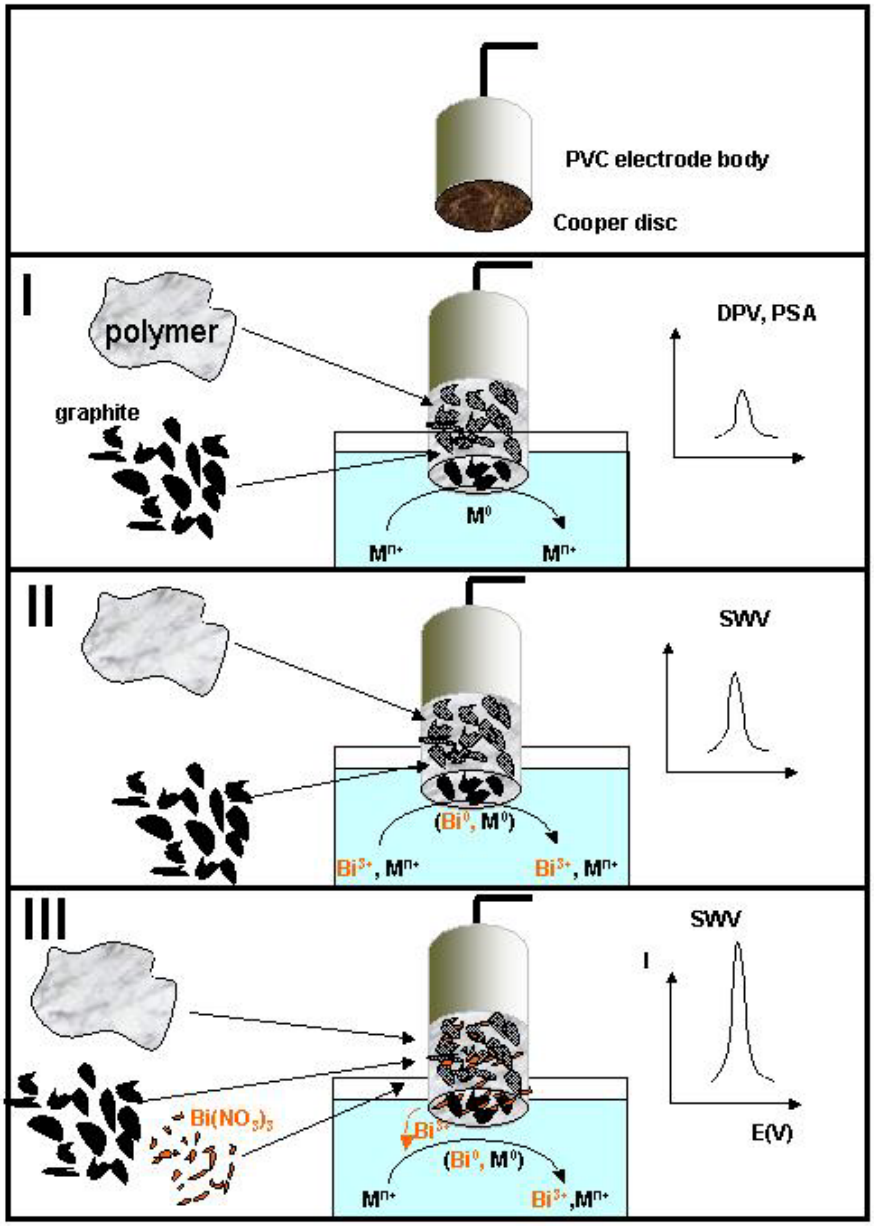

Figure 1. Schematics of the sensing designs. The unmodified or modified GEC pastes have been introduced into a PVC cylindrical sleeve body (upper part) which has an inner electrical copper disc. Shown are: I) Sensing based on GECE sensors without modifications II) Sensing based on Bi-GECE. It represents GECE without modification but in the presence of bismuth in the measuring solution III) Sensing based on $Bi(NO_3)_3$-GECE. It represents GEC modified internally with bismuth nitrate salt.

2.2. Characterisation

2.2.1. Scanning Electron Microscopy

The surface of GECE sensors as well as of glassy carbon electrodes (GCE) were observed by Scanning Electron Microscopy (SEM). Figure 2 (left

images) represents these surfaces. As observed in these images, the surface of GECE (left A) appears to have clusters of material gathered in random areas. Topographically speaking these appear to be of varying heights due to their apparent depth. A SEM image of the glassy carbon electrode for purposes of comparison is also shown (left B). This surface (in this image the PVC tube edge of the glassy carbon electrode is in the upper left hand corner) compared to that of GECE is characterised by a smooth surface and the absence of any clusters. The presence of clusters in the GECE surface results in an increase in its surface area compared to that of the glassy carbon electrode and consequently in the increase of the lead uptake due to an increased physical adsorption.

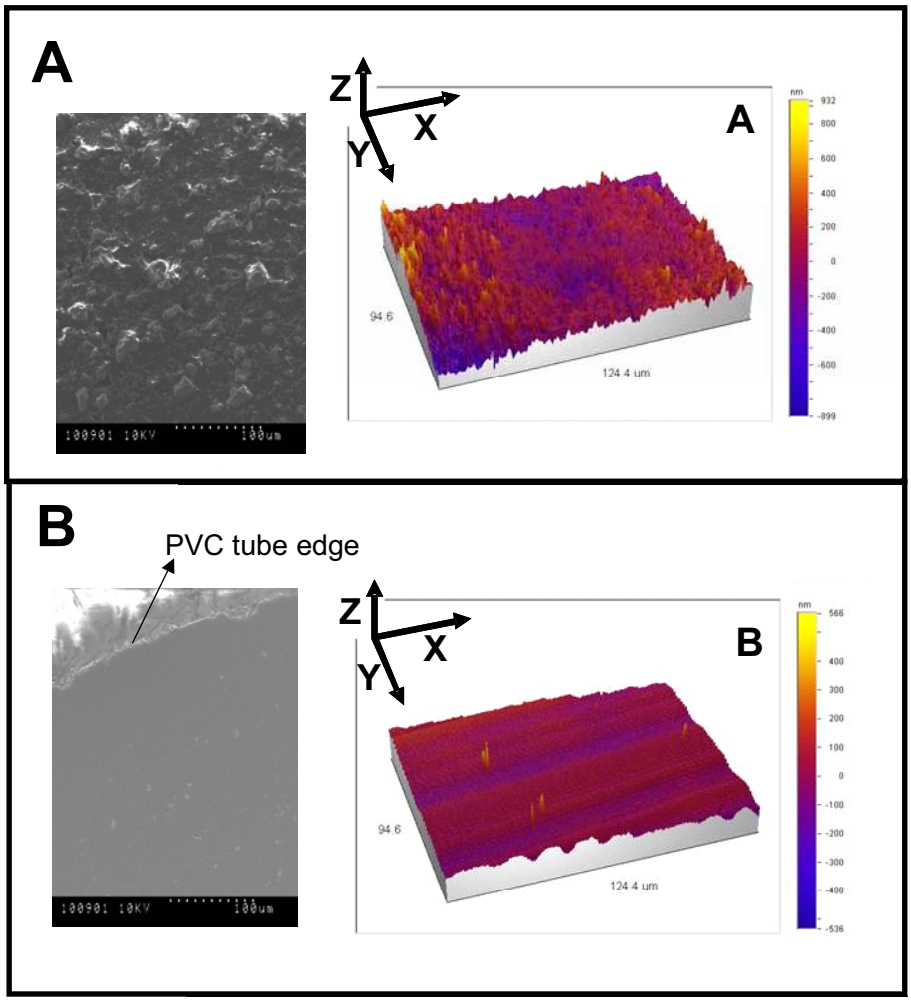

Figure 2. Images of GECE (A) and GCE (B) obtained by using SEM (left; the same accelerated voltage,10 KV, and resolution,100 μm, were used) and white light interferometric profilometry (right; at 50x magnification in each case). The surfaces have been polished in the same way as explained in the text.

2.2.2. Profilometry

To investigate the difference between the surfaces of the GECE and the GCE, the surface topography of each was also examined. Figure 2 (right images) shows 3D topographic maps of the surfaces of the GECE (right, A) and the GCE (right, B). It can be seen that the two electrodes have distinctly different topographies. The GECE surface is characterized by a very rough surface (R.M.S roughness = 151 nm, max. peak to valley height = 1.83 μm), covered with "peaks" and "valleys" which create sub-micron sized "wells". With only a few defects present, the surface of the GCE is much smoother (R.M.S roughness = 50 nm, max. peak to valley height = 1.10 μm). The surface is more undulating, with a structure on the X-Y scale of a few microns possibly due to the polishing procedure, but without the sub-micro "wells" seen in the GECE surface. Therefore there is strong evidence that these "wells" play an important role in the physical adherence of the reduced metals on the surface of the GECE.

3.1. Stripping analysis with non-modified composites

3.1.1. Stripping potentiometry

3.1.1.1. Principle of the method

Potentiometric stripping analysis (PSA) with two modes: (a) constant current and (b) chemical oxidation has been performed. The constant current mode consisted in two steps. In a first step (accumulation), the graphite- epoxy working electrode, the Ag/AgCl reference electrode and the platinum auxiliary electrode were immersed in a stirred 25 ml of 0.1 M sodium acetate solution (pH=3.76) and a constant potential (E_{acc}) of –0.9 V (vs. Ag/AgCl) was applied during a fixed interval time (τ_{acc}) 1 to 30 minutes. In the second step (stripping), a constant current (I_{strip}) of 1 μA was applied while potential is recorded to a limit of –0.2 V during a measurement time of 300 s in unstirred solution. The same procedure, without the removal of the electrodes, was repeated after an addition of a known quantity of heavy metal standard solution to obtain a calibration curve. All experiments were carried out without removal of oxygen.

In PSA with chemical oxidation mode the procedure was the same except the stripping step that was performed by dissolved oxygen in equilibrium with atmosphere.

3.1.1.2. Responses in standard solutions

Figure 3A represent lead calibration curve obtained for a τ_{acc} of 60 s and a I_{strip} of 1 μA. Each point in the calibration curve corresponds to the mean of three parallel measurements performed consecutively in the same cell without polishing the electrode. The error bars are the standard deviations of these measurements. Possible changes of graphite-epoxy electrode surface in contact

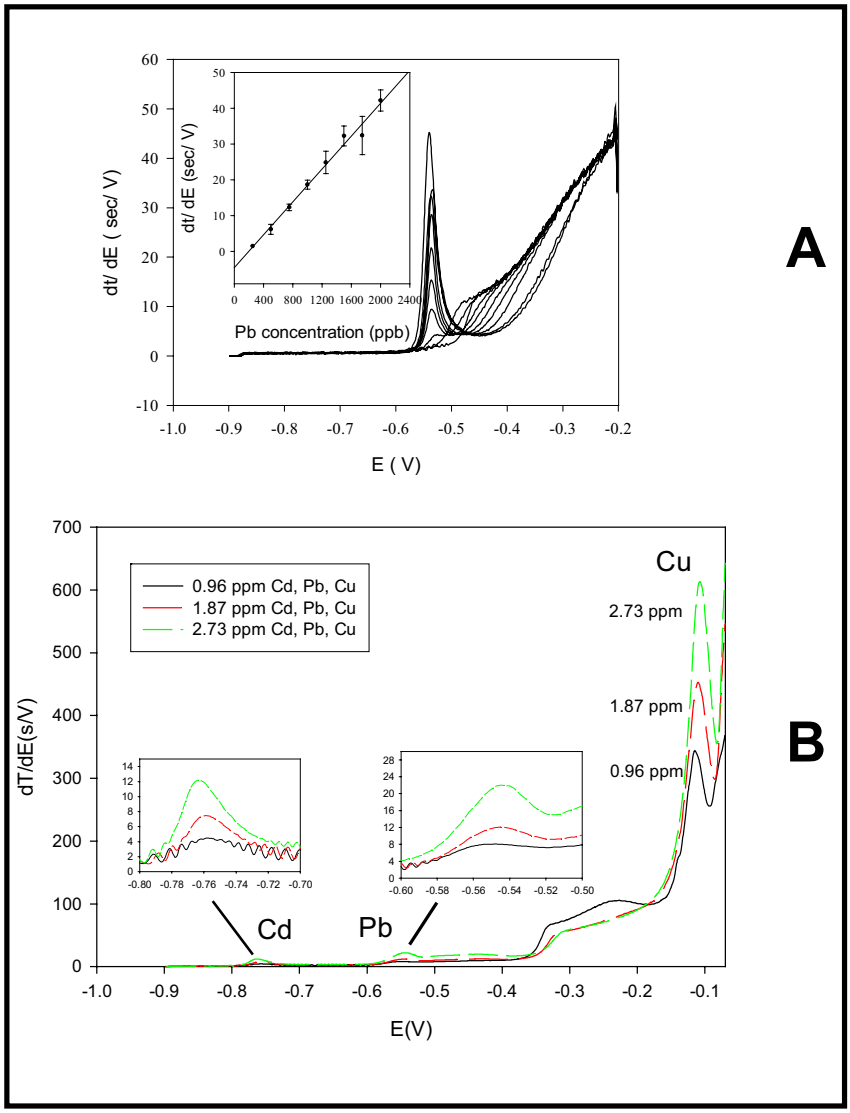

Figure 3. Typical PSA curves using non-modified GECE. (A) Constant current method for different lead concentrations. The composition of the cell was: 25 ml of 0.1 M acetate buffer pH=3.76 with 0.5 ppm of Pb. The other electrodes were: Auxiliary: platinum electrode; reference electrode: Ag/AgCl; Deposition potential: -0.9 V; Accumulation time 60 seconds. Stripping current: 1 μA; Potential limit: -0.2 V ; Max. Time of measurement: 300 sec. (B). Chemical stripping by dissolved oxygen for a mixture of lead, cadmium and copper. Deposition time 60 seconds; other conditions as in A.

with solution should have effect the repeatability of the response. A LD of approximately 200 ppb of lead was determined as the concentration corresponding to three times of the PSA background signal. Taking into consideration that a τ_{acc} of 60 s is used in this work, it would be expected that an increase in this τ_{acc}, would result in a lower LD comparable with those reported for modified glassy carbon electrodes (12 to 15 ppb for a τ_{acc} of 600 sec).

A mixture containing lead with copper and cadmium was also checked using PSA with chemical oxidation mode (Figure 3B). As can be seen from this figure for the same concentration the height of peak associated with copper is approximately 50 times greater than that of cadmium and 20 times greater than that of lead. These results show that the use of GECE is more sensitive for the analysis of copper than for lead and cadmium. The same results were obtained in the case of constant current method although in that case each metal was checked separately. Figure 4 also shows the cadmium and lead peaks are separated well suggesting that these heavy metals may be analysed, using a GECE, in the presence of each other without interferences. This offers an advantage which is not offered by the constant current mode which, showed an overlap between the lead and cadmium response for the gold-coated screen-printed electrode [17]. As observed in the Fig. 4, the copper peak tends to mask the peak associated with lead. High quantities of copper have to be considered for their interference to lead determination. The same copper interference causing a 60 % decrease of lead signal was reported by Palchetti et al. [14].

The repeatability of measurement was checked also for chemical oxidation mode. Results for these PSA peaks in a solution with 2 ppm lead has been studied. The scatter of peak potentials observed in the case of polishing the surface may be associated with the bulk homogeneity of the prepared composite [44]. Smaller potential deviations would be excepted for a better bulk-homogenised composite. It can be observed that the unpolished composite based electrodes give more reproducible peaks compared with polished ones being the relative standard deviations (RSD) of the mean peak signal 7% (n=5) and 11% (n=4) respectively for a 2 ppm lead solution. These RSD values for the GECE are similar with those reported in other works where film mercury or modified glassy carbon electrodes has been used [14].

3.1.2. Stripping voltammetry

3.1.2.1. Method

The differential pulse anodic stripping voltammetry (DPASV) proceeded in two steps. The first one was the accumulation step. In this step, the three electrodes – GEC working electrode, the Ag/AgCl reference electrode and the platinum auxiliary electrode– were immersed in a stirred 25 mL of 0.1 M HCl solution. A conditioning potential of 1 V during 30 sec was applied to clean the electrode from the previous deposited metals; after that an accumulation potential (E_{acc}) of –1.4 V (vs. Ag/AgCl) was applied for a fixed interval time (τ_{acc}) ranging from 1 – 30 min. The second step was the stripping step. In this step the potential was changed within the range of – 0.7 to –0.1 V, using a potential step of 0.0024 V. Modulation time was 0.05 sec and interval time of applied pulses was 0.2 sec. During the stripping step the current is recorded in quiescent solution. To obtain a calibration curve a known quantity of heavy

metal solution was successively added and the above accumulation and stripping procedures were applied, without the removal of the electrodes. All experiments were carried out without removal of oxygen.

Flow through measurements with DPASV were also performed. The working parameters were the same as in the batch measurements except that the metal accumulation step is performed in a flowing stream while the stripping step in a stop mode.

3.1.2.2. Responses in standard solutions

Figure 4A shows the voltammograms for a mixture containing lead, copper and cadmium using an accumulation time of 60 sec. The peaks for each metal are well separated. The corresponding calibration curves (inset Figure 4) are also presented. It can be seen that the sensitivity (change of I_{str} per each

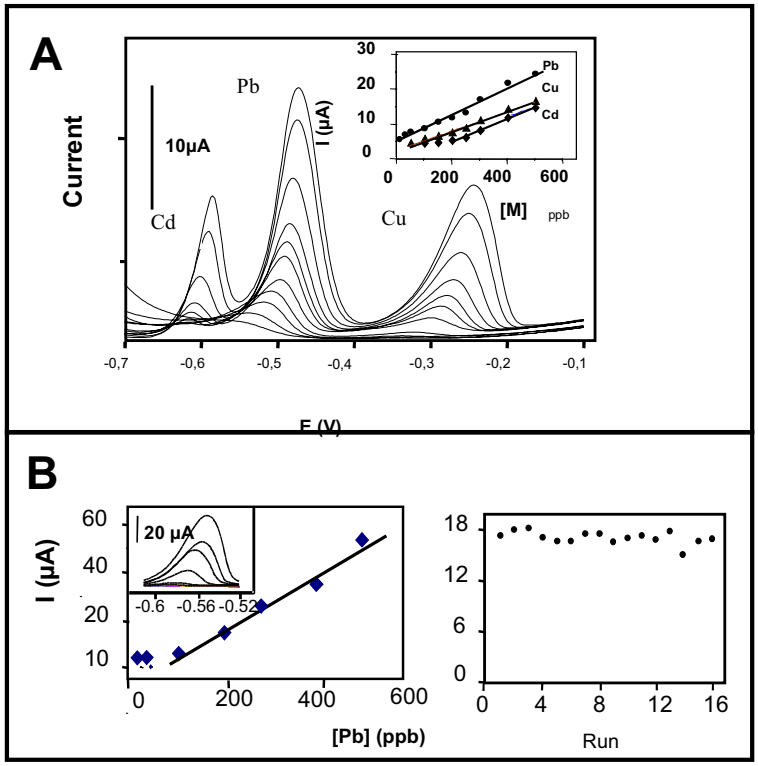

Figure 4 (A) Typical DPASV curves obtained with a graphite-epoxy composite electrode for increasing concentration of Cd, Pb and Cu along with the corresponding calibration curves (inset). The cell composition was: 25 mL 0.1 N HCl; the reference electrode: Ag/AgCl; counter electrode was Pt; accumulation potential, -1.4 V; τ_{acc}, 60 sec; step potential, 0.0024 V; modulation time: 0.05 sec ; interval time 0.2 sec.
(B) Calibration curve in flow through system (B, left) and the corresponding DPASV curves for lead concentrations from 100 to 500 ppb and τ_{acc} 3 min (B, inset left). Stability of the response for a 500 ppb Pb and τ_{acc} 60 s (B, right). Other experimental conditions as in A.

unit of metal concentration change) for lead is higher than copper with cadmium being the lowest. The detection limits (evaluated as the concentration corresponding to 3σ of the DPASV blank signal) were 100 ppb for Cd, 10 ppb for lead and 50 ppb for copper.

A simple flow through system that permits the constant flow of lead solution in 0.1 M HCl was used. The electrochemical cell used permitted the integration of the same three electrode configuration as in the batch measurements. In Figure 4B (left) is presented a typical calibration curve for lead along with the corresponding DPASV (inset, 4B left) for concentrations ranging from 100 to 500 ppb using a 3 min accumulation time. The detection limit was similar to batch measurements. The stability of the system for 16 runs of a 500 ppb lead solution are presented (Figure 4 B, right) showing a 4 % RSD.

3.1.2.3. Real samples

The GECE sensors were used for lead determination in real water samples suspected to be contaminated with lead obtained from water suppliers. The same samples were previously measured by three other methods: a potentiometric FIA system with a lead ion-selective-electrode as detector (Pb-ISE); graphite furnace atomic absorption spectrophotometry (AAS); inductively coupled plasma spectroscopy (ICP). The results obtained for lead determination are presented in Table 1. The accumulation times are given for

Table 1. Results obtained for real water samples using non-modified GECE. Experimental conditions as in Figure 4.

Sample	[Pb] (μg / L)			
	DPASV / τ_{acc} (min)	Pb-ISE	AAS	ICP
1	- / 60	17	<6	<5
2	17 / 6	28	44	36
3	89 / 2	64	88	80
4	50 / 2	122	176	141
5	18 / 10	45	41.3	37
6	263 / 1	175	240	194
7	14 / 20	18	18.1	15
8	121 / 1	158	192	174
9	404 / 1	344	495	398

each measured sample in the case of DPASV. Calibration plots were used to determine the lead concentration. GEC electrode results were compared with each of the above methods by using paired t-Test. The results obtained show that no significative difference appears for the results of GEC electrode compared to other methods. These results show that the application of GEC electrode in real samples is promising but still far from practical application if we take in consideration the relatively high RSD of GEC electrodes. The improvement of the reproducibility of the methods is one of the most important issues in the future research of these materials.

3.2. Bismuth film composite sensors

The analytical use of GECE modified in-situ with bismuth for square wave anodic stripping voltammetry (SWASV) of heavy metals. The use of these types of electrodes as a simpler alternative to the use of mercury or other bismuth modified electrodes for analysis of trace levels of heavy metals has been studied. The applicability of these new surface-modified GECE to real samples (tap water and soil samples) is presented.

3.2.1. Method

Square wave voltammetry stripping measurements were performed by in situ deposition of the bismuth and the target metals in the presence of dissolved oxygen. The three electrodes were immersed into 25 ml electrochemical cell containing 0.1 M acetate buffer (pH 4.5) and 400 µg/l of bismuth. The deposition potential of –1.3 V was applied to the GECE while the solution was stirred. Following the 120 s deposition step, the stirring was stopped and after 15 s the voltammogram was recorded by applying a square-wave potential scan between -1.3 V and -0.3V (with a frequency of 50 Hz, amplitude of 20 mV and potential step of 20 mV). Aliquots of the target metal standard solution were introduced after recording the background voltammograms. A 60 s conditioning step at +0.6 V (with solution stirring) was used to remove the target metals and the bismuth, prior to next cycle.

3.2.2. Responses in standard solutions

The stripping performance of Bi-GECE was tested for lead, cadmium and zinc and the resulting voltammograms were given in Figure 5 (A-C). The square wave stripping voltammograms for increasing concentrations of lead (A) in 20 µg/l steps (a-i), cadmium (B) in 10, 30, 50, 70, 100 µg/l (a-f) and zinc (C) in 500, 700, 1000, 1200 and 1500 µg/l (a-e). The bismuth film electrode displays well-defined and single peaks for all of the metals while sharper peaks were obtained for lead and cadmium compared to zinc (Ep= -0.48 V (Pb), Ep= -0.65 V (Cd) and Ep= -0.84 V (Zn)). Detection limits of 23.1, 2.2 and 600 µg/l can be estimated for lead, cadmium and zinc

respectively based on the signal to noise characteristics of these data (S/N=3). Lower detection limits are expected in connection to longer deposition periods. Also in the concentration ranges mentioned above, the calibration plots (inset) were linear exhibiting the R values of 0.9961, 0.9916 and 0.9965 for lead,

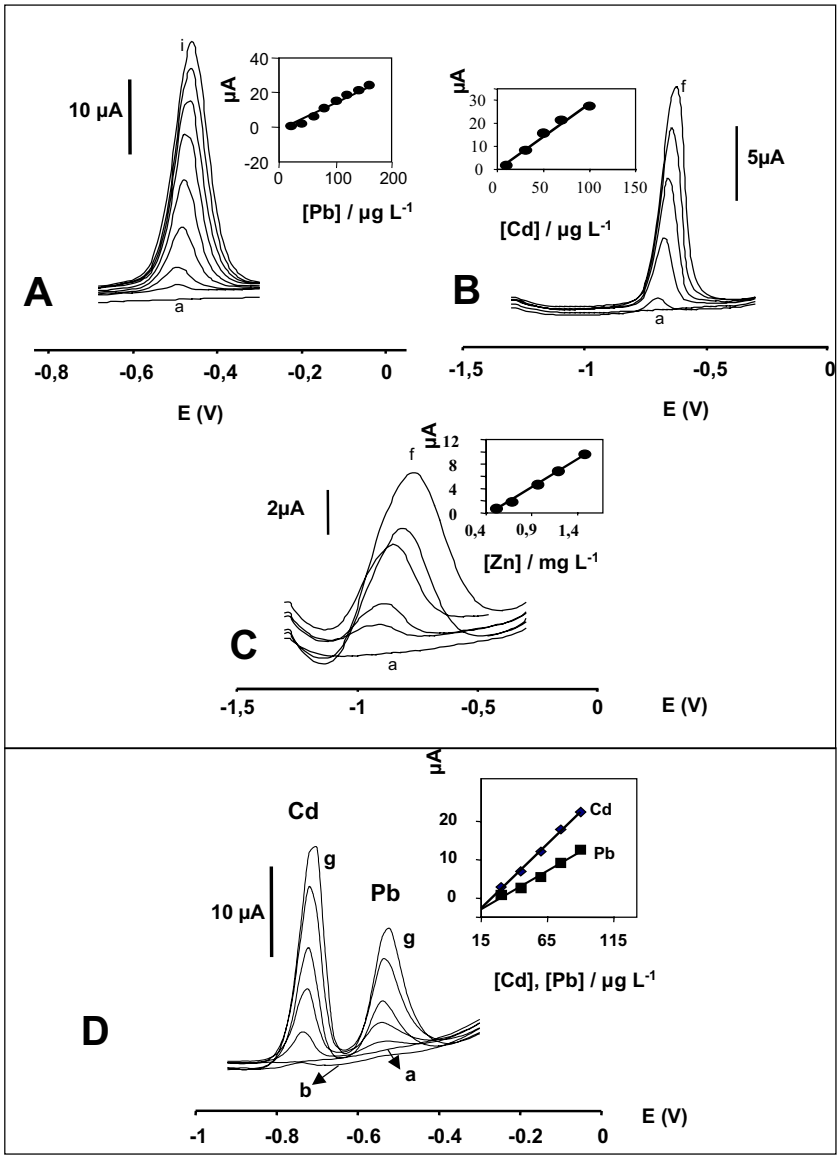

Figure 5. Square wave stripping voltammograms for incresing concentration of lead (A) in 20 µg/l steps (b-i), cadmium (B) in 10 µg/l steps (b-f) and zinc (C) in concentration of 500, 700, 1000, 1200 and 1500 µg/l (b-e) and for simultaneous determination of cadmium and lead (D) for increasing concentrations in 15 µg/l steps (b-g) (concentration range of 15-90 µg/l). Also shown are shown are the corresponding blank voltammograms (a) and as inset the corresponding calibration plots. Solutions 0.1 M acetate buffer (pH 4.5) containing 400 µg/ml bismuth. Square-wave voltammetric scan with a frequency of 50 Hz, potential step of 20 mV and amplitude of 25 mV.

cadmium and zinc respectively. The reproducibility of the Bi-GECE was also tested and found as 2.99%, 1.56% and 2.19% for lead, cadmium and zinc respectively. The difference in peak shapes (sharper for lead and cadmium) and in detection limits of these heavy metals can be explained by the binary and multi component 'fusing' alloys formation of lead and cadmium with bismuth[45]. According to these results, it can be deduced that zinc competes with bismuth for the surface site rather than involving an alloy formation with this metal.

The most attractive property of the Bi-GECE can be observed at the peak potentials of heavy metals. Compared to BiFE on glassy carbon and carbon fibre substrates [22], the approximate positive shifts of peak potential are of 125, 150 and 305 mV for lead, cadmium and zinc respectively. This shifted peak potential can be attributed to the more homogenous and uniform film formation due to the novel supporting material. The rich microstructure of GECE, composed of a mixture of carbon microparticles forming internal microarrays might have a profound effect upon the bismuth film structural features. The obtained peak shifts may be useful for improving resolutions overall taking in the consideration metals like Bi and Cu. The obtained peak widths of 230, 360 and 430 mV for lead cadmium and zinc respectively were similar to other bismuth film electrodes reported previously.

The simultaneous measuring of lead and cadmium with Bi-GECE was also performed as shown at Figure 5D. The Figure displays square wave stripping voltammograms for increasing concentrations of the two metals, cadmium (Ep= -0.72 V) and lead (Ep= -0.54 V), in steps of 15 μg/l between 15-90 μg/l. The well resolved peaks increase linearly with the metal concentration. The voltammogram clearly indicates that 30 μg/l concentrations can be measured simultaneously following a short deposition time of 2 min. In the concentration range from 30-90 μg/l the stripping signals remained undistorted and the resulting calibrating plot (inset) of this concentration range is linear exhibiting the R values of 0.9970 and 0.9985 for lead and cadmium. Detection limits of around 30 μg/l can be estimated for lead and cadmium respectively based on the signal to noise characteristics of these data (S/N=3).

The stripping performances of Bi film on glassy carbon or carbon fibre substrates were examined very carefully by Wang et al. [21] In addition to these materials, GECE (combined with bismuth film), a very easy to prepare and low cost electrode, can also be used successfully for simultaneous stripping analysis of cadmium and lead. Zinc was also tried to be detected simultaneously with lead and cadmium but it was not possible to obtain undistorted and linearly increased peaks. The poor response to zinc can be probably attributed to the preferable accumulation of Bi on GECE rather than of Zn which is result of the competition of these two metals for the GECE surface sites as observed also in other works [22].

3.2.3. Real samples

The performance of Bi-GECE was tested for measuring lead and cadmium in tap water and acetic acid extracted soil sample. The results were summarized at Table 2 in terms of recoveries ± RSD (n=3). For the tap water samples, multiple standard addition method was utilized to recover two concentration levels of 40 and 80 µg/l of spiked metals into 1 ml tap water. The recovered concentrations estimated from x axis interception of the resulted linear plot were 34 and 95 µg/l for lead while 48.5 and 85 µg/l was found for cadmium.

Soil samples, prepared as mentioned in experimental part, have been analysed by using graphite furnace atomic absorption spectrophotometry (AAS). The recoveries of the diluted samples, calculated by using standard addition method, are also presented at Table 2. The recoveries of spiked tap waters and the detected amounts in soil sample demonstrate that Bi-GECE can be applied for various real samples.

Table 2. The recoveries of metals from tap water and soil sample by using Bi-GECE.

Tap water			
Metal	Spiked concentration (µg / L)	Found concentration (µg / L)	Recovery (%)
Pb	40,0	34,0 ± 3,1	85,0 ± 7,6
	80,0	95,0 ± 2,1	118,8 ± 2,7
Cd	40,0	43,3 ±1,2	108,3 ± 3,0
	80,0	85,0 ±5,1	106,6 ± 6,4
Soil extract			
Metal	AAS concentration (µg / l)	Found concentration (µg / l)	Recovery (%)
Pb	88,0	80,0 ± 4,7	90,9 ± 5,4
Cd	24,8	19,0 ± 1,1	80,0 ± 3,5

3.3. Built-in bismuth precursor composite sensors

3.3.1. Method

SWASV measurements were carried out for Pb^{2+}, Cd^{2+} and Zn^{2+}, using the $Bi(NO_3)_3$-GECE as working, Ag/AgCl as reference and platinum as auxiliary electrode. The measurements were carried out in a stirred 25 mL of 0.1 M acetate buffer (pH 4.5). The deposition potential of -1.3 V was applied to the $Bi(NO_3)_3$-GECE while the solution was stirred. Following the 120 s deposition step, the stirring was stopped and after 15 s equilibration, the voltammogram

was recorded by applying a square-wave potential scan between -1.3 and -0.3 V (with a frequency of 50 Hz, amplitude of 20 mV and potential step of 20 mV. Aliquots of the target metal standard solution were introduced after recording the background voltammograms. A 60 s conditioning step at +0.6 V (with solution stirring) was used to remove the target metals and the reduced bismuth, prior to next cycle. The electrodes were washed thoroughly with deionized water between each test.

SWASV measurements were performed using 0.1 and 0.5 M HCl solutions as electrolytic medium in calibrations for lower concentrations of Pb^{2+} (from 1 to 10 ppb) being the experimental conditions the same as for the measurements in acetate buffer.

3.3.2. Responses in standard solutions

The stripping performance of $Bi(NO_3)_3$-GECE was tested for lead and cadmium and the resulting voltammograms were given in Figure 6. The Figure demonstrates the square wave stripping voltammograms for increasing concentration of cadmium (A) in 10 μg/L steps (b–j) and lead (B) in 10 μ/L steps (b–h). Also shown are the corresponding blank voltammograms (a) and the calibration plots (right) over the ranges 10 – 100 μg/L cadmium and 10 – 70 μg/L lead. The $Bi(NO_3)_3$-GECE displays well-defined and single peaks for cadmium (Ep = -0.76 V) and lead (Ep = -0.54 V). Detection limits of 7.23 and 11.81 μg/l can be estimated for cadmium and lead respectively based on the upper limit approach (ULA) [46], which utilizes the one-sided confidence band around the calibration line. Lower detection limits are expected in connection to longer deposition periods. Also in the concentration ranges mentioned above, the calibration plots (right) were linear exhibiting the R values of 0.9968 and 0.9953 for cadmium and lead respectively.

The difference in peak shapes (sharper for lead and cadmium) and in detection limits of these heavy metals can be explained by the binary and multi component ‘fusing’ alloys formation of lead and cadmium with bismuth.

The SWASV for zinc was also checked but the results obtained were not satisfactory. According to these results, it can be deduced that zinc competes with bismuth for the surface site rather than involving an alloy formation with this metal as observed also for Bi-GECE studied previously. [40]

As in the case of Bi-GECE the bismuth film formation onto $Bi(NO_3)_3$-GECE is shown to be a homogenous and uniform one due to the novel supporting material. The rich microstructure of $Bi(NO_3)_3$-GECE, composed of a mixture of carbon microparticles forming internal microarrays might have a profound effect upon the bismuth film structural features. This novel stripping platform may be useful for improving resolutions overall taking in the consideration metals like Bi and Cu. The obtained peak widths of 20 mV for lead and cadmium respectively were similar to other bismuth film electrodes reported previously.

The simultaneous measuring of lead and cadmium with $Bi(NO_3)_3$-GECE was also performed as shown at Figure 4. This figure displays square wave stripping voltammograms for cadmium (Ep= -0.72 V) and lead (Ep= -0.54 V) for increasing concentrations in 10 µg/L steps (Pb) and 20 µg/L steps (Cd) (b – e). The well resolved peaks increase linearly with the metal concentration. The

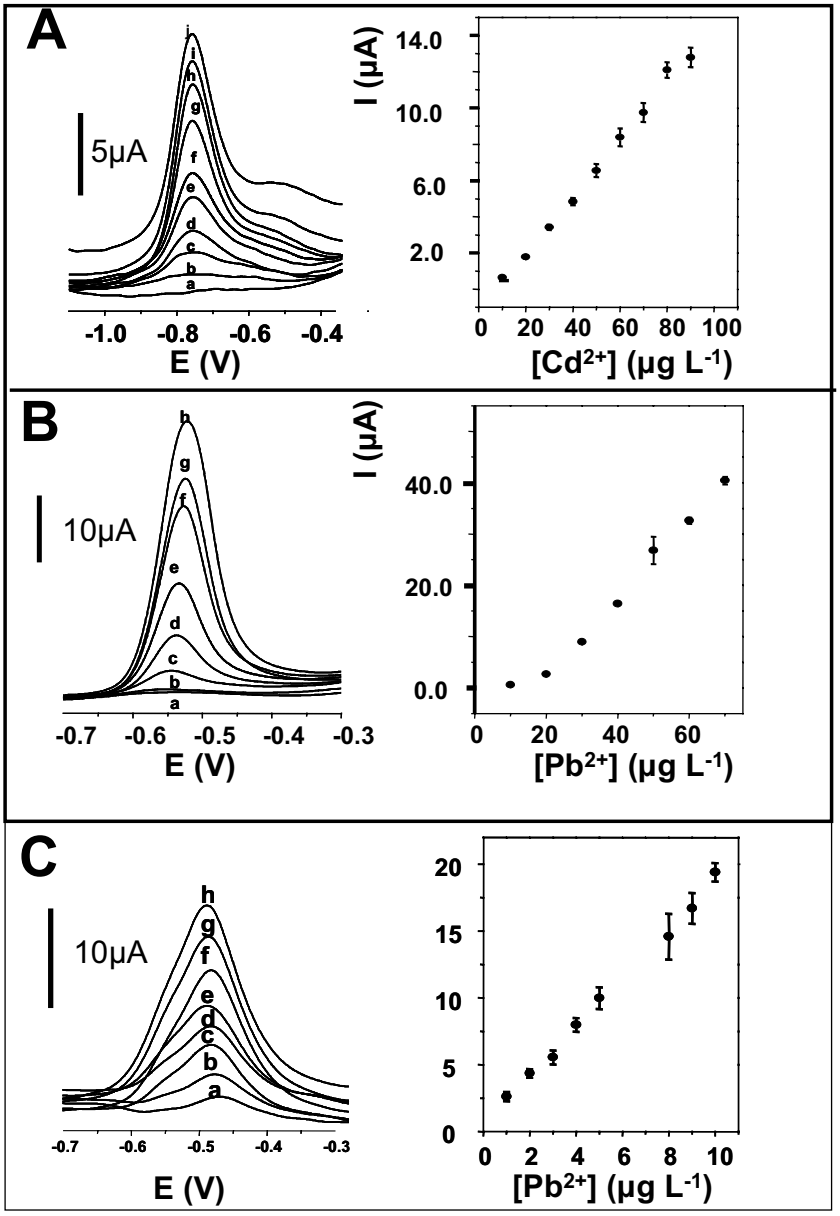

Figure 6. Determination of cadmium and lead for increasing concentrations in 10 µg/L steps (b – e); concentration ranges of 10 – 40 (Cd) and 20 – 80 (Pb) µg/L. Also shown is the blank (a) and the corresponding calibration plots. Solutions 0.1 M acetate buffer (pH 4.5). Square-wave voltammetric scan with a frequency of 50 Hz, potential step of 20 mV and amplitude of 25 mV. Deposition potential of -1.3 V during 120 s.

voltammogram clearly indicates that these metals can be measured simultaneously following a short deposition time of 2 min. In the concentration range from 10-40 μg Cd /L and 20-80 μg Cd /L the stripping signals remained undistorted and the resulting calibrating plots of this concentration range is linear exhibiting the R values of 0.9562 and 0.9762 for lead and cadmium. Detection limits of around 19.1 and 35.8 μg/L can be estimated for lead and cadmium respectively based on the same method [46].

A more sensitive measurement was observed for lead at 0.5 M HCl as measuring solution. Figure 7 represent typical subtractive square-wave stripping voltammograms (removing blanks) for increasing concentration of lead ranging from 1 to 10μg/L steps (a – h). Also shown is the calibration plot (right) over the studied range. This high sensitive response in HCl medium, as expected also from the study of the pH effect is probably related with an improved bismuth release and alloy formation in this medium.

The stability of the $Bi(NO_3)_3$-GECEs in 10 consecutive measurements for 50 ppb cadmium in 0.1M acetate buffer pH 4.5 and using the same surface was tested. The relative standard deviation of this measurement was 9.33%.

Although the $Bi(NO_3)_3$ particles were not uniform in size they were expected to be exposed in a reproducible way onto the freshly obtained $Bi(NO_3)_3$-GECE surfaces after each mechanical polishing procedure. This was confirmed by checking the reproducibility of the measurements for a series of 10 different surfaces of the same $Bi(NO_3)_3$-GECE. The relative

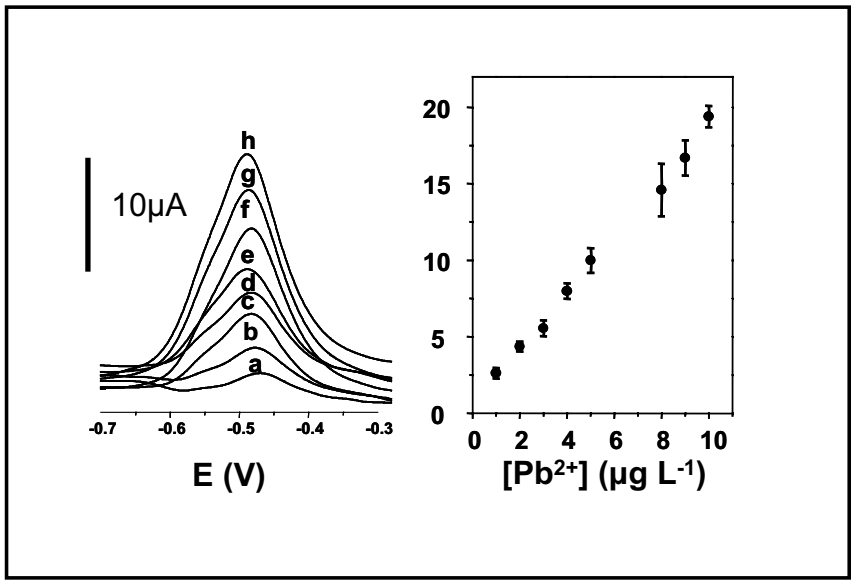

Figure 7. Square-wave stripping voltammograms for increasing concentration of lead: (a) 1, (b) 2, (c) 3, (d) 4, (e) 5, (f) 8, (g) 9, (h) 10 μg/L. Also shown is the corresponding calibration plot (right) over the range 1–10 μg/L lead. The measuring solution was 0.5 M HCl. Other experimental conditions as in Figure 6.

standard deviations of these measurements performed in the same experimental conditions as for the stability study was 10.69 for cadmium measurements.

4. Conclusions

The use of graphite epoxy composite electrodes (GECE) without any modification as a new material to prepare sensors for stripping analysis brings several advantages. Possibly the greatest advantage to be offered by the proposed sensors is the avoidance of the use of harmful mercury or other time consuming procedures to modify glassy carbon or other electrodes. Additionally the metal stripping can be performed without oxygen removal Graphite epoxy electrodes are cheaper and easy to be prepared in the laboratory. Although, higher detection limit compared to the mercury film electrode has been found, this kind of electrode can be envisioned as an attractive alternative for mercury free detection of heavy metals.

The applicability and suitability of Bi-GECE for the determination of cadmium, lead and zinc is also demonstrated. This strategy combine the GECE with bismuth film formation in-situ during the stripping analysis of metals. The coupling of GECE with bismuth film results in sensitive, well-defined and undistorted peaks especially for cadmium and lead.

A novel GECE that incorporate $Bi(NO_3)_3$ salt in the sensing matrix is also developed. The resulted $Bi(NO_3)_3$-GECE is compatible with bismuth-film electrodes for use in stripping analysis of heavy metals. The built-in bismuth property is the distinctive feature of this $Bi(NO_3)_3$ modified GECE which can be utilized for the generation of bismuth adjacently the electrode surface. The developed $Bi(NO_3)_3$-GECE is related with an in-situ bismuth ions generation and film formation without the necessity of external addition of the bismuth in the measuring solution. This sensor is also related with a higher sensitivity and improved detection limits during measurements in HCl medium.

The developed bismuth based GECE sensors compared to unmodified GECE show good stability which is owing to the unique surface morphology resulting in enhanced contact between the GECE matrix and the electrochemically reduced bismuth. Additionally in the case of $Bi(NO_3)_3$-GECE, the avoidance of external bismuth addition improved the sensor integration and consequently its utility .

The possible use of graphite-epoxy material by screen printing technology opens the possibility of mass production of disposable sensors for heavy metal analysis using stripping techniques. The utilization of these sensors for an extensive real heavy metal samples along with other applications are underway in our laboratory.

Acknowledgements

This work was financially supported by Ministry of Education and Culture (MEC) of Spain (Projects BIO2004-02776, MAT2004-05164) and the Spanish foundation Ramón Areces (project 'Bionanosensores'). A.Merkoçi thanks the "Ramón y Cajal" program of MEC (Spain).

References

1. Wang, J.; Tian, B.; Wang, J.; Lu, J.; Olsen, C.; Yarnitzky, C.; Olsen, K.; Hammerstrom, D.; Bennett, W. (1999) 385, 429
2. Bai, Y., Ruan, X., Mo, J., Xie, Y., 1998, Analytica Chimica Acta, 373, 39
3. Maccà, C., Bradshaw, M., Merkoçi, A., Scollary, G., 1997, Analytical Letters, 30, 1223
4. Galus, Z., in Kissinger P.T. and Heineman, W. eds. Laboratory Techniques in Electroanalytical techniques, 2nd ed., Marcel Dekker, Inc., New York, 1996.
5. P.R.M.Silva, P.R.M., El Khakani, M.A., Chaker, M., Dufrense, A., Courchesne, F., 2001, Sensors and Actuators B, 76, 250
6. Merkoçi, A., Vasjari, M., Fabregas, E., Alegret, S., 2000, Mikrochim. Acta, 135, 29
7. Vidal, J., Viñao, R., Castillo, J., 1992, Electroanalysis, 4, 653
8. Wang, J., Hutchins-Kumar, L.D., 1986, Analytical Chemistry, 58, 402
9. Esnafi, A.A., Naeeni, M.A., 2000, Analytical Letters, 33, 1591
10. Seo, K., Kim, S., Park, J., 1998, Analytical Chemistry, 70, 2936
11. Frey, H.H.; McNeil, C. J.; Keay, R.W.; Bannister, J.V., 1998, Electroanalysis, 10: 480
12. Hu, Zh.; Seliskar, C.J.; Heineman, W.R., 1998, Anal.Chim.Acta, 369: 93
13. Degefa, T.H.; Chandravanshi, B.S.; Alemu, H., 1999, Electroanalysis, 11, 1305
14. Palchetti, I.; Upjohn, C.; Turner, A.P.F.; Mascini, M., 2000, Analytical Letters, 33: 1231
15. Wang, J. Stripping Analysis; VCH Publishers: Deerfield Beach, 1985.
16. Achterberg, E. P.; Braungardt, 1999, Anal. Chim. Acta, 400, 381
17. Wang, J.; Tian, B., 1993, Anal. Chem., 65, 1529
18. Nolan, M. A.; Kounaves, S. P., 1999, Anal. Chem., 71, 3567
19. Angnes, L.; Richter, E.M.; Augelli, M.A.; Kume, G.H., 2000, Anal.Chem., 72, 5503
20. Silva, P.R.M.; Khakami, El.; Chaker, M; Dufrense, A.; Courchesne, F., 2001, Sensors and Actuators B, 76, 250.
21. Wang, J., Lu, J., Hocevar, S.B., Farias, P.A., Ogorevc, B., 2000, Anal. Chem., 72, 3218
22. Wang, J., Lu, J., Kirgöz, Ü.A., Hocevar, S.B., Ogorevc, B., 2001, Analytica Chimica Acta, 434, 29
23. Baldo, M.A., Daniele, S., 2004, Analytical Letters, 37, 995
24. Chang, H.P., Johnson, D.C., 1991, Analytica Chimica Acta, 248, 85
25. Flechsig, G.U., Korbout, O., Hocevar, S.B., Thongngamdee, S., Ogorevc, B., Grundler, P., Wang, J., 2002, Electroanalysis, 14, 192.
26. Hutton, E.A., Ogorevc, B., Hocevar, S.B., Weldon, F., Smyth, M.R., Wang, J., 2001, Electrochemistry Communications 3, 707

27. Wang, J., Lu, J., 2000, Electrochemistry Communications 2, 390
28. Kefala, G., Economou, A., Voulgaropoulos, A., Sofoniou, M., 2003, Talanta 61, 603
29. Hutton, E.A., Van Elteren, J.T., Ogorevc, B.I., Smyth, M.R., 2004, Talanta, 63, 849
30. Hocevar, S.B., Ogorevc, B., Wang, J., Pihlar, B., 2002, Electroanalysis, 14, 1707
31. Hocevar, S.B., Wang, J., Deo, R.P., Ogorevc, O., 2002, Electroanalysis, 14, 112
32. Ruschan, G., Newnham, R.E., Runt, J., Smith, E., 1989, Sens. Actuators, 269, 20
33. Alegret, S., 1996, Analyst, 121, 1751
34. Céspedes, F., Fàbregas, E., Alegret, S., 1996, Trends Anal. Chem., 296, 15
35. Céspedes, F., Alegret, S., 2000, Trends Anal. Chem, 276, 19
36. Alegret, S., Fàbregas, E., Céspedes, F., Merkoçi, A., Solé, S., Albareda, M., Pividori, M.I., 1999, Quím. Anal., 23, 18
37. M. Serradell, S. Izquierdo, L. Moreno, A. Merkoçi, S. Alegret, Electroanalysis, 14 1281-1287 (2002)
38. L. Moreno, A. Merkoçi, S. Alegret, Electrochimica Acta, 48 2599-2605 (2003)
39. S.Carrégalo, A. Merkoçi, S. Alegret, Microchimica Acta 147, 245-251 (2004)
40. Ü.A.Kırgöz, S.Marín, M.Pumera, A.Merkoçi, S. Alegret, Electroanalysis, 2004, In press.
41. M.T. Castañeda, B. Pérez, M. Pumera, M. del Valle, A.Merkoçi, S. Alegret, Sent for publication to ACA, 2005.
42. Santandreu, M., Céspedes, F., Alegret, S., Martínez-Fàbregas, E., 1997, Analytical Chemistry, 69, 2080
43. Merkoçi, A., Braga, S., Fàbregas, E., Alegret, S., 1999, Analytica Chimica Acta, 391, 65
44. Ramirez-Garcia, S., Céspedes, F., Alegret, S., 2001, Electroanalysis, 13, 529
45. Gong, G.G., Freedman, L.D., Doak, G.O., Bismuth and bismuth alloys in: M.Grayson (ed.). 1978, Encyclopedia of chemical Technology, Vol. 3, Wiley New York, 912-937p.
46. J. Mocak, A.M. Bond, S. Mitchell, G. Scollary, 1997, Pure & Appl. Chem. 69, 297

III

Gold nanoparticles in DNA and protein analysis. Chapter 38, pages 941-956. ‘Electrochemical sensor analysis’. Amsterdam Elsevier, ISBN-13:978-0-444-53053-0. Editors: S. Alegret and A. Merkoçi, 2007.

Castañeda M. T., Alegret S., Merkoçi A.

Chapter 38

Gold nanoparticles in DNA and protein analysis

María Terra Castañeda, Salvador Alegret and Arben Merkoçi

38.1 INTRODUCTION

According to IUPAC recommendations, a biosensor is a self-contained integrated receptor–transducer device, which is capable of providing selective quantitative or semi-quantitative analytical information using a biological recognition element [1]. Biosensors convert chemical information to an electrical signal through a molecular recognition reaction on a physical transducer. The amount of signal generated is proportional to the concentration of the analyte, allowing for both quantitative and qualitative measurements in time [2].

A biosensor consists of three main components: a biological recognition element or bioreceptor for detection, the transducer, component for readout and an output system. The bioreceptor is a biomolecule, such as enzymes, antibodies, receptors proteins, nucleic acids, cells or tissue sections, which recognises the target analyte. Generally, there are three principal classes of biosensors in terms of their biological component: (1) biocatalytic, depending on the use of pure or crude enzymes to moderate a biochemical reaction and using the chemical transformation of the biomarker as the source of signal; (2) bioaffinity, relying on the use of proteins or DNA to recognise and bind a particular target; and (3) microbe based that use microorganisms as the biological recognition element. These generally involve the measurement of microbial respiration, or its inhibition, by the analyte of interest. Biosensors have also been developed using genetically modified microorganisms (GMOs) that recognise and report the presence of specific environmental pollutants [3–5]. Alternative (bio)recognition molecules include RNA and DNA aptamers [6], molecularly imprinted polymers and templated surfaces [7,8]. The aptamers are functional nucleic acids selected from combinatorial oligonucleotide

Comprehensive Analytical Chemistry 49
Alegret and Merkoçi (Eds)
Volume 49 ISSN: 0166-526X DOI: 10.1016/S0166-526X(06)49038-3

libraries by *in vitro* selection against a variety of targets, such as small organic molecules, peptides, proteins and even whole cells [9].

Recently, introduction of DNA analogous detection systems such as the use of peptide nucleic acid (PNA) technology has attracted considerable attention [10]. The PNAs are synthetic analogues of DNA that hybridise with complementary DNAs or RNAs with high affinity and specificity, essentially because of an uncharged and flexible polyamide backbone. The unique physico-chemical properties of PNAs have led to the development of a variety of research and diagnostic assays where these are used as molecular hybridisation probes [11].

The transducers most commonly employed in biosensors are: (a) Electrochemical: amperometric, potentiometric and impedimetric; (b) Optical: vibrational (IR, Raman), luminescence (fluorescence, chemiluminescence); (c) Integrated optics: (surface plasmon resonance (SPR), interferometery) and (d) Mechanical: surface acoustic wave (SAW) and quartz crystal microbalance (QCM) [4,12].

The biosensors can be divided into: nonlabelled or label-free types, which are based on the direct measurement of a phenomenon occurring during the biochemical reactions on a transducer surface; and labelled, which relies on the detection of a specific label. Research into 'label-free' biosensors continues to grow [13]; however 'labelled' ones are more common and are extremely successful in a multitude of platforms.

Recently, the field of biosensors for diagnostic purposes has acquired a great interest regarding the use of nanomaterials such as DNA and protein markers. Some biosensing assays based upon bioanalytical application of nanomaterials have offered significant advantages over conventional diagnostic systems with regard to assay sensitivity, selectivity and practicality [14–16]. Nanoparticles (NPs) in general [2,17] and quantum dots (QDs) [18] have been used particularly successfully as DNA tags.

Although the spectrum of NPs for labelling applications is relatively broad, this chapter discusses only the application of gold NPs (AuNPs) in electrochemical genosensors and immunosensors and some of the trends in their use for environmental and biomedical diagnostics between other application fields.

38.1.1 Current labelling technologies for affinity biosensors

It is well known that affinity biosensors, usually DNA sensors or immunosensors, require a biorecognition molecule that demonstrates a high affinity and specificity for the target biomarker.

The formation of double-stranded DNA upon hybridisation is commonly detected in connection with the use of an appropriate electroactive hybridisation intercalator or labelling DNA by a simple electroactive molecule or an adequate NP.

Electrochemical detection of hybridisation is mainly based on the differences in the electrochemical behaviour of the labels connected with double-stranded DNA (dsDNA) or single-stranded DNA (ssDNA). The labels for hybridisation detection can be anticancer agents, organic dyes, metal complexes, enzymes or metal NPs. There are basically four different pathways for electrochemical detection of DNA hybridisation: (1) A decrease/increase in the oxidation/reduction peak current of the label, which selectively binds with dsDNA/ssDNA, is monitored. (2) A decrease/increase in the oxidation/reduction peak current of electroactive DNA bases such as guanine or adenine is monitored. (3) The electrochemical signal of the substrate after hybridisation with an enzyme-tagged probe is monitored. (4) The electrochemical signal of a metal NP probe attached after hybridisation with the target is monitored [19].

On the other hand, the main types of immunoassays that can be performed by using labelled antibodies or antigens are: direct sandwich, competitive and indirect assays. The labels can be: enzymes (alkaline phosphatase, peroxidise or glucose oxidase); metal NPs (gold); fluorescent or electrochemiluminescent probes.

38.1.2 Nanoparticles as labels

The use of NPs as labels of DNA molecules [20,21] opened a new alternative for the detection of hybridisation events. NPs labels offer a number of advantages for DNA detection platforms as well as for immunoassays. The NP-based DNA and immunoassays are easy to use, offer good sequence selectivity and sensitivity. Moreover, the NP labelling technology is compatible with chip techniques [22].

Metal NPs have received tremendous attention in the field of bioanalytical science, in particular the sequence-specific DNA detection [23,24]. This is attributed to their unique properties in the conjugation with biological recognition elements (e.g., DNA oligonucleotide probe) as well as in the signal transduction with optical [22,25], electrical [26], microgravimetric [27] and electrochemical [23,28–30] methods.

The commonly used fluorescence labels provide good sensitivity but have various disadvantages. Fluorescent dye labels are expensive, they photobleach rapidly, and the records are not permanent. With metal NPs it seems to be possible to overcome most of the disadvantages

described for fluorescence labelling. Metal NPs in general and particularly gold NPs (AuNPs) can be linked to DNA and other biomolecules without changing their ability to bind to their complementary biomolecule [20,21].

With regard to immunosensors, a number of different reporter groups are used, including enzymes which convert a substrate into a highly coloured product (enzyme-linked immunosorbent assay, 'ELISA') or which digest a substrate to give a photon of light to expose a film (chemiluminescence).

The current research in the field of electrochemical indicators is mainly to find new labels that have powerful electrochemical signals. Metal NPs with well-defined redox properties that can be followed by electrochemical stripping techniques are of great interest [28,31].

38.2 DNA ANALYSIS

Much interest in the development of different non-radioactive DNA sensing techniques for genomics analysis with respect to environmental applications [32] or diagnostics has been shown in the last decade.

The DNA biosensors or genosensors are based on the immobilisation of a single-stranded oligonucleotide on a transducer surface that recognises its complementary DNA sequence via the hybridisation reaction. The immobilisation of oligonucleotides (bioreceptors) onto transducer surfaces plays a crucial role in the performance of the genosensors or the bioanalytical device. Indeed, the bioreceptor must be readily accessible to the analyte [33]. The techniques for the immobilisation of purified oligonucleotides on an electrochemical transducer in the design of genosensors and their corresponding detection methods using these sensors were reviewed in detail by Pividori *et al.* [34]. The most generally employed are the following: (1) entrapment of the bioreceptor within a polymeric matrix such as agar gel, polyacrylamide, polypyrolle matrix or sol–gel matrices [35]; (2) covalent bonding onto surfaces (glassy carbon or carbon paste modified electrodes and polypyrolle, platinum or gold surfaces) by means of bifunctional groups or spacers such as glutaraldehyde, carbodiimide or a self-assembled monolayer of bifunctional silanes; and (3) adsorption of a thiol-modified bioreceptor for self-assembly on a gold surface [33,34].

In a typical configuration of a DNA biosensor, the bioreceptor is an ssDNA called the 'capture probe' that is immobilised by one of the methods described above. The analyte, a complementary ssDNA called

the ‘target DNA’, is recruited to the surface via base-pairing interactions with the capture probe. In most current applications, the target DNA is the product of an amplification reaction (e.g., PCR or related method). This amplification step has two goals: (1) Allow reaching the lower detection limit of the device. (2) Allow incorporating a label into the target DNA that can then be used in the detection. The labels are generally fluorophores or a biotin molecule. When using biotin labelling, additional steps are required for further detection by use of an antibiotin antibody coupled to a fluorophore. The labelling efficiency of the target DNA depends on the polymerase’s ability to incorporate the labelled nucleotides into the growing nucleic acid chain. Since this labelled nucleotide is not the natural substrate for the enzyme, the efficiency of the incorporation is low. An alternative to this approach involves a three-component ‘sandwich’ assay, in which the label is associated with a third DNA sequence (the signalling probe) designed to be complementary to an overhanging portion of the target. This dual hybridisation then eliminates the need to modify the target strand [33].

To date, the detection of the target DNA has been accomplished using fluorescent labels. In addition to their sensitivity, the great diversity of fluorophores allows as to compare gene expressions (e.g., in normal as compared to pathological cells). However, fluorescent labelling has some drawbacks. Fluorescent dyes and the equipment required to image them are expensive; the dyes rapidly photobleach and their manipulation requires special care to avoid interfering signals. As an alternative, NP labels offer excellent prospects for biological sensing due to their low cost, stability and unique physico-chemical properties [33]. The AuNPs functionalised with oligonucleotides are extensively used as tags in many highly sensitive and selective DNA recognition schemes by means of electrochemical sensing. The integration of NPs DNA labelling technology in chips has been also been studied in DNA analysis [23].

The hybridisation of a nucleic acid to its complementary target is one of the most definite and well-known molecular recognition events. Therefore, the hybridisation of a nucleic acid probe to its DNA target can provide a very high degree of accuracy for identifying complementary DNA sequences [32–36].

Diverse techniques for detection of DNA hybridisation have been developed. In most of them, the hybridisation event and electrochemical detection are carried out on the electrode surface [37–41]. In other cases, the electrode only acts as a detector of the hybridisation event

[42–48], which occurs in a separate step, either because it takes place in a microwell [42] or because the hybridisation event occurs on the surface of magnetic beads, which are separated from the hybridisation solution and then redissolved [43,44].

Electrochemical transduction of the hybridisation event can be classified into two categories: label-based and label-free approaches. The label-based approach can be further subdivided into intercalator/groove binder, non-intercalating marker, and NP. The label-free approach is based on the intrinsic electroactivity of the DNA purine bases or the change in interfacial properties (e.g., capacitance and electron transfer resistance) upon hybridisation [49].

The sensitivities of the label-based approach depend mainly on the specific activity of the labels linked to the oligonucleotide probe. Radioisotopic [48], fluorescent [50] and enzymatic [38,40,47] labels have been commonly used. Besides the above labels, NPs have attractive properties to act as DNA tags [18,51]. The fact that NPs present an excellent biocompatibility with biomolecules and display unique structural, electronic, magnetic, optical and catalytic properties have made them a very attractive material to be used as label [52,53].

Cai *et al.* [28] have synthesised AuNPs-labelled ssDNA as a probe to be hybridised with their complementary strand on chitosan-modified glassy carbon electrode (GCE). In their experiments, SH-ssDNA was self-assembled onto an AuNP (16 nm in diameter) (details given previously in Ref. [54]). After hybridisation, the AuNPs tags were detected by differential pulse voltammetry (DPV). The detection limit was 1.0×10^{-9} mol L^{-1} of 32-base synthesised complementary oligonucleotide.

A novel NP-based detection of DNA hybridisation based on magnetically induced direct electrochemical detection of the 1.4 nm Au_{67} QD tag linked to the target DNA was reported by Pumera *et al.* [55]. The Au_{67} NP tag was directly detected after the DNA hybridisation event, without need of acidic (i.e., HBr/Br_2) dissolution [55].

A triple-amplification bioassay that couples the carrier-sphere amplifying units (loaded with numerous AuNP tags) with the 'built-in' preconcentration feature of the electrochemical stripping detection and the catalytic enlargement of the multiple gold particle tags was demonstrated [56]. The gold-tagged beads were prepared by binding biotinylated AuNPs to streptavidin-coated polystyrene spheres. These beads were functionalised with a single-stranded oligonucleotide, which was further hybridised with a complementary oligonucleotide that was linked to a magnetic particle. The numerous AuNP labels associated with one ds-oligonucleotide pair were enlarged by the electroless

TABLE 38.1
Electrochemical genosensors using AuNPs tags, with potential biomedical and environmental applications

Transducer	AuNPs	Detection method	Sample/target DNA	Detection limit	Ref.
SPMBE	20-nm (Sigma)	ASV	Cell culture/ 406-bp HCMV-amplified	5 pM	[42]
PGE	5 ± 1.3 nm (prepared as described in Ref. [61]	DPV	Real PCR amplicons/ factor V Leiden Mutation	0.78 fmol	[29]
SPEs	10 nm (Sigma)	PSA	Synthetic/ breast cancer	4×10^{-9} M	[62]
M-GECE	10 nm (Sigma)	DPV	Synthetic/ breast cancer	33 pmols	[64]
M-GECE	10 nm (Sigma)	DPV	Synthetic/ cystic fibrosis	–	[64]

SPMBE = screen-printed microband electrode, ASV = anodic stripping voltammetry, HCMV = *human cytomegalovirus*, PGE = pencil-graphite electrode, DPV = differential pulse voltammetry, SPEs = screen-printed electrodes, PSA = potentiometric stripping analysis, M-GECE = magnetic graphite–epoxy composite electrode.

deposition of gold and transported to the electrode array with the use of the magnetic particle. Then, the Au assembly was dissolved upon treatment with HBr/Br_2 dissolution and electrochemically analysed by using electrochemical deposition/stripping voltammetry. Such a triple-amplification route offered a dramatic enhancement of the sensitivity.

Several protocols with potential biomedical and environmental application have been developed. Table 38.1 summarises information of some typical electrochemical genosensors based on DNA hybridisation detection using AuNPs tags.

38.2.1 Clinical

Electrochemical assays of nucleic acids based on DNA hybridisation have received considerable attention [34,57–60]. DNA hybridisation biosensors are a very attractive topic in the clinical diagnostics of inherited diseases and the rapid detection of infectious microorganisms.

Authier *et al.* [42] developed an electrochemical DNA detection method for the sensitive quantification of an amplified 406-base pair

human cytomegalovirus DNA sequence (HCMV DNA). The HCMV DNA was extracted from cell culture, amplified by polymerase chain reaction (PCR), and then quantified by agarose gel electrophoresis. The HCMV DNA was immobilised on a microwell surface and hybridised with the complementary oligonucleotide-modified AuNPs (20 nm) followed by the release of Au(III) by treatment with acidic bromine–bromide solution, and the indirect determination of the solubilised Au(III) ions by anodic stripping voltammetry (ASV) at a sandwich-type screen-printed microband electrode (SPMBE). The combination of the sensitive Au(III) determination at a SPMBE with the large number of Au(III) released from each gold NP probe allows detection of as low as 5 pM amplified HCMV DNA fragment.

Ozsoz *et al.* [29] described an electrochemical genosensor based on AuNPs for detection of Factor V Leiden Mutation from PCR amplicons, which were obtained from real samples. The covalently bound amplicons onto a pencil graphite electrode (PGE) were then hybridised with oligonucleotide-AuNPs (the AuNPs, with average diameter of 5 ± 1.3 nm were prepared as reported in the literature [61]). The oxidation signal of AuNPs was measured directly by using DPV at PGE. Direct electrochemical oxidation of the AuNPs was observed at a stripping potential of approximately +1.2 V. The response is greatly enhanced due to the large electrode surface area and the availability of many oxidisable gold atoms in each NP label. The detection limit for PCR amplicons was as low as 0.78 fmol.

Wang *et al.* [62] developed an AuNPs based protocol for the detection of DNA segments related to the breast cancer *BRCA1* gene. This bioassay consisted in the hybridisation of a biotinylated target DNA to streptavidin-coated magnetic bead-binding biotinylated probe and followed by binding of streptavidin-coated AuNPs (5 nm) to the target DNA, dissolution of the AuNPs and electrochemical detection using potentiometric stripping analysis (PSA) of the dissolved gold tag at single-use thick-film carbon electrodes, obtaining a detection limit of 4×10^{-9} M.

The sensitivity of the detection is usually improved by the silver enhancement method. A better detection limit was reported when a silver enhancement method was employed, based on the precipitation of silver on AuNPs tags and its dissolution (in HNO_3) and subsequent electrochemical potentiometric stripping detection [43]. The new silver-enhanced colloidal gold stripping detection strategy represented an attractive alternative to indirect optical affinity assays of nucleic acids and other biomolecules.

Wang *et al.* [63] also reported a new NP-based protocol for detecting DNA hybridisation based on a magnetically induced solid-state electrochemical stripping detection of metal tags. The new bioassay involves the hybridisation of a target oligonucleotide to probe-coated magnetic beads, followed by binding of the streptavidin-coated AuNPs (5 nm) to the captured target, catalytic silver precipitation on the AuNPs tags, a magnetic 'collection' of the DNA-linked particle assembly and solid-state stripping detection (PSA) at a thick-film carbon electrode with a magnet placed below the working electrode. The high sensitivity and selectivity of the new protocol was illustrated for the detection of DNA segments related to the *BRCA1* breast cancer gene. A detection limit of around 150 pg mL^{-1} (i.e., 1.2 fmol) was obtained.

The application of AuNPs as oligonucleotide labels in DNA hybridisation detection assays using a magnetic graphite–epoxy composite electrode (M-GECE) has been reported by Pumera *et al.* [55] (a detailed description of DNA detection using AuNPs as labels is given in Procedure 53–see the accompanying CD-Rom).

Recently, Castañeda *et al.* [64] developed two AuNPs based genosensor designs, for detection of DNA hybridisation. Both assay formats were based on a magnetically induced direct electrochemical detection of the AuNPs tags on M-GECE. The AuNPs tags are also directly detected after the DNA hybridisation event without the need of acidic dissolution.

The first assay is based on the hybridisation between two single-strand biotin-modified DNA probes: a capture DNA probe and a target DNA related to the *BRCA1* breast cancer gene, which is coupled with streptavidin–AuNPs (10 nm). The second assay (Fig. 38.1A–F) is based on hybridisation between three single-strand DNA probes: a biotin-modified capture DNA probe (CF-A), a target DNA, related to cystic fibrosis gene (CF-T) and DNA signaling probe (CF-B) modified with AuNPs via biotin–streptavidin complexation reactions. In this assay, the target is 'sandwiched' between the other two probes. The electrochemical detection of AuNPs by DPV was performed in both cases (a detailed description of DNA detection using AuNPs as labels is given in Procedure 53 in the accompanying CD-Rom).

38.2.2 Environmental

Nucleic acid based affinity and electrochemical biosensors for potential environmental applications have recently been reported. Application areas for these include the detection of chemically induced DNA

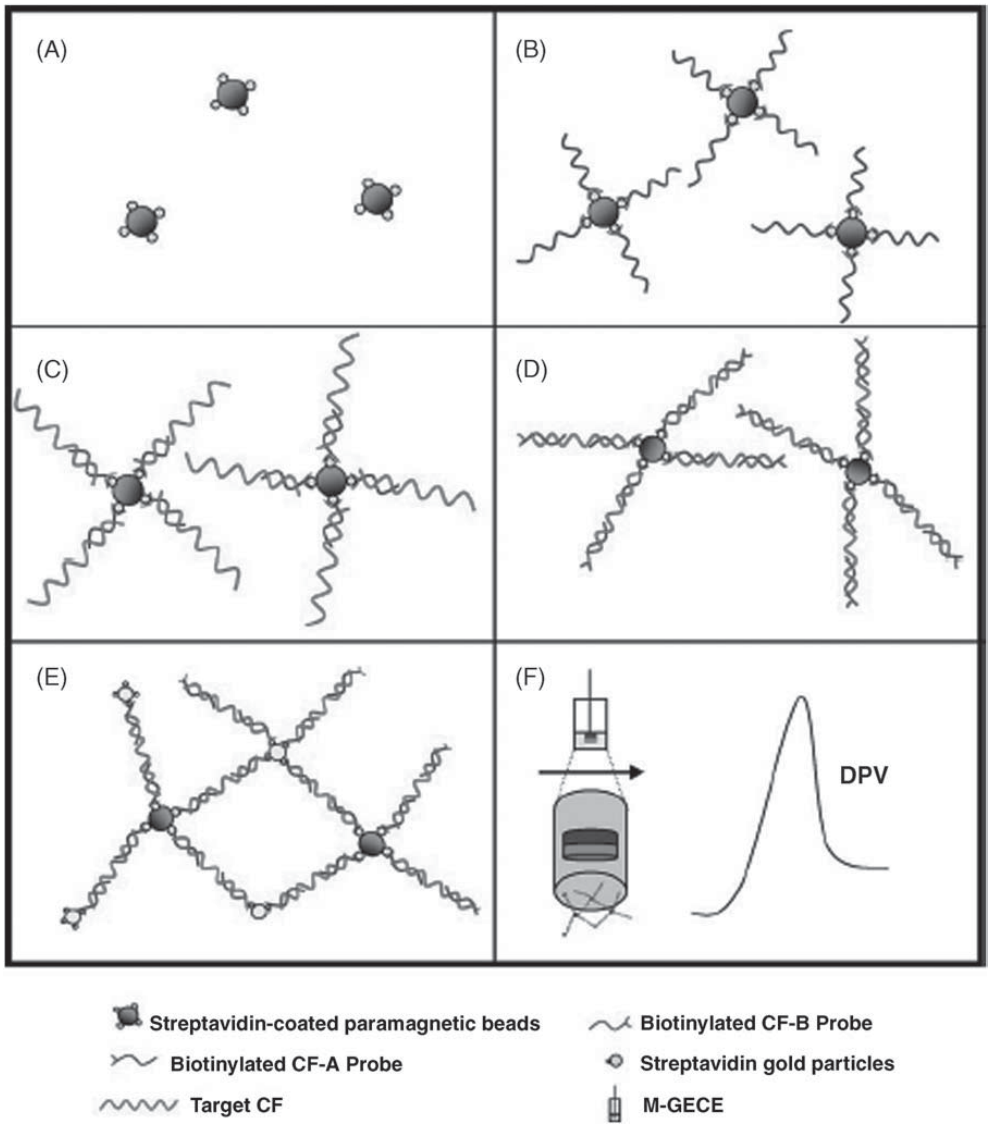

Fig. 38.1. Schematic representation of the sandwich system analytical protocol (not in scale): (A) streptavidin-coated magnetic beads; (B) immobilisation of the biotinylated CF-A probe onto the magnetic beads; (C) addition of CF-T (first hybridisation event); (D) addition of biotinylated CF-B probe (second hybridisation event); (E) tagging by using the streptavidin–gold nanoparticles; (F) accumulation of AuNPs–DNA–magnetic bead conjugate on the surface of M-GECE and magnetically trigged direct DPV electrochemical detection of AuNPs tag in the conjugate. Reprinted from Ref. [64]. Copyright 2006; with permission from Elsevier Science.

damage and the detection of microorganisms through the hybridisation of species-specific sequences of DNA [36].

In the case of DNA biosensors, two strategies are applied to detect pollutants: one is the hybridisation detection of nucleic acid sequences from infectious microorganisms, and the other the monitoring of small pollutants interacting with the immobilised DNA layer (drugs, mutagenic pollutants, etc.) [65].

38.3 PROTEINS ANALYSIS

Proteins are present at various concentrations in samples from very different origins and the determination of their concentration is of particular interest. Biosensors offer an alternative to the classical analytical methods due to their inherent specificity, simplicity, relative low cost and rapid response.

Immunosensors are affinity ligand-based biosensors in which the immunochemical reaction is coupled to a transducer [66]. These biosensors use antibodies as the biospecific sensing element, and are based on the ability of an antibody to form complexes with the corresponding antigen [16]. The fundamental basis of all immunosensors is the specificity of the molecular recognition of antigens by antibodies to form a stable complex. Immunosensors can be categorised based on the detection principle applied. The main developments are electrochemical, optical and microgravimetric immunosensors [66].

The interactions between an antibody and an antigen are highly specific. Such a specific molecular recognition has been exploited in immunosensors to develop highly selective detection of proteins.

Several protocols with potential biomedical and environmental application have been developed. Table 38.2 summarises information of some typical electrochemical immunosensors using AuNPs tags.

38.3.1 Clinical

The development of immunosensors for the detection of diseases has received much attention lately and this has largely been driven by the need to develop hand-held devices for point-of-care measurements [67,68]. Immunosensors can incorporate either the antigen or the antibody onto the sensor surface, although the latter approach has been used most often [67]. Optical [69,70] and electrochemical [70] detection methods are most frequently used in immunosensors [67]. Detection by

TABLE 38.2
Electrochemical immunosensors using AuNPs tags, with potential biomedical applications

Transducer	AuNPs	Detection method	Sample/ antigen	Detection limit	Ref.
MCPE	10 nm (Sigma)	SWASV	–/Mouse IgG	$0.02\,\mu g\,mL^{-1}$	[72]
SPE	18 nm	ASV	–/IgG	$3 \times 10^{-12}\,M$	[73]
Platinum electrode	–	PSA	–/Diptheria antigen	$2.4\,ng\,mL^{-1}$	[76]
GCE	–	ASV	–/Human IgG	$6 \times 10^{-12}\,M$	[75]
TFGE	Protein A labelled with colloidal gold (Sigma)	PSA	Blood serum/ Forest-Spring encephalitis virus	$10^{-7}\,mg\,mL^{-1}$	[77]

MCPE = magnet carbon paste electrode, SWASV = square wave anodic stripping voltammetry, ASV = anodic stripping voltammetry, PSA = potentiometric stripping analysis, SPEs = screen-printed electrodes, TFGE = thick-film graphite electrode, GCE = glassy carbon electrode.

electrochemical immunosensors is generally achieved by using either electroactive labels or enzyme labelling [71].

Liu and Lin [72] have developed a renewable electrochemical magnetic immunosensor by using magnetic beads and AuNPs labels. Anti-IgG antibody-modified magnetic beads were attached to a renewable carbon paste transducer surface by a magnet that was fixed inside the sensor. The magnet carbon paste electrode (MCPE) offers a convenient immunoreaction and electrochemical sensing platform. AuNP (10 nm) labels were capsulated to the surface of magnetic beads by sandwich immunoassay. A highly sensitive electrochemical stripping analysis using square wave anodic stripping voltammetry (SWASV) that offers a simple and fast method to quantify the captured AuNPs tags and avoid the use of an enzyme label and substrate was used. The stripping signal of AuNPs is related to the concentration of target mouse IgG in the sample solution. The detection limit of $0.02\,\mu g\,mL^{-1}$ of IgG was obtained under optimum experimental conditions. Such particle-based electrochemical magnetic immunosensors could be readily used for simultaneous parallel detection of multiple proteins by using multiple inorganic metal NP tracers and are expected to open new opportunities for disease diagnostics and biosecurity. The illustrative representation of the main steps of protocol is shown in Fig. 38.2.

An electrochemical immunoassay using a colloidal gold label (18 nm) that after oxidative gold metal was indirectly determined by ASV at a

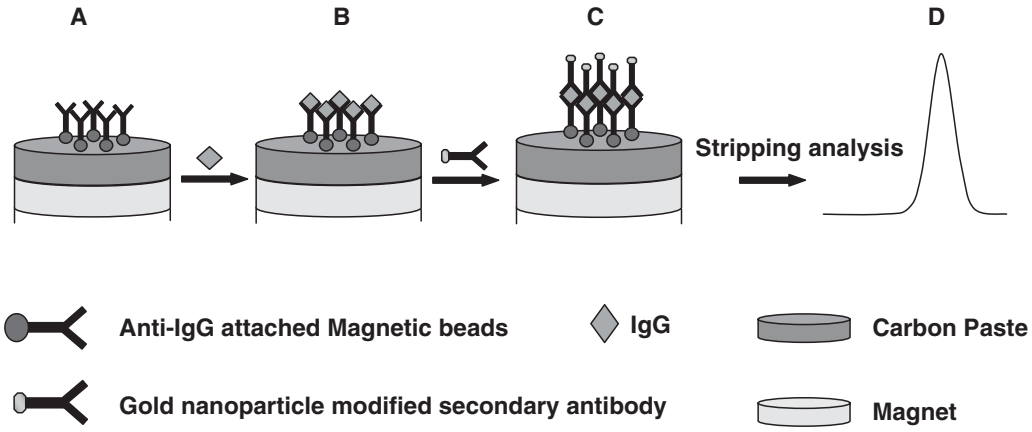

Fig. 38.2. Particle-based electrochemical immunoassay protocol. (A) Introduction of antibody-modified magnetic beads to magnet/carbon paste electrochemical transducer surface; (B) binding of the IgG antigen to the antibodies on the magnetic beads; (C) capture of the gold nanoparticle labelled secondary antibodies; (D) electrochemical stripping detection of AuNPs. Reprinted with permission from Ref. [72].

single-use carbon-based SPE was developed by Dequaire *et al.* [73]. A noncompetitive heterogeneous immunoassay of an IgG was carried out. Primary antibodies specific to goat IgG were adsorbed passively on the bottom of a polystyrene microwell. The goat IgG analyte was first captured by a primary antibody and was then sandwiched by a secondary colloidal gold-labelled antibody. The unbound labelled antibody was removed. To perform the detection, the colloidal gold present in the bound phase was dissolved in an acidic bromine–bromide solution and the Au(III) ions were measured by ASV. A limit of detection in the picomolar range (3×10^{-12} M) was obtained, which is comparable with colorimetric ELISA or with immunoassays based on fluorescent europium chelate labels.

Tang *et al.* [74] developed a potentiometric immunosensor by means of self-assembling AuNPs, polyvinyl butyral and diphtheria antibody to the surface of platinum electrodes. Diphtheria antigen was detected via the change in the electric potential upon antigen–antibody interaction. The detection limit was 2.4 ng mL^{-1} of diphtheria antigen and the linear semilogarithmic range extended from 4.4 to 960 ng mL^{-1}.

An electrochemical immunoassay has been developed by Chu *et al.* [75], based on the precipitation of silver on colloidal gold labels which, after silver metal dissolution in an acidic solution, was indirectly determined by ASV at a glassy carbon electrode. The method was evaluated for a noncompetitive heterogeneous immunoassay of an IgG

as a model. The anodic stripping peak current depended linearly on the IgG concentration over the range of 1.66 ng mL^{-1}–27.25 μg mL^{-1} in a logarithmic plot. A detection limit as low as 1 ng mL^{-1} (i.e., 6×10^{-12} M) human IgG was achieved, which is competitive with colorimetric ELISA or with immunoassays based on fluorescent europium chelate labels.

A direct electrochemical immunoassay system based on the immobilisation of α-1-fetoprotein antibody (anti-AFP), as a model system, on the surface of core-shell Fe_2O_3/Au magnetic nanoparticles (MNP) has been demonstrated. To fabricate such an assay system, anti-AFP was initially covalently immobilised onto the surface of core-shell Fe_2O_3/Au MNP. Anti-AFP-modified MNP (bio-NPs) were then attached to the surface of carbon paste electrode with the aid of a permanent magnet. The performance and factors influencing the performance of the resulting immunosensor were studied. α-1-Fetoprotein antigen was directly determined by the change in current or potential before and after the antigen–antibody reaction versus saturated calomel electrode. The electrochemical immunoassay system reached 95% of steady-state potential within 2 min and had a sensitivity of 25.8 mV. The linear range for AFP determination was from 1 to 80 ng AFP mL^{-1} with a detection limit of 0.5 ng AFP mL^{-1}. Moreover, the direct electrochemical immunoassay system, based on a functional MNP, can be developed further for DNA and enzyme biosensors [76].

Another interesting electrochemical immunosensor including Au-NPs labels for diagnosis of Forest-Spring encephalitis has been proposed by Brainina *et al.* [77]. It comprises a screen-printed thick-film graphite electrode (the transducer) and a layer of the Forest-Spring encephalitis antigen (the biorecognition substance) immobilised on the electrode surface. The procedure includes formation of an antigen–antibody immune complex, localisation of colloidal gold-labelled protein A on the complex, and recording of gold oxidation voltammogram, which provides information about the presence and the concentration of antibodies in blood serum. The response is proportional to the concentration of antibodies over the interval from 10^{-7} to 10^{-2} mg mL^{-1}. The detection limit is 10^{-7} mg mL^{-1}. A sandwich comprising the antigen, an antibody, and protein A labelled with colloidal gold was formed on the sensor surface during the analysis. The gold oxidation current provided information about the concentration of antibodies in test samples. Taking Forest-Spring encephalitis as an example, it was shown that the use of metal-labelled protein A is promising for diagnosis of infectious diseases [77].

38.4 CONCLUSIONS

The development of electrochemical genosensors and immunosensors based on labelling with NPs has registered an important growth, principally for clinical and environmental applications. The electrochemical detection of NP labels in affinity biosensors using stripping methods allows the detailed study of DNA hybridisation as well as immunoreactions with interest in genosensor or immunosensor applications.

Beside different kinds of nanocrystals (or QDs) AuNPs are showing a special interest in several applications. Electrochemical methods used for AuNPs label detection may be very promising taking into account their high sensitivity, low detection limit, selectivity, simplicity, low cost and availability of portable instruments.

The sensitivity of AuNPs detection is usually improved by the silver enhancement method. In this procedure, silver ions are reduced to silver metal by a reducing agent, at the surface of a gold NP, causing it to grow and so facilitating the detection [36].

Many strategies based on DNA hybridisation assays using AuNPs have been developed. Most of them rely on capturing the NP to the hybridised target in a three-component 'sandwich' format.

Actually, special attention is paid in the application of biosensors in environmental analysis. The high cost and slow turnaround times typically associated with the measurement of regulated pollutants clearly indicates a need for environmental screening and monitoring methods that are fast, portable and cost-effective. To meet this need, a variety of field analytical methods have been introduced. Because of their unique characteristics, however, technologies such as DNA sensors and immunosensors based on AuNPs might be exploited to fill specific niche applications in the environmental monitoring area.

The analysis of trace substances in environmental science, pharmaceutical and food industries is a challenge since many of these applications demand a continuous monitoring mode. The use of immunosensors based on AuNPs in these applications should also be appropriate. Although there are many recent developments in the immunosensor field, which have potential impacts [36], nevertheless there are few papers concerning environmental analysis with electrochemical detection based on AuNPs. The application of some developed clinical immunosensors can also be extended to the environmental field.

ACKNOWLEDGEMENTS

Authors thank the Spanish ''Ramón Areces'' foundation (project 'Bionanosensores') and MEC (Madrid) (Projects MAT2005-03553, and the Consolider-Ingenio 2010 CSD2006-00012).

REFERENCES

1 D.R. Thevenot, K. Toth, R.A. Durst and G.S. Wilson, *Pure Appl. Chem.*, 71 (1999) 2333–2348.
2 C.M. Niemeyer, *Angew. Chem. Int. Ed.*, 40 (2001) 4128–4158.
3 S.F. D'Souza, *Biosens. Bioelectron.*, 16 (2001) 337–353.
4 J. Wang, *Anal. Electrochem.*, 2nd ed, Wiley-VCH, New York, 2000.
5 T. Vo-Dinh and B. Cullum, *Fresenius J. Anal. Chem.*, 366 (2000) 540–551.
6 T.S. Misono and P.K.R. Kumar, *Anal. Biochem.*, 342 (2005) 312–317.
7 O. Hayden, R. Bindeus, C. Haderspock, K.J. Mann, B. Wirl and F.L. Dickert, *Sens. Actuators B-Chem.*, 91 (2003) 316–319.
8 O. Hayden and F.L. Dickert, *Adv. Mater.*, 13 (2001) 1480–1483.
9 E.J. Cho, J.R. Collett, A.E. Szafranska and A.D. Ellington, *Anal. Chim. Acta*, 564 (2006) 82–90.
10 G.L. Igloi, *Expert Rev. Mol. Diagn.*, 3 (2003) 17–26.
11 F. Pellestor and P. Paulasova, *Int. J. Mol. Med.*, 13 (2004) 521–525.
12 A.F. Collings and F. Caruso, *Rep. Prog. Phys.*, 60 (1997) 1397–1445.
13 M.A. Cooper, *Anal. Bioanal. Chem.*, 377 (2003) 834–842.
14 P. Alivisatos, *Nanotechnology*, 14 (2003) R15–R27.
15 P. Alivisatos, *Nat. Biotechnol.*, 22 (2004) 47–52.
16 W.C.W. Chan, D.J. Maxwell, X.H. Gao, R.E. Bailey, M.Y. Han and S.A. Nie, *Curr. Opin. Biotechnol.*, 13 (2002) 40–46.
17 M. Huber, T.F. Wei, U.R. Müller, P.A. Lefebvre, S.S. Marla and Y.P. Bao, *Nucleic Acids Res*, 32 (2004) e137.
18 A. Merkoçi, M. Aldavert, S. Marin and S. Alegret, *Trends Anal. Chem.*, 24 (2005) 341–349.
19 K. Kerman, M. Kobayashi and E. Tamiya, *Meas. Sci. Technol.*, 15 (2004) R1–R11.
20 C.A. Mirkin, R.L. Letsinger, R.C. Mucic and J.J. Storhoff, *Nature*, 382 (1996) 607–609.
21 P. Alivisatos, K.P. Johnsson, X. Peng, T.E. Wilson, C.J. Loweth, M.P. Bruchez Jr. and P.G. Schultz, *Nature*, 382 (1996) 609–611.
22 T.A. Taton, C.A. Mirkin and R.L. Letsinger, *Science*, 289 (2000) 1757–1760.
23 W. Fritzsche and T.A. Taton, *Nanotechnology*, 14 (2003) R63–R73.
24 J. Wang, *Anal. Chim. Acta*, 500 (2003) 247–257.
25 Y.C. Cao, R. Jin and C.A. Mirkin, *Science*, 297 (2002) 1536–1540.

26 S.J. Park, T.A. Taton and C.A. Mirkin, *Science*, 295 (2002) 1503–1506.
27 F. Patolsky, K.T. Ranjit, A. Lichtenstein and I. Willner, *Chem. Commun.*, 12 (2000) 1025–1026.
28 H. Cai, Y. Xu, N. Zhu, P. He and Y. Fang, *Analyst*, 127 (2002) 803–808.
29 M. Ozsoz, A. Erdem, K. Kerman, D. Ozkan, B. Tugrul, N. Topcuoglu, H. Ekren and M. Taylan, *Anal. Chem.*, 75 (2003) 2181–2187.
30 T.M.H. Lee, L.L. Li and I.M. Hsing, *Langmuir*, 19 (2003) 4338–4343.
31 H. Cai, Y.Q. Wang, P.G. He and Y.Z. Fang, *Chem. J. Chinese Universities*, 24 (2003) 1390–1394.
32 K. Shanmugam, S. Subramanayam, S.V. Tarakad, N. Kodandapani and S.F. D'Souza, *Anal. Sci.*, 17 (2001) 1369–1374.
33 B. Foultier, L. Moreno-Hagelsieb, D. Flandre and J. Remacle, *IEE Proc. Nanobiotechnol.*, 152 (2005) 3–12.
34 M.I. Pividori, A. Merkoci and S. Alegret, *Biosens. Bioelectron.*, 15 (2000) 291–303.
35 K. Vivek, T. Vijay and J. Huangxian, *Crit. Rev. Anal. Chem.*, 36 (2006) 73–106.
36 L.D. Mello and L.T. Kubota, *Food Chem*, 77 (2002) 237–256.
37 E. Williams, M.I. Pividori, A. Merkoçi, R.J. Forster and S. Alegret, *Biosens. Bioelectron.*, 19 (2003) 165–175.
38 M.I. Pividori, A. Merkoçi and S. Alegret, *Biosens. Bioelectron.*, 19 (2003) 473–484.
39 A. Erdem, K. Kerman, B. Meric, U.S. Akarca and M. Ozsoz, *Anal. Chim. Acta*, 422 (2000) 139–149.
40 M.I. Pividori, A. Merkoçi, J. Barbé and S. Alegret, *Electroanalysis*, 15 (2003) 1815–1823.
41 D. Hernández-Santos, M. Díaz-González, M.B. González-García and A. Costa-García, *Anal. Chem.*, 76 (2004) 6887–6893.
42 L. Authier, C. Grossiord and P. Brossier, *Anal. Chem.*, 73 (2001) 4450–4456.
43 J. Wang, R. Polsky and D. Xu, *Langmuir*, 17 (2001) 5739–5741.
44 J. Wang, G. Liu and A. Merkoçi, *Anal. Chim. Acta*, 482 (2003) 149–155.
45 M. Fojta, L. Havran, M. Vojtiskova and E. Palecek, *J. Am. Chem. Soc.*, 126 (2004) 6532–6533.
46 E. Palecek, R. Kizek, L. Havran, S. Billova and M. Fojta, *Anal. Chim. Acta*, 469 (2002) 73–83.
47 J. Wang, D. Xu, A. Erdem, R. Polsky and M.A. Salazar, *Talanta*, 56 (2002) 931–938.
48 S.F. Wolf, L. Haines, J. Fisch, J.N. Kremsky, J.P. Dougherty and K. Jacobs, *Nucleic Acids Res*, 15 (1987) 2911–2926.
49 T.M. Lee and I.-M. Hsing, *Anal. Chem. Acta*, 556 (2006) 26–37.
50 P.O. Part, E. López and G. Mathis, *Anal. Biochem.*, 195 (1991) 283–289.
51 S.G. Penn, L. He and M. Natan, Nanoparticles for bioanalysis, *Curr. Opin. Chem. Biol.*, 7 (2003) 609–615.

52 Z. Zhong, K.B. Male and J.H.T. Luong, *Anal. Lett.*, 36 (2003) 3097–3111.
53 D. Hernández-Santos, M.B. González-García and A. Costa-García, *Electroanalysis*, 14 (2002) 1225–1235.
54 A. Doron, E. Katz and I. Willner, *Langmuir*, 11 (1995) 1313–1317.
55 M. Pumera, M.T. Castañeda, M.I. Pividori, R. Eritja, A. Merkoçi and S. Alegret, *Langmuir*, 21 (2005) 9625–9629.
56 A. Kawde and J. Wang, *Electroanalysis*, 16 (2004) 101–107.
57 J. Wang, *Anal. Chim. Acta*, 469 (2002) 63–71.
58 F. Lucarelli, G. Marrazza, A.P. Turner and M. Mascini, *Biosens. Bioelectron.*, 19 (2004) 515–530.
59 J.J. Gooding, *Electroanalysis*, 14 (2002) 1149–1156.
60 A. Kouřilová, S. Babkina, K. Cahová, L. Havran, F. Jelen, E. Paleček and M. Fojta, *Analytical Letters*, 38 (2005) 2493–2507.
61 L.M. Demers, C.A. Mirkin, R.C. Mucic, R.A. Reynolds, R.L. Letsinger, R. Elghanian and G. Viswanadham, *Anal. Chem.*, 72 (2000) 5535–5541.
62 J. Wang, D. Xu, A.-N. Kawde and R. Polsky, *Anal. Chem.*, 73 (2001) 5576–5581.
63 J. Wang, D. Xu and R. Polsky, *J. Am. Chem. Soc.*, 124 (2002) 4208–4209.
64 M.T. Castañeda, A. Merkoçi, M. Pumera and S. Alegret, *Biosens. Bioelectron.*, 22 (2007) 1961–1967.
65 J. Wang, G. Rivas, X. Cai, E. Palecek, P. Nielsen, H. Shiraishi, N. Dontha, D. Luo, C. Parrado and M. Chicharro, *Anal. Chim. Acta*, 347 (1997) 1–8.
66 P.B. Luppa, L.J. Sokoll and D.W. Chan, *Clin. chim. Acta*, 314 (2001) 1–26.
67 R.I. Stefan, J.F. van Staden and H.Y. Aboul-Enein, *Fresenius J. Anal. Chem.*, 366 (2000) 659–668.
68 A. Warsinke, A. Benkert and F.W. Scheller, *Fresenius J. Anal. Chem.*, 366 (2000) 622–634.
69 M.J. Gomara, G. Ercilla, M.A. Alsina and I. Haro, *J. Immunol. Methods*, 246 (2000) 13–24.
70 V. Koubova, E. Brynda, L. Karasova, J. Skvor, J. Homola, J. Dostalek, P. Tobiska and J. Rosicky, *Sens. Actuators B Chem*, 74 (2001) 100–105.
71 I.E. Tothill, *Comput. Electron. Agric.*, 30 (2001) 205–218.
72 G. Liu and Y. Lin, *J. Nanosci. Nanotechnol.*, 5 (2005) 1060–1065.
73 M. Dequaire, C. Degrand and B. Limoges, *Anal. Chem.*, 72 (2000) 5521–5528.
74 D. Tang, R. Yuan, Y. Chai, X. Zhong, Y. Liu and J. Dai, *Biochem. Eng.*, 22 (2004) 43–49.
75 X. Chu, X. Fu, K. Chen, G.L. Shen and R.Q. Yu, *Biosens. Bioelectron.*, 20 (2005) 1805–1812.
76 D. Tang, R. Yuan and Y. Chai, *Biotechnol. Lett.*, 28 (2006) 559–565.
77 K. Brainina, A. Kozitsina and J. Beikin, *Anal. Bioanal. Chem.*, 376 (2003) 481–485.

IV

DNA analysis by using gold nanoparticle labels. Procedure 53, e381–388. ‘Electrochemical sensor analysis’. Amsterdam Elsevier, ISBN-13:978-0-444-53053-9. Editors: S. Alegret and A. Merkoçi, 2007.

Castañeda M. T., Pumera M., Alegret S., Merkoçi A.

Procedure 53

DNA analysis by using gold nanoparticle as labels

María Teresa Castañeda, Martin Pumera, Salvador Alegret and Arben Merkoçi

53.1 OBJECTIVES

(a) To construct a magnetic graphite epoxy composite electrode (M-GECE).
(b) To detect DNA hybridization electrochemically by labelling with gold nanoparticles and using an M-GECE.

53.2 MATERIALS AND INSTRUMENTS

- Graphite powder (particle size 50 μm, BDH, U.K.); epoxy resin (Epotek H77A) and hardener (Epotek H77B), (both of Epoxy Technology, USA); cylindrical PVC sleeve (6-mm i.d., 8-mm o.d. and 16-mm long); copper disk (6-mm o.d. and 0.5-mm thickness); copper wire; neodymium magnet (diameter 3 mm, height 5 mm, Halde Gac Sdad, Barcelona, Spain, catalog number N35D315); abrasive paper and alumina paper (polishing strips 301044-001, Orion, Spain); small spatula; glass of precipitates.
- Tris(hydroxymethyl)methylamine (TRIS), sodium chloride, sodium citrate, ethylenediamine tetraacetic acid disodium salt (EDTA), lithium chloride, Tween 20, streptavidin 10 nm colloidal gold labelled, hydrochloric acid (37%), nitric acid, streptavidin-coated paramagnetic beads (MB) with a diameter of 2.8 μm, Dynabeads M-280 Streptavidin (Dynal Biotech, Oslo, Norway); biotinylated probe oligonucleotides which sequences are shown in Table 53.1.
- The buffers, hybridization solution and supporting electrolyte are prepared as follows:
  – TTL buffer: 100 mM Tris-HCl, pH 8.0; 0.1% Tween 20; and 1 M LiCl.

Comprehensive Analytical Chemistry 49
Alegret and Merkoçi (Eds)
Volume 49 ISSN: 0166-526X DOI: 10.1016/S0166-526X(06)49096-6

TABLE 53.1
Oligonucleotide sequences used in assays[a]

Probe	Sequence
Capture DNA (BC-A)	biotin-5 'GAT TTT CTT CCT TTT GTT C3'
Target DNA (BC-T)[b]	biotin-5'GAA CAA AAG GAA GAA AAT C3'
Capture DNA (CF-A)	5'TGC TGC TAT ATA TAT-biotin-3'
Signaling DNA (CF-B)	biotin-5'GAG AGT CGT CGT CGT3'
Target DNA (CF-T)[c]	5'ATA TAT ATA GCA GCA GCA GCA GCA GCA GAC GAC GAC GAC TCT C3'
One base mismatch (CF-MX1)	5'ATA TAT AAA GCA GCA GCA GCA GCA GCA GAC GAC GAC GAC TCT C3'
Three base mismatch (CF-MX3)	5'ATA TAT CCC GCA GCA GCA GCA GCA GCA GAC GAC GAC GAC TCT C3'
Noncomplementary (CF-NC)	5'GGT CAG GTG GGG GGT ACG CCA GG3'

[a]Underlined nucleotides correspond to the mismatches.
[b]Target related to BRCA1 breast cancer gene.
[c]Target related to cystic fibrosis gene.

- TT buffer: 250 mM Tris-HCl, pH 8.0; and 0.1% Tween 20.
- TTE buffer: 250 mM Tris-HCl, pH 8.0; 0.1% Tween 20; and 20 mM Na2EDTA, pH 8.0.
- Hybridization solution: 750 mmol/L NaCl, 75 mmol/L sodium citrate.
- HCl 0.1 M as supporting electrolyte.

All stock solutions are prepared using deionised and autoclaved water.

- Platinum auxiliary electrode, (model 52–67 1, Crison, Spain); double junction Ag/AgCl reference electrode (Orion 900200) and magnetic graphite composite electrode (M-GECE) as working electrode.
- Autolab PGSTAT 20 (Eco Chemie, The Netherlands) connected to a personal computer for differential pulse voltammetry (DPV) measurements; TS-100 Thermo Shaker (Spain) used during the binding of streptavidin-coated paramagnetic beads with biotinylated probe and hybridization events. MCB 1200 biomagnetic processing platform (Sigris, CA, USA) in order to carry out the magnetic separation.

53.3 CONSTRUCTION OF THE M-GECE

- Construct the transducer body as follows: Take a connection female of 2 mm diameter and place a metallic thread and then solder this connection at its extreme to the center of the copper disk with the concavity up. Clean the copper disk previously by dipping it in HNO_3 solution (1:1) in order to remove copper oxide and rinsing it well with bidistilled water.

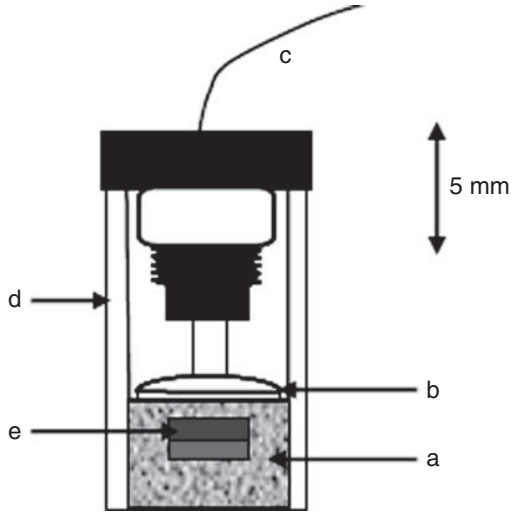

Fig. 53.1. Details of magnetic graphite–epoxy composite electrode with incorporated magnet. (a) Conducting graphite–epoxy composite; (b) copper disc facilitating electrical contact between the composite material and copper wire; (c) leading to the electrochemical workstation; (d) plastic sleeve; (e) permanent neodymium magnet. With permission from Ref. [1].

- Introduce this connection into the cylindrical PVC sleeve (6-mm i.d., 8-mm o.d. and 16-mm long). The metallic thread allows that the connection should remain fixed well in the end of the cylindrical PVC sleeve, whereas at another end there stays a cavity approximately 3-mm deep in which is placed the conducting composite and the permanent magnet [1]. Figure 53.1 shows the details of the M-GECE [1].
- On the other hand, manually mix epoxy resin and hardener in the ratio 20:3 (w/w) using a spatula. When the resin and hardener are well mixed, add the graphite powder (particle size 50 μm) in the ratio 20:80 (w/w) and mix thoroughly for 30 min to obtain a homogeneous paste of graphite–epoxy composite. Place the resulting paste into the cylindrical PVC sleeve, onto the copper disk.
- Incorporate the neodymium magnet into the body of the paste of graphite–epoxy composite, 2 mm under the surface of the electrode [1] and continue placing the paste until filling all the cavity. Cure the conducting composite at 40°C during 1 week. Once the resin is hardened, polish the surface first with abrasive paper and then with alumina paper.

53.4 ELECTROCHEMICAL DETECTION OF THE HYBRIDIZATION OF DNA STRAND RELATED TO BRCA1 BREAST CANCER GENE USING A TWO STRANDS ASSAY FORMAT

- Transfer 100 μg of streptavidin-coated microspheres (MB) into 0.5-mL Eppendorf tube. Separate, decant and wash the MB once with 100 μL of TTL buffer and then separate, decant and resuspend in 20 μL of TTL buffer. Add the desired amount of BC-A (capture DNA). Incubate the resulting solution for 15 min at temperature of 25°C and 400 rpm in a TS-100 ThermoShaker, so as to ensure immobilization.
- Separate the MB with the immobilized BC-A from the incubation solution, decant and wash sequentially with 100 μL of TT, 100 μL of TTE and 100 μL of TT buffers with the appropriate magnetic separation steps and then decant and resuspend in 50 μL of hybridization solution. The suspension of MB-modified with BC-A is ready for the hybridization.
- Add to the previous suspension (50 μL of MB/BC-A conjugate) the desired amount of BC-T (target DNA). Incubate at 42°C for 15 min and 800 rpm in TS-100 Thermo Shaker in order to carry out the hybridization reaction. Wash the formed MB/BC-A/BC-T conjugate twice with 100 μL of TT buffer and resuspend in 20 μL of TTL buffer. It is ready for adding streptavidin–gold nanoparticles (Au-NPs) label.
- Add the desired amount of Au-NPs to the resulting MB/BC-A/BC-T conjugate and then incubate for 15 min at 25°C and 400 rpm in TS-100 Thermo Shaker. Wash the resulting MB/BC-A/BC-T/Au-NPs conjugate twice with 100 μL of TT buffer and then separate, decant and resuspend in 50 μL of hybridization solution.
- Bring the surface of M-GECE into contact for 60 s with the solution containing the MB/BC-A/BC-T/Au-NPs conjugate that is accumulated on it due to the inherent magnetic field of the electrode. The M-GECE is ready for the immediate DPV detection of Au-NPs labels anchored onto the surface through the conjugate.

53.5 ELECTROCHEMICAL DETECTION

- Choose differential pulse voltammetry (DPV) analysis mode in the Autolab software program.
- Establish the parameters: Deposition potential, +1.25 V; duration, 120 s; conditioning potential, 1.25 V; step potential, 10 V; modulation amplitude, 50 mV.

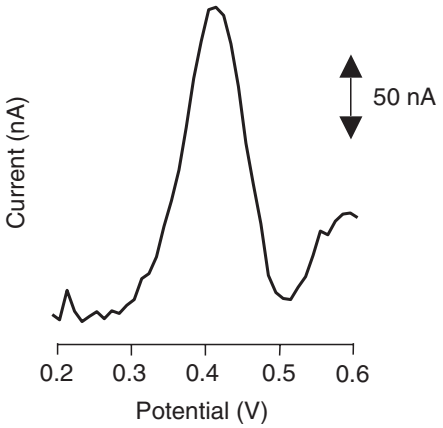

Fig. 53.2. DPV hybridization response of 2.5 μg mL^{-1} of: BC-T on magnetic graphite–epoxy composite electrode. Conditions: amount of paramagnetic beads, 50 μg; amount of AuNPs, 9×10^{12}; hybridization time, 15 min; hybridization temperature, 42°C; oxidation potential, +1.25 V; oxidation time, 120 s; DPV scan from +1.25 V to 0 V; step potential, 10 mV; modulation amplitude, 50 mV; scan rate, 33.5 mV s^{-1}; non-stirred solution. With permission from Ref. [3].

- Immerse the three electrodes: M-GECE as working electrode, the Ag/AgCl as reference electrode and the platinum as auxiliary electrode in a 10 mL electrochemical cell containing HCl 0.1 M.
- The electrochemical oxidation of Au-NPs to $AuCl_4^-$ is performed at +1.25 V (vs. Ag/AgCl) for 120 s in the nonstirred solution. Immediately after the electrochemical oxidation step, is performed DPV. During this step scan the potential from +1.25 V to 0 V (step potential 10 mV, modulation amplitude 50 mV, scan rate 33.5 mV s^{-1}, no stirred solution).
- The result is an analytical signal due to the reduction of $AuCl_4^-$ at potential +0.4 V [2]. The DPV peak height at a potential of +0.4 V is used as the analytical signal in all of the measurements.
- The background subtraction protocol involving saving the response for the blank solution and subtracting it from the analytical signal is used.

Figure 53.2 shows a typical DPV hybridization response of BC-T on M-GECE [3].

53.6 ELECTROCHEMICAL DETECTION OF THE HYBRIDIZATION OF DNA STRAND RELATED TO CYSTIC FIBROSIS GENE, USING A SANDWICH ASSAY FORMAT

- Transfer 100 μg of MB into 0.5 mL Eppendorf tube. Wash the MB once with 100 μL of TTL buffer and then separate, decant and

resuspend in 20 μL of TTL buffer. Add the desired amount of CF-A (capture DNA). Incubate the resulting solution for 15 min at temperature of 25°C and 400 rpm in a TS-100 ThermoShaker, so as to ensure immobilisation.

- Separate the MB with the immobilised CF-A from the incubation solution and wash sequentially with 100 μL of TT, 100 μL of TTE and 100 μL of TT buffers with the appropriate magnetic separation steps and then decant and resuspend in 50 μL of hybridization solution. The suspension of MB modified with CF-A is ready for the first hybridization.
- Add to the previous suspension (50 μL of MB/CF-A conjugate) the desired amount of CF-T (Target DNA). Incubate at 25°C for 15 min and 800 rpm in TS-100 Thermo Shaker in order to carry out the first hybridization reaction. The formed MB/CF-A/CF-T conjugate is separated, decanted and washed twice with 100 μL of TT buffer. Separate, decant and resuspend in 50 μL of hybridization solution. It is ready for the second hybridization.
- Add to the previous suspension (50 μL of MB/CF-A/CF-T conjugate) the desired amount of CF-B (Signaling DNA). Incubate at 25°C during 15 min and 800 rpm, in TS-100 Thermo Shaker in order to carry out the second hybridization reaction. The formed MB/CF-A/CF-T/CF-B conjugate is separated, decanted and washed twice with 100 μL of TT buffer. Separate, decant and resuspend in 20 μL of TTL buffer. It is ready for adding Au-NPs label.
- Add the desired amount of Au-NPs to the resulting MB/CF-A/CF-T/CF-B conjugate and then incubate during 15 min at 25°C and 400 rpm in TS-100 Thermo Shaker. The MB/CF-A/CF-T/CF-B/Au-NPs sandwich conjugate is formed. Wash twice with 100 μL of TT buffer separate, decant and resuspend in 50 μL of hybridization solution.
- Carry out the magnetic collection onto the surface of the M-GECE as described in the final point of Section 53.4.
- The electrochemical detection is performed in the same way as previously described in Section 53.5.

53.7 DISCUSSION

The voltammogram shown in Fig. 53.2 demonstrates the efficacy of the genomagnetic assay using as target a DNA strand related to the BRCA1 breast cancer gene.

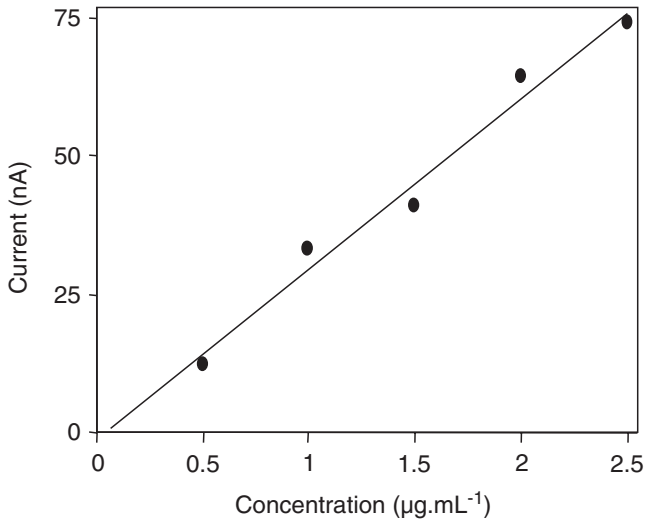

Fig. 53.3. Calibration plot for BC-T DNA over the 0.5–2.5 $\mu g\,mL^{-1}$ range with a correlation coefficient of 0.9784. DL: 0.198 $\mu g\,mL^{-1}$ of BC-T (33 pmols in 50-μL sample volume). Conditions: Hybridization time, 15 min; amount of paramagnetic beads, 50 μg; oxidation potential, +1.25 V; oxidation time, 120 s. With permission from Ref. [3].

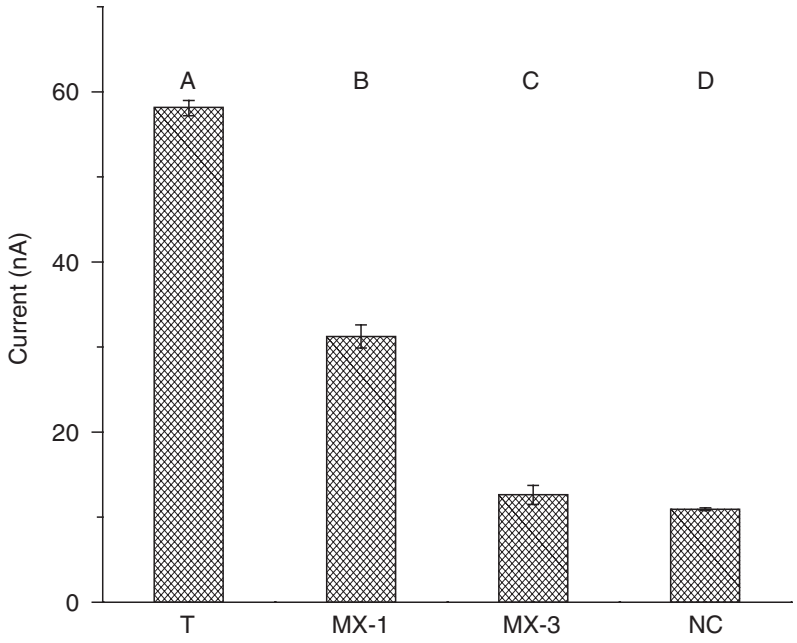

Fig. 53.4. Histogram that shows the current intensities of DPV peaks obtained for the hybridization responses of 8 $\mu g\,mL^{-1}$ of target associated with cystic fibrosis (*T*), single-base mismatch (MX-1), three-base mismatch (MX-3), and non-complementary DNA (NC) on magnetic graphite–epoxy composite electrode. Error bars show the mean and the standard deviations of the measurements taken from three independent experiments. Conditions: Hybridization temperature, 25°C; amount of MB, 100 μg. Other conditions as in Fig. 53.2. With permission from Ref. [3].

Figure 53.3 shows the BC-T defined concentration dependence. The calibration plot was linear over the concentration range studied [3].

Experiments for the detection of a single, three-base mismatch and non-complementary DNA were carried out in both assays. The results demonstrated an efficient discrimination. Figure 53.4 displays these results in sandwich assay, where the difference in current intensities is observed: higher for CF-T (Fig. 53.4A), which represents the efficient hybridization electrochemical response on the M-GECE; lower responses for CF-MX1 (Fig. 53.4B) and significantly lower for CF-MX3 (Fig. 53.4C) and CF-NC (Fig. 53.4D) [3].

SELECTED LITERATURE

1 M. Pumera, M.T. Castañeda, M.I. Pividori, R. Eritja, A. Merkoçi and S. Alegret, *Langmuir*, 21 (2005) 9625–9629.
2 M. Pumera, M. Aldavert, C. Mills, A. Merkoçi and S. Alegret, *Electrochim. Acta*, 50 (2005) 3702–3707.
3 M.T. Castañeda, A. Merkoçi, M. Pumera and S. Alegret, *Biosens. Bioelectron.*, 22 (2007) 1961–1967.

V

Electrochemical sensing of DNA using gold nanoparticles. *Electroanalysis*, 2007, 19, 743-753.

Castañeda M. T., Merkoçi A., Alegret S.,

Review

Electrochemical Sensing of DNA Using Gold Nanoparticles

M. T. Castañeda,[a,b,c] *S. Alegret,*[b] *A. Merkoçi*[a]*

[a] Institut Català de Nanotecnologia, Campus UAB, 08193 Bellaterra, Barcelona, Catalonia, Spain
*e-mail: arben.merkoci.icn@uab.es
[b] Grup de Sensors i Biosensors, Departament de Química, Universitat Autònoma de Barcelona, 08193 Bellaterra, Catalonia, Spain
[c] On leave from: Departamento de Ciencias Básicas, Universidad Autónoma Metropolitana-Azcapotzalco, 022000, México, D. F., Mexico

Received: October 21, 2006
Accepted: December 11, 2006

Abstract
The electrochemical properties of gold nanoparticles (AuNPs) have led to their widespread use as DNA labels. This fact has improved the design strategies for the electrochemical detection of DNA through hybridization event monitoring. The reported DNA hybridization detection modes are based on either AuNP detection after dissolving or the direct detection of the AuNP/DNA conjugates anchored onto the genosensor surface. Various enhancement strategies have been reported so as to improve the detection limit. Most are based on catalytic deposition of silver onto AuNP. Other strategies based on the use of AuNPs as carrier/amplifier of other labels will be also revised. The developed techniques are characterized by sensitivities and specificities that enable further applications of the developed DNA sensors in several fields.

Keywords: Gold nanoparticles, DNA labeling, DNA sensing, DNA immobilization, DNA hybridization, stripping voltammetry

DOI: 10.1002/elan.200603784

1. Introduction

Nanotechnology refers to research and technology development at the atomic, molecular, and macromolecular scale, leading to the controlled manipulation and study of structures and devices with length scales in the 1 to 100 nm range. Objects at this scale, such as nanoparticles (NPs) take on novel properties and functions that differ markedly from those seen in the bulk scale [1].

NPs represent an excellent biocompatibility with biomolecules and display unique structural, electronic, magnetic, optical and catalytic properties which have made them a very attractive material [2] as labels in the detection of DNA hybridization [3] using optical methods, i.e. surface plasmon resonance (SPR) [4] or various electrochemical techniques [5] between other applications.

Metal NPs have been known since antiquity and AuNPs, known for their use in staining glass, have been the subject of systematic study since 1857 with the pioneering work of Faraday on the color of colloidal gold [6].

Gold nanoparticles (AuNPs) are the most frequently used in bioanalysis among all the metal NPs. Colloidal gold or AuNPs is a suspension of submicrometer-sized particles of gold in a solvent usually water. The AuNPs suspension has usually either an intense red color (for particles less than 100 nm), or a dirty yellowish color (for larger particles) [7]. The NPs themselves can come in a variety of shapes: spheres, [8–11] rods, [12–16] cubes, [17, 18] triangles, [9, 19–21] ellipsoidal, [22] are some of the more frequently observed ones. AuNPs of different shapes and sizes were reported by Dos Santos et al. [23].

Michael Faraday was the first scientific to attribute the red color of colloidal gold to its finely divided state and the modern scientific evaluation of colloidal gold did not begin until his work [6] and later by the other pioneering works of Turkevich [24] and Frens [8]. Synthesis of novel AuNPs with unique properties is subject of substantial research, with applications in a wide variety of areas, including medicine, electronics, nanotechnology [7]. Particularly important are optical, electrical, magnetic and catalytic properties. The intrinsic properties of a metal nanostructure can be tuned by controlling its size, shape, and crystallinity. [20, 25].

The size and properties of AuNPs are highly dependent on the preparation conditions [26]. The shown biocompatibility [27] makes the AuNPs as very interesting for several bioanalytical applications in general and for biosensor application particularly. They have become of great importance in different DNA detection methods such as optical, [28, 29] or electronic [30]. Optical biosensors based on fluorescence are extraordinarily sensitive, and arrays containing thousands of unique probe sequences have been constructed [31].

Blab et al. [32] reported a novel optical readout scheme for AuNPs-based DNA microarrays on "Laser-Induced Scattering around a NanoAbsorber" which provides direct counting of individual NPs present on each array spot and stable signals, without any silver enhancement. Given the detection of nanometer-sized particles the linear dynamic

range of the method is particularly large and well suited for microarray detection.

Owing to their attractive properties AuNPs have been the most extensively NPs used so far in electrochemical biosensor applications in general and for DNA analysis particularly [33–35]. The aim of this review is to summarize the recent advances in AuNPs-based electrochemical DNA sensors emphasizing their use as DNA labels.

2. Synthesis and Characterization

2.1. Synthesis

After the first reported synthesis by Faraday [6], standard protocols for the preparation of AuNPs in aqueous solution were established by Turkevich [24, 36] and refined later by G. Frens [8]. Generally monodisperse spherical AuNPs, suspended in water with a diameter of around 10–20 nm, have been used to be produced. $HAuCl_4$, dissolved in deionized water and heated then until boiling is used and then sodium citrate solution is added. The color of the solution will gradually change from faint yellowish to wine-red. The sodium citrate first acts as a reducing agent, and later the negative citrate ions around the AuNPs surface introducing the charge that repels the particles and prevents them from aggregating. The formation of AuNPs can be observed by a change in color since small NPs of gold are red. Subsequently several other methods have been developed to prepare AuNPs with different sizes and shapes [37–40]. Several reducing agents/modes such as citric acid, [8, 24, 41] sodium borohydride ($NaBH_4$), [38, 42, 43] sodium ascorbate, [44] amines, [41, 45] and sonochemical [46] or electrochemical [38, 47] reduction have been reported. The stability of the colloidal suspension is the most important prerequisite in utilizing AuNPs. In order to stabilize the NPs, to control their size and shape and to prevent them from aggregating organic ligands as typical colloid chemical stabilizers or electron-donor ligands, like phosphines, amines or thiols, which stabilize the particles electrostatically or sterically [48] have been also used.

Alkylthiol passivated AuNPs of around 5–6 nm have been reported by Brust et al. [42] by using $NaBH_4$ as reducing agent. Ultrasound has become an important tool for the synthesis of metal NPs [49]. Based on this method [50] AuNPs have been produced by using hydroxyl and sugar pyrolysis radicals as reducing agents.

Colloidal solutions containing AuNPs of various sizes (5 to 80 nm) were prepared by a new method introduced by Slouf et al. [51]. They used a combination of the techniques already described [24] based on several-step reduction of $HAuCl_4$ water solution by combination of $Na(BH_4)$ and NH_2 OH solutions. Recently, Newman and Blanchard [41] reported the controlled formation of AuNPs using amine reducing. The reduction of $HAuCl_4$ occurs due to transfer of electrons from the amine to the metal ion, resulting in the formation of Au^0, with the subsequent formation of AuNPs.

Kimling et al. [52] have examined in detail the growth of AuNPs by reduction by citrate and ascorbic acid to explore the parameter space of reaction conditions. It is found that AuNPs can be produced in a wide range of sizes, from 9 to 120 nm, with defined size distribution, following the earlier work of Turkevich [24] and Frens [8].

The synthesized AuNPs have been characterized by means of various optical (spectroscopic, microscopic etc.) or electrochemical techniques so as to obtain information about structure, morphology, size and composition including their electrochemical behavior.

2.2. Optical Characterization

Transmission electron microscopy (TEM) has been used extensively as a way of AuNPs characterization. Nevertheless other techniques such as scanning electronic microscopy (SEM), scanning tunneling microscopy (STM), atomic force microscopy (AFM) and X-ray powder diffractometry (XRD) have been also used.

In a study reported by Dos Santos et al. [23] AuNPs of different shapes and sizes produced through the reaction of fulvic acid (FA) and gold tetrachloric acid were characterized by high-resolution transmission electron microscopy (HRTEM) and their optical field enhancing properties tested in surface-enhanced Raman scattering (SERS). Nuclear magnetic resonance (NMR) spectroscopy and TEM were also used to characterize AuNPs stabilized by 2,2′ :6′,2″-terpyridinyloctanethiol [53].

Chirea et al. [54] described the construction and characterization of structural and charge transport properties of electrostatically layer-by-layer self-assembled polielectrolyte/AuNPs films composed of cationic poly(L-lysine) (pLys) and mercaptosuccinic acid stabilized AuNPs with an average diameter of 2.5 nm. The assemblies were characterized using UV-vis absorption spectroscopy, AFM as well as electrochemical methods.

Frenkel et al. [55] characterized their thiol-protected AuNPs by using TEM to measure their size distribution and extended X-ray absorption fine-structure (EXAFS) to measure their coordination numbers and nearest-neighbor distances. The authors presented a self-consistent analysis of the EXAFS spectroscopy data of ligand-stabilized metal nanoclusters. Their method employs the measurement of the coordination numbers and metal-metal bond-length decrease that can be correlated with the average diameter and structure of the NPs in the framework of the surface tension model and different structural motifs. To test the method, they synthesized and analyzed a series of dodecanethiol-stabilized AuNPs where the only control parameter was the gold/thiol ratio, varied between 6:1 and 1:6.

Recently, Scaffardi et al. [56] sized AuNPs by optical extinction spectroscopy. The measurement of optical extinction is used to determine the size of nearly spherical AuNPs suspended in solution, produced by a 'reverse micelles' process. For the small particles used in their work there had a very good agreement between the determina-

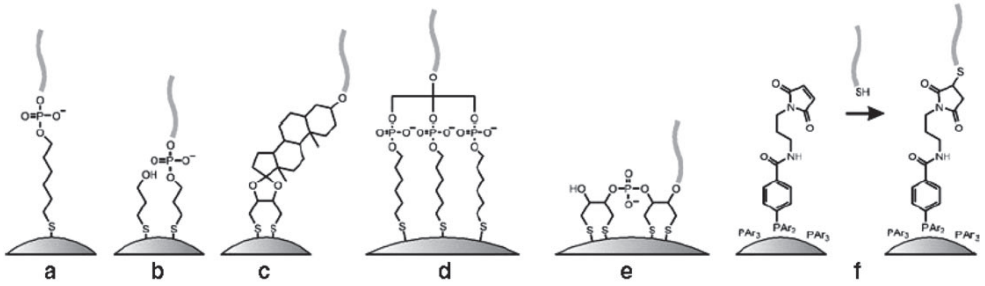

Fig. 1. Schematic of the methods used for conjugating oligonucleotides to gold nanoparticles. a) Thiol-modified and b) disulfide-modified oligonucleotides spontaneously bind to gold nanoparticle surfaces. Asymmetric disulfide modification adds an additional mercaptoalcohol ligand to the Au surface, but the density of oligonucleotides formed on the nanoparticle surface is the same as for thiol-terminal oligonucleotides. c) Di and d) trisulfide modified conjugates. e) Oligothiol–nanoparticle conjugates. Although four thiol connections are shown, any number are possible via sequential addition of a commercial dithiane phosphoramidite during solid-phase oligonucleotide synthesis. f) Oligonucleotide conjugates from Nanoprobes' phosphine-modified nanoparticles. Adapted from *Nanotechnology*, **2003**, *14*, R63.

tion of the radius by optical methods and TEM techniques. Extinction measurements with a commercial spectrophotometer can be an economical and simple alternative when special electronic microscopy (TEM or SEM) is not available.

2.3. Electrochemical Characterization

Quinn et al. [57] reported the preparation of hexanethiol-capped Au (C6S-Au) particles to obtain thiol protected AuNPs (0.81 nm, Au_{147}) so-called monolayer protected clusters (MPCs) with improved monodispersity. In order to investigate MPCs redox properties electroanalytical techniques: Cyclic voltammetry (CV), differential pulse voltammetry (DPV), and chronoamperometry at a Pt microelectrode were used. A DPV response for the as-prepared Au_{147} MPCs showing 15 evenly spaced (ΔV) peaks characteristic of charge injection to the metal core was obtained. The authors presented the first report of 15 quantized double layer charging peaks at room temperature which is a clear confirmation that MPCs are indeed multivalent redox species.

The reaction of the phosphine-protected AuNPs $Au_{55}(PPh_3)_{12}Cl_6$ ("Au_{55}") with hexanethiol ($C_6H_{13}SH$) and other thiols with the aim to obtain relatively monodisperse NPs was described by Balasubramanian et al. [58]. The voltammetry of the reaction product with $C_6H_{13}SH$ displays a well-defined pattern of peaks qualitatively reminiscent of Au_{38} NPs, but with quite different spacing (0.74 ± 0.01 V) between the potentials of initial oxidation and reduction steps (electrochemical gap). Correction of this "molecule-like" gap for charging energy indicates a HOMO-LUMO gap energy of about 0.47 V. CV and Osteryoung square-wave voltammetry (OSWV) were carried out in a single compartment cell containing 1.4 mm Pt disk working, Pt wire counter, and Ag wire quasireference electrodes (QRE), under argon.

AuNPs electrodeposited onto glassy carbon-electrodes (AuNPs/GC) in the presence of two different additives: cysteine and iodide ions were studied by Deab et al. [59]. The electrochemical characterization of the AuNPs/GC was performed via the measurements of the reductive desorption patterns of a thiol (e.g., cysteine) self-assembled monolayer as well as the CV response toward the oxygen reduction reaction in alkaline medium.

The redox behavior of a ruthenium-terpyridine complex of AuNPs (Ru–Tpy–Au, core size 5.5 nm) was studied also by CV using platinum wire as counter and glassy carbon or gold as working electrodes [53].

3. DNA Immobilization

Owing their large specific surface area and high surface free energy, AuNPs can strongly adsorb DNA. The negative charges as a result of the adsorption of citrate (used in most of the fabrication processes) enhance the electrostatic adsorption between AuNPs and DNA strands. DNA can also be immobilized onto AuNPs through special functional groups such as thiols and others, which can interact strongly with AuNPs [60–62].

DNA oligonucleotides that contain several adenosyl phosphothiolate residues at their ends have been used to interact directly with the metal surface of NPs [63]. A limited number of linkers to immobilize DNA oligonucleotides onto AuNPs has been used [64, 65]. Figure 1 is a schematic of the methods used for conjugating oligonucleotides to AuNPs. Monomaleimido gold clusters have been coupled with thiolated DNA oligomers to synthesize probes for homogeneous nucleic acid analyses and ensure a 1:1 DNA/AuNP connection with interest for sensitivity improvements [66, 67] (See Fig. 2).

The synthesis of a novel trithiol-capped oligodeoxyribonucleotide and AuNPs conjugates prepared from it, was reported by Li et al. [61] This novel trithiol DNA oligonu-

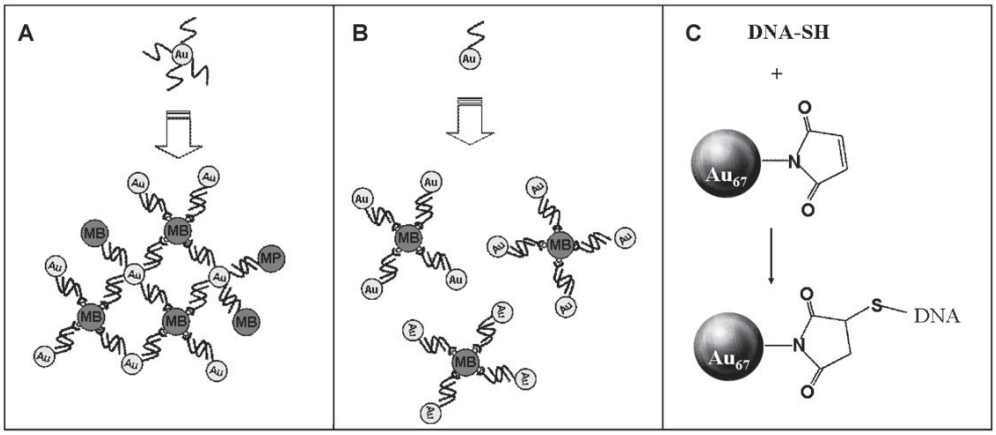

Fig. 2. Schematics of A) Formation of particle-linked DNA network structure due to the interconnection between magnetic beads (MB) in the case where AuNPs modified with more than one DNA strands are used; B) The previous network is not created by using the 1:1 Au-DNA connection (C). The reaction of maleimido-Au67 with thiol-oligonucleotide that make possible the 1:1 Au-DNA connection. Adapted from *Langmuir*, **2005**, *21*, 9625.

cleotide can be used to stabilize particles >30 nm in diameter which is essential for many diagnostic applications [61].

Cai et al. [68] immobilized the oligonucleotide with a mercaptohexyl group at the 5′-phosphate end onto the 16 nm diameter AuNPs, which were self-assembled on a cysteamine-modified gold electrode and discovered that the saturated immobilization quantities of singlestrand DNA on the modified electrode were about 10 times larger than that on a bare gold electrode.

4. Applications in DNA Analysis

The analysis of specific gene sequences in the diagnostic laboratory is usually based on DNA hybridization in which the target gene sequence is identified by a DNA probe able to form a double stranded hybrid with its complementary nucleic acid with high efficiency and specificity [69]. NPs in general and AuNPs particularly offer attractive properties to act as DNA hybridization tags [70] with interest in developing sensitive electrochemical genosensors.

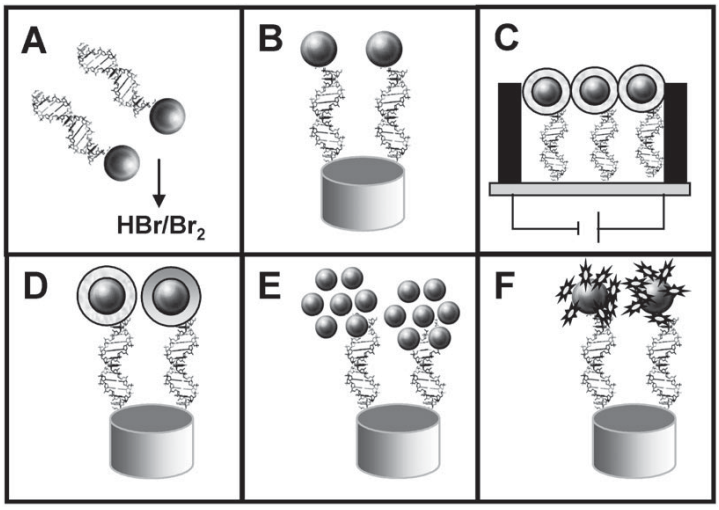

Fig. 3. Schematic (not in scale) of the different strategies used for the integration of gold nanoparticles (AuNPs) into DNA sensing systems: A) Previous dissolving of AuNP by using HBr/Br_2 mixture followed by Au(III) ions detection; B) direct detection of AuNPs anchored onto the surface of the genosensor; C) conductometric detection, D) enhancement with silver or gold followed by detection; E) AuNPs as carriers of other AuNPs; F) AuNPs as carriers of other electroactive labels.

Figure 3 is a schematic of the most important strategies used to integrate AuNPs in DNA detection systems. These strategies consist of: (A) The electrochemical detection of AuNP label by detecting the gold ions released after acidic dissolving; (B) Direct detection of AuNPs anchored onto the surface of a conventional genosensor (based on stripping voltammetry); (C) Silver enhancement using conductometric technique; (D) Enhancement of AuNPs anchored to conventional genosensor surface by using silver or gold; (E) Using of AuNPs as carriers for other electroactive labels.

Details of the above strategies will be discussed in the following sections.

4.1. Detection Based on AuNPs Dissolving

AuNPs bound to a DNA can be detected indirectly, by oxidatively dissolving the AuNPs into aqueous metal ions and then electrochemically sensing the ions. The great majority of the AuNPs-based assays have been based on chemical dissolution of the AuNPs tags in a hydrobromic acid/bromine (HBr/Br_2) solution followed by accumulation and stripping analysis of the resulting Au(III) solution.

Authier et al. [71] developed an electrochemical DNA detection method for the sensitive quantification of an amplified 406-base pair human cytomegalovirus DNA sequence (HCMV DNA). The HCMV DNA was extracted from cell culture, amplified by polymerase chain reaction (PCR), and then quantified by agarose gel electrophoresis. The HCMV DNA was immobilized on a microwell surface and hybridized with the complementary oligonucleotide-modified AuNPs, followed by the release of Au by treatment with a HBr/Br_2 solution, and the indirect determination of the solubilized Au(III) ions by ASV at a sandwich-type screen-printed microband electrode (SPMBE). AuNPs of 20-nm were used. The combination of the sensitive Au(III) determination at a SPMBE with the large number of Au(III) released from each gold nanoparticle probe allows detection of as low as 5 pM amplified HCMV DNA fragment. Wang et al. [72] developed an AuNPs based protocol for the detection of DNA segments related to the breast cancer *BRCA1* gene. This bioassay consisted in the hybridization of a biotinylated target DNA to streptavidin coated magnetic bead-binding biotynilated probe and followed by binding of streptavidin-coated AuNPs (5 nm) to the target DNA, dissolution of the AuNPs and electrochemical detection using potentiometric stripping analysis (PSA) of the dissolved gold tag at single use thick film carbon electrodes, obtaining a detection limit of 4×10^{-9} M.

The sensitivity of the detection is usually improved by the silver enhancement method. A better detection limit was reported when a silver enhancement method was employed, based in the precipitation of silver on AuNPs tags and its dissolution (in HNO_3) and subsequent electrochemical potentiometric stripping detection The new silver-enhanced colloidal gold stripping detection strategy represented an attractive alternative to indirect optical affinity assays of nucleic acids and other biomolecules. The high sensitivity and selectivity of the new protocol was illustrated for the detection of DNA segments related to the *BRCA1* breast-cancer gene. A detection limit of around 150 pg mL^{-1} (i.e., 1.2 fmol) was obtained [73, 74].

The same group reported a new strategy for amplifying particle-based electrical DNA detection based on oligonucleotides functionalized with polymeric beads carrying numerous AuNPs tags which an ultrasensitive electrochemical stripping detection of the dissolved gold tags was carried out [75].

4.2. Direct Detection

The HBr/Br_2 solution is highly toxic and therefore methods based on direct electrochemical detection of AuNPs tags anchored onto the surface of the DNA genosensor, which would replace the chemical oxidation agent, are urgently need [67].

Direct detection of AuNPs but not in connection with the detection of DNA hybridization was reported earlier by our group and Costa-García's group [76, 77]

The application of AuNPs as oligonucleotide labels in DNA hybridization detection assays using a magnetic graphite-epoxy composite electrode (M-GECE) has been reported by Pumera et al. [67]. The novel gold nanoparticle-based protocol for detection of DNA hybridization was based on a magnetically trigged direct electrochemical detection of gold quantum dot tracers. It relies on binding target DNA (DNA1) with Au_{67} quantum dot in a ratio 1:1, followed by a genomagnetic hybridization assay between Au_{67}-DNA1 and complementary probe DNA (DNA2) marked paramagnetic beads. DPV was used for a direct voltammetric detection of resulting Au_{67} quantum dot-DNA1/DNA2-paramagnetic bead conjugate on M-GECE. The electrochemical oxidation of Au_{67} quantum dots to $AuCl^{4-}$ was performed at +1.25 V (vs Ag/AgCl) for 120 s in the nonstirred solution. Immediately after the electrochemical oxidation step, DPV was performed. During this step the potential was scanned from +1.25 V to 0 V, resulting in an analytical signal due to the reduction of $AuCl^{4-}$ at potential +0.4 V. The DPV peak height at a potential of +0.4 V was used as the analytical signal in all of the measurements. The background subtraction protocol involving saving the response for the blank solution and subtracting it from the analytical signal was used.

Castañeda et al. [78] reported two Au-NPs based genosensors designs for detection of DNA hybridization. Both assay formats were also based on a magnetically induced direct electrochemical detection of the Au-NPs tags on M-GECE. The first assay is based on the hybridization between 2 single strands biotin modified DNA probes: a capture DNA probe and a target DNA related to the *BRCA1* breast cancer gene, which is coupled with streptavidin-AuNPs (10 nm). The second assay is based on hybridization between 3 DNA strands: a biotin modified capture DNA probe, a target DNA, related to cystic fibrosis gene, and DNA signaling probe modified with AuNPs via biotin–

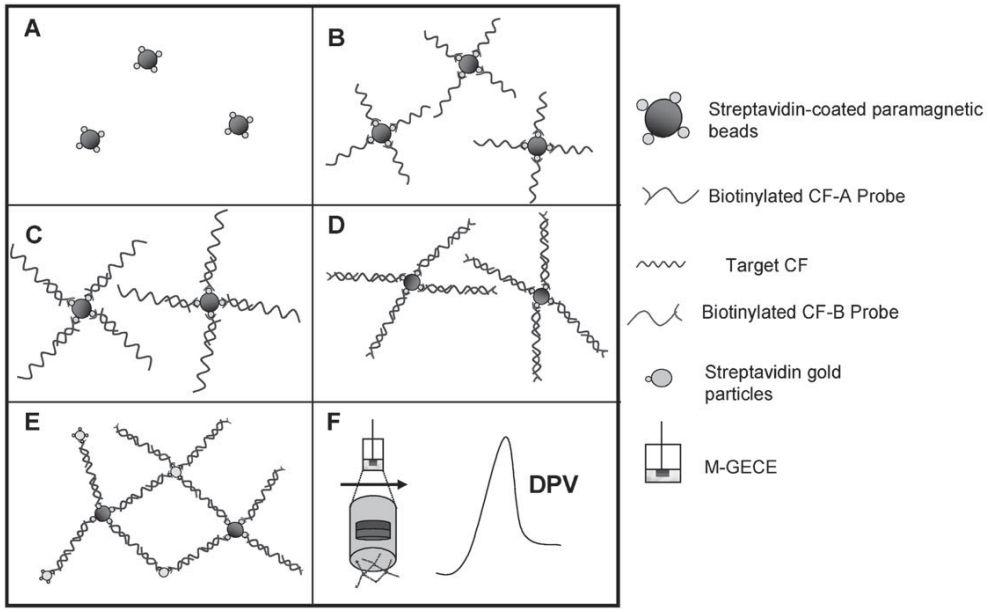

Fig. 4. Schematic representation of the sandwich system analytical protocol (not in scale): A) Introduction of streptavidin-coated magnetic beads; B) immobilization of the biotinylated CF-A probe onto the magnetic beads; C) addition of CF-T (first hybridization event); D) addition of biotinylated CF-B probe (second hybridization event); E) tagging by using the streptavidin – gold nanoparticles; F) accumulation of Au-NPs-DNA-magnetic bead conjugate on the surface of M-GECE and magnetically trigged direct DPV electrochemical detection of Au-NPs tag in the conjugate. CF: cystic fibrosis gene; Target CF: DNA target related to CF; CF-A: Capture probe for target CF; CF-B: signaling probe related to CF target. Adapted from *Biosens. Bioelectron*. **2006**, doi:10.1016/j.bios.2006.08.031

streptavidin complexation reactions. In this assay the target is 'sandwiched' between the others two probes. The Au-NPs tags were directly detected after the DNA hybridization event without the need of acidic dissolution. The electrochemical detection of AuNPs by DPV was performed in both cases with the same conditions described previously [67] (See Fig. 4).

An electrochemical genosensor based on AuNPs for detection of Factor V Leiden mutation from PCR amplicons which were obtained of real samples was described by Ozsoz et al. [79] The authors covalently bound amplicons to a pencil graphite electrode (PGE) and hybridized oligonucleotide-AuNPs conjugate a these electrode-bound targets. The oxidation signal of AuNPs was measured directly by using DPV at PGE. Direct electrochemical oxidation of the AuNPs was observed at a stripping potential of approximately +1.2 V. The response is greatly enhanced due to the large electrode surface area and the availability of many oxidizable gold atoms in each nanoparticle label. The detection limit for PCR amplicons was as low as 0.78 fmol.

4.3. Enhancement Methods

Enhancements by precipitation of silver onto the AuNPs labels have been reported so as to achieve amplified signals and lower detection limits [73, 80]. The use of other particles as AuNPs labels carriers are also used.

4.3.1. Enhancement with Silver

Mirkin's group [30] has developed an electronic DNA detection approach with high sensitivity and selectivity. In their approach, a small array of microelectrodes with 20 μm gaps between the electrodes leads is constructed, and probe sequences are immobilized on the substrate between the gaps. Using a three-component sandwich approach, hybridized target DNA is used to recruit AuNPs-tagged reporter strands between the electrodes leads. The NPs labels are then developed in the silver enhancer solution, leading to the precipitation of silver metal onto the AuNPs. The deposition of silver closes the electrical connection between the two flanking microelectrodes, and target captured is signaled by a sharp drop in the resistance of the circuit. The binding events localize AuNPs in an electrode gap; silver deposition facilitated by these NPs bridges the gap and leads to readily measurable conductivity changes. With this method, they demonstrated a sensitivity of 500 fM with a point mutation selectivity factor of 100000:1. in target DNA.

Silver enhanced technology, using voltammetry techniques, has been used also by Cai et al. [81] The DNA target was immobilized onto a chitosan-modified glassy carbon electrode (GCE) and hybridized with gold nanoparticle-modified DNA probes. This electrode was subjected to silver enhancer solution for 8 min to coat the gold particle with a thick shell of metallic silver. The voltammetric signal was increased by 88 times after silver enhancement strategy.

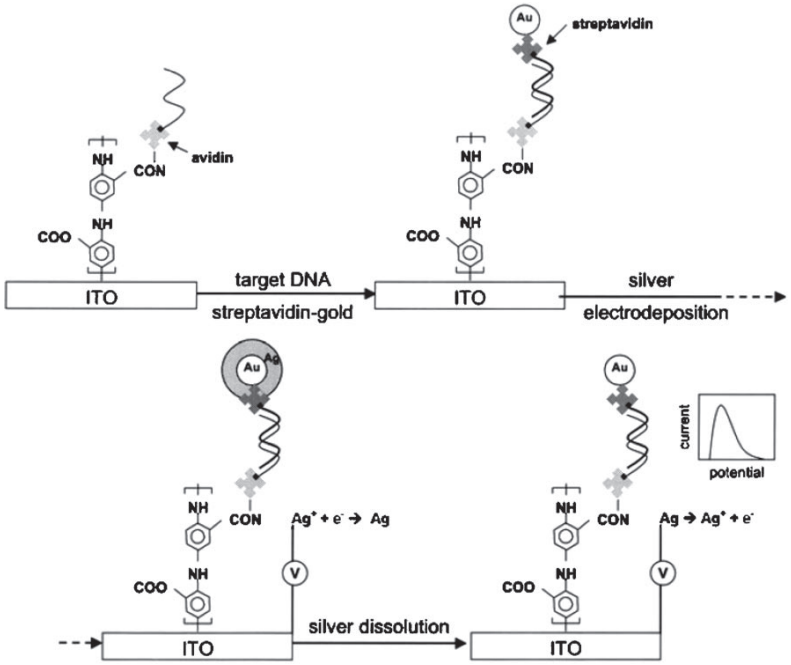

Fig. 5. Schematic of the DNA hybridization assay protocol with the gold nanoparticle-catalyzed silver electrodeposition approach on the electroconductive polymer-modified ITO electrode. With permission from *Electroanalysis* **2004**, *16*, 1628.

The same group reported [82] an electrochemical methodology that enables the rapid identification of different DNA sequences on microfabricated electrodes. Their approach starts with an electropolymerization process on a patterned indium tin oxide (ITO)-coated glass electrode, followed by a selective immobilization of biotin-tagged probes on individually addressable spots via the biotin–streptavidin linkage. An exemplary target mixture containing *E. coli* and *Stachybotrys chartarum*, an airborne pathogen, is then introduced. Recognition of the DNA hybridization event of the immobilized probes with the target pathogen PCR products or synthetic oligonucleotides is achieved by chronopotentiometric stripping utilizing the catalytic silver electrodeposition process on the DNA-linked nanogold shells. The ability to selectively immobilize different oligonucleotide probes together with a sensitive electrochemistry-based detection for multiple species, as demonstrated in this study, is an important step forward for the realization of a portable bioanalytical microdevice for the rapid detection of pathogens.

Lee et al. [83] reported an improved electrochemistry-based sequence-specific detection technique by modifying the electrode surface using polyelectrolytes or utilizing the electrode whose surface exhibits the lowest background signal. The electrochemical DNA-hybridization detection utilizing AuNPs labels in combination with silver enhancement was successfully demonstrated on the gold and indium tin oxide (ITO) electrodes. For the gold electrode, a significant reduction in the background silver staining was achieved by modifying the electrode surface with polyelectrolyte multilayer films of poly-allylamine hydrochloride (PAH) and poly-styrenesulfonate (PSS). The DNA probe was immobilized onto the (PAH/PSS)3-modified gold electrode via an avidin–biotin interaction for the sequence-specific detection of target sequences. For the ITO electrode, its inherent low silver-deposition property was exploited to develop a sensitive DNA-detection platform. The electrode was modified with a SAM of MPA, to which a thiol-modified probe was attached through a disulfide linkage [83].

Later the same group [84] reported a simple, rapid and sensitive method for the electrochemical AuNPs-based DNA detection with an electrocatalytic silver deposition process. The catalytic silver electrodeposition on AuNPs surfaces using an ITO as the electrode material instead of carbon paste, at certain potentials, without any chemical pretreatments of the electrode was performed. The ITO electrode surface was first coated with an electroconductive polymer, poly(2-aminobenzoic acid), to enable the chemical attachment of avidin molecules for the subsequent probe immobilization. The AuNPs labels were bound to the formed hybrids, via streptavidin–biotin interaction. Finally, silver was electrodeposited on the AuNPs surface and quantified directly by scanning the electrode to obtain the silver oxidation signal (See Figure 5).

4.3.2. Enhancement with Gold

Dequaire et al. [85] developed a new efficient protocol for the sensitive quantification of a 35 base-pair human

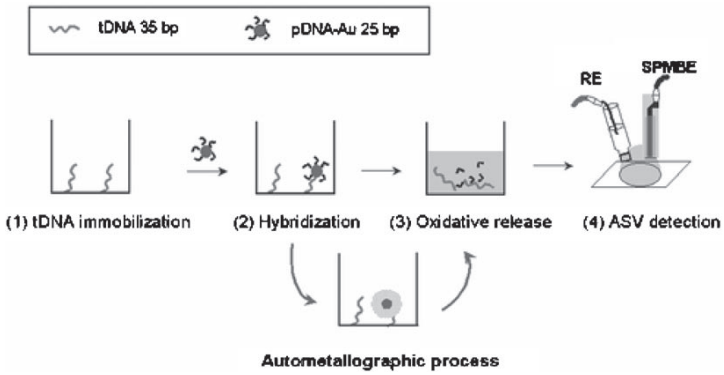

Fig. 6. Schematic representation of the electrochemical DNA Hybridization assay involving a colloidal gold label conjugate and its enlargement by catalytic gold deposition. With permission from *Analyst* **2006**, *131*, 923.

cytomegalovirus nucleic acid target (tDNA). In this assay, the hybridization of the target adsorbed on the bottom of microwells with an oligonucleotide-modified AuNPs detection probe (pDNA-Au) was monitored by the anodic stripping detection of the chemically oxidized gold label at a SPMBE. Thanks to the combination of the sensitive Au(III) determination at a SPMBE with the large amount of Au(III) released from each pDNA-Au, pM detection limits of tDNA can be achieve. Further enhancement of the hybridization signal based on the autocatalytic reductive deposition of ionic gold (Au(III)) on the surface of the AuNPs labels anchored on the hybrids was first envisaged by incubating the commonly used mixture of Au(III) and hydroxylamine (NH_2OH). However, due to a considerable nonspecific current response and of poor reproducibility it was not possible to significantly improve the analytical performances of the method under these conditions. This strategy, which led to an efficient increase of the hybridization response, allowed detection of tDNA concentrations as low as 600 aM and thus offers great promise for ultrasensitive detection of other hybridization events (See Fig. 6).

4.4. AuNPs as Amplification Units

AuNPs can be used as carrier for other AuNPs or other electroactive labels enhancing by this way the DNA detection compared to the use of single labels (single AuNP or a single electroactive molecule).

4.4.1. Carriers of AuNP Labels

A new strategy for amplifying particle-based electrical DNA detection based on oligonucleotides functionalized with polymeric beads carrying numerous AuNPs tags was described by Kawde and Wang [75]. The gold-tagged beads were prepared by binding biotinylated metal NPs to streptavidin-coated polystyrene spheres. Such use of carrier-sphere amplification platforms was combined with catalytic enlargement of the multiple gold tags and an ultrasensitive electrochemical stripping detection of the dissolved gold tags. This amplified electrical transduction allows detection of DNA targets down to the 300 amol level, and offers great promise for ultrasensitive detection of other biorecognition events.

4.4.2. AuNPs as Carriers for other Electroactive Labels

Another signal amplification strategy is to attach electroactive 6-ferrocenylhexanethiol molecules onto the AuNPs labels [86, 87].AuNPs/streptavidin conjugates covered with 6-ferrocenylhexanethiol were attached onto a biotinylated DNA detection probe of a sandwich DNA complex. Due to the elasticity of the DNA strands, the ferrocene caps on gold nanoparticle/streptavidin conjugates are positioned in close proximity to the underlying electrode modified with a mixed DNA capture probe/hexanethiol self-assembled monolayer

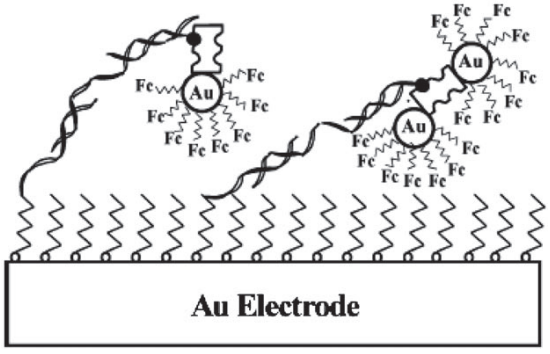

Fig. 7. Schematic representation of the amplified electrochemical detection of DNA hybridization via oxidation of the ferrocene caps on the AuNPs/streptavidin conjugates. For clarity, 1-hexanethiol, DNA, streptavidin, and 6-ferrocenylhexanethiol molecules are not draw to scale. The scheme pictorially reflects the fact that one streptavidin molecule could be linked to one or two ferrocenylalkanethiol-modified AuNPs. With permission from *Anal. Chem*. **2003**, *75*, 3941.

Table 1. Electrochemical genosensors using AuNPs as label. GE: gold electrode; DPV: differential pulse voltammetry; ASV: anodic stripping voltammetry; SPMBE: sandwich-type screen-printed microband electrode; PSA: potentiometric stripping analysis; SPEs: screen-printed electrodes; M-GECE: magnetic graphite-epoxy composite electrode, GCE: classy carbon electrode.

AuNPs size	Electrode	Detection technique	Detection mode	Enhancement	Detection limit	References
1.4 nm	M-GECE	DPV	Direct	None	12 nM	[67]
20 nm	SPMBE	ASV	HBr/Br_2	None	5 pM	[71]
5 nm	SPEs	PSA	HBr/Br_2	None	5 ng	[72]
5 nm	SPE	PSA	Direct	Silver	1.2 fmol	[74]
10 nm	M-GECE	DPV	Direct	None	33 pmol	[78]
5 ± 1.3 nm	PGE	DPV	Direct	None	0.78 fmol	[79]
16.3 nm	Chitosan- modified GCE	DPV	–	Silver	50 pM	[81]
15 nm	SPMBE	ASV	HBr/Br_2	Gold	600 aM	[85]

and can undergo reversible electron-transfer reactions. A detection level, down to 2.0 pM (10 amol for the 5 μL of sample needed) for oligodeoxynucleotide samples was obtained. The amplification of the voltammetric signals was attributed to the attachment of a large number of redox (ferrocene) markers per DNA duplex formed [86] (See Fig. 7).

5. Conclusions

Various electrochemical strategies to detect DNA hybridization by employing gold nanoparticles (AuNPs) as labels have already emerged. The majority of AuNP based DNA assays have been based on chemical dissolution of gold nanoparticle tag in a HBr/Br_2 solution followed by accumulation and stripping analysis of the resulting gold ions solution. The HBr/Br_2 solution is highly toxic and therefore methods based on direct electrochemical detection of AuNP tags, which replace the chemical oxidation agent, have been also reported.

Silver or even gold precipitation onto AuNP-DNA conjugates have been reported so as to improve the detection limit. Table 1 summarizes some of the results obtained by using different strategies. Although clear improvements have been demonstrated by the same authors upon comparing their results (with and without enhancement) it is not so clear the improvement when comparing different laboratories. The improvements by using enhancement strategies seem to be a compromise between signal augmentation and the reproducibility. The enhancements strategies by precipitation of gold or silver onto AuNPs or the use of AuNPs as carriers of other AuNPs or electroactive labels require a careful attention so as to avoid the irreproducibility problems.

Most of the electrochemical strategies reported up to date suffer from the fact that the hybridization event is still separated from the detection. Only in few cases these two processes are already integrated being the whole electrochemical assay compacted in a classical sensor model.

The electrochemical detection of AuNPs using stripping methods can further be improved. The use of microelectrode including arrays may probably improve the detection limits allowing their application in the study of other biomolecules interactions. The potential for detecting single molecule interactions by detecting individual gold colloid label opens the way toward new applications.

The electrochemical properties of AuNPs make them extremely easy to detect using simple instrumentation. In addition, these electrochemical properties may allow designing simple and inexpensive electrochemical systems for detection of ultrasensitive, multiplexed assays.

Clearly, AuNPs have a promising future in designing DNA sensors. Their utilization will be driven by the need for smaller detection platforms with lower limits of detection. Further efforts should be directed to enhancement strategies so as to avoid efficiently take their advantages.

Obviously the DNA electrochemical detection by using AuNPs will have an important impact on the development of specific and sensitive assays for clinical diagnosis, detection of pathogenic microorganisms in foods and the environment as well as for other applications including proteomics.

6. Acknowledgements

Spanish "Ramón Areces" foundation (project 'Bionanosensores') and MEC (Madrid) (Projects MAT2005 – 03553, BIO2004 – 02776 and CONSOLIDER NANOBIOMED are acknowledged.

7. References

[1] S. E. McNeil, *J. Leukocyte Biol.* **2005**, *78*, 585.
[2] D. Hernández-Santos, M. B. González-García, A. Costa-García, *Electroanalysis* **2002**, *14*, 1225.
[3] S. G. Penn, L. He, M. Natan, *Curr. Opin. Chem. Biol.* **2003**, *7*, 609.
[4] S. Schultz, D. R. Smith, J. J. Mock, D. A. Schultz, *Proc. Natl. Acad. Sci*. **2000**, *97*, 996.
[5] J. J. Gooding, *Electroanalysis* **2002**, *14*, 1149.
[6] M. Faraday, *Phil. Trans. Roy. Soc. London* **1857**, *147*, 145.
[7] C. N. Ramachandra Rao, G. U. Kulkarni, P. J. Thomasa, P. P. Edwards, *Chem. Soc. Rev.* **2000**, *29*, 27.

[8] G. Frens, *Nat. Phys. Sci.* **1973**, *241*, 20.
[9] S. S. Shiv, B. Suresh , S. Murali , *J. Nanosci. Nanotechnol.* **2005**, *5*, 1721.
[10] B. DeBenedetti, D. Vallauri, F. A. Deorsola, M. Martínez García, *J. Electroceramics* **2006**, *17*, 37.
[11] Z. Jian, Z. Xuang, W. Yongchang, *Microelectr. Eng.* **2005**, *77*, 58.
[12] J. H. Song, F. Kim, D. Kim, P. D. Yang, *Chem.-Eurp. J.* **2005**, *11*, 910.
[13] R. Krishnaswamy, H. Remita, M, Impéror-Clerc, C. Even, P. Davidson, B. Pansu, *Chem. Phys. Chem.* **2006**, *7*, 1510.
[14] B. D. Busbee, S. O. Obare, C. J. Murphy, *Adv. Mater.* **2003**, *15*, 414.
[15] E. Hao, R. C. Bailey, G. C. Schatz, J. T. Hupp, S. Li, *Nano Lett.* **2004**, *4*, 327.
[16] F. Kim, J. H. Song, P. D. Yang, *J. Am. Chem. Soc.* **2002**, *124*, 14316.
[17] Y. G. Sun, Y. N. Xia, *Science* **2002**, *298*, 2176.
[18] S. Hyuk Im, Y. Tack Lee, B. Wiley, Y. Xia, *Angew. Chem. Int. Ed.* **2005**, *44*, 2154.
[19] X. Zhang, A. V. Whitney, J. Zhao, E. M. Hicks, R. P. Van Duyne, *J. Nanosci. Nanotechnol.* **2006**, *6*, 1.
[20] R. C. Jin, Y. W. Cao, C. A. Mirkin, K. L. Kelly, G. C. Schatz, J. G. Zheng, *Science* **2001**, *294*, 1901.
[21] R. Jin, Y. C. Cao, E. Hao, G. S. Metraux, G. C. Schatz, C. A. Mirkin, *Nature* **2003**, *425*, 487.
[22] C. K. Tsung, W. Hong, Q. Shi, X. Kou, M. H. Yeung, J. Wang, G. D. Stucky, *Adv. Funct. Mater.* **2006**, *16*, 2225.
[23] D. S. dos Santos, Jr., R. A. Alvarez-Puebla, O. N. Oliveira, Jr., R. F. Aroca, *J. Mater. Chem.* **2005**, *15*, 3045.
[24] J. Turkevich, P. C. Stevenson, J. Hiller, *Discuss. Faraday Soc.* **1951**, *11*, 55.
[25] M. A. El-Sayed, *Acc. Chem. Es.* **2001**, *34*, 257.
[26] S. A. Miscoria, G. D. Barrera, G. A.Rivas, *Electroanalysis* **2005**, *17*, 1578.
[27] S. Liu, H. Ju, *Electroanalysis* **2003**, *15*, 1488.
[28] Y. W. C. Cao, R. C. Jin, C. A. Mirkin, *Science* **2002**, *297*, 1536.
[29] A. Csáki, P. Kaplanek, R. Möller, W. Fritzsche, *Nanotechnology* **2003**, *14*, 1262.
[30] S. J. Park, T. A. Taton, C. A. Mirkin, *Science* **2002**, *295*, 1503.
[31] J. R. Epstein, I. Biran, D. R. Watt, *Anal. Chim. Acta* **2002**, *469*, 3.
[32] G. A. Blab, L. Cognet, S. Berciaud, I. Alexandre, D. Husar, J. Remacle, B. Lounis, *Biophys. J.* **2006**, *90*, L13.
[33] Y. Zhuo, R. Yuan, Y. Q. Chai, D. P. Tang, Y. Zhang, N. Wang, X. L. Li, Q. Zhu, *Electrochem. Commun.* **2005**, *7*, 355.
[34] Y. Xiao, F. Patolsky, E. Katz, J. F. Hainfeld, I. Willner, *Science* **2003**, *299*, 1877.
[35] H. Cai, Y. Xu, N. N. Zhu, P. G. He, Y. Z. Fang, *Analyst* **2002**, *127*, 803.
[36] J. Turkevich, G. Kim, *Science* **1970**, *169*, 873.
[37] Z. Zhong, K. B. Male, J. H. T. Luong, *Anal. Lett.* **2003**, *36*, 3097.
[38] M. A. Hayat, *Colloidal Gold, Principle, Methods and Applications,* Vol. 1, Academic Press, New York **1989**, ch. 2, pp. 13 – 31.
[39] W. J. Parak, D. Gerion, T. Pellegrino, D. Zanchet, Ch. Micheel, S. C.Williams, R. Boudreau, M. A. Le Gros, C. A. Larabell, A. P. Alivisatos, *Nanotechnology* **2003**, *14*, R-15.
[40] G. Bauer, J. Hassmann, H. Walter, J. Haglmüller, C. Mayer, T. Schalkhammer, *Nanotechnology* **2003**, *14*, 1289.
[41] J. D. S. Newman, G. J. Blanchard, *Langmuir* **2006**, *22*, 5882.
[42] M. Brust, M. Walter, D. Bethell, D. J. Schiffrin, R. Whyman, *J. Chem. Soc. Chem. Commun.* **1994**, 801.
[43] L. Wang, G. Wei, L. Sun, Z. Liu, Y. Song, T. Yang, Y. Sun, Yujing, C. Guo, Z. Li, *Nanotechnology* **2006**, *17*, 2907.
[44] A. V. Stanishevsky, H. Williamson, H. Yockell-Lelievre, L. Rast, A. M. Ritcey, *J. Nanosci. Nanotechnol.* **2006**, *6*, 2013.
[45] C. Subramaniam, R. T. Tom, T. J. Pradeep, *Nanopart. Res.* **2005**, *7*, 209.
[46] Y. Mizukoshi, T. Fujimoto, Y. Nagata, R. Oshima, Y. Maeda, *J. Phys. Chem.* **2000**, *B104*, 6028.
[47] M. Zhou, S. Chen, S. Zhao, *Chem. Lett.* **2006**, *35*, 332.
[48] W. W. Weare, S. M. Reed, M. G. Warner, J. E. Hutchison, *J. Am. Chem. Soc.* **2000**, *122*, 12890.
[49] S. Zhu, H. Zhou, M. Hibino, I. Honma, M. Ichihara, *Adv. Funct. Mater.* **2005**, *15*, 381.
[50] J. Zhang, J. Du, B. Han, Z. Liu, T. Jiang, Z. Zhang, *Angew. Chem. Int. Ed.* **2006**, *45*, 1116.
[51] M. Šlouf, R. Kužel, Z. Matěj, *Z. Kristallogr. Suppl.* **2006**, *23*, 319.
[52] J. Kimling, M. Maier, B. Okenve, V. Kotaidis, H. Ballot, A. Plech, *J. Phys. Chem. B* **2006**, *110*, 15700.
[53] M. Ito, T. Tsukatani, H. Fujihara, *J. Mater. Chem.* **2005**, *15*, 960.
[54] M. Chirea, V García-Morales, J. A. Manzanares, C.Pereira, R. Gulaboski, F. Silva, *J. Phys. Chem. B* **2005**, *109*, 21808.
[55] A. I. Frenkel, S. Nemzer, I. Pister, L. Soussan, T. Harris, Y. Sun, M. H. Rafailovich, *J. Chem. Phys.* **2005**, *123*, 184701.
[56] L. B. Scaffardi, N. Pellegri, O. de Sanctis, J. O. Tocho, *Nanotechnology* **2005**, *16*, 158.
[57] B. M. Quinn, P. Liljeroth, V. Ruiz, T. Laaksonen, K. Kontturi, *J. Am. Chem. Soc.* **2003**, *125*, 6644.
[58] R. Balasubramanian, R. Guo, A. J. Mills, R. W. Murray, *J. Am. Chem. Soc.* **2005**, *127*, 8126.
[59] M. S. El-Deab, T. Sotomura, T. Ohsaka, *J. Electrochem. Soc.* **2005**, *152*, C1.
[60] N. M. Niemeyer, *Angew. Chem. Int. Ed.* **2001**, 4128.
[61] Z. Li, R. Jin, C. A. Mirkin, R. L. Letsinger, *Nucleic Acids Res.* **2002**, *30*, 1558.
[62] T. H. Galow, A. K. Boal, V. M. Rotello, *Adv. Mater.* **2000**, *12*, 576.
[63] F. Patolsky, K. T. Ranjit, A. Lichtenstein, I. Willner, *Chem. Commun.* **2000**, 1025.
[64] H. Mattoussi, J. M. Mauro, E. R. Goldman, G. P. Anderson, V. C. Sundar, F. V. Mikulec, M. G. Bawendi, *J. Am. Chem. Soc.* **2000**, *122*, 12142.
[65] R. L. Letsinger, R. Elghanian, G. Viswanadham, C. A. Mirkin, *Bioconjugate Chem.* **2000**, *11*, 289.
[66] B. Dubertret, M. Calame, A. J. Libchaber, *Nat. Biotechnol.* **2001**, *19*, 365.
[67] M. Pumera, M. T. Castañeda, M. I. Pividori, R. Eritja, A. Merkoçi, S. Alegret, *Langmuir* **2005**, *21*, 9625.
[68] H. Cai, C. Xu, P. He, Y. Fang, *J. Electroanal. Chem.* **2001**, *510*, 78.
[69] F. Lucarelli, G. Marrazza, A. P. F. Turner, M. Mascini, *Biosens. Bioelectron.* **2004**, *19*, 515.
[70] A. Merkoçi, M. Aldavert, S. Marín, S. Alegret, *Trends. Anal. Chem.* **2005**, *24*, 341.
[71] L. Authier, C. Grossiord, P. Brossier, B. Limoges, *Anal. Chem.* **2001**, *73*, 4450.
[72] J. Wang, D. Xu, A.-N. Kawde, R. Polsky, *Anal. Chem.* **2001**, *73*, 5576.
[73] J. Wang, R. Polsky, D. Xu, *Langmuir* **2001**, *17*, 5739.
[74] J. Wang, D. Xu, R. Polsky, *J. Am. Chem. Soc.* **2002**, *124*, 4208.
[75] A-N. Kawde, J. Wang, *Electroanalysis* **2004**, *16*, 101.
[76] M. Pumera, M. Aldavert, C. Miles, A. Merkoçi, S. Alegret, *Electrochim. Acta* **2005**, *50*, 3702.
[77] M. B. González García, A. Costa García, *Bioelectrochem. Bioenerg.* **1995**, *38*, 389.
[78] M. T. Castañeda, A. Merkoçi, M. Pumera, S. Alegret, *Biosens. Bioelectron.* **2006**, DOI: 10.1016/j.bios.2006.08.031.

[79] M. Ozsoz, A. Erdem, K. Kerman, D. Ozkan, B. Tugrul, N. Topcuoglu, H. Ekren, M. Taylan, *Anal. Chem.* **2003**, *75*, 2181.
[80] L. L. Li, H. Cai, T. M. H. Lee, J. Barford, I. M. Hsing, *Electroanalysis* **2004**, *16*, 81.
[81] H. Cai, Y. Wang, P. He, Y. Fang, *Anal. Chim. Acta* **2002**, *469*, 165.
[82] H. Cai, C. Shang, H. Ming, *Anal. Chim. Acta* **2004**, *523*, 61.
[83] T. M. H. Lee, L. L. Li, I. M. Hsing, *Langmuir* **2003**, *19*, 4338.
[84] T. M. H. Lee, H. Cai, I.-Ming Hsing, *Electroanalysis* **2004**, *16*, 1628.
[85] M. R. Dequaire, B. Limoges, P. Brossiera, *Analyst* **2006**, *131*, 923.
[86] J. Wang, J. Li, A. J. Baca, J. Hu, F. Zhou, W. Yan, D-W. Pang, *Anal. Chem.* **2003**, *75*, 3941.
[87] A. J. Baca, F. Zhou, J. Wang, J. Hu, J. Li, J. Wang, Z. S. Chikneyan, *Electroanalysis* **2004**, *16*, 73.

VI

Magnetically trigged direct electrochemical detection of DNA hybridization based Au67 Quantum Dot – DNA – paramagnetic bead conjugate. *Langmuir*. 2005, 21, 9625-9629.

Pumera M., Castañeda M. T., Pividori M. I., Eritja R., Merkoçi A., Alegret S.

Magnetically Trigged Direct Electrochemical Detection of DNA Hybridization Using Au_{67} Quantum Dot as Electrical Tracer

Martin Pumera,[†] Maria Teresa Castañeda,[†] Maria Isabel Pividori,[†] Ramon Eritja,[‡] Arben Merkoçi,*[,†] and Salvador Alegret[†]

Grup de Sensors i Biosensors, Departament de Química, Universitat Autònoma de Barcelona, 08193 Bellaterra, Catalonia, Spain, and Institut de Biologia Molecular de Barcelona, C.S.I.C., E-08034 Barcelona, Catalonia, Spain

Received July 15, 2005

A novel gold nanoparticle-based protocol for detection of DNA hybridization based on a magnetically trigged direct electrochemical detection of gold quantum dot tracers is described. It relies on binding target DNA (here called DNA1) with Au_{67} quantum dot in a ratio 1:1, followed by a genomagnetic hybridization assay between Au_{67}−DNA1 and complementary probe DNA (here called DNA2) marked paramagnetic beads. Differential pulse voltammetry is used for a direct voltammetric detection of resulting Au_{67} quantum dot−DNA1/DNA2−paramagnetic bead conjugate on magnetic graphite−epoxy composite electrode. The characterization, optimization, and advantages of the direct electrochemical detection assay for target DNA are demonstrated. The two main highlights of presented assay are (1) the direct voltammetric detection of metal quantum dots obviates their chemical dissolution and (2) the Au_{67} quantum dot−DNA1/DNA2−paramagnetic bead conjugate does not create the interconnected three-dimensional network of Au−DNA duplex−paramagnetic beads as previously developed nanoparticle DNA assays, pushing down the achievable detection limits.

1. Introduction

There is a high demand for the detection of specific DNA sequences in various fields, including molecular diagnostic of human genetic diseases or bacterial/viral infections. The high sensitivity of electrochemical transducers, coupled with the low cost and low power requirements led to the explosive research activity in the area of electrochemical DNA biosensors.[1−3] The DNA recognition event can be detected using different strategies, including intrinsic electroactivity of the nucleic acid,[4−6] DNA duplex intercalators,[7,8] electroactive markers,[9−11] enzyme labels,[12−17] and metal nanoparticles/quantum dots.[18−21] The nanoparticles offer attractive properties to act as DNA tags.[22] Sensitivity, long lifetime along with multiplexing capability have led to an explosive growth of gold nanoparticle/quantum dot based DNA electrochemical assays in recent years.[17−24] The vast majority of these nanoparticle-based assays have been based on chemical dissolution of the gold nanoparticle tag (in a hydrobromic acid/bromine mixture) followed by accumulation and stripping analysis of the resulting Au^{3+} solution. The HBr/Br_2 solution is highly toxic and therefore methods based on direct electrochemical detection of gold nanoparticle tags, which would replace the chemical oxidation agent, are urgently needed. A pioneering work on direct solid-state detection of silver precipitate on gold nanoparticle−DNA conjugates was reported by Wang et al.[25] However, this method was based on direct detection of precipitated silver, not the gold nanoparticle tag itself. Direct detection of colloidal gold nanoparticles but not in connection with the detection of DNA hybridization was reported earlier by our group and Costa Gracía's group.[26,27]

* To whom correspondence should be addressed. E-mail: arben.merkoci@uab.es. Tel: +34-93-581-1976. Fax: +34-93-581-2379.

[†] Universitat Autònoma de Barcelona.

[‡] C.S.I.C.

(1) Palecek, E.; Fojta, M. *Anal. Chem.* **2001**, *73*, 75A.
(2) Wang, J. *Anal. Chim. Acta* **2003**, *500*, 247.
(3) Pividori, M. I.; Merkoçi, A.; Alegret, S. *Biosens. Bioelectron.* **2000**, *15*, 291.
(4) Jelen, F.; Yosypchuk, B.; Kourilova, A.; Novotny, L.; Palecek, E. *Anal. Chem.* **2002**, *74*, 4788.
(5) Wang, J.; Kawde, A.-N.; Erdem, A.; Salazar, M. A. *Analyst* **2001**, *126*, 2020.
(6) Wang, J.; Kawde, A.-N. *Electrochem. Commun.* **2002**, *4*, 349.
(7) Kara, P.; Kerman, K.; Ozkan, D.; Meric, B.; Erdem, A.; Ozkan, Z.; Ozsoz, M. *Electrochem. Commun.* **2002**, *4*, 705.
(8) Erdem, A.; Kerman, K.; Meric, B.; Ozsoz, M. *Electroanalysis* **2001**, *13*, 219.
(9) Wang, J.; Polsky, R.; Merkoçi, A.; Turner, K. L. *Langmuir* **2003** *19*, 989.
(10) Ihara, T.; Nakayama, M.; Murata, M.; Nakano, K.; Maeda, M. *Chem. Commun.* **1997**, 1609.
(11) Kertez, V.; Whittemore, N. A. Inamati, G.; Manoharan, M.; Cook, P.; Baker, D.; Chambers, J. Q. *Electroanalysis* **2000**, *12*, 889.
(12) Caruana, D. J.; Heller, A. *J. Am. Chem. Soc.* **1999**, *121*, 769.
(13) Wang, J.; Xu, D.; Erdem, A.; Polsky, R.; Salazar, M. A. *Talanta* **2002**, *56*, 931.
(14) Lumley, T.; Campbell, C.; Heller, A. *J. Am. Chem. Soc.* **1996**, *118*, 5504.
(15) Alfonta, L.; Singh, A. K.; Willner, I. *Anal. Chem.* **2001**, *73*, 91.
(16) Pividori, M. I.; Merkoçi, A.; Barbe, J.; Alegret, S. *Electroanalysis* **2003**, *15*, 1815.
(17) Pividori, M. I.; Merkoçi, A.; Alegret, S. *Biosens. Bioelectron.* **2003**, *19*, 473.
(18) Wang, J.; Liu, G.; Merkoçi, A. *J. Am. Chem. Soc.* **2003**, *125*, 3214.
(19) Authier, L.; Grossiord, C.; Brossier, P.; Limoges, B. *Anal. Chem.* **2001**, *73*, 4450.
(20) Wang, J.; Xu, D.; Kawde, A.-N.; Polsky, R. *Anal. Chem.* **2001**, *73*, 5576.
(21) Wang, J.; Liu, G. D.; Polsky, R.; Merkoçi, A. *Electrochem. Commun.* **2002**, *4*, 722.
(22) Merkoçi, A.; Aldavert, M.; Marin, S.; Alegret, S. *Trends Anal. Chem.* **2005**, *24*, 341.
(23) Hernandez-Santos, D.; Gonzales-García, M. B.; Costa Garcia, A. C. *Electroanalysis* **2002**, *14*, 1225.
(24) Katz, E.; Willner, I.; Wang, J. *Electroanalysis* **2004**, *16*, 19.
(25) Wang, J.; Xu, D.; Polsky, R. *J. Am. Chem. Soc.* **2002**, *124*, 4208.
(26) Pumera, M.; Aldavert, M.; Mills, C.; Merkoçi, A.; Alegret, S. *Electrochim. Acta* **2005**, *50*, 3702.
(27) Gonazales-Gracía, M. B.; Costa García, A. *Bioelectrochem. Bioenerg.* **1995**, *38*, 389.

10.1021/la051917k CCC: $30.25
Published on Web 09/02/2005

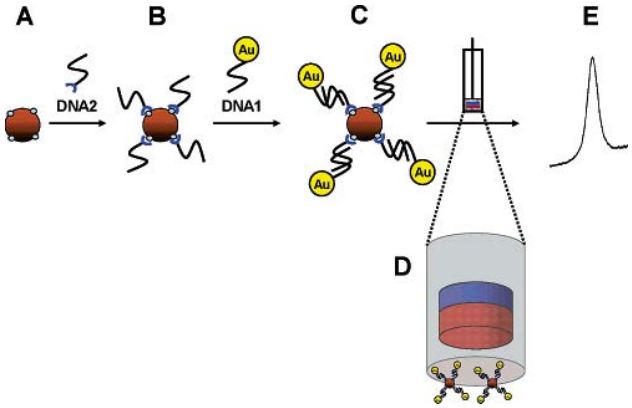

Figure 1. Schematic representation of the analytical protocol (not in scale): (A) introduction of streptavidin coated paramagnetic beads; (B) immobilization of the biotinylated probe (DNA2) onto the paramagnetic beads; (C) addition of the 1:1 Au_{67}−DNA1 target; (D) accumulation of Au_{67}−DNA1/DNA2−paramagnetic bead conjugate on the surface of magnetic electrode; (E) magnetically trigged direct DPV electrochemical detection of gold quantum dot tag in Au_{67}−DNA1/DNA2−paramagnetic bead conjugate.

We report here a novel nanoparticle-based detection of DNA hybridization based on magnetically induced direct electrochemical detection of the 1.4 nm Au_{67} quantum dot tag linked to the target DNA. The Au_{67} nanoparticle tag is directly detected after the DNA hybridization event, without need of acidic (i.e., HBr/Br_2) dissolution.

Figure 1A−E represents the main steps involved in the assay. The binding of the probe DNA2 to the paramagnetic beads (A) is achieved via the streptavidin−biotin interaction. The resulting DNA2 modified paramagnetic beads (B) are hybridized then with the target DNA1, marked with Au_{67} nanoparticle in the ratio 1:1. The resulting Au_{67}-DNA1/DNA2 paramagnetic bead conjugate (C) is collected magnetically on the surface of a transducer with built-in magnet (Figure 1D; see more details in the Supporting Information), which is triggering the direct electrochemical detection (E).[5,6] The formed Au_{67}−DNA1/DNA2−paramagnetic bead conjugates with a single DNA duplex link between the nanoparticle and the paramagnetic bead ensure their individual handling and consequently the sensitivity of the assay is not hindered by sharing one gold tag by several DNA strands as it was in previous assays.[20,25] Figure 2 is a schematic that shows such phenomena compared to the case where more than one DNA strand is connected to the gold nanoparticle giving a particle-linked DNA network structure due to the interconnection between magnetic beads.[9]

The favorable properties of magnetically trigged direct detection scheme of DNA hybridization using Au_{67} as a marker will be reported in following sections.

2. Experimental Section

2.1. Apparatus. All voltammetric experiments were performed using an electrochemical analyzer Autolab 20 (Eco-Chemie, The Neetherlands) connected to a personal computer. Electrochemical experiments were carried out in a 5 mL voltammetric cell at room temperature (25 °C), using three electrode configuration. A platinum electrode served as an auxiliary electrode and an Ag/AgCl as reference electrode. Graphite composite electrodes were prepared as described in section 2.2.

The binding of strepavidin coated paramagnetic beads with biotinilated probe and hybridization event were performed in TS-100 ThermoShaker (Spain). Magnetic separation was carried out with the MCB 1200 biomagnetic processing platform (Sigris, CA).

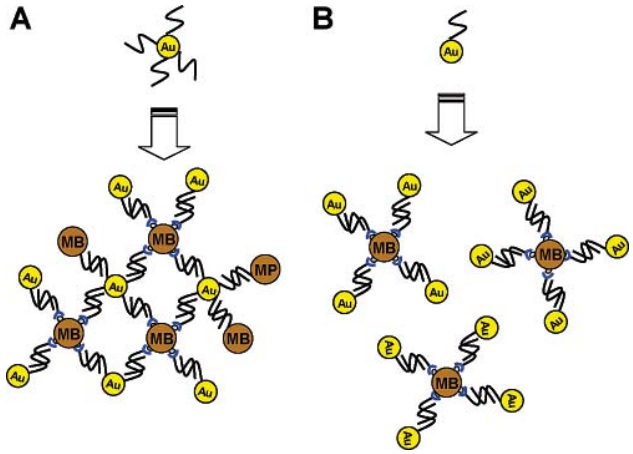

Figure 2. Schematic that shows the formation of particle-linked DNA network structure due to the interconnection between paramagnetic beads (MB) in the case where Au quantum dots modified with more than one DNA strands are used (A). Such network is not created by using the 1:1 Au−DNA connection (B), employed in this work.

2.2. Electrode Preparation. Graphite-epoxy composite electrode without incorporated magnet were prepared as described previously.[28,29] Briefly, epoxy resin (Epotek H77A, Epoxy Technology, USA) and hardener (Epotek H77B) were mixed manually in the ratio 20:3 (w/w) using a spatula. When the resin and hardener were well-mixed, the graphite powder (particle size 50 μm, BDH, U.K.) was added in the ratio 1:4 (w/w) and mixed for 30 min. The resulting paste was placed into a cylindrical PVC sleeve (6 mm i.d.). Electrical contact was completed using a copper disk connected to a copper wire. The conducting composite was cured at 40 °C for one week. Magnetic graphite-epoxy composite electrodes were prepared in similar way by incorporating the neodymium magnet (diameter 3 mm, heigth 1.5 mm, Halde Gac Sdad, Bacelona, Spain, catalog number N35D315) into the body of graphite epoxy composite, 2 mm under the surface of the electrode (see Figure S1, Supporting Information). Prior to use, the surface of the electrode was polished with abrasive paper and then with alumina paper (polishing strips 301044−001, Orion, Spain).

2.3. Reagents. All stock solutions were prepared using deionized and autoclaved water. Tris(hydroxymethyl)methylamine (TRIS), sodium chloride and ethylenediamine tertraacetic acid disodium salt (EDTA) were purchased from Sigma-Aldrich, hydrochloric acid (37%) was purchased from PanReac (Barcelona, Spain). Streptavidin coated paramagnetic beads Dynabeads M-280 (diameter 2.8 μm) were purchased from Dynal Biotech, Oslo, Norway. Biotinylated probe oligonucleotide was received from AlfaDNA, Canada. Thiolated oligomers were synthesized in our laboratory according described procedure[30] and had the following sequences:

target (DNA1): 5′TCT CAA CTC GTA-phosphate-$O(CH_2)_3$−CONH−$CH(CH_2SH)$−CONH−$(CH_2)_6$−OH

immobilized probe (DNA2): 5′TAC GAG TTG AGA-biotin

noncomplementary: thiohexyl-5′CGA GTC ATT GAG TCA TCG AG

The 1.4 nm maleimido-Au_{67} quantum dots were obtained from Nanoprobes Inc., NY and were characterized by ^{252}Cf plasma desorption mass spectrometry.[31] Maleimido-Au_{67} nanoparticles statistically carry one reactive maleimido molecule incorporated

(28) Cespedes, F.; Martinez-Fabregas, E.; Bartroli, J.; Alegret, S. *Anal. Chim. Acta* **1993**, *273*, 409.
(29) Santandreu, M.; Cespedes, F.; Alegret, S.; Martinez-Fabregas, E. *Anal. Chem.* **1997**, *69*, 2080.
(30) Torre, B. G.; Morales, J. C.; Avino, A.; Iacopino, D.; Ongaro, A.; Fitzmaurice, M. D.; Doyle, H.; Redmond, G.; Eritja, R. *Helv. Chim. Acta* **2002**, *85*, 2594.
(31) NcNeal, C. J.; Hughes, J. M.; Pignolet, L. H.; Nelson, L. T. J.; Garder, T. G.; Fackler, J. P.; Winpenny, R. E. P.; Irgens, L. H.; Vigh, G.; MacFarlane, R. D. *Inorg. Chem.* **1993**, *32*, 5582.

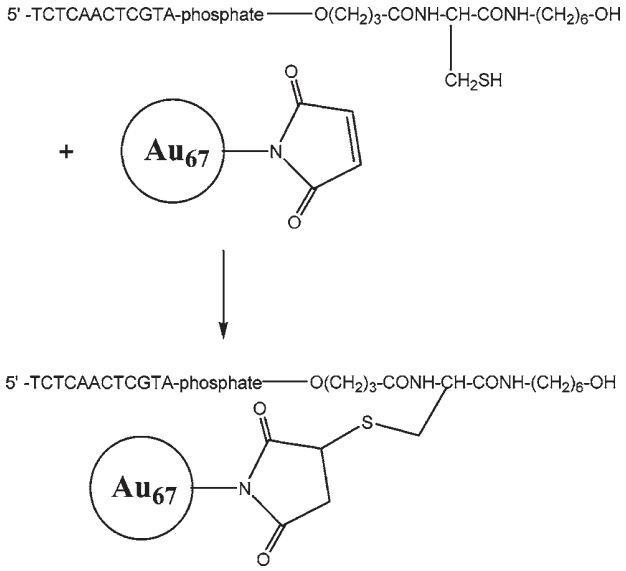

Figure 3. Schematic of the reaction of maleimido−Au_{67} with thiol-oligonucleotide.

into phosphine shelf. The 2 times concentrated binding and washing buffer (2×B&W) contained 10 mM Tris HCl (pH 7.5), 1 mM EDTA and 2.0 M NaCl. The binding and washing buffer (B&W) was prepared from 2×B&W by diluting with the deionized autoclaved water.

2.4. Procedures. *Preparation of the Au Quantum Dot Modified DNA (1:1 Au_{67}-DNA1).* The binding of maleimido-Au_{67} quantum dot to the thiol DNA1 in the ratio *1:1* was preformed as described previously (for reaction scheme, see Figure 3).[30] Briefly, aliquots of lyophilized maleiimido-Au_{67} nanoparticles (6 nmols) were mixed with thiol-oligonucloetides (6 nmols) dissolved in 10% 2-propanol. The resulting mixtures were kept overnight at room temperature and the resulting solutions stored in refrigerator until further use. Purity control of discrete Au_{67} nanocrystal−DNA1 conjugates was performed by gel electrophoresis in 2% agarose gel at 80 V, with electrophoresis time 20 min, using 0.5× TRIS-borate-EDTA (TBE) buffer as a running buffer (see Figure S2, Supporting Information).[32,33]

Immobilization of the DNA Probe (DNA2) onto Paramagnetic Beads. The binding of the biotinylated probe with streptavidin coated paramagnetic beads was carried out using a slightly modified procedure recommended by Dynal Biotech.[34] Briefly, 100 μg of streptavidin coated paramagnetic beads was transferred into 1.5 mL ependorf tube. The beads were washed with 100 μL B&W buffer three times. The paramagnetic beads were then resuspended in 50 μL of B&W buffer, and 5 μg of probe DNA2 were added. The volume was adjusted to 100 μL, and the concentration of NaCl was adjusted to 1.0 M by 2×B&W buffer and autoclaved water. The resulting solution was incubated for 15 min at temperature 25 °C with gentle mixing in a TS-100 Thermo Shaker. The paramagnetic beads with immobilized probe were then separated from the incubation solution and washed 3 times with 100 μL of B&W buffer.

The preparation process was completed by resuspending the DNA2 modified beads in 50 μL of B&W buffer and it was ready for the following hybridization.

Hybridization Procedure and Electrochemical Detection. The desired amount of Au_{67} marked DNA1 was added in the solution (50 μL) of DNA2 modified beads in B&W buffer prepared previously, and the volume was adjusted to 100 μL keeping the NaCl concentration at 1.0 M by adding 2×B&W buffer and autoclaved water. The hybridization reaction was carried out during 15 min at 42 °C in TS-100 Thermo Shaker (if not stated otherwise). The final Au_{67}-DNA1/DNA2−paramagnetic bead conjugates were washed 3 times with 100 μL of B&W buffer and resuspended in 50 μL of B&W buffer. The surface of magnetic graphite−epoxy composite electrode was then brought into contact for 60 s with the solution containing Au_{67}−DNA1/DNA2−paramagnetic beads conjugates which accumulated on it due to the inherent magnetic field of the electrode. The electrochemical oxidation of Au_{67} quantum dots to $AuCl_4^-$ was performed at +1.25 V (vs Ag/AgCl) for 120 s (if not stated otherwise) in the nonstirred solution. Immediately after the electrochemical oxidation step, differential pulse voltammetry (DPV) was performed. During this step the potential was scanned from +1.25 V to 0 V (step potential 10 mV, modulation amplitude 50 mV, scan rate 33.5 mV s^{-1}, nonstirred solution), resulting in an analytical signal due to the reduction of $AuCl_4^-$ at potential +0.4 V.[26] The DPV peak height at a potential of +0.4 V was used as the analytical signal in all of the measurements. The background subtraction protocol involving saving the response for the blank solution and subtracting it from the analytical signal was used.

3. Results and Discussion

The attractive performance of the new magnetically trigged electrochemical detection of DNA hybridization using Au_{67} quantum dots as DNA tags is illustrated in Figure 4. A well-defined signal is observed for 500 nM target DNA solution (Figure 4A). Three base mismatch DNA (500 nM) had a significantly lower signal (Figure 4B). A negligible gold signal is observed for 1000 nM noncomplementary DNA (Figure 4C). Effective magnetic triggering of the transducing event is demonstrated in Figures 4A and 4D, showing the hybridization response on the magnetic and nonmagnetic electrode, respectively. The magnetic electrode displays a well-defined signal, reflecting the effective magnetic attraction of the Au_{67}−DNA1/DNA2−paramagnetic bead conjugates to its surface (Figure 4A). In contrast, no electrochemical response is observed for the same conjugate at the conventional electrode without a built-in magnet as expected from the absence of magnetic or adsorptive accumulation of paramagnetic beads (Figure 4D).

Various parameters involved in the new genomagnetic protocol were examined and optimized. Figure 5A shows the influence of the amount of the paramagnetic beads upon the voltammetric response. The response increases linearly up to 50 μg beads, reaching a maximum at 100 μg, and slightly decreases thereafter. This behavior corresponds to the fact that with an increasing amount of paramagnetic beads the surface of the magnetic electrode becomes saturated with the beads, and therefore, the further increase of the bead amount does not lead to an increase of the signal. Subsequent work employed 100 μg paramagnetic beads. Another parameter that affects the detection of DNA is hybridization time (Figure 5B). The DPV response increases with hybridization time between 2 and 15 min and then levels off.

The influence of the hybridization temperature was studied in the interval of 25−42 °C. The resulting electrochemical signals show low temperature dependence (see Figure S3, Supporting Information), the response increased 12 % in the studied interval. For optimal discrimination of noncomplementary DNA, it is important to maintain the temperature of hybridization approximately 10 °C under the melting point of the DNA hybrid, which is for used the Au_{67} quantum dot−DNA1/DNA2 conjugate 51.2 °C.[30] The hybridization time 15 min at a temperature of 42 °C was chosen as optimal for the proposed DNA hybridization detection.

Relevant parameters influencing the electroanalytical DPV response of the gold quantum dot tag in the Au_{67}−DNA1/DNA2−paramagnetic bead conjugate were investigated (Figure 6). Optimization of the electrooxidation

(32) Loweth, C. J.; Caldwell, W. B.; Peng, X.; Alivisatos, A. P.; Schultz, P. G. *Angew. Chem., Int. Ed. Engl.* **1999**, *38*, 1808.
(33) Zanchet, D.; Micheel, C. M.; Parak, W. J.; Gerion, D.; Alivisatos, A. P. *Nano Lett.* **2001**, *1*, 32.
(34) Dynal Biotech, Technote 010 for product 112.05.

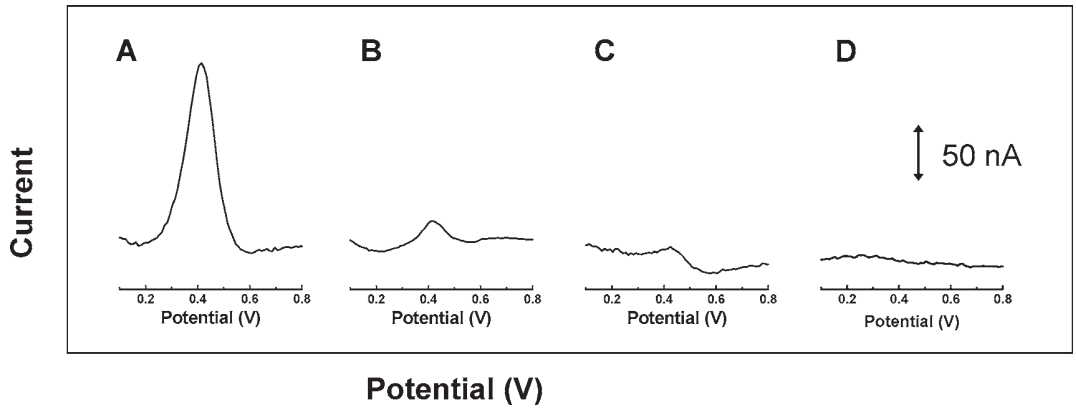

Figure 4. DPV hybridization response of 500 nM target (A), 500 nM three-base mismatch (B), 1000 nM noncomplementary DNA (C) on magnetic graphite-epoxy composite electrode. DPV hybridization response of the 500 nM target on the nonmagnetic graphite-epoxy composite electrode (D). Conditions: hybridization time, 15 min; hybridization temperature, 42 °C; amount of paramagnetic beads, 100 μg; electrooxidation potential, +1.25 V; electrooxidation time, 120 s, DPV scan from +1.25 V to 0 V, step potential 10 mV, modulation amplitude 50 mV, scan rate 33.5 mV s^{-1}, nonstirred solution.

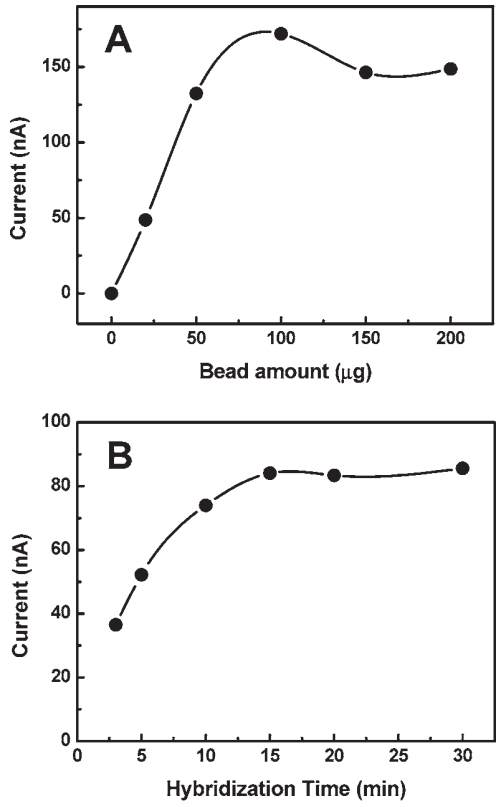

Figure 5. Effect of the amount of paramagnetic beads (A) and hybridization time (B) upon the hybridization response of the target DNA. Conditions A: concentration of target, 500 nM; hybridization time, 15 min. Conditions B: concentration of target, 250 nM; amount of paramagnetic beads, 100 μg. Other conditions as in Figure 4A.

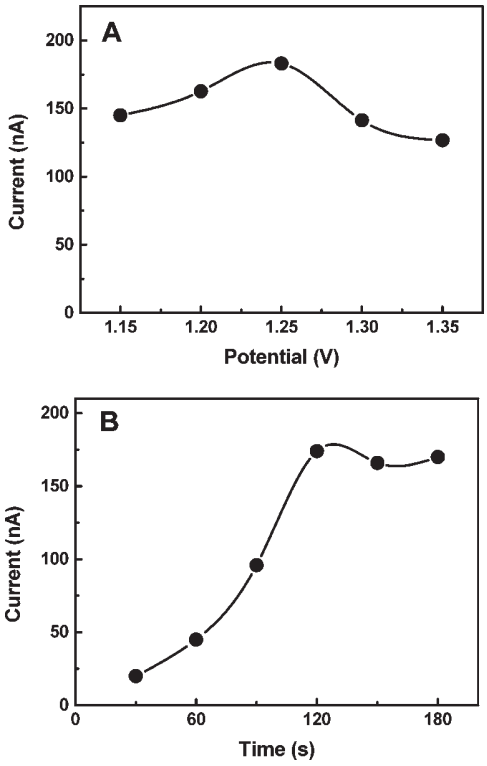

Figure 6. Effect of electrooxidation potential (A) and electrochemical oxidation time (B) on the magnetic graphite epoxy composite electrode DPV response to 500 nM target. Other conditions, as in Figure 4A.

potential of the Au_{67} quantum dots was performed in an interval of +1.15 to +1.35 V. The DPV response increases from +1.15 V when reaching a maximum at +1.25 V, and it decreases thereafter (Figure 6A). Hence, a potential of +1.25 V was selected as optimal for electrooxidation of Au_{67} quantum dots. Figure 6B shows the influence of the electrochemical oxidation time of the Au_{67} upon the DPV signal. The signal displays an increase in the interval from 30 to 120 s and levels off thereafter. This leads to the conclusion that the electrooxidation interval of 120 s is sufficient for reaching the steady-state response.

This new Au_{67} quantum dot-based DNA hybridization detection protocol shows defined concentration dependence (Figure 7). The calibration plot was linear over the range from 10 to 40 nM of target DNA with a sensitivity of 0.97 nA nM^{-1} and an intercept of −0.83 nA (correlation coefficient of 0.991). The limit of detection (based on upper limit approach[35]) was 12 nM of target DNA. Such a detection limit is comparable to LOD of HBr/Br_2 dissolution based 5 nm-Au nanoparticle−DNA−paramagnetic bead assay (15 nM),[20] but it is achieved with much smaller, 1.4 nm, Au nanoparticles (containing 45 times less gold atoms than the 5 nm Au nanoparticle). This reflects a

(35) Mocak, J.; Bond, A. M.; Mitchell, S.; Scollary, G. *Pure Appl. Chem.* **1997**, *69*, 297.

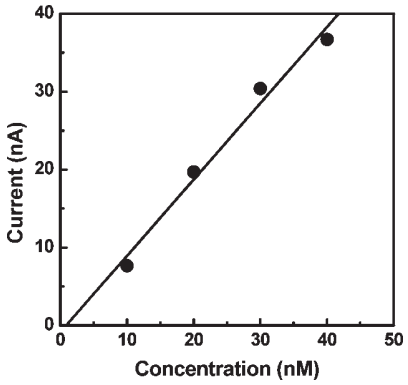

Figure 7. Calibration plot for target DNA. Hybridization time, 20 min; amount of paramagnetic beads, 50 μg. Other conditions, as in Figure 4A.

high sensitivity of presented direct electrochemical detection of the Au_{67} quantum dot−DNA1/DNA2−paramagnetic bead protocol. Further improvement of the detection limit by using larger gold nanoparticles can be readily envisaged. For example, assuming an increase of nanoparticle diameter from 1.4 to 10 nm (7 times increase), a 340-fold enhancement of sensitivity can be expected (assuming that the sensitivity is proportional to the cube of the particle diameter and that the steric effect of the bigger gold nanoparticle is negligible).[19]

Very good precision is an attractive feature of the presented magnetically trigged Au_{67} quantum dot marked DNA hybridization detection. It reflects a well-defined and highly reproducible magnetic collection of Au_{67}−DNA1/DNA2−paramagnetic bead conjugates on the surface of the electrode with a built-in magnet and also a well defined structure of these conjugates, without any irreproducible three-dimensional Au−paramagnetic bead DNA linked network, typical for previously developed configurations.[20,25] A series of six repetitive hybridization measurements of 40 nM of the Au_{67} marked target DNA resulted in a relative standard deviation of 4%, which compares favorably to an RSD values of 7% (ref 25) and 11% (ref 20) of nanoparticle chemical dissolution DNA assays.

Conclusion

We have demonstrated the proof of the concept of magnetically trigged direct electrochemical detection for monitoring DNA hybridization. The new method couples the high sensitivity and reproducibility with effective genomagnetic discrimination against noncomplementary DNA. The elimination of the need of acid dissolution greatly simplifies particle-based electrical bioassays and obviates the need for a toxic HBr/Br_2 solution. The use of a 1:1 Au_{67} quantum dot−DNA conjugate avoids the creation of an interconnected network of Au−DNA−paramagnetic beads compared to previously developed DNA assays (which relied on multiple duplex links between magnetic beads and nanoparticles) pushing down the achievable detection limits and facilitating potential manipulation of individual Au_{67} quantum dot−DNA1/DNA2−paramagnetic beads conjugates in microfluidic channel arrays, offering the possibility of parallel multiple DNA detection.[36] Moreover, the magnetically trigged Au_{67} quantum dot direct detection methodology described above can be applied to different bioassays (i.e., immunoassay). Besides their biosensing utility, the DNA-mediated assembly structures should have a profound impact in the fields of nanotechnology and nanoelectronics. Current effort in our laboratory aims at the broadening of the application range of above-described quantum dot direct detection protocol and at the development of microfluidic devices integrating all of the steps of genomagnetic protocol on the lab-on-a-chip platform.

Acknowledgment. This work was financially supported by MEC (Spain) (Projects BIO2004-02776 and MAT2004-05164) and by the Spanish "Ramón Areces" foundation (Project 'Bionanosensores'). A.M. thanks the "Ramón y Cajal" program of the Ministry of Science and Technology (Spain). M.P. is grateful for the support from the Marie Curie Intra-European Fellowship from European Community under 6th FP (Project MEIF-CT-2004-005738). The authors are grateful to R. D. Powel (Nanoprobes Inc.) for gold nanoparticle characterization information.

Supporting Information Available: Details of magnetic graphite−epoxy composite electrode, the scan of gel electrophoresis purity control of the Au_{67} quantum dot−DNA1 conjugate, and a graph showing the influence of temperature upon the hybridization response. This material is available free of charge via the Internet at http://pubs.acs.org.

LA051917K

(36) Fan, Z. H.; Mangru, S.; Granzow, R.; Heaney, P.; Ho, W.; Dong, Q.; Kumar, R. *Anal. Chem.* **1999**, *71*, 4851.

Supporting Information

Magnetically trigged direct electrochemical detection of DNA hybridization using Au_{67} quantum dot as electrical tracer

Martin Pumera, Maria Teresa Castañeda, Maria Isabel Pividori, Ramon Eritja, Arben Merkoçi[*]*, Salvador Alegret*

Table of Contents

Figure S1

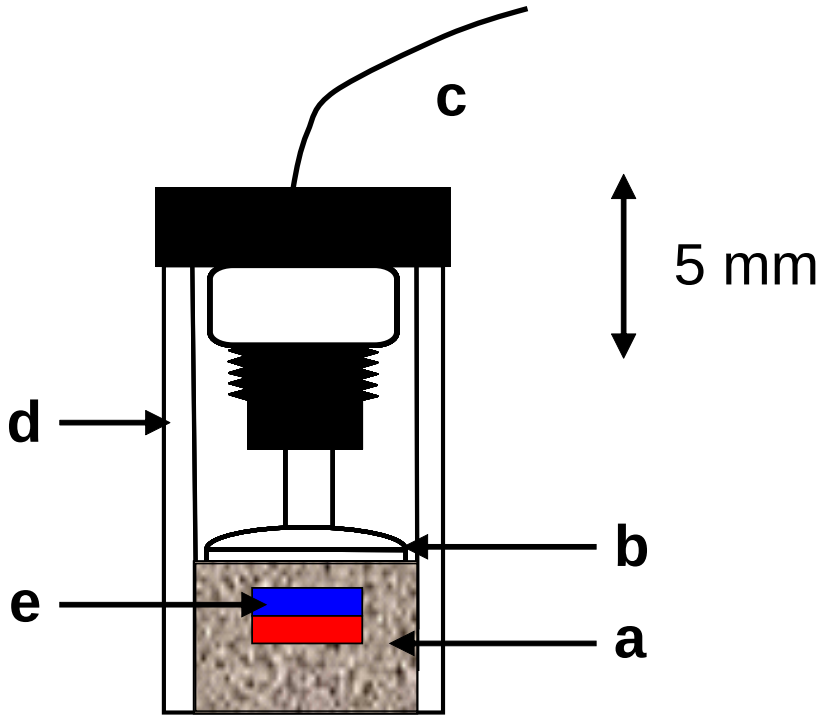

Details of magnetic graphite-epoxy composite electrode with incorporated magnet. (a) conducting graphite-epoxy composite; (b) copper disc facilitating electrical contact between the composite material and copper wire (c) leading to the electrochemical workstation; (d) plastic sleeve; (e) permanent neodymium magnet.

Figure S2

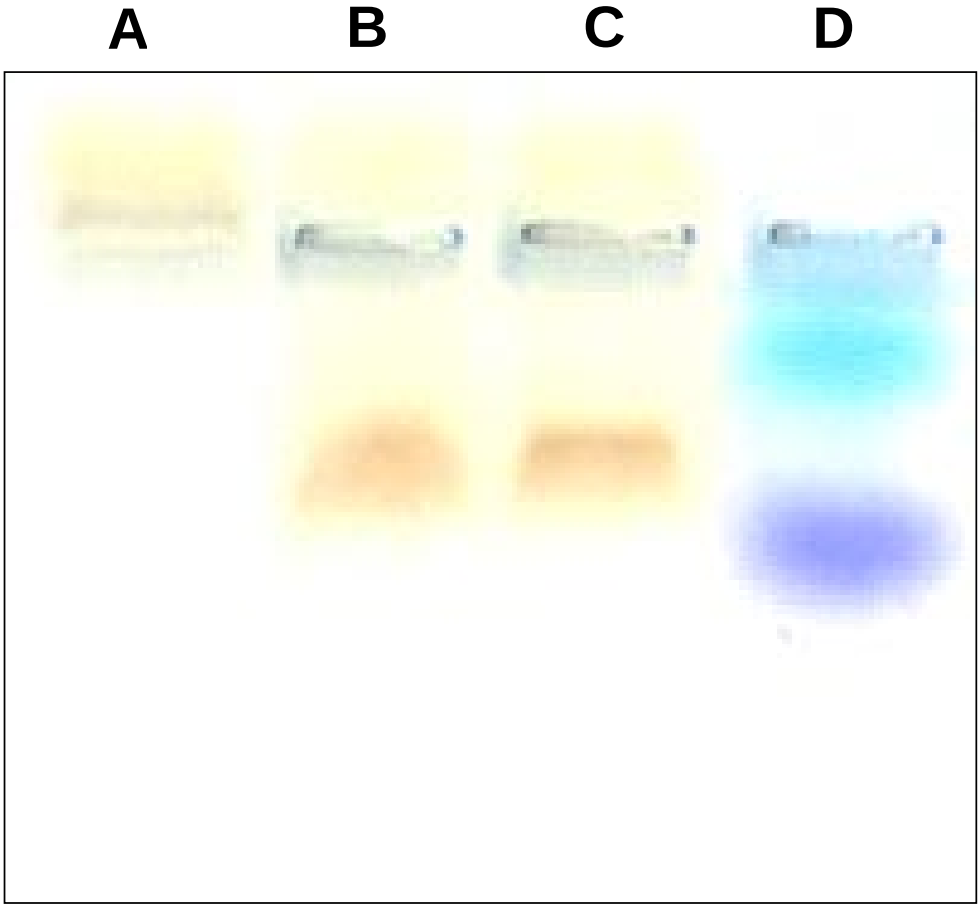

Purity control of discrete Au_{67} nanocrystal-DNA conjugates. (A) maleimido Au_{67} nanocrystals; (B) target DNA marked with Au_{67} nanoparticle; (C) non-complementary DNA marked with Au_{67} nanoparticle; (D) bromophenol blue and xylenecyanol dyes. Conditions: gel electrophoresis in 2% agarose gel at 80 V, with electrophoresis time 20 min, using 0.5× TRIS-borate-EDTA (TBE) buffer as a running buffer.

Figure S3

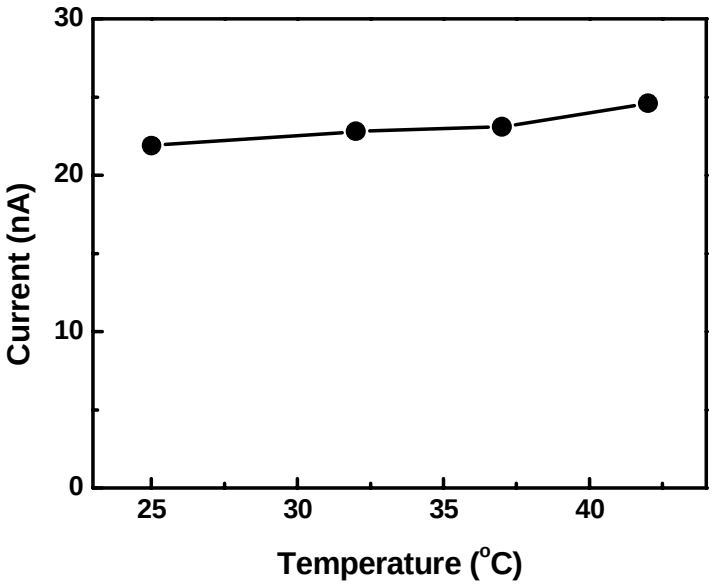

Effect of the hybridization temperature upon the hybridization response (DPV current) of the target DNA modified with Au quantum dots. Target DNA concentration, 25 nM; hybridization time, 20 minutes; amount of paramagnetic beads, 50 μg; electrooxidation potential, +1.25 V; electrooxidation time 120 s, DPV scan from +1.25 V to 0 V, step potential 10 mV, modulation amplitude 50 mV, scan rate 33.5 $mV.s^{-1}$, non-stirred solution.

VII

Electrochemical genosensors for biomedical applications based on gold nanoparticles. *Biosens, Bioelectron*. 2007, 22, 1961-1967.

Castañeda M. T., Merkoçi A., Pumera M., Alegret S.

Available online at www.sciencedirect.com
ScienceDirect
Biosensors and Bioelectronics 22 (2007) 1961–1967
BIOSENSORS & BIOELECTRONICS
www.elsevier.com/locate/bios

Electrochemical genosensors for biomedical applications based on gold nanoparticles

M.T. Castañeda [1], A. Merkoçi *, M. Pumera, S. Alegret

Grup de Sensors i Biosensors, Departament de Química, Universitat Autònoma de Barcelona, E-08193 Bellaterra, Barcelona, Spain

Received 24 April 2006; received in revised form 13 August 2006; accepted 18 August 2006
Available online 27 September 2006

Abstract

Two gold nanoparticles-based genomagnetic sensors designs for detection of DNA hybridization are described. Both assays are based on a magnetically induced direct electrochemical detection of gold tags on magnetic graphite-epoxy composite electrodes. The first design is a two strands assay format that consists of the hybridization between a capture DNA strand which is linked with paramagnetic beads and another DNA strand related to BRCA1 breast cancer gene used as a target which is coupled with streptavidin-gold nanoparticles. The second genomagnetic sensor design is a sandwich assay format with more application possibilities. A cystic fibrosis related DNA strand is used as a target and sandwiched between two complementary DNA probes: the first one linked with paramagnetic beads and a second one modified with gold nanoparticles via biotin–streptavidin complexation reactions. The electrochemical detection of gold nanoparticles by differential pulse voltammetry was performed in both cases. The developed genomagnetic sensors provide a reliable discrimination against noncomplementary DNA as well against one and three-base mismatches. Optimization parameters affecting the hybridization and analytical performance of the developed genosensors are shown for genomagnetic assays of DNA sequences related with the breast cancer and cystic fibrosis genes.

Keywords: Gold nanoparticles; Genomagnetic sensor; DNA hybridization; Breast cancer; Cystic fibrosis

1. Introduction

Recent advances in the electrochemical detection of nucleic acids have allowed the development of new types of genosensors. Sequence specific DNA detection has been a topic of significant interest for its application in diagnosis of pathogenic and genetic diseases (Palecek and Jelen, 2002; Wang et al., 2003a) between other fields.

Extensive research has been fueled by the need for practical, robust, and highly sensitive and selective detection devices that can address the deficiencies of conventional technologies. Nucleic acid-based electrochemical detection involves the generation of an electrical signal mediated by nucleic acid hybridization and serves as the basis for the DNA detection technology for which the detection of DNA hybridization by means of biosensors (genosensors) is a topic of major scientific and technological interest (Pividori et al., 2000; Palecek and Fojta, 2001; Wang, 2003).

Various are the field to which the genosensors are being applied. Hernández-Santos et al. (2004), reported the potential applicability of screen-printed genosensors in the diagnosis of a human infectious pulmonary disease.

Millan and Mikkelsen (1993) were the first in exploring the use of electrochemical reactions for signaling DNA hybridization. A number of formats for electrochemical detection are described in the literature, including hybridization with probes conjugated to a redox-active label (Kerman et al., 2004). The DNA recognition event can be detected using enzyme labels (Wang et al., 2002; Pividori et al., 2003a, 2003b) between others. On the other hand recently the field of molecular diagnostics has acquired a great interest in the use of nanoparticles (NPs) as DNA and protein markers. Significant advantages over conventional diagnostic systems with regard to assay sensitivity, selectivity, and practicality have been offered by some NPs-based assays (Alivisatos, 2003, 2004). NPs have been successfully used as labels in nucleic acid (Huber et al., 2004; Niemeyer, 2001;

* Corresponding author. Tel.: +34 935811976; fax: +34 935812379.
E-mail address: arben.merkoci@uab.es (A. Merkoçi).
[1] On leave from Departamento de Ciencias Básicas, Universidad Autónoma Metropolitana-Azcapotzalco, 022000 México, D.F., Mexico.

0956-5663/$ – see front matter © 2006 Elsevier B.V. All rights reserved.
doi:10.1016/j.bios.2006.08.031

Wang et al., 2001). Quantum dots are also widely used due to their attractive properties to act as DNA tag (Merkoçi et al., 2005). Wang et al. (2003b) have developed a technique in which employing NPs labels with different redox potentials. Nevertheless gold nanoparticles (Au-NPs) the most reported NPs have been an attractive material in research for a long time (Mirkin et al., 1996). Colloidal Au-NPs are promising nanomaterials that play an important role in the design of genosensors (Shipway et al., 2000). The redox properties of Au-NPs have led to their widespread use as electrochemical labels in nucleic acid detection. Ozsoz et al. (2003), immobilized target DNA on an electrode, followed by hybridization with complementary probes labeled with Au-NPs.

A novel NPs-based detection of DNA hybridization based on magnetically induced direct electrochemical detection of the 1.4 nm Au_{67} quantum dot tag linked to the target DNA was reported earlier by our group (Pumera et al., 2005a).

Herein we report two Au-NPs-based genosensors designs, including for the first time a sandwich assay, for detection of DNA hybridization. Both assay formats were based on a magnetically induced direct electrochemical detection of the Au-NPs tag on magnetic graphite-epoxy composite electrode (M-GECE). The Au-NPs tags also are directly detected after the DNA hybridization event without the need of acidic dissolution as was reported previously (Pumera et al., 2005a).

The illustrative representations of the main steps of hybridization assays for the two strands assay as well as for the sandwich format are shown in Figs. 1 and 2, respectively.

The first assay called here the two strands assay (Fig. 1A–E) is based on the hybridization between two single-strands biotin modified DNA probes: a capture DNA probe (BC-A) and a target DNA (BC-T), related to the *BRCA1* breast cancer gene, which in a clinical situation would be derived from patient samples. The second assay (Fig. 2A–F) is based on hybridization between three single strand DNA probes: a biotin modified capture DNA probe (CF-A), a DNA target (CF-T), related to cystic fibrosis gene, which also in a clinical situation would be derived from patient samples, and a biotin modified DNA signaling probe (CF-B). In this assay the CF-T is 'sandwiched' between the CF-A and CF-B probes.

Parameters involved in both genomagnetic protocols that influence the results of hybridization reactions were analyzed and optimized.

The protocols proposed in this work that could represent a practical potential of emerging electrochemical DNA detection technologies for use as novel alternatives in current molecular diagnostic applications will be shown in the following sections.

2. Materials and methods

2.1. Apparatus

Differential pulse voltammetry (DPV) was performed with an electrochemical analyzer Autolab PGSTAT 20 (Eco Chemie, The Netherlands) connected to a personal computer. Electrochemical measurements were carried out in a 10 mL voltammetric cell at room temperature (25 °C). The electrode system consisted of a platinum electrode that served as an auxiliary electrode, an Ag/AgCl as reference electrode and magnetic graphite composite electrode as working electrode (if not stated otherwise). The binding of streptavidin coated paramagnetic beads with biotinylated probe and hybridization events were carried out on a TS-100 Thermo Shaker (Spain). Magnetic separation was carried out on a MCB 1200 biomagnetic processing platform (Sigris, CA)

2.2. Reagents

All stock solutions were prepared using deionized and autoclaved water. Tris(hydroxymethyl)methylamine (Tris), sodium chloride, sodium citrate, ethylenediamine tertraacetic acid disodium salt (EDTA), lithium chloride, Tween 20, and the streptavidin 10 nm colloidal gold labeled were purchased from Sigma-Aldrich. Hydrochloric acid (37%) was purchased from PanReac (Barcelona, Spain). Streptavidin coated paramagnetic beads Dynabeads M-280 Streptavidin (diameter 2.8 μm) was purchased from Dynal Biotech, Oslo, Norway. Biotinylated probe oligonucleotides were received from Alpha DNA, Canada and their sequences are showed in Table 1.

The buffers and hybridization solution were prepared as follows:

- TTL buffer: 100 mM Tris–HCl, pH 8.0; 0.1% Tween 20; and 1 M LiCl.
- TT buffer: 250 mM Tris–HCl, pH 8.0; and 0.1% Tween 20.
- TTE buffer: 250 mM Tris–HCl, pH 8.0; 0.1% Tween 20; and 20 mM Na_2 EDTA, pH 8.0.
- Hybridization solution: 750 mmol/L NaCl, 75 mmol/L sodium citrate.

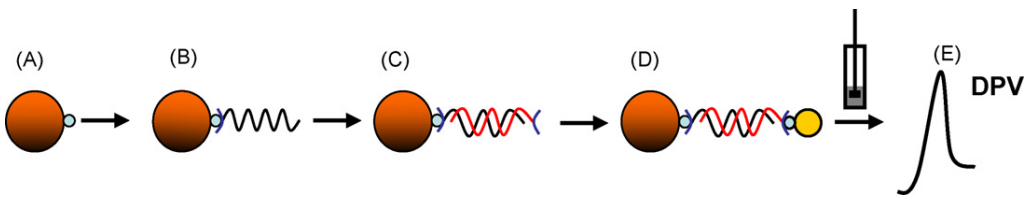

Fig. 1. Schematic representation of the first analytical protocol (not in scale): (A) introduction of the streptavidin-coated magnetic beads; (B) immobilization of the biotinylated BC-A probe onto the magnetic beads; (C) addition of the biotinylated BC-T probe, hybridization event; (D) addition and capture of the streptavidin-gold nanoparticles; (E) accumulation of final Au-NPs-BC-T/BC-A-magnetic beads conjugate on the surface of the M-GECE and magnetically trigged direct DPV electrochemical detection of Au-NPs tag in the conjugate.

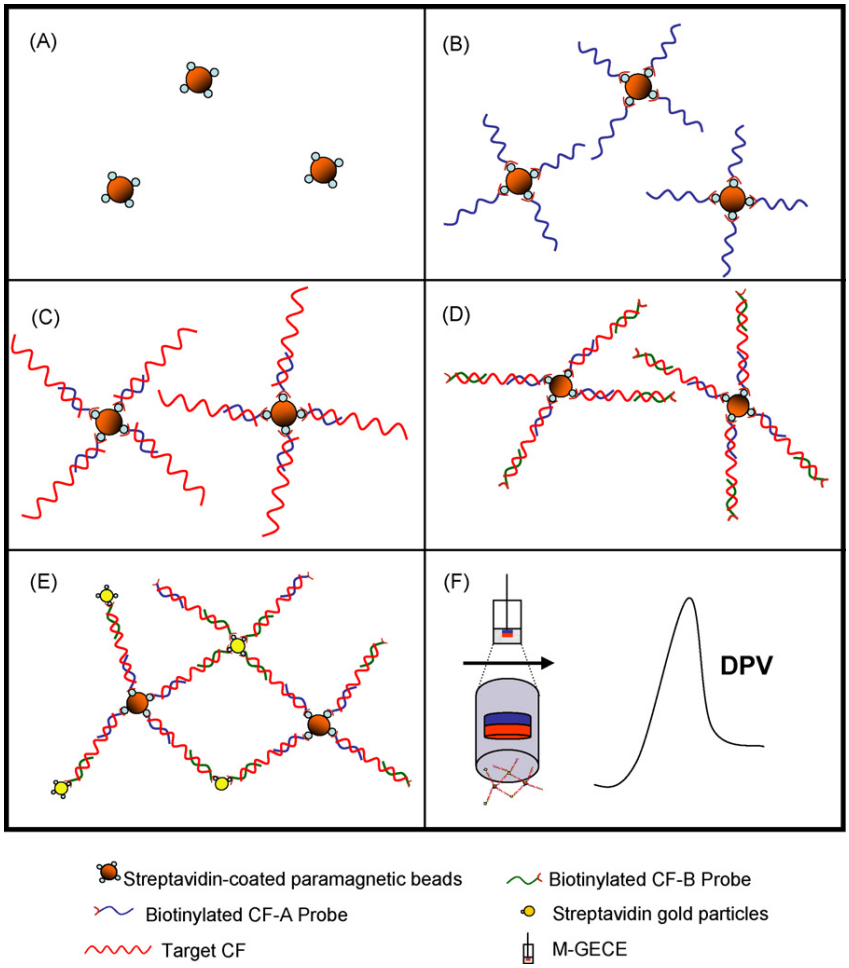

Fig. 2. Schematic representation of the sandwich system analytical protocol (not in scale): (A) streptavidin-coated magnetic beads; (B) immobilization of the biotinylated CF-A probe onto the magnetic beads; (C) addition of CF-T (first hybridization event); (D) addition of biotinylated CF-B probe (second hybridization event); (E) tagging by using the streptavidin-gold nanoparticles; (F) accumulation of Au-NPs-DNA-magnetic bead conjugate on the surface of M-GECE and magnetically trigged direct DPV electrochemical detection of Au-NPs tag in the conjugate.

2.3. Electrodes construction

Graphite-epoxy composite electrodes without incorporated magnet were prepared as described previously (Céspedes et al., 1993; Santandreu et al., 1997). Briefly, epoxy resin (Epotek H77A, Epoxy Technology, USA) and hardener (Epotek H77B) were mixed manually in the ratio 20:3 (w/w) using a spatula. When the resin and hardener were well mixed, the graphite

Table 1
Oligonucleotides sequences used in assays

Probe	Sequence[a]
Capture DNA (BC-A)	Biotin-5′GAT TTT CTT CCT TTT GTT C3′
Target DNA (BC-T)[b]	Biotin-5′GAA CAA AAG GAA GAA AAT C3′
Three base mismatch (BC-MX3)	Biotin-5′GAA CAA ATC TAA GAA AAT C3′
Noncomplementary (BC-NC)	Biotin-5′GGT CAG GTG GGG GGT ACG CCA GG3′
Capture DNA (CF-A)	5′TGC TGC TAT ATA TAT-biotin-3′
Signaling DNA (CF-B)	Biotin-5′GAG AGT CGT CGT CGT3′
Target DNA (CF-T)[c]	5′ATA TAT ATA GCA GCA GCA GCA GCA GCA GAC GAC GAC GAC TCT C3′
One base mismatch (CF-MX1)	5′ATA TAT AAA GCA GCA GCA GCA GCA GCA GAC GAC GAC GAC TCT C3′
Three base mismatch (CF-MX3)	5′ATA TAT CCC GCA GCA GCA GCA GCA GCA GAC GAC GAC GAC TCT C3′
Noncomplementary (CF-NC)	5′GGT CAG GTG GGG GGT ACG CCA GG3′

[a] Underlined nucleotides correspond to the mismatches.
[b] Target related to *BRCA1* breast cancer gene.
[c] Target related to cystic fibrosis gene.

powder (particle size 50 μm, BDH, UK) was added in the ratio 1:4 (w/w) and mixed for 30 min. The resulting paste was placed into a cylindrical PVC sleeve (6 mm i.d.). Electrical contact was completed using a copper disk connected to a copper wire. The conducting composite was cured at 40 °C during 1 week. Magnetic graphite-epoxy composite electrodes were prepared in similar way by incorporating the neodymium magnet (diameter 3 mm, height 1.5 mm, Halde Gac Sdad, Barcelona, Spain, catalog number N35D315) into the body of graphite-epoxy composite, 2 mm under the surface of the electrode (Pumera et al., 2005a). Before each use, the surface of the electrode was wet with doubly distilled water and then thoroughly smoothed, first with abrasive paper and then with alumina paper (polishing strips 301044-001, Orion).

2.4. Procedure for the two strands assay format

2.4.1. Immobilization of the capture DNA probe (BC-A) onto paramagnetic beads

The binding of the biotinylated probe with MB was carried out using a modified procedure recommended by Bangs Laboratories (1999). Briefly, 100 μg of MB (Fig. 1A) were transferred into 0.5 mL Eppendorf tube. The MB were washed once with 100 μL of TTL buffer and then separated, decanted and resuspended in 20 μL TTL buffer and the desired amount of BC-A was added (Fig. 1B). The resulting solution was incubated during 15 min at temperature of 25 °C with gentle mixing in a TS-100 Thermo Shaker. The MB with the immobilized BC-A were then separated from the incubation solution and washed sequentially with 100 μL of TT buffer, 100 μL of TTE buffer and 100 μL of TT buffer and then resuspended in 50 μL of hybridization solution and it was ready for the hybridization.

2.4.2. Hybridization procedure

The desired amount of BC-T was added in the solution (50 μL) of MB/BC-A conjugate obtained in the previous step. The hybridization reaction was carried out during 15 min at 42 °C in TS-100 Thermo Shaker (if not stated otherwise). The hybridized BC-T/BC-A/MB conjugate (Fig. 1C) was then washed twice with 100 μL of TT buffer and resuspended in 20 μL of TTL buffer and it was ready for adding Au-NPs label.

2.4.3. Binding of the streptavidin-coated Au-NPs

The desired amount of streptavidin-gold nanoparticles was added to the resulting MB/BC-A/BC-T conjugate and then incubated with gentle mixing during 15 min at 25 °C in TS-100 Thermo Shaker. The resulting MB/BC-A/BC-T/Au-NPs conjugate (Fig. 1D) was washed twice with 100 μL of TT buffer and then separated, decanted and resuspended in 50 μL of hybridization solution. The surface of M-GECE was then brought into contact during 60 s with the solution containing the final conjugate which is accumulated on it due to the inherent magnetic field of the electrode (Fig. 1E). It was ready for the immediate magnetically trigged direct DPV electrochemical detection of Au-NPs tag in the conjugate.

2.4.4. Electrochemical detection

The electrochemical oxidation of Au-NPs to $AuCl_4^-$ was performed at +1.25 V (versus Ag/AgCl) for 120 s (if not stated otherwise) in the nonstirred solution. Immediately after the electrochemical oxidation step, DPV was performed. During this step the potential was scanned from +1.25 to 0 V (step potential 10 mV, modulation amplitude 50 mV, scan rate 33.5 mV s^{-1}, nonstirred solution), resulting in an analytical signal due to the reduction of $AuCl_4^-$ at potential +0.4 V (Pumera et al., 2005b). The DPV peak height at a potential of +0.4 V was used as the analytical signal in all of the measurements. The background subtraction protocol involving saving the response for the blank solution and subtracting it from the analytical signal was used.

2.5. Procedure for the sandwich assay format

2.5.1. Immobilization of the capture DNA probe (CF-A) onto paramagnetic beads

This step was similar to the previously described one. Briefly, 100 μg of MB (Fig. 2A) were transferred into 0.5 mL Eppendorf tube, washed once with 100 μL of TTL buffer, separated, decanted and resuspended in 20 μL TTL buffer. The desired amount of CF-A was added (Fig. 2B). The resulting solution was incubated during 15 min at 25 °C with gentle mixing in a TS-100 Thermo Shaker. The MB with immobilized CF-A were separated, washed sequentially with 100 μL of TT buffer, 100 μL of TTE buffer and 100 μL of TT buffer, decanted and resuspended in 50 μL of hybridization solution and it was ready for the first hybridization.

2.5.2. First hybridization procedure

The desired amount of CF-T was added in the solution (50 μL) of MB/CF-A conjugate obtained in the previous step. The first hybridization reaction was carried out at 25 °C during 15 min in TS-100 Thermo Shaker (if not stated otherwise). The MB/CF-A/CF-T conjugate (Fig. 2C) was separated, washed twice with 100 μL of TT buffer, decanted and resuspended in 50 μL of hybridization solution and it was ready for the second hybridization.

2.5.3. Second hybridization procedure

The desired amount of CF-B was added in the solution (50 μL) of MB/CF-A/CF-T conjugate obtained previously. This second hybridization reaction was also carried out at 25 °C during 15 min in TS-100 Thermo Shaker (if not stated otherwise). The resulting MB/CF-A/CF-T/CF-B conjugate (Fig. 2D) was then washed twice with 100 μL of TT buffer and resuspended in 20 μL of TTL buffer and it was ready for adding Au-NPs label.

2.5.4. Binding of the streptavidin coated Au-NPs

The desired amount of streptavidin-gold nanoparticles was added to the resulting MB/CF-A/CF-T/CF-B conjugate and then incubated with gentle mixing during 15 min at 25 °C in TS-100 Thermo Shaker. The resulting MB/CF-A/CF-T/CF-B/Au-NPs conjugate (Fig. 2E) was washed twice with 100 μL of TT buffer separated, decanted and resuspended in 50 μL of hybridization solution. The surface of M-GECE was then brought into contact

with the solution containing the final conjugate in the similar way as previously described (Fig. 2F).

2.5.5. Electrochemical detection

This was performed in the same way as for the two strands assay format previously described.

3. Results and discussion

3.1. Two strands assay format

Fig. 3 shows the voltammograms that demonstrate the efficacy of the genomagnetic assay using as target a DNA strand related to the BRCA1 breast cancer gene. In Fig. 3A a well-defined signal is observed for 2.5 μg mL^{-1} of BC-T. The Fig. 3B shows a significantly much lower signal for 2.5 μg mL^{-1} of BC-MX3. A practically null gold signal is observed for 2.5 μg mL^{-1} of BC-NC (Fig. 3C). The discrimination of BC-MX3 and BC-NC is significantly better than that reported previously by our group (Pumera et al., 2005a).

The results obtained show that the magnetically trigged direct electrochemical detection of NPs tags corresponds to an effective hybridization along with an efficient magnetic attraction of the MB/BC-A/BC-T/Au-NPs conjugate onto the sensor surface with the tiny magnet inside (M-GECE). In contrast no electrochemical response is observed for the same conjugate at GECE (without a built-in magnet), because of the absence of magnetic or adsorptive accumulation of paramagnetic beads (Fig. 3D).

Fig. S1A–C (see Fig. S1, Supplementary Information) displays the effect of amount of the Au-NPs (A), MB (B) and hybridization time (C) upon the hybridization response. The amounts of MB and Au-NPs affect the quantity of bound probes and captured tags, respectively, which have a great effect upon the sensitivity. Fig. S1A shows the obtained peak currents using a number of NPs between 3×10^{12} and 13×10^{12}, reaching a maximum in 9×10^{12} and showing a low decrement thereafter probably due to some excess washing in the final step. All further work employed 9×10^{12} NPs tags. Fig. S1B displays increment in the current response between 25 and 50 μg MB showing very slightly increases thereafter. We considered 50 μg as a maximum because the further increases of MB did not led a significant increment of the signal. Subsequent work employed 50 μg of MB. This behavior corresponds to the fact that with an increasing amount of paramagnetic beads the surface of the magnetic electrode becomes saturated with the beads, and therefore, the further increase of the bead amount does not lead to an increase of the signal.

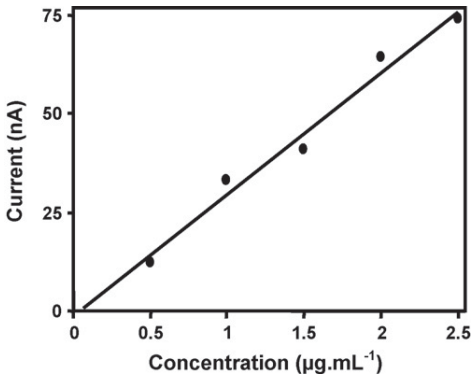

Fig. 4. Calibration plot for BC-T DNA over the 0.5–2.5 μg mL^{-1} range with a correlation coefficient of 0.9784. Hybridization time, 15 min; amount of paramagnetic beads, 50 μg. Other conditions, as in Fig. 3A.

Another important parameter that affects the detection of DNA is hybridization time (Fig. S1C). The DPV response increases with hybridization time between 5 and 15 min and then show a leveling off. The influence of the hybridization temperature was studied previously in the interval of 25–42 °C (not shown). The hybridization time 15 min at a temperature of 42 °C was chosen as optimal for this assay.

Fig. 4 shows the BC-T defined concentration dependence. The calibration plot was linear over a concentration range from 0.5 to 2.5 μg mL^{-1} of BC-T, with a correlation coefficient of 0.9784 and a detection limit (DL) of 0.198 μg mL^{-1} of BC-T, based on upper limit approach (Mocak et al., 1997). Such DL corresponds to 33 pmols in the 50 μL sample volume. This DL is lower in comparison to that reported by Wang et al. (2002) for the breast-cancer *BRCA1* gene using screen-printed electrodes and labeling with alkaline-phosphatase. By the other side our DL is higher in comparison to that obtained with other electrochemical assays, e.g. the genosensor based on colloidal Au-NPs developed by Ozsoz et al. (2003) and the genomagnetic based on guanine oxidation signal developed by Erdem et al. (2005), both by using pencil graphite electrode; however, these assays

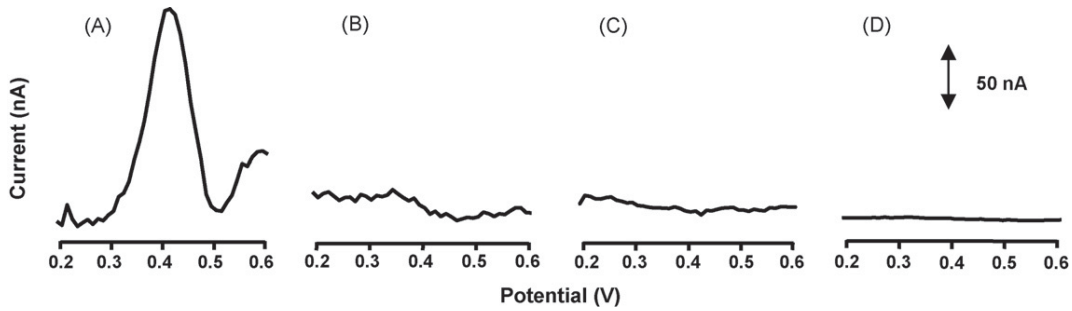

Fig. 3. DPV hybridization response of 2.5 μg mL^{-1} of: BC-T (A), BC-MX3 (B), BC-NC (C) on magnetic graphite-epoxy composite electrode and 2.5 μg mL^{-1} of BC-T on non-magnetic graphite-epoxy composite electrode (D). Conditions: amount of paramagnetic beads, 50 μg; amount of Au nanoparticles, 9×10^{12}; hybridization time, 15 min; hybridization temperature, 42 °C; oxidation potential, +1.25 V; oxidation time, 120 s; DPV scan from +1.25 to 0 V; step potential, 10 mV; modulation amplitude, 50 mV; scan rate, 33.5 mV s^{-1}; non-stirred solution.

differ substantially from the protocol described in this paper. On the other hand the detection limits reported in both assays correspond to polymerase chain reaction (PCR) amplicons, being not the case in this manuscript.

Current work in our laboratory aims to improve the DL by using different strategies including the silver enhancement so as to augment the hybridization signal coming from Au-NPs.

The technology reported herein offers various advantages such as the simplicity, sensitivity along with the effective discrimination against mismatched and noncomplementary oligomers. The immobilization of the probe onto the magnetic beads rather than onto the electrode surface (as reported by Wang et al., 2002) offers also greater versatility. The proposed method could provide a useful approach for future applications in clinical diagnostic.

3.2. Sandwich assay format

Fig. S2A–D (Supplementary Information) shows a typical differential pulse voltammogram (A); the effect of hybridization time (B), hybridization temperature (C) and amount of MB upon the hybridization response.

Fig. S2A represents a typical differential pulse voltammogram for the signals of Au at M-GECE after hybridization with CF-T in the sandwich assay. Low Au signals (not shown) were observed when single and three-mismatch and noncomplementary oligonucleotides were examinated.

The influence of the hybridization time on this genomagnetic sensor was also studied (Fig. S2B) between 5 and 30 min. The DPV response increased with hybridization time between 5 and 15 min and then decreased. The highest signal was obtained to 15 min as in the assay previously described. This time was chosen as optimal for further studies.

The influence of the hybridization temperature was also investigated in this assay in the interval from 25 to 42 °C (Fig. S2C). The highest signal was observed at 25 °C. This temperature was chosen as optimal for this assay. Fig. S2C displays low temperature dependence due to that the response increased only 10% in the studied interval.

Fig. S2D displays the effect of the amount of MB. An increment in the hybridization response between 25 and 100 μg MB is observed showing a sudden decreases thereafter. This phenomenon although not observed for the previous assay is probably related to the decrease of the sensor conductivity upon increasing the thickness of the adsorbed MB layer. Subsequent work employed 100 μg of MB chosen as the optimal quantity. The amount of MB is of great importance because of its influence in the immobilization of CF-A which will determine the sensitivity and reproducibility of the genosensor.

Other relevant parameters influencing the electroanalytical DPV response of the Au-NPs gold such as electrooxidation potential and electrochemical oxidation time were investigated and optimized previously (Pumera et al., 2005a). Hence, a potential of +1.25 V and 120 s were selected as optimal for electrooxidation of Au-NPs upon the DPV signal, to both assays.

Fig. 5 shows the hybridization detection studies with CF-T. Data are given in vertical bars that show the current intensities of DPV signals obtained for the hybridization responses of 8 μg mL^{-1} of: CF-T, CF-MX1, CF-MX3 and CF-NC on M-GECE. Error bars show the mean and the standard deviations of the measurements taken from three independent experiments. In Fig. 5A is observed the higher current intensity which represents the efficient hybridization electrochemical response on the M-GECE because of magnetic attraction of the MB/CF-A/CF-T/CF-B/Au-NPs conjugate to its surface. Lower responses for CF-MX1 (Fig. 5B) and significantly lower for CF-MX3 (Fig. 5C) and CF-NC (Fig. 5D) are observed according to the difference in current intensities. The discriminations can be improved by avoiding the nonspecifically adsorbed oligonucleotides by a better control of the washing step or increasing the concentration of CF-A.

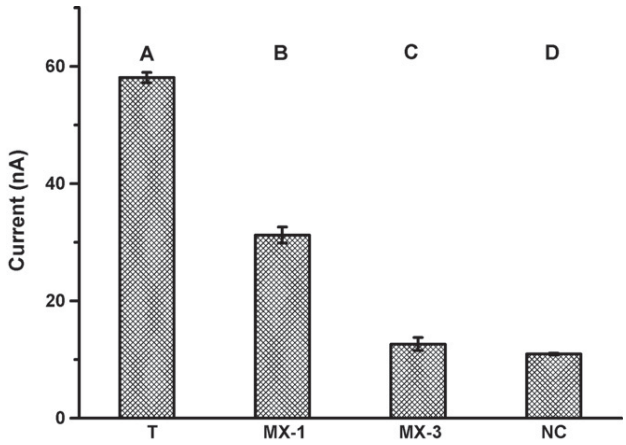

Fig. 5. Histogram that shows the current intensities of DPV peaks obtained for the hybridization responses of 8 μg mL^{-1} of: target associated with cystic fibrosis (T), single-base mismatch (MX1), three-base mismatch (MX3), and noncomplementary DNA (NC) on magnetic graphite-epoxy composite electrode. Error bars show the mean and the standard deviations of the measurements taken from three independent experiments. Conditions: Hybridization time, 15 min; hybridization temperature, 25 °C; amount of paramagnetic beads, 100 μg; electrooxidation potential, +1.25 V; electrooxidation time, 120 s; DPV scan from +1.25 to 0 V; step potential, 10 mV; modulation amplitude, 50 mV; scan rate, 33.5 mV s^{-1}; nonstirred solution.

4. Conclusions

We have reported a simple strategy for rapid and precise electrochemical detection of DNA hybridization by labeling with Au-NPs and using an M-GECE that makes the detection much easier. Experiments for the detection of a single and three-base mismatch were carried out and the results demonstrated an efficient, rapid and accurate detection of single and three base mismatch. The developed methods have a sufficient detection limit for real-world analysis in regard to diagnosis. These bioassays also eliminate the use of toxic chemical such as HBr/Br_2 solution which is commonly used in acid dissolution of Au-NPs tag (Wang et al., 2001; Authier et al., 2001).

The proposed electrochemical detection formats are simple, sensitive enough, have a low cost, fast response time and are potentially useful for fast clinical screenings. The application of

the developed designs can be extended to other fields such as environmental related analysis where fast DNA analysis is of special importance.

Current effort in our laboratory is directed to the optimization of the experimental conditions in order to improve the sensitivity and reproducibility in order to adapt these assays to the pathogenic microorganism detection.

Acknowledgements

This work was financially supported by the Spanish "Ramón Areces" foundation (project 'Bionanosensores') and MEC (Madrid) (Projects MAT2005-03553, BIO2004-02776 and CONSOLIDER NANOBIOMED and "Ramón y Cajal" program, A.M.).

Appendix A. Supplementary data

Supplementary data associated with this article can be found, in the online version, at doi:10.1016/j.bios.2006.08.031.

References

Alivisatos, P., 2003. Nanotechnology 14, R15–R27.
Alivisatos, P., 2004. Nat. Biotechnol. 22, 47–52.
Authier, L., Grossiord, C., Brossier, P., Limognes, B., 2001. Anal. Chem. 73, 4450–4456.
Bangs Laboratories Inc., TechNote 101, 1999.
Céspedes, F., Martínez-Fabregas, E., Bartroli, J., Alegret, S., 1993. Anal. Chim. Acta 273, 409–417.
Erdem, A., Ozkan, D., Karadeniz, H., Kara, P., Sengonul, A., Arzu, A., Ozsoz, M., 2005. Electrochem. Commun. 7, 815–820.
Hernández-Santos, D., Díaz-González, M., González-García, M.B., Costa-García, A., 2004. Anal. Chem. 76, 6887–6893.
Huber, M., Wei, T.F., Muller, U.R., Lefebvre, P.A., Marla, S.S., Bao, Y.P., 2004. Nucl. Acids Res. 32, e137.
Kerman, K., Kobayashi, M., Tamiya, E., 2004. Measure. Sci. Technol. 15, 1–11.
Merkoçi, A., Aldavert, M., Marin, S., Alegret, S., 2005. Trends Anal. Chem. 24, 341–349.
Millan, K.M., Mikkelsen, S.R., 1993. Anal. Chem. 65, 2317–2323.
Mirkin, C.A., Letsinger, R.L., Mucic, R.C., Storhoff, J.J., 1996. Nature 382, 607–609.
Mocak, J., Bond, A.M., Mitchell, S., Scollary, G., 1997. Pure Appl. Chem. 69, 297–328.
Niemeyer, C.M., 2001. Angew. Chem., Int. Ed. 40, 4128–4158.
Ozsoz, M., Erdem, A., Kerman, K., Ozkan, D., Tugrul, B., Topcuoglu, N., 2003. Anal. Chem. 75, 2181–2187.
Palecek, E., Jelen, F., 2002. Crit. Rev. Anal. Chem. 3, 261–270.
Palecek, E., Fojta, M., 2001. Anal. Chem. 73, 75A–83A.
Pividori, M.I., Merkoçi, A., Alegret, S., 2000. Biosens. Bioelectron. 15, 291–303.
Pividori, M.I., Merkoçi, A., Barbe, J., Alegret, S., 2003a. Electroanalysis 15, 1815–1823.
Pividori, M.I., Merkoçi, A., Alegret, S., 2003b. Biosens. Bioelectron. 19, 473–484.
Pumera, M., Castañeda, M.T., Pividori, M.I., Eritja, R., Merkoçi, A., Alegret, S., 2005a. Langmuir 21, 9625–9629.
Pumera, M., Aldavert, M., Mills, C., Merkoçi, A., Alegret, S., 2005b. Electrochim. Acta 50, 3702–3707.
Santandreu, M., Cespedes, F., Alegret, S., Martinez-Fabregas, E., 1997. Anal. Chem. 69, 2080–2085.
Shipway, A.N., Katz, E., Willner, I., 2000. Chem. Phys. Chem. 1, 18–52.
Wang, J., Xu, D., Kawde, A.-N., Polsky, R., 2001. Anal. Chem. 73, 5576–5581.
Wang, J., Polsky, R., Merkoci, A., Turner, K.L., 2003a. Langmuir 19, 989–991.
Wang, J., 2003. Anal. Chim. Acta 500, 247–257.
Wang, J., Liu, G.D., Merkoci, A., 2003b. J. Am. Chem. Soc. 125, 3214–3215.
Wang, J., Xu, D., Merkoci, Erdem, A., Polsky, R., Salazar, M.A., 2002. Talanta 56, 931–938.

SUPPLEMENTARY INFORMATION

Electrochemical genosensors for biomedical applications based on gold nanoparticles

M.T. Castañeda*, A. Merkoçi, M. Pumera, S. Alegret**

Table of Contents

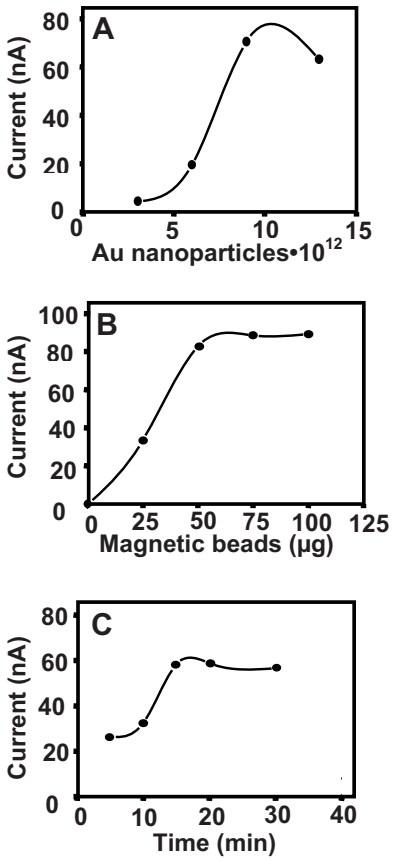

Fig. S1. *Effect of Au nanoparticles, (A); amount of paramagnetic beads (B) and hybridization time (C) upon the hybridization response of the BC-T DNA. Conditions: concentration of target, 2.5* µg.mL^{-1}*; hybridization time to (A) and (B), 15 min; amount of Au nanoparticles to (B) and (C), 13 x 10^{12}; amount of paramagnetic beads to (A) and (C) 50 µg; Other conditions: hybridization temperature, 42 ºC; oxidation potential, +1.25 V; oxidation time, 120 s; DPV scan from +1.25 V to 0 V; step potential, 10 mV; modulation amplitude, 50 mV; scan rate, 33.5 mV.s^{-1}; non-stirred solution.*

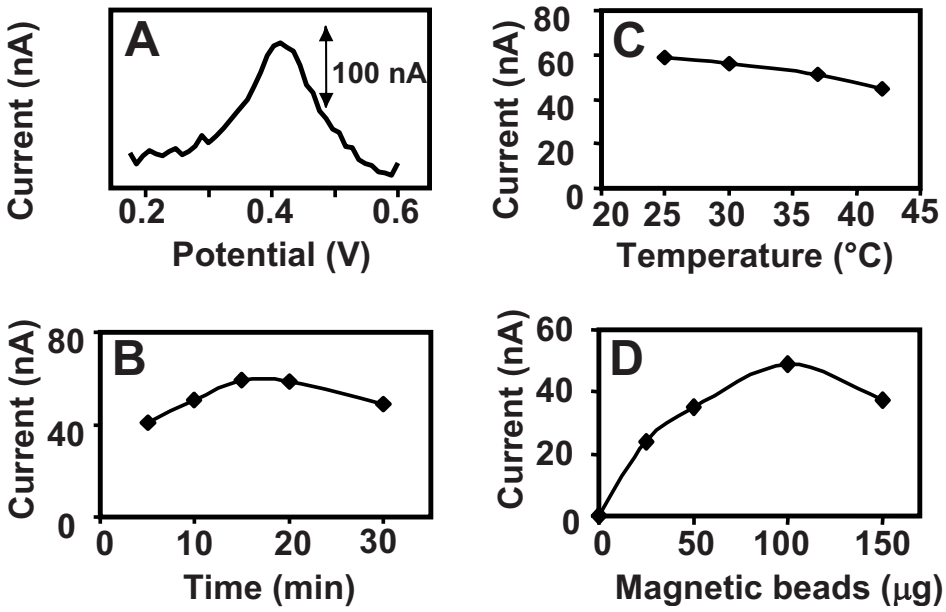

Fig. S2. *Typical differential pulse voltammogram for the oxidation signals of Au (A) during the sandwich assay to 8* μg.mL^{-1} of CF-T. *Effect of the hybridization time (B), hybridization temperature and (C) and amount of magnetic beads (D) upon the hybridization response of CF-T. Conditions A: hybridization time, 15 min; hybridization temperature, 25 ºC; amount of paramagnetic beads, 100 μg; electrooxidation potential, +1.25 V; electrooxidation time, 120 s; DPV scan from +1.25 V to 0 V, step potential 10 mV, modulation amplitude 50 mV, scan rate 33.5 mV s^{-1}, nonstirred solution.*
Conditions (B-D): Concentration of target, 8 μg.mL^{-1}. *Conditions B: amount of paramagnetic beads, 100 μg; hybridization temperature, 25 ºC. Conditions C: amount of paramagnetic beads, 100 μg; hybridization time, 15 min. D: hybridization time, 15 min; hybridization temperature, 25 ºC. Other conditions as in A.*

VIII

Double-codified gold nanolabels for enhanced immunoanalysis. *Analytical Chemistry*, 2007, 79, 5232-5240.

Ambrosi A., Castañeda M. T., Killard A. J., Smyth M. R, Alegret S., Merkoçi A.,

Anal. Chem. **2007,** *79,* 5232−5240

Double-Codified Gold Nanolabels for Enhanced Immunoanalysis

Adriano Ambrosi,[†,‡,§] Maria Teresa Castañeda,[†,‡,||] Anthony J. Killard,[§] Malcolm R. Smyth,[§] Salvador Alegret,[‡] and Arben Merkoçi*[,†]

Nanobioelectronics & Biosensors Group, Institut Català de Nanotecnología, Barcelona, Catalonia, Spain, Group of Sensors & Biosensors, Autonomous University of Barcelona, Barcelona, Catalonia, Spain, and School of Chemical Sciences, Dublin City University, Dublin 9, Ireland

A novel double-codified nanolabel (DC-AuNP) based on gold nanoparticle (AuNP) modified with anti-human IgG peroxidase (HRP)-conjugated antibody is reported. It represents a simple assay that allows enhanced spectrophotometric and electrochemical detection of antigen human IgG as a model protein. The method takes advantage of two properties of the DC-AuNP label: first, the HRP label activity toward the OPD chromogen that can be related to the analyte concentration and measured spectrophotometrically; second, the intrinsic electrochemical properties of the gold nanoparticle labels that being proportional to the protein concentration can be directly quantified by stripping voltammetry. Beside these two main direct determinations of human IgG, a secondary indirect detection was also applicable to this system, exploiting the high molar absorptivity of gold colloids, by which, the color intensity of their solution was proportional to the concentration of the antigen used in the assay. Paramagnetic beads were used as supporting material to immobilize the sandwich-type immunocomplexes resulting in incubation and washing times shorter than those typically needed in classical ELISA tests by means of a rapid magnetic separation of the unbound components. A built-in magnet graphite−epoxy−composite electrode allowed a sensibly enhanced adsorption and electrochemical quantification of the specifically captured AuNPs. The used DC-AuNP label showed an excellent specificity/selectivity, as a matter of fact using a different antigen (goat IgG) a minimal nonspecific electrochemical or spectrophotometric signal was measured. The detection limits for this novel double-codified nanoparticle-based assay were 52 and 260 pg of human IgG/mL for the spectrophotometric (HRP-based) and electrochemical (AuNP-based) detections, respectively, much lower than those typically achieved by ELISA tests. The developed label and method is versatile, offers enhanced performances, and can be easily extended to other protein detection schemes as well as in DNA analysis.

Gold nanoparticles have been used for analytical and biomedical purposes for many years. Rapid and simple chemical synthesis, a narrow size distribution, and efficient coating by thiols or other bioligands has enabled gold nanoparticles (AuNPs) to be used as transducers for several biorecognition binding applications. Properties such as their electron dense core, highly resonant particle plasmons, direct visualization of single nanoclusters by scattering of light, catalytic size enhancement by silver deposition, and electrochemical properties made them very attractive for several applications in biotechnology.

Gold nanoparticles have been used for several purposes. Bioconjugated gold nanoparticles for recognizing and detecting specific DNA sequences that function as both a nanoscaffold and a nanoquencher (efficient energy acceptor) have been reported.[1] Gold nanoparticles conjugated to antibodies are widely used in the field of light and electron microscopy, for visualizing proteins in biological samples.[2] The sensitivity of the detection is usually improved by the silver enhancement method. Beside these applications, an increased interest is shown for their use to quench the fluorescence,[3] tune the enzyme specificity,[4] visualize cellular or tissue components by electron microscopy,[5] electrical contacting or "wiring" between electrodes and redox enzymes,[6] tailoring the DNA loading by changing the nanoparticle size,[7] and labeling DNA strands for sensor and analytical applications.

The combination of biomolecules with gold nanoparticles provides interesting tools for several biological components. Oligonucleotide-functionalized gold nanoparticles have become the basis for an increasing number of diagnostic applications that

* To whom correspondence should be addressed. E-mail: arben.merkoci.icn@uab.es. Tel: +34935811976. Fax: +34935812379.

[†] Institut Català de Nanotecnología.

[‡] University of Barcelona.

[§] Dublin City University.

[||] On leave from: Universidad Autónoma Metropolitana-A, México, D. F., Mexico.

(1) Maxwell, D. J.; Taylor, J. R.; Nie, S. *J. Am. Chem. Soc.* **2002**, *124*, 9606−9612.
(2) Horisberger, M. *Scanning Electron Microsc.* **1981**, *11*, 9−31.
(3) Huang, T.; Murray, R. W. *Langmuir* **2002**, *18*, 7077−7081.
(4) You, C. C.; Agasti, S. S.; De, M.; Knapp, M. J.; Rotello, V. M. *J. Am. Chem. Soc.* **2006**, *128*, 14612−14618.
(5) De la Fuente, J. M.; Berry, C. C.; Riehle, M. O.; Curtis, A. S. G.; *Langmuir* **2006**, *22*, 3286−3293.
(6) Zayats, M.; Katz, E.; Baron, R.; Willner, I. *J. Am. Chem. Soc.* **2005**, *127*, 12400−12406.
(7) Hurst, S. J.; Lytton-Jean, A. K. R.; Mirkin, C. A. *Anal. Chem.* **2006**, *78*, 8313−8318.

10.1021/ac070357m CCC: $37.00
Published on Web 06/19/2007

compete with molecular fluorophores in certain settings.[8] The use of gold nanoparticles for protein analysis is also a very interesting research field. Gold nanoparticle/protein conjugates are finding increasing application as biochemical sensors, enzyme enhancers, nanoscale building blocks, and immunohistochemical probes.[9,10]

Nanoparticles in general and gold nanoparticles in particular offer attractive properties to act as DNA tags.[11] Their sensitivity, long lifetime, and multiplexing capability have led to extensive applications in electrochemical assays in recent years.[12] Most of the reported assays have been based on chemical dissolution of gold nanoparticle tag (in a hydrobromic acid/bromine mixture) followed by accumulation and stripping analysis of the resulting Au^{3+} solution. Due to the toxicity of the HBr/Br_2 solution, direct solid-state detection of silver precipitate on gold nanoparticle−DNA conjugates was reported by Wang et al.[13] However, this method was based on direct detection of precipitated silver, not the gold nanoparticle tag itself. Direct detection of colloidal gold nanoparticles but not in connection with the detection of DNA hybridization was reported earlier by our and Costa-García's groups.[14,16] A novel nanoparticle-based detection of DNA hybridization based on magnetically induced direct electrochemical detection of 1.4-nm Au_{67} quantum dot tag linked to the target DNA had been reported previously by our group. The Au_{67} nanoparticle tag is directly detected after the DNA hybridization event, without the need of acidic (i.e., HBr/Br_2) dissolution.[17,18]

The combination of optical and electrochemical properties of gold nanoparticles with the catalytic activity of the horseradish peroxidase (HRP) enzyme will be demonstrated now with a new double-codified (DC) label. It represents a gold nanoparticle modified with a model anti-human IgG peroxidase-conjugated antibody (anti-human IgG-HRP). The used label offers several analytical routes for immunodetection. Spectrophotometric analysis based on either gold nanoparticle absorption or HRP enzymatic activity and the electrochemical detection based on gold nanoparticle will be presented and compared. Optical sensitivity enhancement attributable to the use of gold nanoparticles as a multi-IgG-HRP carrier, which therefore amplify the enzymatic signal, as well as the high sensitivity in the direct electrochemical detection, represents the most important achievements due to the use of this double-codified nanolabel, which can potentially be exploited in several other future applications.

EXPERIMENTAL SECTION

Chemicals and Instruments. Streptavidin-coated magnetic beads (M-280) were purchased from Dynal Biotech. Biotin conjugate-goat anti-human IgG (sigma B1140, developed in goat and γ-chain specific), human IgG from serum, goat IgG from serum, anti-human IgG peroxidase conjugate (Sigma A8667, developed in goat and whole molecule), *o*-phenylenediamine dihydrochloride (OPD), hydrogen tetrachloroaurate(III) trihydrate ($HAuCl_4 \cdot 3H_2O$, 99.9%), trisodium citrate, and hydrogen peroxide were purchased from Sigma-Aldrich. All buffer reagents and other inorganic chemicals were supplied by Sigma, Aldrich, or Fluka, unless otherwise stated. All chemicals were used as received, and all aqueous solutions were prepared in doubly distillated water.

The phosphate buffer solution (PBS) consisted of 0.01 M phosphate-buffered saline, 0.137 M NaCl, and 0.003 M KCl (pH 7.4). Blocking buffer solution consisted of a PBS solution with added 5% (w/v) bovine serum albumin (BSA; pH 7.4). The binding and washing (B&W) buffer consisted of a PBS solution with added 0.05% (v/v) Tween 20 (pH 7.4). The measuring medium for the electrochemical measurements consisted of a 0.1 M HCl solution. OPD−H_2O_2 solution for spectrophotometric analysis was prepared by dissolving one Sigma OPD tablet in 25 mL of phosphate−citrate buffer (pH 5.0), and then immediately before the analysis, 10 μL of a 30% H_2O_2 solution was added.

All voltammetric experiments were performed using an electrochemical analyzer Autolab 20 (Eco-Chemie, The Netherlands) connected to a personal computer. Electrochemical experiments were carried out in a 5-mL voltammetric cell at room temperature (25 °C), using a three-electrode configuration. A platinum electrode served as an auxiliary electrode and an Ag/AgCl as reference electrode. Graphite composite working electrodes were prepared as described in construction of the Graphite−Epoxy Compositie−Magnet Electrodes. The binding of streptavidin-coated paramagnetic beads with biotinylated primary antibody and all the incubations were performed in a TS-100 ThermoShaker. Magnetic separation was carried out with an MCB1200 biomagnetic processing platform (Sigris). The spectrophotometric measurements were performed using a Tecan Sunrise absorbance microplate reader. Transmission electron micrographs were taken using a Jeol JEM-2011 (Jeol Ltd., Tokyo, Japan). Scanning electron microscopy characterizations were performed with a Jeol JSM-6300 (Jeol Ltd.) linked to an energy-dispersive spectrometer LINK ISIS-200 (Oxford Instruments, Bucks, England) for the energy-dispersive X-ray analysis.

Synthesis and Characterization of Gold Nanoparticles. Gold nanoparticles were synthesized by reducing tetrachloroauric acid with trisodium citrate, a method pioneered by Turkevich et al.[19] Briefly, 200 mL of 0.01% $HAuCl_4$ solution was boiled with vigorous stirring, and 5 mL of a 1% trisodium citrate solution was added quickly to the boiling solution. When the solution turned deep red, indicating the formation of gold nanoparticles, the solution was left stirring and cooling down. Transmission electron micrographs were recorded (see Figure S1A−C Supporting Information) in order to measure the size. To verify the Au metallic structure, a fast Fourier transform of crystalline planes distances was measured (see Figure S1D), and the corresponding data are

(8) Lytton-Jean, A. K. R.; Mirkin, C. A. *J. Am. Chem. Soc.* **2005**, *127*, 12754−12755.
(9) Ackerson, C. J.; Jadzinsky, P. D.; Jensen, G. J.; Kornberg, R. D. *J. Am. Chem. Soc.* **2006**, *128*, 2635−2640.
(10) Stoeva, S. I.; Lee, J.-S.; Smith, J. E.; Rosen, S. T.; Mirkin, C. A. *J. Am. Chem. Soc.*; **2006**, *128*, 8378−8379.
(11) Merkoçi, A.; Aldavert, M.; Marin, S.; Alegret, S. *Trends Anal. Chem.* **2005**, *24*, 341−349.
(12) Katz, E.; Willner, I.; Wang, J. *Electroanalysis* **2004**, *16*, 19−44.
(13) Wang, J.; Xu, D.; Polsky, R. *J. Am. Chem. Soc.* **2002**, *124*, 4208.
(14) Hernández-Santos, D.; Gonzáles-García, M. B.; Costa García, A. C.; *Electroanalysis* **2002**, *14*, 1225−1235.
(15) Pumera, M.; Aldavert, M.; Mills, C.; Merkoçi, A.; Alegret, S. *Electrochim. Acta* **2005**, *50*, 3702−3707.
(16) Gonzáles-García, M. B.; Costa-García, A. *Bioelectrochem. Bioenerg.* **1995**, *38*, 389−392.
(17) Pumera, M.; Castañeda, M. T.; Pividori, M. I.; Eritja, R.; Merkoçi, A.; Alegret, S. *Langmuir* **2005**, *21*, 9625−9629.
(18) Castañeda, M. T.; Merkoçi, A.; Pumera, M.; Alegret, S. *Biosens. Bioelectron.* In press.
(19) Turkevich, J.; Stevenson, P.; Hillier, *J. Discuss. Faraday Soc.* **1951**, *11*, 55−75.

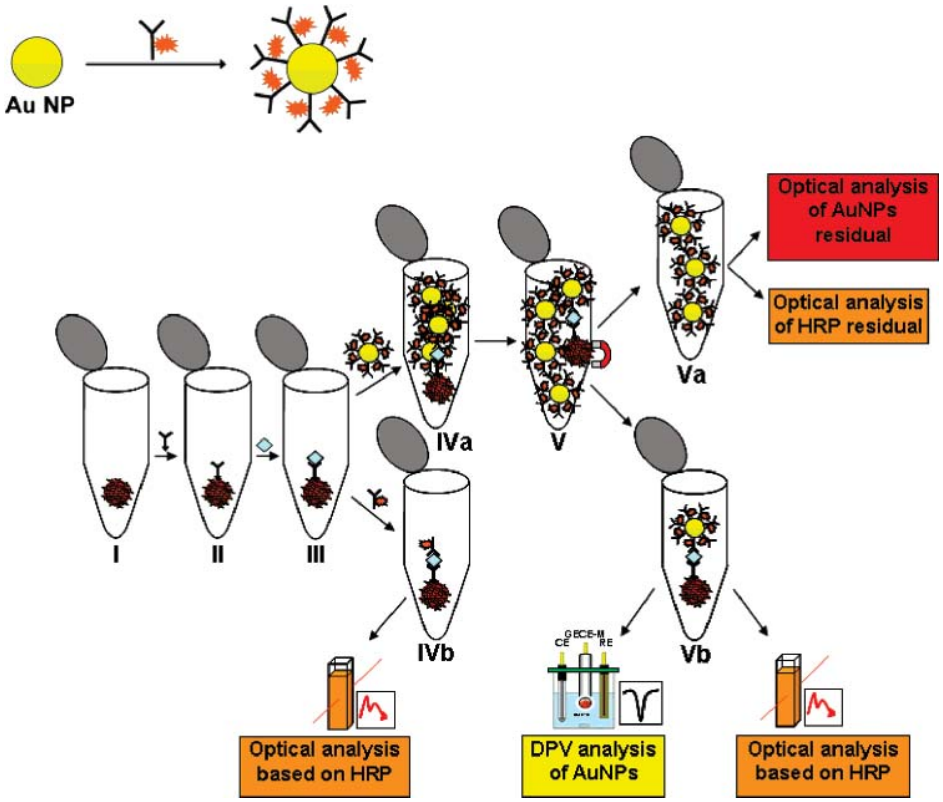

Figure 1. Schematic (not in scale) of (upper part) preparation of double-codified label using AuNPs (13 nm) and anti-human IgG peroxidase-conjugated antibody (anti-human-HRP) and (lower part) general assay procedure and characterizations, consisting of the following steps. (I) Introduction of streptavidin-coated paramagnetic beads (MBs). (II) Incubation with the primary biotinylated anti-human IgG antibody. (III) Incubation with different concentrations of the antigen human IgG. (IVa) Incubation with gold-labeled anti-human-HRP. (V) Separation of the magnetic bead immunocomplex from unbound gold-labeled anti-human-HRP. (Va) Gold-labeled anti-human-HRP residual for spectrophotometric analysis of gold and HRP. (IVb) Incubation with anti-human-HRP and spectrophotometric calibration based on HRP. (Vb) Magnetic bead immunocomplex with gold-labeled anti-human-HRP ready for double detection: spectrophotometric based on HRP and electrochemical based on direct DPV analysis of AuNPs.

shown in the table (inset in Figure S1). A UV−vis spectrum was recorded (see Figure S2A Supporting Information) and showed the characteristic absorbance peak of gold at 520 nm. Finally an energy-dispersive X-ray analysis was also performed (see Figure S2B).

Preparation of the Double-Codified Au Nanoparticle Label (DC-AuNP). The DC-AuNP, which represents a gold-labeled anti-human IgG−peroxidase conjugate antibody, was prepared by following the published procedure.[20] A schematic of the DC-AuNP preparation is given in Figure 1 (upper part). The conjugation process was carried out by adding the minimum antibody concentration determined by gold aggregation test (See more details at Supporting Information.) plus 10% (a total of 7.7 μg of antibody was added) to the appropriate gold solution volume (10 mL) adjusted to pH 9.0. The mixture was stirred for 10 min and then, to remove the excess of antibody, it was centrifuged at 15000*g* for 1 h at 4 °C. The clear supernatant was carefully removed, and the precipitated gold conjugates were resuspended in 10 mL of B&W buffer and stored at 4 °C.

Preparation of Magnetic Beads Sandwich-Type Immunocomplexes. The binding of the biotinylated anti-human IgG with streptavidin-coated paramagnetic beads was carried out using a slightly modified procedure recommended by Dynal Biotech.[21] In Figure S3 (Supporting Information) are shown scanning electron micrographs of the paramagnetic beads used.

Figure 1 (lower part) is a schematic of the whole assay steps used in this work. Briefly, 150 μg (15 μL from the stock solution) of streptavidin-coated paramagnetic beads (MB) (I in Figure 1) were transferred into a 0.5-mL Eppendorf tube. The MBs were washed twice with 150 μL of B&W buffer. The MBs were then resuspended in 108 μL of B&W buffer and 42 μL (from stock solution 0.36 mg/mL) of biotinylated anti-human IgG was added. The resulting MB and anti-human IgG solution was incubated for 30 min at temperature 25 °C with gentle mixing in a TS-100 ThermoShaker. The formed MB/anti-human IgG (II in Figure 1) were then separated from the incubation solution and washed three times with 150 μL of B&W buffer. The preparation process was followed by the resuspension of the MB/anti-human IgG in 150 μL of blocking buffer (PBS−BSA 5%) to block any remaining active surface of MBs, and the mixture was incubated at 25 °C for 20 min. After the washing steps with B&W buffer, the MB/anti-human IgG were incubated at 25 °C for 30 min with 150 μL of human IgG antigen at different concentrations forming by this

(20) Beesley, J. *Colloidal Gold. A new perspective for cytochemical marking*; Royal Microscopical Society Handbook 17; Oxford Science Publications. Oxford University Press: Oxford, England, 1989.

(21) Dynal Biotech, Technote 010 for product 112.05.

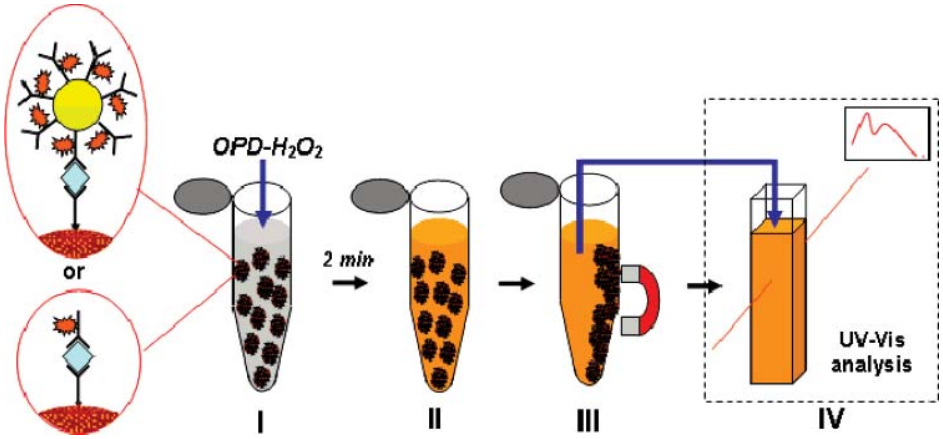

Figure 2. Spectrophotometric analysis procedure consisting of the following. (I) Addition to the MB immunocomplex suspension with or without AuNPs of the OPD−H_2O_2 solution (OPD ready to use from tablets, H_2O_2 0.01%) as a specific enzymatic substrate for HRP. (II) After 2 min, the solution turns orange due to the water-soluble yellow-orange reaction product of peroxidase with OPD with an absorbance maximum at 492 nm and an intensity proportional to the concentration of the enzyme label. (III) MB immunocomplexes are separated from the solution using a magnet and then transferred to the measuring cuvette for UV−vis analysis. (IV) Absorbance measurements are carried out at 492 nm after blocking the reaction with 3 M HCl.

way the immunocomplex MB/anti-human IgG/Human IgG (III in Figure 1). Finally, after the washing steps, the MB/anti-human IgG/human IgG immunocomplexes were labeled either with DC-AuNP or with anti-human-HRP.

Labeling with DC-AuNP. The washed MB/anti-human IgG/human IgG immunocomplex (III in Figure 1) was resuspended and incubated at 25 °C for 30 min with 150 μL of the previously prepared gold-labeled anti-human−HRP conjugate (DC-AuNP) solution (IVa in Figure 1) forming the sandwich-type immunocomplex: MB/anti-human IgG/human IgG/DC-AuNP. This complex was further characterized as follows. After the magnetic separation of the excess of DC-AuNP conjugate (V in Figure 1), a spectrophotometric analysis was carried out based on either HRP (optical analysis of HRP residual) or AuNP (optical analysis of AuNP residual), both present in the remaining excess of DC-AuNP (Va in Figure 1) not anchored to the MB through the interaction with the antigen human IgG. This spectrophotometric analysis was carried out as follows using a Tecan Sunrise absorbance microplate reader. The separated solution of residual DC-AuNP (Va in Figure 1) was divided into two parts. Part I, 140 μL, was transferred to a 96-well plastic plate and used directly for the analysis of gold by measuring the absorbance at 520 nm. Part II, 10 μL, was transferred to another plate and used for the reaction between HRP and OPD (150 μL), which generates a colored solution. After 2 min, the HRP/OPD reaction was stopped by adding 50 μL of 3 M HCl, and the absorbance measurement was carried out at 492 nm.

Labeling with Anti-Human-HRP. The washed MB/anti-human IgG/human IgG immunocomplex (III in Figure 1) was resuspended and incubated at 25 °C for 30 min with 150 μL of the anti-human-HRP (7 μg/mL) without AuNPs. The immunocomplex prepared with anti-human-HRP was used for comparison studies with the DC-AuNP. Details are shown in the next section.

Spectrophotometric Analysis. The two magnetic bead sandwich immunocomplexes prepared without AuNP (MB/anti-human IgG/human IgG/anti-human HRP; see IVb in Figure 1) and with AuNP (MB/anti-human IgG/human IgG/DC-AuNP; see Vb in Figure 1) in the secondary antibody conjugate were analyzed spectrophotometrically in order to evaluate the benefits in using AuNPs. The analysis procedure is well described in Figure 2. The magnetic bead sandwich-type immunocomplexes purified magnetically as described previously (see Figure 1, IVb and Vb) were analyzed in a similar way. Each sandwich immunocomplex was resuspended in the Eppendorf tube with 150 μL of a preliminarily prepared solution of OPD−H_2O_2 (I in Figure 2). After the optimized time of 2 min (data not shown), the solution color changed to yellow-orange in relation to the concentration of HRP present in the complexes (II in Figure 2), which is proportional to the concentration of the human IgG used during the assay procedure. The reaction was then arrested by adding 50 μL of 3 M HCl, which denatures the enzyme and ensures the same reaction time in all the tubes. Using an external magnet, the magnetic beads were then separated from the solution (III in Figure 2), which was subsequently transferred to a 96-well plastic plate for the spectrophotometric analysis (IV in Figure 2) performed by measuring the absorbance at 492 nm.

Construction of the Graphite−Epoxy Composite−Magnet Electrodes. Graphite-epoxy composite electrode without incorporated magnet (GECE) were prepared as described previously.[22,23] Briefly, epoxy resin (Epotek H77A, Epoxy Technology) and hardener (Epotek H77B) were mixed manually in the ratio 20:3 (w/w) using a spatula. When the resin and hardener were well-mixed, the graphite powder (particle size 50 μm, BDH) was added in the ratio 1:4 (w/w) and mixed for 30 min. The resulting paste was placed into a cylindrical PVC sleeve (6-mm i.d.). Electrical contact was completed using a copper disk connected to a copper wire. The conducting composite was cured at 40 °C for one week. Magnetic graphite−epoxy composite electrodes (GECE-M) were prepared in similar way by incorporating a neodymium magnet (diameter 3 mm, height 1.5 mm; Halde Gac Sdad, Barcelona, Spain, Catalog No. N35D315) into the body of graphite−epoxy composite, 2 mm under the surface of the

(22) Céspedes, F.; Martinez-Fabregas, E.; Bartroli, J.; Alegret, S. *Anal. Chim. Acta* **1993**, *273*, 409−417.
(23) Santandreu, M.; Cespedes, F.; Alegret, S.; Martinez-Fabregas, E. *Anal. Chem.* **1997**, *69*, 2080−2085.

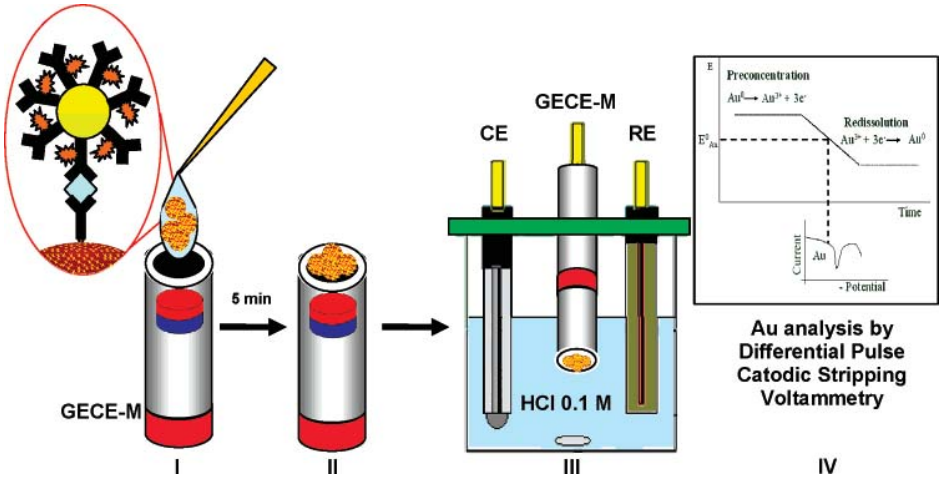

Figure 3. Electrochemical analysis procedure consisting of the following. (I) Deposition of 50 μL of the MB−AuNP immunocomplex sample onto the electrode surface. (II) Adsorption of the added immunocomplex on the electrode surface for 5 min at open circuit. (III) Introduction of the electrode without a washing step in the measurement cell containing 0.1 M HCl as electrolyte buffer. (IV) Electrochemical analysis consisting of a preconcentration step at 1.25 V for 150 s, followed by a DP cathodic scan from 1.25 to 0 V, and measurement of the peak current at 0.45 V (step potential 10 mV, amplitude 50 mV, scan rate 33 mV/s (vs Ag/AgCl).

electrode (Figure S4 Supporting Information). Prior to the use, the surface of the electrode was polished with abrasive paper and then with alumina paper (polishing strips 301044-001, Orion) and rinsed carefully with double-distilled water.

Electrochemical Analysis. Figure 3 is a schematic of the steps followed for the electrochemical analysis. The MB/anti-human IgG/human IgG/DC-AuNP immunocomplex was resuspended in 150 μL of double-distilled water. A 50-μL aliquot of this suspension was brought into contact for 5 min with the surface of the magnetic graphite−epoxy composite electrode in order to allow AuNP to accumulate on it. The inherent magnetic field of the electrode certainly improved the accumulation process, keeping the magnetic beads well immobilized. After 5 min, the electrode was transferred without any washing steps to an electrochemical cell containing 0.1 M HCl. A preconcentration process to oxidize AuNPs to $AuCl_4^-$ was performed at +1.25 V (vs Ag/AgCl) for 120 s in a stirred solution. Immediately after the electrochemical oxidation, differential pulse voltammetry (DPV) was performed by scanning from +1.25 to 0 V (step potential 10 mV, modulation amplitude 50 mV, scan rate 33.5 mV s^{-1}, nonstirred solution), resulting in an analytical signal due to the reduction of $AuCl_4^-$ at potential +0.45 V[14].

RESULTS AND DISCUSSION

Preparation of the DC-AuNP. The gold aggregation test was performed to detect salt-induced colloidal gold aggregation and find by this way the antibody concentration to be used for conjugation with gold nanoparticles. The antibody concentration that prevents gold aggregation was determined by measuring the difference between the absorbance at 520 nm and at 580 nm and plotting it against the concentration used (see Figure S7 Supporting Informtion). The minimum antibody concentration giving the highest absorbance difference was 7 μg for 1 mL of gold nanoparticles and that corresponded to the number of protein molecules of 10 for each gold nanoparticle. This result was verified by theoretical calculations. We used the covering ratio calculations to define the configuration called spherical code (or spherical packing).[24] Anti-human-HRP was approximated to a sphere of a radius of 5.6 nm[25] and, using the geometrical model of sphere packing around a single central sphere, resulted that 13 spheres of radius 5.6 nm can be arranged around a single central sphere of radius 6.5 nm (gold nanoparticle). The good correspondence between theoretical and experimental results confirms that the gold aggregation test is a simple and valid method to control protein conjugation to gold nanoparticles. Transmission electron micrographs (see Figure S5 Supporting Information) show gold nanoparticles surrounded by anti-human-HRP antibodies. The multiple small dots present inside the biological mass could be associated with Fe atoms of the prosthetic heme group of HRP enzymes.

Spectrophotometric Analysis. An ultrasensitive and simple method for detecting and quantifying biomarkers is essential for early diagnosis of diseases. Due to their extremely high extinction coefficients at 520 nm, AuNPs are a very good candidate. Moreover, different agglomeration states of AuNPs can result in distinctive color changes. These extraordinary optical features make AuNPs an ideal color reporting group for signaling molecular recognition events and render the nanomolar concentration detection possible.[26] In addition to AuNP optical properties, the DC-AuNP modified with HRP is sensitive to the OPD chromogen, showing by this way an alternative optical detection. Taking into account the above DC-AuNP properties, two optical detection procedures were developed and optimized for analyte quantitation: indirect analysis of DC-AuNP labels remaining in solution after the final incubation with the immunocomplex (Va in Figure 1) and based on both the gold nanoparticle absorptivity and the HRP activity; direct analysis of DC-AuNP labels specifically attached to the MB immunocomplexs (Vb in Figure 1) and based only on the HRP activity. This direct optical detection of DC-AuNP

(24) http://mathworld.wolfram.com/SphericalCode.html.
(25) Green, A. J.; Johnson, C. J.; Adamson, K. L.; Begent, R. H. *J. Phys. Med. Biol.* **2001**, *46*, 1679−1693.
(26) Jin, R.; Wu, G.; Li, Z.; Mirkin, C. A.; Schatz, G. C. *J. Am. Chem. Soc.*; **2003**; *125*, 1643−1654.

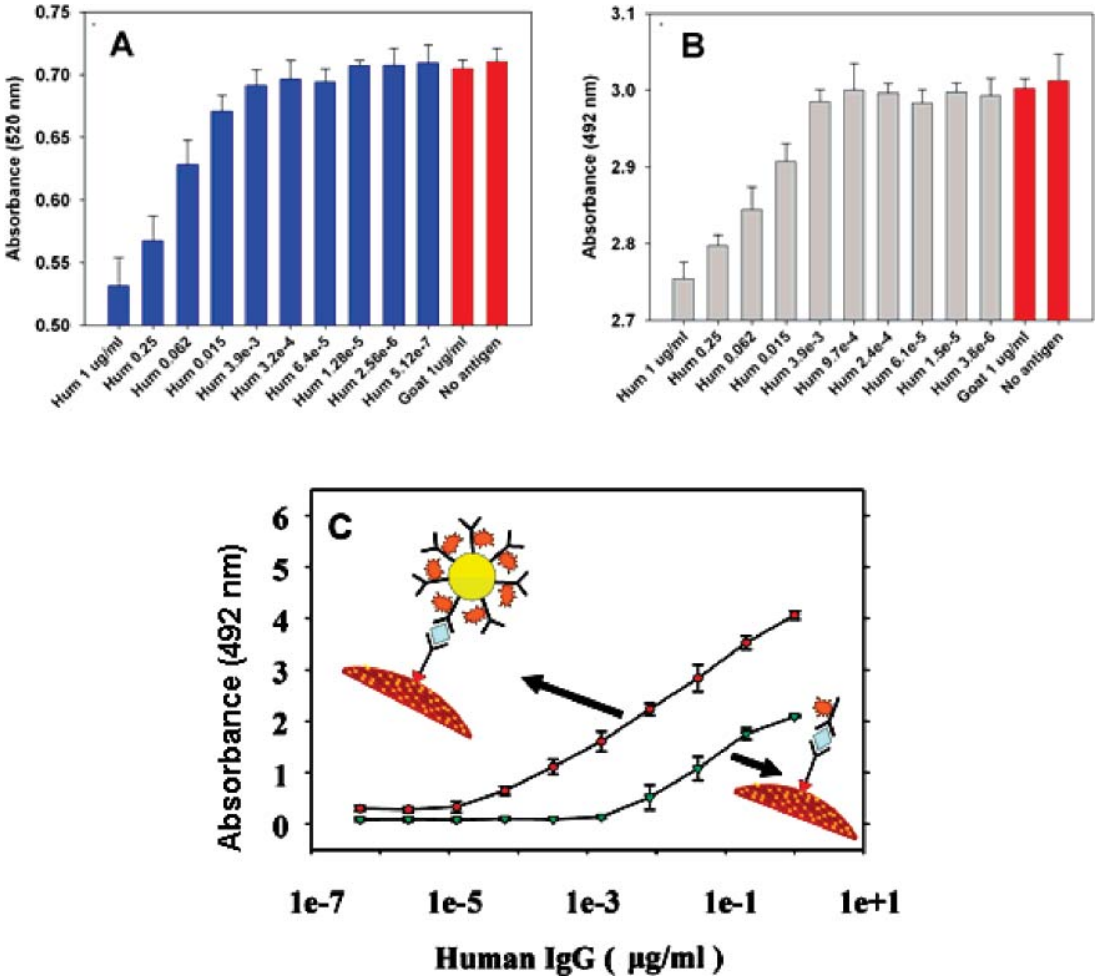

Figure 4. Upper part. Spectrophotometric analyses of magnetically separated DC-AuNP labels remaining in solution as excess after the incubation with MB/anti-human IgG/human IgG complexes. Graph A shows the absorbance at 520 nm related to the amount of AuNPs, and graph B shows the absorbance at 492 nm related to the amount of anti-human-HRP after the reaction with OPD. In both cases, it can be seen that, for an increased concentrations of the antigen (human IgG), the amount of the DC-AuNP label remaining in solution decreased as a proof of the specific interaction with the antigen. The red bars (in both A and B) represent the signals recorded when a nonspecific antigen was used (goat IgG, first red bar) or the antigen was missing (second red bar) in the immunoassay. Experimental conditions are explained above. Lower part. Calibration curves for the direct spectrophotometric detections of human IgG recorded using anti-human-HRP (green) and DC-AuNP (red) as labels. Experimental conditions are explained in the Experimental Section.

label was performed in parallel with the direct analysis of the anti-human-HRP label (IVb in Figure 1) for comparison purposes.

Indirect Spectrophotometric Determination of Human IgG. Figure 4 (A and B bars) shows the signals recorded for the analysis based on gold nanoparticle (at 520 nm) (see A bars) and based on HRP (at 492 nm after reaction with OPD) (see B bars) for all the human IgG antigen concentrations used during the preparation of the MB/anti-human IgG/human IgG/DC-AuNP immunocomplexes. The solutions used correspond to the excess (residual) of DC-AuNP conjugate (Va in Figure 1) nonconnected/remained in solution after the magnetic separation of the sandwich-type immunocomplex: MB/anti-human IgG/human IgG/DC-AuNP. An increased signal (absorbance at 520 nm for AuNP (Figure 6A) and at 492 nm for HRP/OPD chromogen (Figure 6B)) is related to the increase of DC-AuNP residual and consequently to the decrease of the bound human IgG in the previously separated MB/anti-human IgG/human IgG/ DC-AuNP immunocomplex. Two negative controls (red bars) are also included in Figure 4, which correspond to the sample with a nonspecific antigen (goat IgG 1 μg/mL) and the blank sample (without human IgG added), respectively. It can be clearly seen that, for increasing concentrations of the human IgG antigen, the concentration of AuNP and HRP present in the residual separated DC-AuNP conjugate solution decreases, proving that a specific interaction was effectively occurring. These two indirect spectrophotometric analyses allowed the quantification of human IgG as low as 16 and 36 ng/mL by using AuNP- and HRP-related signals, respectively.

Direct Spectrophotometric Determination of Human IgG. The sandwich-type immunocomplex MB/anti-human IgG/human IgG/DC-AuNP (Vb in Figure 1) obtained by magnetic separation from the unbound DC-AuNP (detected as described previously) was observed by transmission electron microscopy (see Figure 5). The images in the upper part clearly show the gold nanoparticles (black dots) attached to the magnetic beads (big black spheres) through the immunocomplex component interaction. These gold nanoparticles are, as a matter of fact, not present in the lower images that represent the sandwich-type immunocomplex MB/

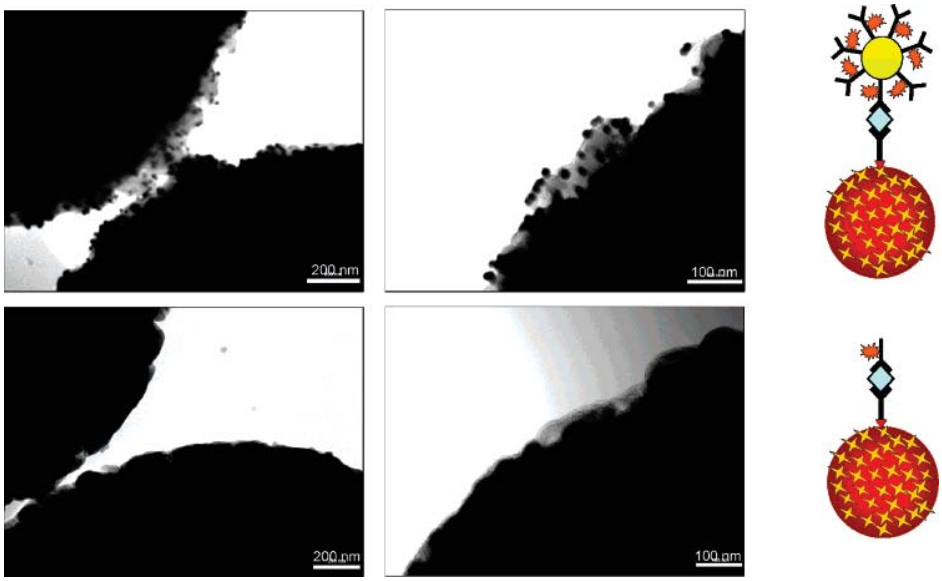

Figure 5. Transmission electron micrographs of sandwich-type immunocomplex MB/anti-human IgG/human IgG/DC-AuNP (upper part images) and MB/anti-human IgG/human IgG/anti-human-HRP (lower part images) obtained by the magnetic separation from the unbound DC-AuNP and anti-human-HRP, respectively.

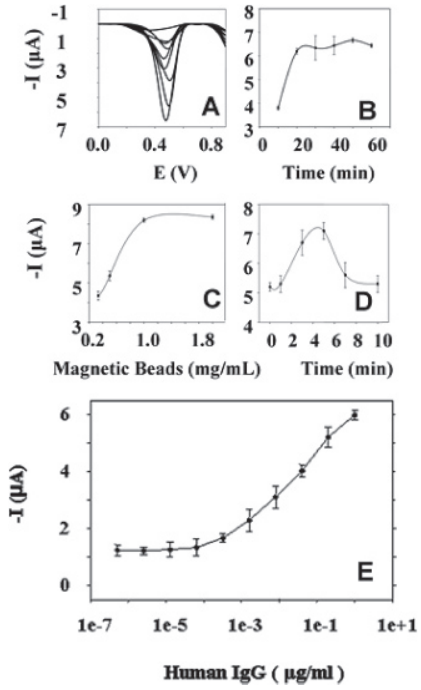

Figure 6. (A) Typical DPV curves corresponding to AuNPs analysis for human IgG concentrations of 2.5×10^{-6}, 1.3×10^{-5}, 3.2×10^{-4}, 1.6×10^{-3}, 0.008, 0.04, 0.2, and 1 μg/mL. It is also shown the response for 0.1 M HCl buffer solution only. (B) Graph of the optimization of the incubation time. (C) Magnetic beads concentration optimization graph. (D) Optimization graph for the adsorption time of MB-immuno-AuNP complexes on the electrode surface. (E) Human IgG calibration curves recorded using the DPV analysis of AuNP-labeled. Experimental conditions as explained in the Experimental Section.

anti-human IgG/human IgG/anti-human-HRP prepared without gold nanoparticles (see IVb in Figure 1). A direct spectrophotometric analysis based on the HRP-related signal was carried out for the DC-AuNP-based immunocomplex, and the results were compared with the analysis of the MB/anti-human IgG/human IgG/anti-human-HRP immunocomplex (IVb in Figure 1) obtained after the magnetic separation of the unbound anti-human-HRP.

Figure 4C shows the two calibration curves of human IgG for both immunocomplexes. It can be seen that, using the DC-AuNPs as label, an optical signal enhancement due to the higher number of anti-human IgG-HRP conjugates carried on the AuNPs (~10 HRP/1 AuNP) occurred. Although the sensitivity of the assay was almost the same (0.3617 Abs/in μg·mL) for both spectrophotometric detections, the limit of detection using the gold-labeled anti-human-HRP conjugate (DC-AuNP) was ~50 times lower than that obtained using the HRP-labeled anti-human IgG (2.4 ng of human IgG/mL) reaching the value of 52 pg of human IgG/mL (that corresponds to 0.33 pM). The increased absorbance achieved using AuNPs is due to a higher number of HRP. However, the resulting LOD decreased because of a lower nonspecific signal. In fact, the bottom line of the calibration curve using the DC-AuNP label, representing the nonspecific signal, is just a bit higher than the bottom line in the curve without AuNPs (Figure 4C). This could be explained only by the fact that, during the washing steps, the nonspecific interactions can be eliminated more easily when the antibody is attached to gold than when it is alone. That keeps the nonspecific line at a value lower than that at which it should be considering the signal enhancement. The detection limit obtained using DC-AuNP label is much lower than that using an enzyme-linked immunosorbent assay (ELISA), in which the electrochemical oxidation of enzyme-generated hydroquinone was measured,[27] and is comparable to the reported limit (190 fM) for the selective multiplexed detection of three protein cancer markers utilizing a new multiplexed version of the bio bar code amplification reported by the Mirkin group.[10]

Electrochemical Measurements. The use of enzymes as labels in immunosensing systems in general and particularly those based on electrochemical methods is one of the most important strategies reported so far. Various kinds of enzymes such as

(27) Wilson, M. S.; Nie, W. *Anal. Chem.* **2006**, *78*, 2507−2513.

urease,[28] alkaline phosphatase,[29] or HRP[30] have been used as labels for immunosensors based on electrochemical detections.

While elegant biosensing designs utilizing optical properties of AuNP have been demonstrated, it is desirable to expand these rather facile/sensitive detection methodologies to new and more versatile applications with special interest to the development of novel biosensor devices: integrated and small, low cost, and easy to be used.

The methods based on electrochemical detection offer unique opportunities for such applications. Direct DPV detection of AuNPs is of particular interest. We have been exploring these unique properties of AuNPs in DNA sensing.[17] The proof of concept of a magnetically trigged direct electrochemical detection for monitoring DNA hybridization shows several advantages. The developed method couples high sensitivity and reproducibility with effective genomagnetic discrimination against noncomplementary DNA. The elimination of the need for acid dissolution greatly simplifies particle-based electrical bioassays and obviates the use of toxic HBr/Br_2 solutions. The same detection principle is now applied for the DC-AuNP labeled immunocomplex.

The sandwich-type immunocomplex MB/anti-human IgG/human IgG/ DC-AuNP (Vb in Figure 1) obtained after magnetic separation of the unbound DC-AuNP was directly detected using the differential pulse cathodic scan. The results obtained (Figure 6) show an attractive performance of the magnetically trigged electrochemical detection of the immunoreaction based on DC-AuNP labeling. The DPV response of the immunocomplex was studied previously (results not shown), and the DPV peak height at +0.45 V potential was chosen and used as the analytical signal in all of the measurements. Figure 6A shows typical DPV curves corresponding to the DC-AuNPs connected to the immunocomplex for human IgG concentrations ranging from $2{,}5 \times 10^{-6}$ to 1 μg/mL. Optimizations of the entire procedure were carried out using the described electrochemical conditions with the fixed concentration of the antigen human IgG of 1 μg/mL. In contrast, no electrochemical response was observed for the same immunocomplex at the same electrode but without the built-in magnet as expected from the absence of magnetic or adsorptive accumulation of the paramagnetic beads.

Various parameters involved in the preparation of DC-AuNP-based immunocomplexes as well as in the electrochemical detection were examined and optimized. The graph in Figure 6B represents the incubation time optimization of the biological elements at 25 °C. It can be seen that, using the magnetic beads as a supporting material, the biological interactions can be completed in 20 min, which is much shorter than typical incubation times used in ELISA procedures with plastic plate supports.[31] Longer incubation time did not improve the signal. Figure 6C shows the optimization of the magnetic bead concentration. The response increases linearly up to 1 mg of magnetic beads/mL and remains almost constant thereafter. A 1:10 dilution of the paramagnetic bead stock solution (10 mg/mL) resulted therefore as the best to be used. Figure 6D represents the optimization of the deposition time of MB immunocomplexes on the electrode surface, before the electrochemical measurement. Precisely, after the final wash to eliminate the excess DC-AuNP label, the MB immunocomplexes were resuspended in water and then 50 μL from the suspension was dropped onto the electrode surface and left for different time periods to be adsorbed.

An increase of the voltammetric peak related to AuNPs for increasing adsorption times on the electrode surface is observed up to 5 min. This increase is correlated to a higher number of AuNPs coming through the MB immunocomplexes and attracted onto the electrode surface by the magnet underneath. Adsorption times longer than 5 min caused a signal decrease, and this is probably due to a blocking effect taking place on the surface and caused by the thicker layer of magnetic beads more and more attracted to the electrode surface. A direct consequence of that seems to be the reduced number of AuNPs that can actually "be seen" (touch the surface) by the electrode. The signal should indeed have reached a plateau, but in fact, it decreased. The adsorption time of 5 min was then chosen for further characterizations as the best in terms of DPV sensitivity.

Figure 6E shows the calibration curve for the DPV analysis of the MB immunocomplex. A sensitivity of 0.5066 $\mu A/\ln \mu g \cdot mL^{-1}$ can be observed with a detection limit of 0.26 ng of human IgG for 1 mL of sample (that corresponds to 1.7 pM).

The method showed a very good precision, which represents an attractive and important feature for novel electrochemical immunoassays. The results obtained are related to the well-defined and highly reproducible magnetic collection of the MB/anti-human IgG/human IgG/DC-AuNP immunocomplexes on the electrode surface and overall to the direct detection of AuNPs without the need of any preliminary dissolving step that might affect the sensitivity as well as the reproducibility of the method (a series of 3 repetitive immunoreactions for 1 μg of human IgG/mL showed a RSD of ~3%).

The use of DC-AuNP label resulted in a significantly improved response for both the electrochemical and the spectrophotometric detection techniques, compared to the classical immunoassays exploiting HRP or other enzymes as labels. The lowest detection limit was obtained using spectrophotometric detection (52 pg/mL or 0.33 pM); however, electrochemical analysis was the most sensitive and with a limit of detection (260 pg/mL or 1.69 pM) still much lower or comparable with those reported by other authors based on either electrochemical or optical detections.[32] Protein detection using HPLC, including coupling it with a mass spectrometer via an electrospray ionization or a matrix-assisted laser desorption/ionization (MALDI), is nowadays a very potential laboratory technique. The utility of the above methodology (MALDI) was demonstrated last by the analysis of low amounts of protein routinely in the microgram to submicrogram range, with examples approaching the nanogram range as a potential limit (MALDI).[33]

The results obtained show that besides the optical−electrochemical versatility, the DC-AuNP label brings interesting advantages related to the sensitive, direct, and easy electrochemical

(28) Solé, S.; Alegret, S.; Céspedes, F.; Fàbregas, E.; Caballero, T. D. *Anal. Chem.* **1998**, *70*, 1462−1467.
(29) Santandreu, M.; Céspedes, F.; Solé, S.; Fàbregas, E.; Alegret, S. *Biosens. Bioelectron.* **1998**, *13*, 7−17.
(30) Zacco, E.; Pividori, M. I.; Alegret, S.; Galve, R.; Marco, M. P. *Anal. Chem.* **2006**, *78*, 1780−1788.
(31) http://www.chemicon.com/resource/ANT101/a2C.asp.
(32) Wang, M.; Wang, L.; Yuan, H.; Ji, X.; Sun, C.; Ma, L.; Bai, Y.; Li, T.; Li, J. *Electroanalysis* **2004**, *16*, 757−764.
(33) Perlman, D. H.; Huang, H.; Dauly, C.; Costello, C. E.; McComb, M. E. *Anal. Chem.* **2007**, *79*, 2058−2066.

application and opens new possibilities for in-field analysis in connection with low-cost and easy-to-use instrumentation.

CONCLUSIONS

A versatile gold-labeled detection system based on either a spectrophotometric or an electrochemical method was developed. In our procedure, a double-codified label consisting of gold nanoparticles conjugated to an HRP-labeled anti-human IgG antibody, is used to detect human IgG as a model protein. Streptavidin-modified paramagnetic beads were used as supporting material for the preparation of the sandwich-type immunocomplexes. A magnetic separation was then used to isolate the complexes from the unbound components, reducing considerably incubation and washing times. A permanent magnet inserted inside a graphite−epoxy composite electrode allowed an efficient and very reproducible collection of the MB immunocomplexes on the electrode surface for enhanced adsorption and subsequently the direct electrochemical determination of AuNPs. The DC-AuNP label allows us to perform immunoassays using both the electrochemical and the spectrophotometric techniques, obtaining for both detection methods better results in terms of detection limits (0.33 and 1.69 pM for the antigen by the optical−HRP-based and the electrochemical−AuNP-based analysis, respectively), and in terms of method sensitivity, if compared to the classical enzyme-linked immunosorbent assays.

This proof of concept of a double-codified immunodetection method shows a very good performance, it is rapid, straightforward, and inexpensive (no special equipment is required). In addition, this system establishes a general detection methodology that can be applied to a variety of immunodetection and DNA detection systems including lab-on-a-chip technology.

ACKNOWLEDGMENT

A.M. thanks the Spanish "Ramón Areces" foundation (project 'Bionanosensores') and MEC (Madrid) for the following Projects: MAT2005-03553, Consolider-Ingenio 2010, Proyecto CSD2006-00012, and also the support of Enterprise Ireland under the Technology Development Fund TD/03/107.

SUPPORTING INFORMATION AVAILABLE

Characterizations of the used AuNP and DC-AuNP labels including details on the electrode used. This material is available free of charge via the Internet at http://pubs.acs.org.

Received for review February 20, 2007. Accepted May 15, 2007.

AC070357M

Supporting Information

Double-Codified Gold Nanolabels for Enhanced Immunoanalysis

Adriano Ambrosi[1,2,3], *Maria Teresa Castañeda*[1,2,4], *Anthony J. Killard*[3], *Malcolm R. Smyth*[3]

Salvador Alegret[2], *Arben Merkoçi*[1*]

[1]Nanobioelectronics & Biosensors Group, Institut Català de Nanotecnología, Barcelona, Catalonia, Spain; [2] Group of Sensors & Biosensors, Autonomous University of Barcelona, Barcelona, Catalonia, Spain.[3] School of Chemical Sciences, Dublin City University, Dublin 9, Ireland, [4]On leave from: Universidad Autónoma Metropolitana-A, México, D. F., Mexic.

*Corresponding author: arben.merkoci.icn@uab.es

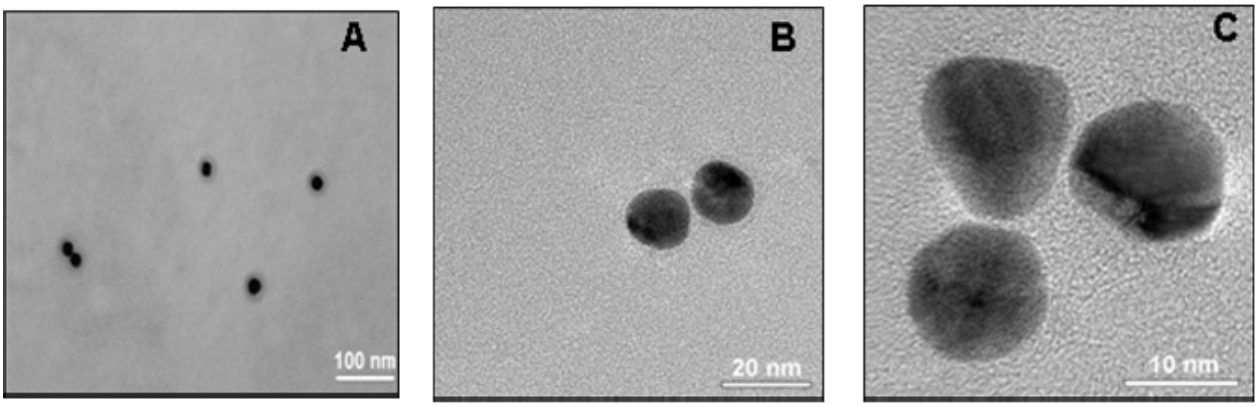

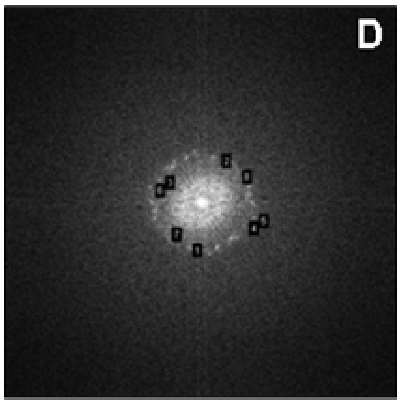

FFT of TEM Au NPs 1-600000X-6

Spot	d-Spacing(nm)	Rec Pos (1/nm)	Degrees to Spot 1	Degrees to x-axis	Amplitude
1	0.2330	4.292	0.00	-107.21	712203.69
2	0.2346	4.263	179.29	72.08	712203.69
3	0.2322	4.307	101.25	151.54	856670.55
4	0.2302	4.344	78.59	-28.61	856670.55
5	0.2046	4.887	90.77	-16.44	445662.77
6	0.2069	4.833	88.86	163.93	445662.77
7	0.2419	4.134	32.60	-139.81	880580.50
8	0.2420	4.133	146.72	39.51	880580.50

FFT of TEM Au NPs 3-500000X-3

Spot	d-Spacing(nm)	Rec Pos (1/nm)	Degrees to Spot 1	Degrees to x-axis	Amplitude
1	0.2404	4.159	0.00	133.66	5573096.19
2	0.2382	4.185	179.95	-46.28	5573096.19
3	0.2407	4.155	121.63	12.04	5282600.92
4	0.2415	4.141	58.68	-167.66	5282600.92
5	0.2439	4.102	61.30	72.36	283544.47
6	0.2418	4.135	119.48	-106.86	283544.47
7	0.1371	7.292	150.93	-17.27	313793.48
8	0.1381	7.241	29.24	162.90	313793.48

Figure S1. Transmission electron micrographs of AuNPs (13 nm) at A) 50000X, B) 200000X and C) 500000X magnifications. D) FFT of crystalline planes of one AuNP. Planes distances measured correspond to the cubic system of Au. The AuNP sample was diluted in doubly-distilled water and ultrasonicated for 20 min prior the analysis.

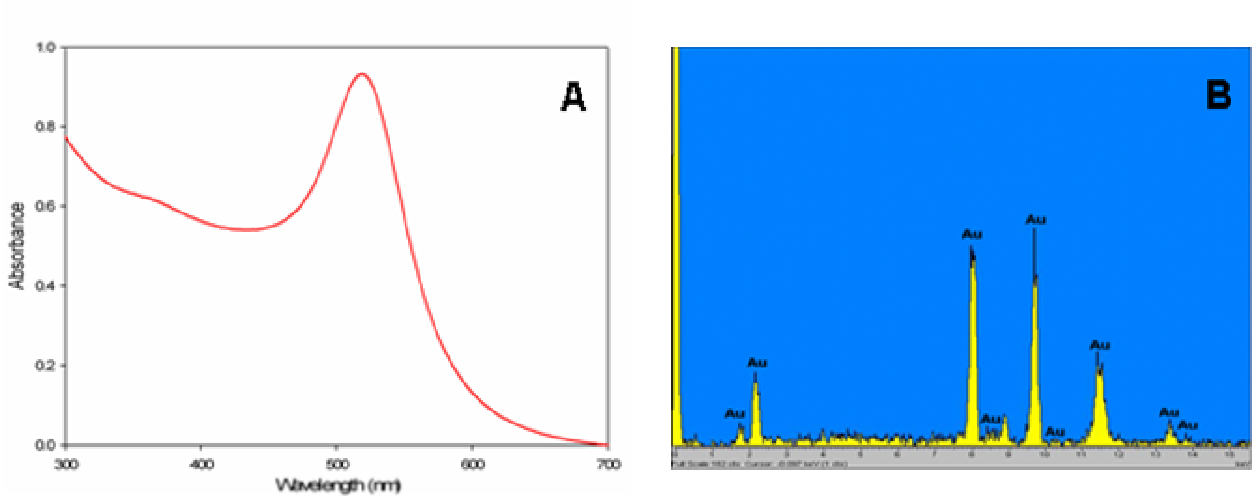

Figure S2. A) UV-Vis spectrum of AuNPs with the characteristic absorbance peak at 520 nm. B) Energy-dispersive X-ray spectroscopy result (EDX spectrum) of AuNPs.

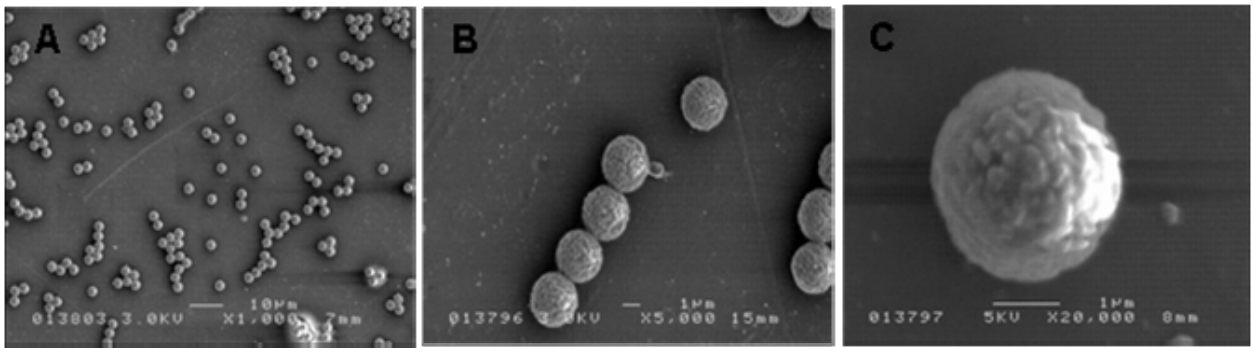

Figure S3. Scanning electron micrographs of streptavidin-coated magnetic beads (2,8 μm) at (A) 1000X, (B) 5000X and (C) 20000X magnification. The MB sample was diluted with doubly-distilled water and ultrasonicated for 20 min prior the analysis.

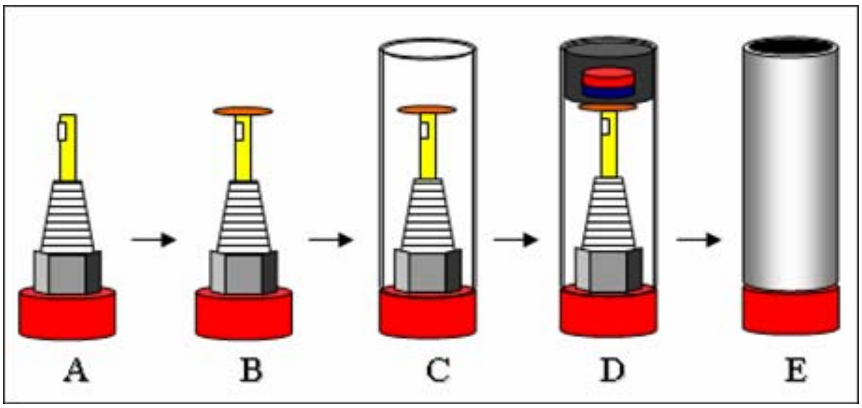

Figure S4. Schematic (not in scale) of the graphite-epoxy composite-magnet electrode (GECE-M) preparation. A) Electrode connector body. B) Copper disk attachment on top of the connector. C) Mount of the PVC body. D) Introduction of the graphite-epoxy paste including a permanent neodymium magnet on top of the copper disk up to the upper border. E) The ready to use GECE-M assembled after a curing step at 40°C for one week.

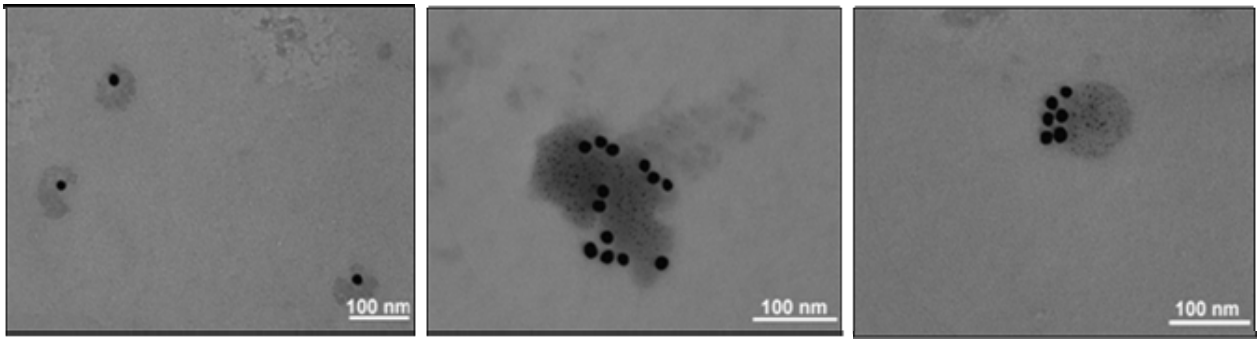

Figure S5. Transmission electron micrographs showing anti-human-HRP antibodies conjugated to AuNPs. The small spots around the black AuNPs can be associated to iron metals present in the heme group of HRP. The experimental conditions of the conjugate preparation are explained in section 3 of the main text.

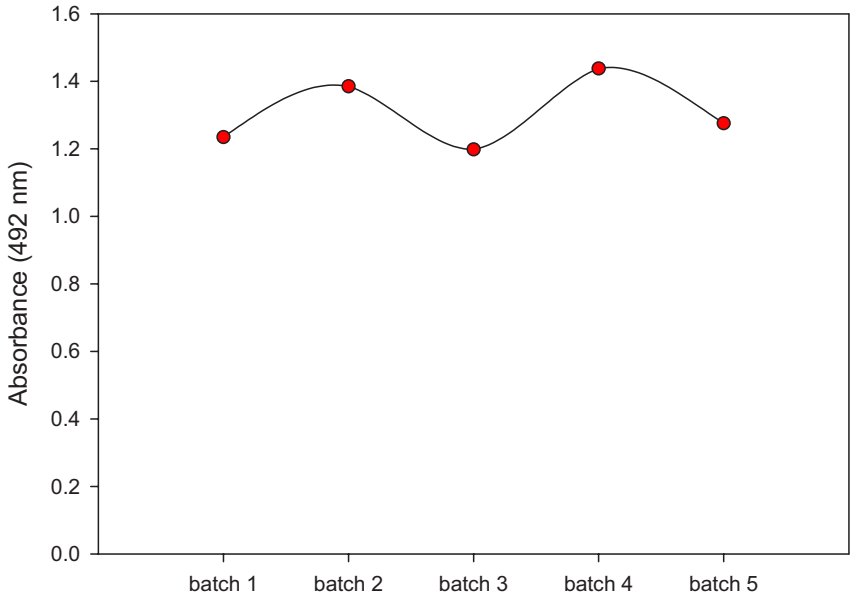

Figure S6. Batch to batch reproducibility of double-codified gold nanolabels. 5 batches of DC-AuNP labels were prepared as described in the paragraph 1.3 of the main text. The method reproducibility was evaluated spectrophotometrically measuring the absorbance at 492 nm after the reaction between HRP on AuNPs and OPD chromogen. Precisely, 5 µL of the DC-AuNP label solution (diluted 1:2) from each batch were transferred to a 96-wells plastic plate; then 160 µL of OPD solution were added simultaneously. The reaction between HRP and OPD, generating a coloured solution, was stopped after 2 min adding 50 µL of HCl 3M. The absorbance at 492 nm was then measured for each batch with a Tecan Sunrise Absorbance Microplate Reader. The absorbance is proportional to the amount of HRP attached to AuNPs. The graph shows the values measured for the 5 batches. This is not an absolute quantitation of HRP carried by each AuNP, but only a relative comparison between the 5 batches. The standard deviation for the 5 measurements was calculated to be 0.101. RSD = 7.8 %

Gold aggregation test

Gold aggregation test was preliminarily carried out to judge the minimum antibody concentration to use for conjugation. Precisely, gold colloid (13 nm) solution was adjusted to pH 9 with NaOH 0.01M; then several solutions with different concentrations of anti-human-HRP in water were prepared to a volume of 30 μL and added to 200 μL of gold solution. After 5 min, 30 μL of 10% NaCl solution were added. NaCl causes the aggregation of gold nanoparticles and shifts the maximum absorbance peak from 520 to 580 nm. (see Figure S7)

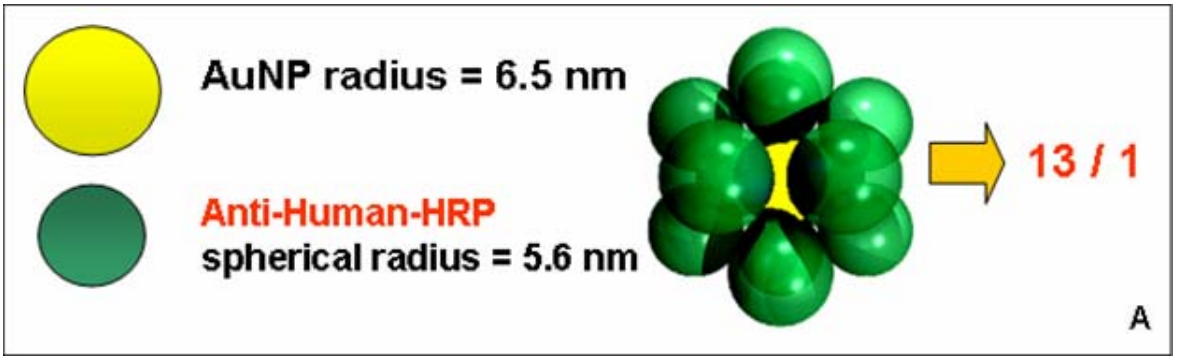

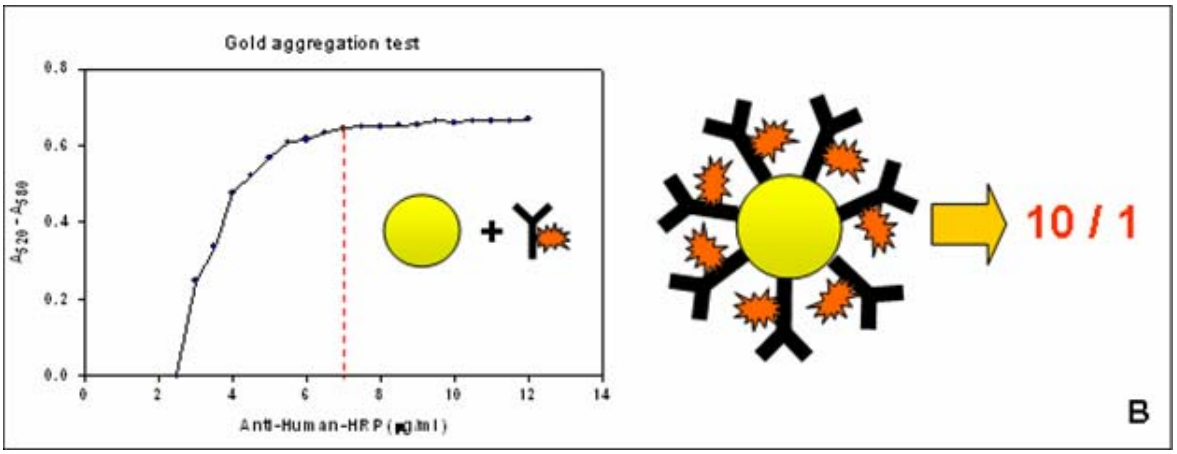

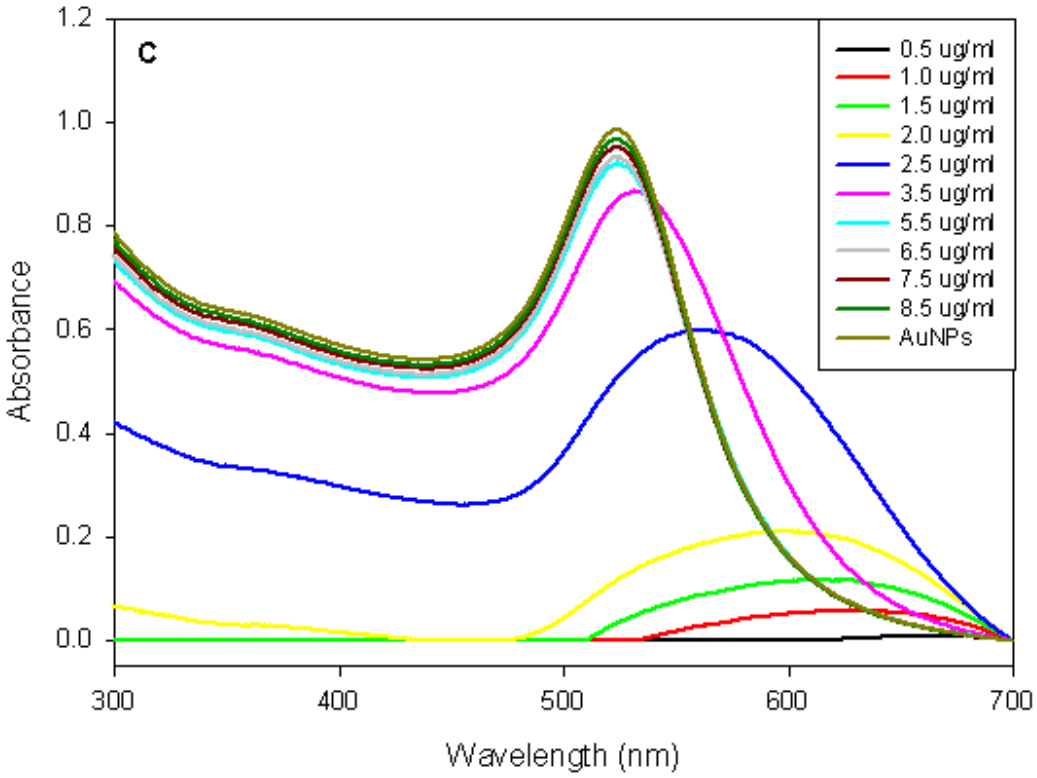

Figure S7. A) Geometrical and B) Experimental results for the conjugation of Anti-human-HRP antibody to AuNPs (13 nm). Considering the AuNP radius and approximating the anti-human-HRP molecule as a sphere of radius 5.6 nm, resulted from geometrical calculation a possible ratio anti-human-HRP / AuNPs of 13/1. From the experimental results, 7.0 μg/mL of anti-human-HRP were necessary to fully cover each AuNP and this corresponded to a molar ratio anti-human-HRP / AuNPs of 10/1. There is a good correspondence between theoretical (13/1) and experimental result (10/1). Theoretical results were based on the geometrical model of sphere packing around a single central sphere as explained in section 3.1. in the main text. C) AuNP spectra recorded after the addition of increasing concentrations of anti-human-HRP antibody and NaCl (10%). The increase of anti-human-HRP stabilizes the AuNPs preventing their aggregation that is visible from the shift of the maximum absorbance peak from 520 to 580 nm. It can be seen how the spectrum of AuNP-anti-human-HRP conjugate solutions becomes more and more similar to that of pure AuNPs (upper line).

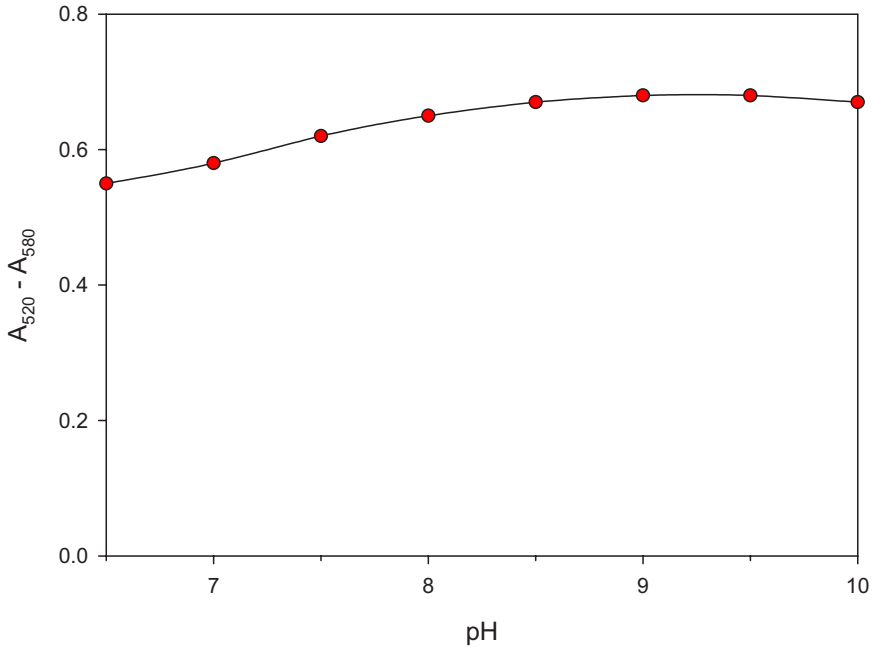

Figure S8. Optimal pH for the conjugation of anti-human IgG-HRP to AuNPs. A preliminary titration was carried out in order to verify the optimal pH for the conjugation of anti-human IgG-HRP to AuNPs. The pH of gold NP solutions was adjusted with either HCl or NaOH 0.01 M (buffers can not be used because cause the aggregation of gold NPs) to the values: 6.5, 7, 7.5, 8, 8.5, 9, 9.5, 10. 200 µL from each solution were transferred to 8 wells of a 96-wells plastic plate. Then 30 µL of anti-human-HRP at the fixed concentration of 10 µg/mL were added to each well. After 5 min 30 µL of 10% NaCl solution were added to each solution to cause gold aggregation. Finally, a spectrophotometric measurement was carried out recording the absorbance at 520 and 580 nm. The optimal pH at which the antibody more efficiently prevent gold aggregation resulted to be around 9 giving the highest absorbance difference.

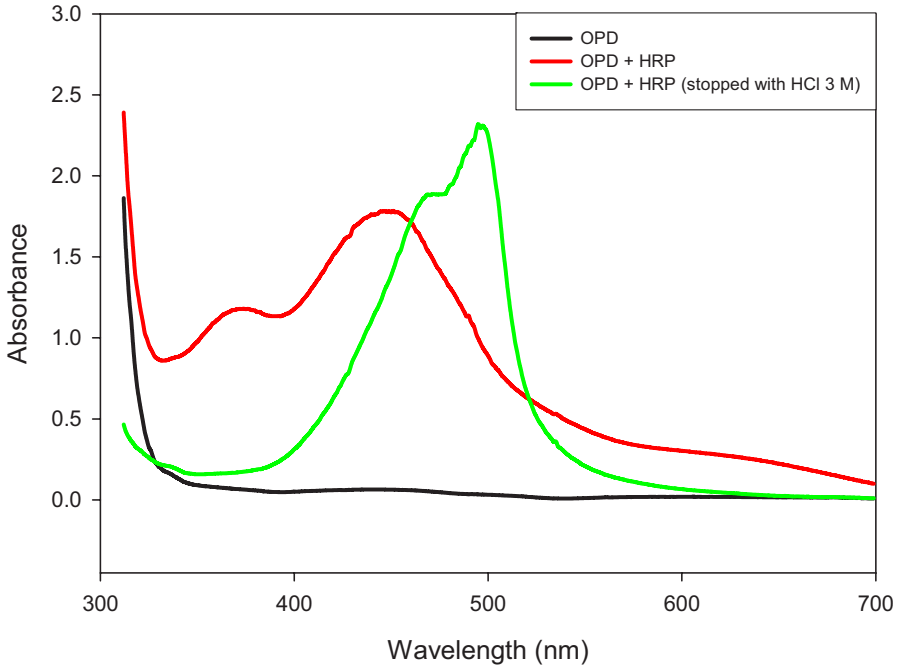

Figure S9. UV-Vis spectrum of OPD solution before the reaction with HRP (black), after the reaction with HRP (red) and after the reaction with HRP stopped by the addition of HCl 3 M. It can be seen that the use of a strong acid to stop the reaction causes the shift of the maximum absorbance peak from 450 to 492 nm.

Chapter 8. ANNEX

I

Electrochemical detection of DNA Hybridization Using Micro and Nanoparticles. Humana Press methods book on biosensors, 2007. Accepted.
Castañeda M. T., Alegret S., Merkoçi A.

DEPARTMENT OF HEALTH AND HUMAN SERVICES Public Health Service

National Institute of Health
National Cancer Institute
6130 Executive Blvd.
Rockville, MD 20852
Phone: 301-402-4185
FAX: 301-402-7819
E. Mail:rasoolya@mail.nih.gov

Wednesday, January 16, 2008

Dr.Arben Merkoçi
Research Professor & Group Leader
Nanobioelectronics & Biosensors Group
Institut Català de Nanotecnologia
Barcelona, Catalonia, Spain
www.nanocat.org

Dear Dr. Merkoçi:

I would like to thank you and your team for submitting two manuscripts for the Humana Press methods book on biosensors.

We have reviewed and accepted for publication the two manuscripts listed below and we sent them to the publisher:
1. Electrochemical Detection of DNA Hybridization Using Micro and Nanoparticles
(María Teresa Castañeda, Salvador Alegre, Arben Merkoçi) and
2. Electrochemical Immunosensing Using Micro and Nanoparticles
(Alfredo de la Escosura, Adriano Ambrosi, Salvador Alegret, Arben Merkoçi)

The aim of the book is to address the topic from an experimental perspective, and to publish detailed practical protocols so that a reader can both understand the technology and also be able to do similar experiments.

Thanks again for your contributions which I hope will advance the field and help standardize methodologies.

Best regards,

Avi Rasooly, Ph.D.

Program Director
Cancer Diagnosis Program,
DCTD, NCI
EPN 6035A
6130 Executive Blvd.
Rockville, MD 20852
Phone: 301-402-4185
FAX: 301-402-7819

Electrochemical Detection of DNA Hybridization Using Micro and Nanoparticles

María Teresa Castañeda[1,2¥], *Salvador Alegret*[3], *Arben Merkoçi*[1*]

[1]Nanobioelectronics & Biosensors Group, Institut Català de Nanotecnologia, Barcelona, Catalonia, Spain; [2]Group of Sensors & Biosensors, Autonomous University of Barcelona, Barcelona, Catalonia, Spain.

[¥]On leave from: Departamento de Ciencias Básicas, Universidad Autónoma Metropolitana-Azcapotzalco, 02200, México, D. F., Mexic.

*Corresponding author: E-mail: arben.merkoci.icn@uab.es Tel: +34935811976; fax: +34935812379

i. Abstract

A novel, rapid and sensitive protocol for the electrochemical detection of DNA hybridization that take the advantage of a magnetic separation/mixing process and the use of monomaleimide-gold nanoparticles of 1.4 nm diameter as label is presented. A sandwich-type assay is formed in this protocol by the capture probe DNA immobilized on the surface of magnetic beads and the double hybridization of the target (cystic fibrosis related DNA), first with the immobilized probe, and then with signaling probe DNA labelled with monomaleimide-gold nanoparticles. When the assay is completed the final conjugate is transferred onto genomagnetic sensor surface (graphite epoxy composite electrode with a magnet inside) used as working electrode and then the direct determination of gold nanoparticles by differential pulse voltammetry striping technique is carried out. This protocol is quite promising for numerous applications in different fields as clinical analysis, environmental control as well as other applications.

ii. Key Words: Gold nanoparticles, DNA analysis, magnetic beads, cystic fibrosis, genosensor, electrochemical detection.

1. Introduction

Developments in nanotechnology have driven to research of nanomaterials in the 1 to 100 nm range offering great potential in a variety of applications such as detection of infectious diseases (***1***), environmental monitoring (***2***), detection of pathogens (***3***), proteomics (***4***), genomics (***5***), drug delivery (***6***), catalytic (*7*) and others bioanalysis. (***8***) Materials at this scale, such as metal nanoparticles (NPs) take on novel properties and functions that differ markedly from those seen in the bulk scale (***8***). The NPs themselves can come in a variety of shapes of which the most commonly prepared are: spheres (***9,10***), rods (***11***), cubes (***12***), triangles (***10***) and ellipsoids *(**13***).

Metal NPs represent an excellent biocompatibility with biomolecules and display unique structural, electronic, magnetic, optical and catalytic properties which in combination with their size have made them a very attractive material in biology (***14***–***18***). The attractive physicochemical properties of gold nanoparticles (AuNPs) are highly affected by its shape and size (***19,20***). The size and properties of AuNPs are highly dependent on their preparation conditions (*7,**21***). Dos Santos et al. have reported the synthesis of AuNPs of different shapes and sizes (***22***).

Currently synthesis of novel AuNPs with unique properties and with applications in a wide variety of areas is subject of substantial research (***23,24***).

Among noble-metal nanoparticles, gold nanoparticles (AuNPs) have been the most extensively used in electrochemical biosensor applications. This is also due to the fact that the biochemical activity of the labelled receptor biomolecules (i.e. proteins and DNA among others) is retained when AuNPs are coupled to them (***25***–*27*). Particularly AuNPs have been

successfully used as electroactive label in the detection of DNA sequences, based on the highly specific hybridization of complementary strands of DNA (***2,5,28–31***).

On the other hand microscopic magnetic beads on the micron size scale have become useful platforms in order to immobilize biomolecules at different biological assays such those related to antibodies (***4***), oligonucleotides (***28,30–32***) and another applications (***32–34***). Dynabeads® M-280 Streptavidin (Dynal Biotech, Oslo, Norway) of 2.8 μm diameter which are uniform, superparamagnetic, polystyrene beads with a monolayer of streptavidin covalently attached to the hydrophobic bead surface are commonly used. Using a magnetic separator the beads allow isolation and subsequent handling of target molecules in a highly specific manner. Capture, washing steps and detection are easily performed and optimised.

Herein we present an AuNPs-based electrochemical DNA hybridization detection protocol involving the use of nanoparticles –monomaleimide-Nanogold (AuNPs) 1.4 nm diameter– as labels (*see* **Fig. 1A-B**) and microparticles –magnetic beads (MB) 2.8 μm diameter– as platform for DNA probe immobilization (*see* **Fig. 1C-D**). In this approach a DNA biosensor (genosensor) design is based on a sandwich detection strategy in which a cystic fibrosis related DNA strand used as target is sandwiched between two complementary DNA probes: the capture probe DNA immobilized on MB via streptavidin-biotin and the signaling probe DNA modified with thiol and labelled with AuNPs via reaction of thiol group with monomaleimide so as to ensure a 1:1 AuNP-DNA probe connection. Differential pulse voltammetry is used for a direct voltammetric detection of AuNPs onto magnetic graphite-epoxy composite electrode (GECE-M).

2. Materials

2.1 Apparatus

1. Electrochemical analyzer Autolab PGSTAT 20 (Eco Chemie, The Netherlands) connected to a personal computer for differential pulse voltammetry (DPV) analyses.
2. Platinum electrode (model 52-67 1, Crison, Spain); that served as an auxiliary electrode.
3. Double junction Ag/AgCl (Orion 900200, Spain) as reference electrode.
4. Magnetic graphite epoxy composite electrode (GECE-M) as working electrode (home made as described at section *3.1.2)*.
5. TS-100 Thermo Shaker (Spain) for the binding of streptavidin-coated paramagnetic beads (MB) with biotinylated probe (Immobilization DNA) and hybridization events.
6. MCB 1200 biomagnetic processing platform (Sigris, CA, USA), in order to carry out the magnetic separation.
7. Power supply, 3000V/300mA/300W (Code PS3003, Ecogen, S.R.L., Spain).
8. A BlueMarine 100 (Inverness Medical Ibérica, S.A.U., Barcelona, Spain) horizontal electrophoresis unit tray is used in order to carry out the gel electrophoresis.
9. High resolution transmission electron micrographs are taken using a Jeol JEM-2011 electronic microscope (Jeol Ltd., Tokyo, Japan).

2.2 Reagents

1. Tris (hydroxymethyl) methylamine (Tris), sodium chloride, sodium citrate, ethylenediamine tertraacetic acid disodium salt (EDTA), lithium chloride, tween 20, boric acid, nitric acid, 65%, bovine serum albumin (BSA), (Molecular Biology reagent, Ref. B428, glycerol (G8773-500mL), 2-Propanol and bromophenol blue sodium salt (B8026) from Sigma-Aldrich.
2. Agarose (Molecular Biology grade, Roche).
3. Xylenecyanol FF, (95600-10G, Fluka).

4. Hydrochloric acid to 37% (PanReac, Barcelona, Spain).
5. Streptavidin-coated paramagnetic beads of diameter 2.8 μm (concentration: 10 mg/mL) –Dynabeads M-280 Streptavidin– (Dynal Biotech, Norway).
6. Monomaleimide-Nanogold, 1.4 nm diameter (Nanoprobes Inc., NY.).
7. Epoxy resin (Epotek H77A) and hardener (Epotek H77B), (Epoxy Technology, Inc., USA).
8. Graphite powder of particle size 50 μm, (BDH, U.K.).

2.3 Oligonucleotides

1. Biotinylated probe oligonucleotide and no modified oligonucleotides from Alpha DNA, Canada.
2. Oligonucleotide modified with thiol (–SH) group is synthesized in our laboratory on an automatic Applied Biosystems DNA synthesizer, model 392, and according described procedure (***35***).
3. Oligonucleotides sequences used in the assay are listed in **Table 1**.

3. Methods

3.1 Electrode construction

3.1.1 Transducer body construction

1. Take a connection female of 2 mm of diameter, place a metallic thread and then solder this connection in its extreme to the centre of the copper disk (6 mm o.d. and

0.5 mm thickness), with the concavity up. (*See* **Fig. 2A**) Previously clean the copper disk by dipping it in HNO_3 solution (1:1) in order to remove copper oxide and rinsing it well with bi-distilled water in order to avoid the decrease of the electrical conductivity of the transducer.

2. Introduce this connection into a cylindrical PVC sleeve (6 mm i.d., 8 mm o.d. and 20 mm longitude). (See Fig. 2B)
3. The metallic thread allows that the connection should remain fixed well in the end of the cylindrical PVC sleeve, whereas in another end there stays a cavity of approximately 3 mm deep in which will be placed the conducting paste (–graphite-epoxy composite– which preparation is described at section 3.2.1) and a permanent magnet. (*See* **Fig. 2C**)

3.1.2 GECE- M preparation

1. Mix manually epoxy resin and hardener in a ratio 20:3 (w/w) using a small spatula.
2. When the resin and hardener are well-mixed, add the graphite powder in the ratio 20:80 (w/w) and mix thoroughly for 30 min to obtain a homogeneous paste of graphite-epoxy composite.
3. Place the resulting conducting paste of graphite epoxy composite into the cylindrical transducer body where a neodymium magnet (diameter 3 mm, height 1.5 mm, Halde Gac Sdad, Spain, catalog number N35D315) has been introduced, 2 mm under the surface of the electrode in such a way that the small neodymium magnet stays between 2 layers of graphite epoxy composite. (*See* **Fig. 2C**)
4. Electrical contact is completed using the copper disk connected to a copper wire into a cylindrical PVC sleeve (6 mm i.d., 8 mm o.d. and 160 mm longitude) leading to the electrochemical workstation. (*See* **Fig. 2D**)

5. Cure the conducting composite in a dry heat oven cured at 40 °C for one week. **Fig. 2G** shows a summarized scheme (not in scale) of GECE-M preparation.
6. Once the resin is hardened, prior to use, the surface of the electrode is polished with abrasive paper and then with alumina paper (polishing strips 301044-001, Orion, Spain) and rinsed carefully with bidistilled water (*See* **Note 1**). The prepared electrode will be ready for later measurements in a three electrode set-up (see figure 2E) connected with the measuring system (see figure 2F) as will be described in the next sections.

3.2 Buffers and solutions preparation

1. TTL buffer: 100mM Tris–HCl, pH 8.0; 0.1% Tween 20; and 1M LiCl.
2. TT buffer: 250mM Tris–HCl, pH 8.0; and 0.1% Tween 20.
3. TTE buffer: 250mM Tris–HCl, pH 8.0; 0.1% Tween 20; and 20mM Na_2 EDTA, pH 8.0.
4. Hybridization solution: 750 mmol/L NaCl, 75 mmol/L sodium citrate.
5. Supporting electrolyte: HCl 0.1M as supporting electrolyte.
6. 5X Tris-Borate-EDTA Buffer (TBE) as running buffer, Composition of 10X TBE Buffer, for 1 Liter: 108g Tris, 55 g Boric acid, 40 mL 0.5M EDTA (pH 8.0) and MilliQ water to 1 L. The pH is 8.3 and requires no adjustment. Dilute 1 in 20 to obtain 5X TBE buffer
7. 1X TBE Buffer: 10X TBE 100 mL and MilliQ water 900 mL
8. Dyes: Bromophenol blue and xylenecyanol FF. For a 10X concentrated solution, the composition is the following: 0.2% xylenecyanol FF, 0.2 % bromophenol blue, 50% glycerol and 10X TBE buffer MilliQ Water. For preparing 100 mL add: 0. 2 g of

xylenecyanol, 0.2 g of bromophenol blue, 50 g of glycerol, 10 mL TBE 10X and 40 mL of MilliQ water. Add 1 μL by each 9 mL of solution.

9. BSA at 10%: Weigh 10 g of BSA powder and place it in a 125 mL flask, then add 100 mL of hybridization solution (prepared previously as in 4) to the flask. Swirl to mix the solution. (*See* **Notes 2** and **3**)

3.3 Functionalization of monomaleimide-Nanogold 1.4 nm

Monomaleimide-Nanogold 1.4 nm *(*AuNPs) is functionalized with signaling DNA (CF-B). This oligonucleotide modified with thiol (–SH) group is directly bound to the surface of AuNPs tags.

1. The binding (*See* **Fig. 3A**) is carried out via reaction of maleimido-thiol group as has been described previously (***35***). Briefly:
2. Mix aliquots of lyophilized AuNPs (6 nmols) with CF-B (6 nmols) and dissolve in 10% 2-propanol.
3. Keep the mixture overnight at room temperature and store the resulting solution in refrigerator until further use.
4. The maleimido group reacts specifically with sulfhydryl groups when the pH of the reaction mixture is between pH 6.5 and 7.5 and forms a stable thioether linkage that is not reversible. *(See* **Fig. 4)**
5. The obtained DNA-functionalized AuNPs carry a negative surface charge provided by the anionic thiolated oligonucleotide.

3.4 Agarose gel electrophoresis of the DNA-functionalized AuNPs

To verify the purity of the functionalization of AuNPs with CF-B a gel electrophoresis is carried out. The sample of CF-B/AuNPs conjugate and control dyes (bromophenol blue and xylenecyanol FF) are loaded in the wells of a 2% agarose gel and 80 V is applied along the gel, with electrophoresis time of 20 min, using 0.5X tris-borate-EDTA (TBE) buffer as a running buffer. A detailed description of the procedure is given in the following two sections.

3.4.1 Agarose gel to the 2%

1. Weight 1 g of agarose powder and place it in a 125 or 250 mL flask. (*See* **Note 4**)
2. Add 50 mL of 1X TBE buffer to the flask. Swirl to mix the solution.
3. Place the flask in the microwave. Heat on high until the solution is completely clear and no small floating particles are visible (about 2 minutes). Swirl the flask frequently to mix the solution and prevent the agarose from burning. (*See* Fig. 5A)
4. Cool the solution to 55 ºC before pouring the gel into the plastic casting tray. (*See* **Note 5**)
5. While the mixture cools, cover the ends of the gel tray with masking tape.
6. Place the plastic comb in the slots on the side of the gel tray. The comb teeth should not touch the bottom of the tray.
7. Pour the agarose mixture into the gel tray until the comb teeth are immersed about 6 mm or 1/4" into the agarose. Pour slowly to avoid bubbles. (*See* Fig. 5B) (*See* **Note 6**)
8. Allow the agarose gel to cool until solidified. The gel will appear a cloudy white colour and will feel cool to the touch (about 20 minutes).

3.4.2 Gel electrophoresis

1. Remove the comb from the wells by pulling straight up on the comb. Gently remove the tape from both ends of the gel tray.

2. Place the gel tray in the gel box with the wells closest to the negative (black) electrode.
3. Add enough 1X TBE buffer to fill the electrophoresis chamber and submerge the gel about 1/4 of inch.
4. Pipette 20 µL of control dyes into the first well and 20 µL of MB-CFA conjugate in the next well. Remember to record on the sketch the order the samples and controls were loaded.
5. Close the top of the electrophoresis chamber. Plug the leads into the electrophoresis chamber. The black lead is the negative lead and should be plugged in closest to the wells. The red lead is the positive lead and should be plugged in furthest from the wells. (*See* Fig. 6A)
6. Plug the other end of the leads into the power source and turn it on. Run the gel at 80 volts until the loading dye has travelled 1/2 of the way down the gel approximately (about 20 minutes). (*See* Fig. 6B)
7. Turn off the power supply. On plug the leads and the power supply before opening the electrophoresis chamber.
8. Observe the migration of the CF-B/AuNPs conjugate towards the '+' electrode and the discrete band of the conjugate, which indicate its successful preparation.
9. Choose to photograph/photocopy/scan the gel or view it on the overhead projector. (*See* **Fig. 7**)
10. The obtained conjugate as resulted from functionalization could then assemble with target DNA.

3.5 Sandwich assay format procedure

3.5.1 Immobilization of capture DNA probe onto paramagnetic beads

The binding of the biotinylated capture DNA probe (CF-A) with magnetic beads (MB) is carried out using a modified procedure recommended by Bangs Laboratories (***36***), as follows:

1. Transfer 50 µg (5µL) of MB into 0.5 mL Eppendorf tube. (*See* **Note 7**)
2. Wash the MB once with 100 µL of TTL buffer using gentle rotation or occasional mixing by gently tapping the tubes. (*See* **Note 8**)
3. Separate magnetically by placing the tube on MCB 1200 biomagnetic processing platform (magnet) for 1 min (see **Fig. 8**). (*See* **Note 9**)
4. Remove the supernatant with a micropipette while the tube remains on the magnet. (*See* **Note 10**)
5. Resuspend gently in 20 µL TTL buffer, removing the tube from the magnet previously. (*See* **Note 11**)
6. Add 200 pmoles of biotin modified capture DNA probe (CF-A), (**Fig. 3B-I**), then adjust the volume to 100 µL by adding deionised and autoclaved water.
7. Incubate resulting MB/CF-A conjugate during 15 min at temperature of 25 °C with gentle mixing in a TS-100 Thermo Shaker (*see* **Note 12**) in order to immobilize CF-A.
8. When the immobilization was complete separate magnetically the resulting MB/CFA conjugate (MB with the immobilized CF-A), from the incubation solution by placing the tube on the magnet for 1 minute.
9. Remove the supernatant with a micropipette while the tube remains on the magnet.
10. Wash sequentially with 100 µL of TT buffer, 100 µL of TTE buffer and 100 µL of TT buffer using gentle rotation or occasional mixing by gently tapping the tubes.
11. Separate magnetically by placing the tube on the magnet for 1 minute.

12. Remove the supernatant with a micropipette while the tube remains on the magnet.
13. Resuspend gently in 50 μL of hybridization solution and it is ready for the first hybridization.

3.5.2 First hybridization

1. Add 38 pmoles (if no stated otherwise) of target DNA (CF-T) in the solution (50 μL) of the MB/CF-A conjugate obtained in the previous step (*see* **Fig. 3B-II**).
2. Adjust the volume to 100 μL by adding deionised and autoclaved water.
3. Incubate at 42 °C with gentle mixing during 15 min. (*See* **Note 13**)
4. When the hybridization was complete separate magnetically the obtained MB/CF-A/CF-T conjugate by placing the tube on the magnet for 1 min.
5. Wash twice with 100 μL of TT buffer using gentle rotation or occasional mixing by gently tapping the tubes.
6. Remove the supernatant with a micropipette while the tube remains on the magnet.
7. Resuspend gently in 50 μL of hybridization solution and it is ready for the second hybridization.

3.5.3 Second hybridization

1. Add 38 pmoles (*see* **Note 14**) AuNPs functionalized with CF-B in the ratio 1:1 in the solution (50 μL) of the MB/CF-A/CF-T conjugate obtained in the previous step. (*See* **Fig. 3B-III**)
2. Add the necessary volume of BSA at 10% and autoclaved water in order to obtain a final volume of 100 μL and a final concentration of the BSA of 5% approximately. (*See* **Note 15**)
3. Incubate at 42 °C with gentle mixing during 15 min.

4. When the hybridization was complete wash the resulting MB/CF-A/CF-T/CF-B-AuNPs conjugate three times with 100 μL of TT buffer, using gentle rotation or occasional mixing by gently tapping the tubes
5. Separate magnetically by placing the tube on the magnet for 1 minute.
6. Remove the supernatant with a micropipette while the tube remains on the magnet.
7. Resuspend in 50 μL of hybridization solution and it is ready for to do the corresponding measurement.
8. Place the solution containing the final conjugate on the surface of GECE-M during 60 s which is accumulated on it due to the inherent magnetic field of the electrode. (*See* **Fig. 3B-IV**) (*See* **Note 16**)
9. Finally carry out the direct DPV electrochemical detection of Au-NPs tags in the conjugate after the DNA hybridization event, without the need of acidic (i.e. HBr/Br_2) dissolution (***28***,***30***), according the established conditions. (*See* **Fig. 3B-V**)

3.5.4. Control assay

An identical procedure as described above except the addition of target (step II at Fig. 3) in order to evaluate the nonspecific adsorption onto GECE-M at sandwich assay, simultaneously was carried out.

3.5.5. Discrimination study

To study the discrimination between CF-MX1 (one base mismatch), CF-MX3 (three base mismatch), CF-NC (noncomplementary) and the CF-T (target DNA) (See sequences in Table 1) in order to demonstrate the selectivity of the genomagnetic sandwich assay protocol should be made following the same protocol above described.

3.5.5 Conditions of Electrochemical detection

1. The electrochemical detection is an extensively used method to analyze specific DNA sequences by means of the hybridization event due to its simplicity, selectivity, low instrumentation costs and high sensitivity.
2. The amount of AuNPs tag was determined by DPV voltammetry as follows:
3. Choose differential pulse voltammetry (DPV) analysis mode in the Autolab software program.
4. Establish the following parameters: Deposition potential, +1.25 V; duration, 120 s; conditioning potential, 1.25 V; step potential, 10 V; modulation amplitude, 50 mV.
5. Run a blank by triplicate immersing the three electrodes: GECE-M as working electrode, the Ag/AgCl as reference electrode and the platinum electrode as auxiliary in an electrochemical cell containing 10 mL of HCl 0.1M as supporting electrolyte. (*See* **Fig. 2E**) Save the responses
6. Rinse the electrodes with Milli-Q water.
7. Place the sample on the surface of GECE-M during 60 s which is accumulated on it due to the inherent magnetic field of the electrode.
8. Carry out the sample measurement immersing also the three electrodes in the electrochemical cell containing 10 mL of HCl 0.1M as supporting electrolyte. Save the response. (*See* **Fig. 2F**)
9. The electrochemical oxidation of Au-NPs to $AuCl_4^-$ is performed at +1.25 V (vs. Ag/AgCl) for 120 s (*see* **Note 17**) in the nonstirred solution. Immediately after the electrochemical oxidation step, is performed DPV. During this step scan the potential from +1.25 V to 0 V with step potential 10 mV, modulation amplitude 50 mV, scan rate 33.5 mV s^{-1}, no stirred solution.

10. Subtract the response saved for the blank from the sample response using the Autolab software.
11. Save the result which is an analytical signal due to the reduction of $AuCl_4^-$ at potential +0.4 V. (*37*) Use the DPV peak height at the potential of +0.4 V as the analytical signal in all of the measurements. **Fig. 9a** shows the typical differential pulse voltammogram (DPV) for the oxidation signal of Au during the sandwich assay to 38 pmoles of CF-T. The Au reduction signal current is proportional to the amount of AuNPs, which corresponds to the concentration of hybridized DNA target. The quantitative result is obtained from the corresponding calibrate plot. (Not shown). **Fig. 9b** shows the DPV response (almost negligible) to control assay owing to the fact that the sandwich is not formed.

4. Notes

1. Before each use, the surface of the electrode was wet with doubly distilled water and then thoroughly smoothed, first with abrasive paper and then with alumina paper.
2. All stock solutions are prepared using deionised and autoclaved water.
3. Store all stock solutions in refrigerator (4ºC) until its use.
4. 50 mL are needed for a single gel.
5. Higher temperatures will melt the plastic tray.
6. Push any bubbles to the side farthest from the wells or to eliminate them.
7. The amount of MB used in this protocol is the result of an optimization between 25 and 150 µg for the same concentration of CF-T (38 pmoles). Results no shown.

8. Carry out all the washed, using gentle rotation or occasional mixing by gently tapping the tubes, approximately during 1 minute.
9. Do not remove the tube from the magnet during the separation process.
10. Avoid touching the inside wall of the tube (where the beads attract to the magnet) with the pipette tip.
11. Before each different addition into Eppendorf tube, remove the tube from the magnet.
12. The influence of the time and the temperature of hybridization on DPV response is also optimized. Result no shown.
13. All the incubations were carried out at TS-100 Thermo Shaker.
14. Should be added as minimum the same concentration as CF-T DNA.
15. With the BSA used as blocking agent and the effective washing steps non-specific adsorption is eliminated.
16. This protocol can be adapted for other fields such as biotechnological and environmental.
17. The influence of time and potential of electrochemical oxidation of Au-NPs to $AuCl_4^-$ upon the DPV signal also are studied in order to establish the optimal values.

Acknowledgments

This work is supported by the Spanish "Ramón Areces" foundation (project 'Bionanosensores') and MEC (Madrid) thorough the following projects: MAT2005-03553, and Consolider-Ingenio 2010 (CSD2006-00012).

References

1. Pejcic, B., De Marco, R., and Parkinson, G. (2006) The role of biosensors in the detection of emerging infectious diseases. *Analyst*, **131**, 1079–1090.

2. Cai, H., Shang, Ch., and Hsing I. M. (2004) Sequence-specific electrochemical recognition of multiple species using nanoparticle labels. *Anal. Chim. Acta,* **523**, 61–68.

3. Lin, F. Y. H., Sabri, M., Alirezaie, J., Li, D., and Sherman, P. M. (2005) Development of a Nanoparticle-Labeled Microfluidic Immunoassay for Detection of Pathogenic Microorganisms. *Clin. Diagn. Lab. Immunol.* **12**, 418–425.

4. Ambrosi, A., Castañeda, M. T., Killard, A. J., Smyth, M. R., Alegret, S., and Merkoçi, A., (2007) Double-codified gold nanolabels for enhanced immunoanalysis. *Anal. Chem.*, **79**, 5232–5240.

5. Zhang, J., Song, S., Zhang, L., Wang, L., Wu, H., Pan, D., and Fan, Ch. (2006) Sequence-Specific Detection of Femtomolar DNA via a Chronocoulometric DNA Sensor (CDS): Effects of Nanoparticle-Mediated Amplification and Nanoscale Control of DNA Assembly at Electrodes. *J. Am. Chem. Soc.*, **128**, 8575–8580.

6. Sinha, R., Kim, G. J. and Nie, S., and Dong M. Shin (2006) Nanotechnology in cancer therapeutics: bioconjugated nanoparticles for drug delivery. *Mol. Cancer Ther.* **5**, 1909-1917.

7. Cuenya, B. R., Hyeon Baeck, S., Jaramillo, T. F., and McFarland, E. W. (2003) Size-and Support-Dependent Electronic and Catalytic Properties of Au^0/Au^{3+} Nanoparticles Synthesized from Block Copolymer Micelles. *J. Am. Chem. Soc*., **125**, 12928-12934.

8. McNeil, S. E. (2005) Nanotechnology for the biologist. *J. Leukocyte Biol.,* **78**, 585–594.

9. DeBenedetti, B., Vallauri, D., Deorsola, F. A., and Martínez García, M. (2006) Synthesis of TiO_2 nanospheres through microemulsion reactive precipitation. *J. Electroceramics*, **17**, 37–40

10. S. Shiv, S., Suresh, B., and Murali, S. (2005) Synthesis of Gold Nanospheres and Nanotriangles by the Turkevich Approach. *J. Nanosci. Nanotechnol*., **5**, 1721–1727.

11. Tai H. H., Koo H.-J., and Chung, B. H. (2007) Shape-Controlled Syntheses of Gold Nanoprisms and Nanorods Influenced by Specific Adsorption of Halide Ions. *J. Phys. Chem. C*, **111**, 1123–1130.

12. Hyuk Im, S., Tack Lee, Y., Wiley B., and Xia, Y., (2005) Large-Scale Synthesis of Silver Nanocubes: The Role of HCl in Promoting Cube Perfection and Monodispersity. *Angew. Chem. Int.Ed.,* **44**, 2154–2157.

13. Mendoza-Reséndez, R., Bomati-Miguel O., Morales, M. P., Bonville, P., and Serna C. J. (2004) Microstructural characterization of ellipsoidal iron metal nanoparticles. *Nanotechnology,* **15**, S254–S258.

14. Hernández-Santos, D., González-García, M. B., and Costa-García, A., (2002) Metal-nanoparticles based electroanalysis. *Electroanalysis*, **14**,1225–1235.

15. Alivisatos, P. (2004) The use of nanocrystals in biological detection. *Nat. Biotechnol*., **22**, 47–52.

16. Rosi, N. L., and Mirkin, C. A. (2005) Nanostructures in biodiagnostics. *Chem. Rev.,* **105**, 1547–1562.

17. Azzazy, H. M. E., Mansour M. M. H., and Kazmierczak, S. C. (2006) Nanodiagnostics: A New Frontier for Clinical Laboratory Medicine. *Clinical Chemistry,* **52**, 1238–1246.

18. Katz, E., and Willner, I. (2004) Integrated nanoparticle-biomolecule hybrid systems: Synthesis, properties and applications*. I. Angew. Chem. Int. Ed.* **43**, 6042–6108.

19. Liz-Marzan, L. M., (2004) Nanometals: Formation and color. *Materials Today*, **7**, 26–31.

20. Burda, C., Chen, X., Narayanan, R., and El-Sayed, M. A. (2005) Chemistry and Properties of Nanocrystals of Different Shapes. *Chemical Reviews*, **105**, 1025–1102.

21. Miscoria, S.A., Barrera, G. D., and Rivas, G. A. (2005) Enzymatic biosensor based on carbon paste electrodes modified with gold nanoparticles and polyphenol oxidase. *Electroanalysis* **17**, 1578–1582.

22. Dos Santos, Jr., D. S., Alvarez-Puebla, R. A., Oliveira, Jr., O. N., and Aroca, R. F. (2005) Controlling the size and shape of gold nanoparticles in fulvic acid colloidal solutions and their optical characterization using SERS. *J. Mater. Chem*., **15**, 3045–3049.

23. Panda, B. R., and Chattopadhyay, A. (2007) Synthesis of Au Nanoparticles at "all" pH by H_2O_2 Reduction of $HAuCl_4$. *J. Nanosci. Nanotechnol.,* **7**, 1911-1915.

24. Luo, Y., and Sun X., (2007) Sunlight-Driving Formation and Characterization of Size-Controlled Gold Nanoparticles. *J. Nanosci. Nanotechnol.,* **7**, 708-711.

25. Castañeda, M. T., Alegret, S., and Merkoçi, A. (2007) Electrochemical sensing of DNA using gold nanoparticles, *Electroanalysis*, **19**, 743-753.

26. Merkoçi¸ A. (2007) Electrochemical biosensing with nanoparticles. *FEBS Journal,* **274**, 310–316.

27. Luo, X., Morrin, A., Killard, A. J., and Smyth, M. R. (2006) Application of Nanoparticles in Electrochemical Sensors and Biosensors. *Electroanalysis*, **18**, 319–326.

28. Pumera, M., Castañeda, M. T., Pividori, M. I., Eritja, R., Merkoçi A., and Alegret, S. (2005) Magnetically Trigged Direct Electrochemical Detection of DNA Hybridization Using Au_{67} Quantum Dot as Electrical Tracer. *Langmuir*, **21**, 9625–9629.

29. Ozsoz, M., Erdem, A., Kerman, K., Ozkan, D., Tugrul, B., and Topcuoglu, N. (2003) Electrochemical Genosensor Based on Colloidal Gold Nanoparticles for the Detection of Factor V Leiden Mutation Using Disposable Pencil Graphite Electrodes. *Anal. Chem*., **75**, 2181–2187.

30. Castañeda, M. T., Merkoçi, A., Pumera, M., and Alegret, S., (2007) Electrochemical genosensors for biomedical applications based on gold nanoparticles. *Biosens. Bioelectron*., **22**, 1961–1967.

31. Wang, J., Xu, D., Kawde, A. N., and Polsky R. (2001) Metal nanoparticle-based electrochemical stripping potentiometric detection of DNA hybridization. *Anal. Chem.,* **73,** 5576–5581.

32. Palecek, E., Fojta, M., and Jelen, F. (2002) New approaches in the development of DNA sensors: hybridization and electrochemical detection of DNA and RNA at two different surfaces. *Bioelectrochemistry*, **56**, 85–90.

33. Gijs, M.A.M., (2004) Magnetic bead handling on-chip: new opportunities for analytical applications. *Microfluidics and Nanofluidics*, **1**, 22–40.

34. Lim, C.T., and Zhang Y. (2007) Bead-based Microf luidic Immunoassays: The Next Generation. *Biosens. Bioelectron*., **22**, 1197–1204.

35. Torre, B. G., Morales, J. C., Avino, A., Iacopino, D., and Ongaro, A. Fitzmaurice, D., Murphy, D., Doyle, H., Redmond, G., and Eritja, R. (2002) Synthesis of Oligonucleotides Carrying Anchoring Groups and Their Use in the Preparation of Oligonucleotide -Gold Conjugates. *Helv. Chim. Acta*, **85**, 2594–2607.

36. Bangs Laboratories Inc., TechNote 101 (1999).

37. Pumera, M., Aldavert, M., Mills, C., Merkoçi, A., and Alegret, S. (2005) Direct Voltammetric Determination of Gold Nanoparticles Using Graphite-Epoxy Composite Electrodes. *Electrochim. Acta,* **50**, 3702–3707.

Figure Captions

Fig. 1. HR-TEM images of monomaleimide-Nanogold 1.4 nm diameter (AuNPs) at: (**A**) 400000X and **(B)** 500000X; and paramagnetic beads 2.8 μm diameter (MB) at: (**C**) 600X and (**D**) 4000X magnifications.

Fig. 2. Pictures of transducer body construction (A-B): GECE-M preparation (C-D); system of three electrodes, from left to right: auxiliary, working and reference immersed into electrochemical cell (E); electrochemical analyzer Autolab PGSTAT 20 connected to a personal computer, at which DPV electrochemical detection of AuNPs was carried out (F).

Fig. 3. Functionalization of monomaleimide-Nanogold 1.4 nm diameter (**A**). Schematic representation (not in scale) of the analytical protocol (**B**): Immobilization of the biotinylated CF-A probe onto streptavidin-coated paramagnetic beads (MB), (**3B-I**); addition of the Target CF to the first hybridization event, (3**B-II**); addition of monomaleimide-nanogold (AuNPs) functionalized with signalling thiolated CF-B probe to the second hybridization event, (**3B-III**); accumulation of final conjugate on the surface of the M-GECE, (3**B-IV)** and magnetically trigged direct DPV electrochemical detection of AuNPs tags in the conjugate, (3**B-V)**.

Fig. 4. Monomaleimide-Nanogold with thiol-oligonucleotide reaction scheme.

Fig. 5. Agarose gel preparation. The mixture of agarose and 1X TBE buffer is heated at microwave (A) until its complete dissolution. The dissolution formed is cooled up to

55ºC and then poured slowly into the gel tray (B) and left to be solidified at room temperature.

Fig. 6. Gel electrophoresis apparatus. From left to right: Cover electrophoresis chamber with the corresponding black and red leads, chamber electrophoresis and gel tray with the plastic comb inside (A); Power supply (B).

Fig. 7. Image of the agarose gel to 2 % in which the corresponding bands of control of bromophenol blue and xylenecyanol dyes (**1**) and DNA/monomaleimide-Nanogold 1.4 nm conjugate (**2**) are observed. Conditions: 80 V, electrophoresis time 20 min, using 0.5X Tris-borate-EDTA buffer as running buffer.

Fig. 8. MCB 1200 biomagnetic processing platform. (Sigris, CA, USA) in which magnetic separations are carried out.

Fig. 9. Typical differential pulse voltammogram (DPV) for the oxidation signals of Au during the sandwich assay to 38 pmoles of CF-T (a) and sandwich assay without CF-T used as control (b). Conditions: hybridization time, 15 min; hybridization temperature, 42 ºC; amount of paramagnetic beads, 50 μg; electrooxidation potential, +1.25 V; electrooxidation time, 120 s; DPV scan from +1.25 V to 0 V, step potential 10 mV, modulation amplitude 50 mV, scan rate 33.5 mV s^{-1}, nonstirred solution.

Table 1. Oligonucleotides used in this protocol

Name	Probe sequence[a]
Capture DNA (CF-A)	5'TGC TGC TAT ATA TAT-biotin-3'
Signaling DNA (CF-B)	Thiol-5'GAG AGT CGT CGT CGT3'
Target DNA (CF-T)[b]	5'ATA TAT ATA GCA GCA GCA GCA GCA GCA GAC GAC GAC GAC TCT C3'
One base mismatched DNA (CF-MX1)	5'ATA TAT AAA GCA GCA GCA GCA GCA GCA GAC GAC GAC GAC TCT C3'
Three base mismatched DNA (CF-MX3)	5'ATA TAT CCC GCA GCA GCA GCA GCA GCA GAC GAC GAC GAC TCT C3'
Noncomplementary DNA (CF-NC)	5'GGT CAG GTG GGG GGT ACG CCA GG3'

[a] Underlined nucleotides correspond to the mismatches.
[b] Target related to cystic fibrosis gene.

FIGURES

Figure 1

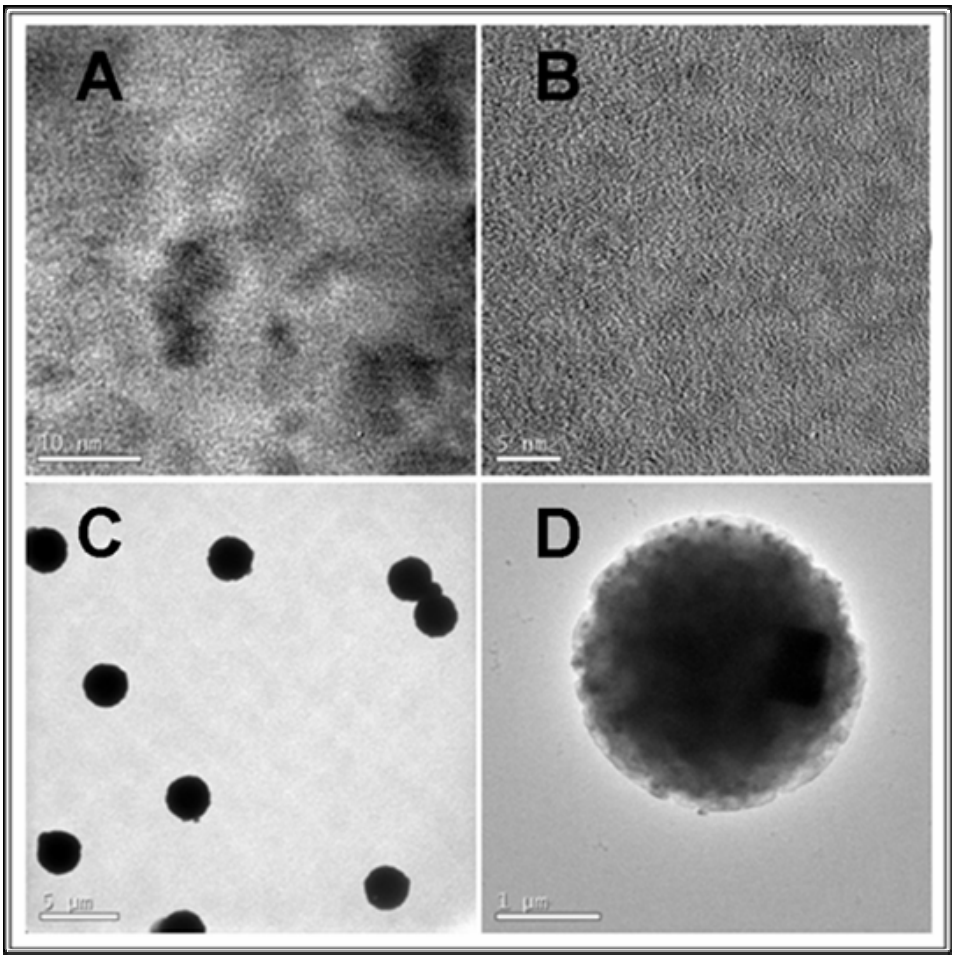

Figure 2

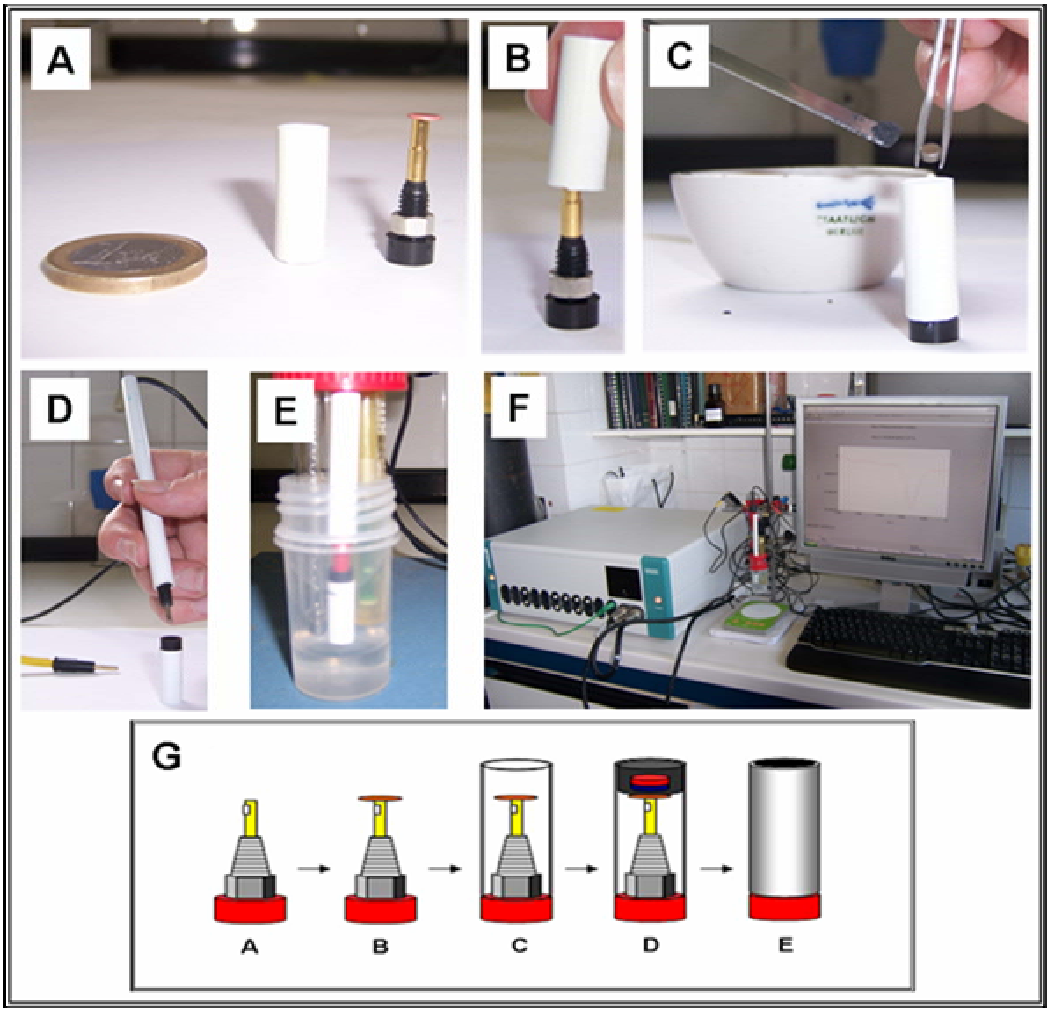

Figure 3

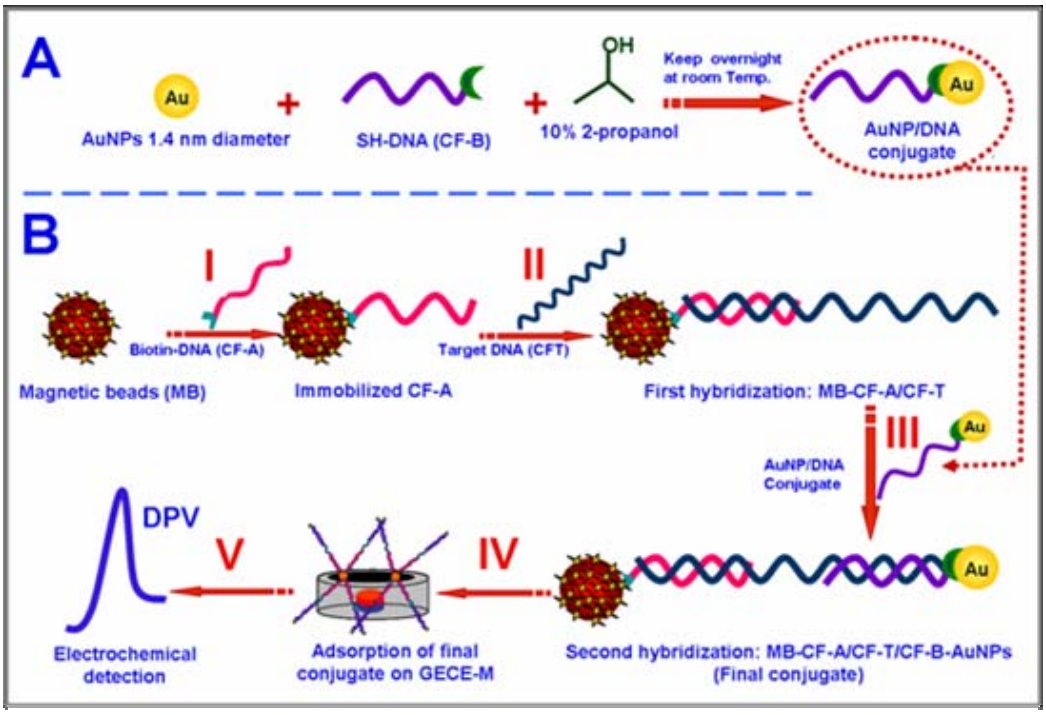

Figure 4

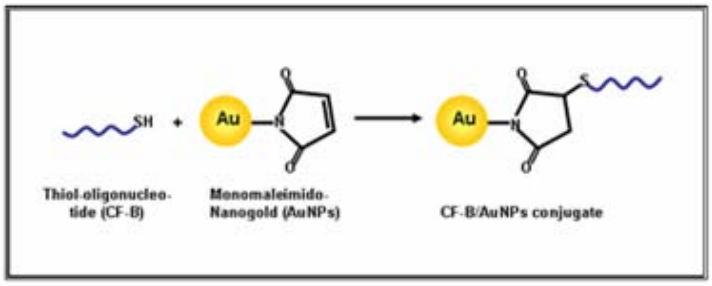

Figure 5

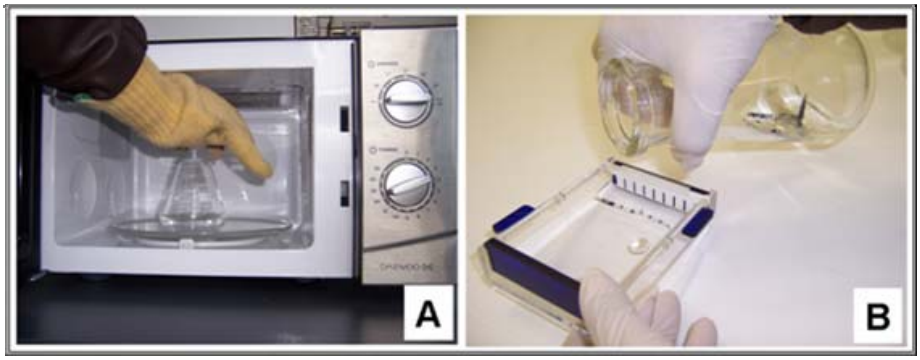

Figure 6

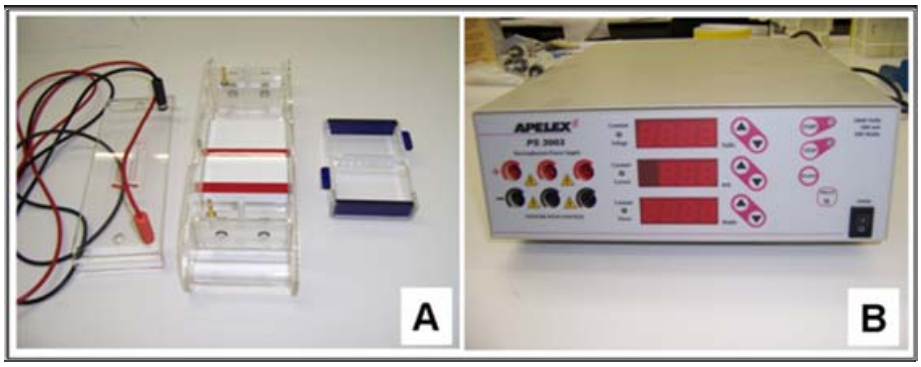

Figure 7

Figure 8

Figure 9